Alma Mater Studiorum – Università di Bologna

DOTTORATO DI RICERCA IN

SCIENZE BIOMEDICHE E NEUROMOTORIE

Ciclo XXXIII

Settore Concorsuale: 05/D1

Settore Scientifico Disciplinare: BIO/09

NEUROPHYSIOLOGICAL, MOLECULAR AND PATHOPHYSIOLOGICAL ASPECTS OF SYNTHETIC TORPOR

Presentata da: Fabio Squarcio

Coordinatore Dottorato

Prof. Pietro Cortelli

Supervisore

Prof. Roberto Amici

Co-Supervisore

Prof.ssa Elisabetta Ciani

Esame finale anno 2020

Out of the cradle
onto dry land
here it is
standing:
atoms with consciousness;
matter with curiosity.

Stands at the sea,
wonders at wondering: I
a universe of atoms
an atom in the universe.

(Richard Feynman, 1955)

ABSTRACT

Synthetic torpor is a peculiar physiological condition resembling natural torpor, in which even non-hibernating species can be induced through different pharmacological approaches. The growing interest in the induction of a safe synthetic torpor state in non-hibernating species stems from the possible applications that it may have in a translational perspective. In particular, the deeper understanding of the functional changes occurring during and after synthetic torpor may lead to the standardization of a safe procedure to be used also in humans and to the implementation of new therapeutic strategies. Some of the most interesting and peculiar characteristics of torpor that should be assessed in synthetic torpor and may have a translational relevance are: the reversible hyperphosphorylation of neuronal Tau protein, the strong and extended neural plasticity, which may be related to Tau regulatory processes, and the development of radioresistance.

In this respect, in the present thesis, rats were induced into synthetic torpor by the pharmacological inhibition of the raphe pallidus, a key brainstem thermoregulatory area, in order to assess: i) whether a reversible hyperphosphorylation of Tau protein occurs at the spinal cord level, also testing the possible involvement of microglia activation in this phenomenon; ii) sleep quality after synthetic torpor and its possible involvement in the process of Tau dephosphorylation; iii) whether synthetic torpor has radioprotective properties, by assessing histopathological and molecular features in animals exposed to X-rays irradiation.

The results showed that: i) a reversible hyper-phosphorylation of Tau protein also occurs in synthetic torpor in the dorsal horns of the spinal cord; ii) sleep regulation after synthetic torpor seems to be physiological, and sleep deprivation speeds up Tau dephosphorylation; iii) synthetic torpor induces a consistent increase in radioresistance, as shown by analyses at both histological and molecular level.

TABLE OF CONTENTS

INDEX OF ABBREVIATIONS

2-DG: 2-deoxy-D-glucose
5'-AMP: 5'-adenosine monophosphate
ACh: AcetylCholine
aCSF: Artificial cerebrospinal fluid
Adcyap1: Adenylate cyclase activating polypeptide 1
ADP: Adenosine diphosphate
ADS: Antibody dilution solution
Amb: Nucleus ambiguus
AMP: Adenosine monophosphate
AMPA: α-amino-3-hydroxy-5-methyl-4-isoxazolepropionic acid
AMPK: AMP protein kinase
ANS: Autonomic nervous system
Arc: Arcuate nucleus of the hypothalamus
ATP: Adenosine triphosphate
avMLPA: Anterior and ventral portions of the medial and lateral preoptic area
AVPe: Anteroventral periventricular nucleus
BAT: Brown adipose tissue
BER: Base excision repair
CA3: CA3 field of the hippocampus
cAMP: Cyclic AMP
Cb-Cx: Cerebellum cortex
Cdk: Cyclin dependent kinases
CHA: N6-cyclohexyladenosine
ChAT: Choline-acetil transferase
CKI: Cdk inhibitors
CNS: Central nervous system
CREB: cAMP response element-binding protein
DH: Dorsal horn of the spinal cord
DMH: Dorsomedial nucleus of the hypothalamus
dMV: Dorsal motor nucleus of the vagus nerve
DSB: Double-strand break
EEG: Electroencephalogram
fEPSPs: Field excitatory postsynaptic potentials
GSK3-β: Glycogen-synthase kinase-3-β
H_2S: Hydrogen sulphide
HPc: Hibernation protein complex
HSP: Heat shock proteins
HSPCs: Hematopoietic stem cells
IR: Ionizing radiation
LC: Locus coeruleus
LH: Lateral hypothalamus
LPB: Lateral parabrachial nucleus

LPBd: Dorsal portion of the LPB
LPBel: External lateral subdivision of the LPB
LTD: Long-term depression
LTP: Long-term potentiation
MAP: Microtubule-associated protein
MM: Medial mammillary nucleus
MnPO: Median preoptic nucleus
MPA: Medial preoptic area
MR: Metabolic rate
NE: Norepinephrine
NER: Nucleotide excision repair
NMDA: N-methyl-D-aspartate receptors
NPY: Neuropeptide Y
NFT: Neurofibrillary tangles
NTS: Nucleus of the solitary tract
nuEMG: Nuchal electromyography
OER: Oxygen enhancement ratio
PAG: Lateral periaqueductal grey area
PBS: Phosphate buffered saline
PCD: Programmable cell death
P-Cx: Parietal cortex
PHF: Paired helical filaments
P-GSK3-β: GSK3-β phosphorylated on serine 9
PKA: cAMP-dependent protein kinase
POA: Preoptic Area
PRh: Perirhinal cortex
PV: Paraventricular nucleus of the thalamus
PVH: Paraventricular hypothalamic nucleus
QRFP: Pyroglutamylated RFamide peptide
RPa: Raphe pallidus
RVLM: Rostral ventrolateral medulla
RVMM: Ventromedial medullary areas
SCN: Suprachiasmatic nucleus of the hypothalamus
SHY: Synaptic homeostasis hypothesis
SNS: Sympathetic nervous system
SWA: Slow-wave activity
T_1AM: 3-iodothyronamine
Ta: Ambient temperature
Tb: Body temperature
TH: Thyroid hormone
Thy: Hypothalamic temperature
TNF: Tumor necrosis factor
TR: Thyroid hormone receptor
TRH: Thyrotropin-releasing hormone

TRP: Transient receptor potential channels
UCP1: Uncoupling protein 1
Vglut2: Vesicular glutamate transporter 2
VH: Ventral horn of the spinal cord
VLPAG: Ventrolateral part of the periaqueductal grey matter
VLPO: Ventrolateral preoptic nucleus
WSN: Warm sensitive neurons

1. INTRODUCTION

1.1 THERMOREGULATION

All living beings produce heat, which is partially eliminated in the environment and in part it remains inside the body. The heat is usually considered as a waste product from the biochemical machine, but this is not always the case. For organisms that have the ability to maintain a constant temperature, it represents an indispensable product to reach an adequate thermal level. Indeed, in vertebrates the maximum of the efficacy is in a tiny range of body temperature (Tb) between 0 and 45 °C (Scotto, 2006).

In fact, despite life exists in a universe with temperatures ranging from near absolute zero (–273°C) to > 1,000,000°C, the Tb of most living organisms falls into only a tiny portion of this range: from 0 to 45°C. Most organisms cannot operate at a Tb below 0 °C, since water freezes at this temperature, which results in a loss of most cell functions and, typically (although not always), makes it impossible for a cell to survive. Life, as we know it, is also nearly impossible at a Tb above 45°C, as enzymes that catalyze biochemical reactions start denaturing at this temperature (Romanovsky, 2018).

Nonetheless, within these extremes, even slight variation of Tb from the ideal value can have significant effects, because every biological process involves many biochemical reactions that depend on the temperature.

Based on the ability of the animals to maintain their Tb constant they can be divided in two main categories:

● Poikilotherms (from Greek poikilos which means mutable)

● Homeotherms (from Greek Omoios which means equal, same)

Poikilotherms, which include the plants and most of the animals, except bird and mammals, are organisms whose internal temperature fluctuates as the environmental temperature varies, moreover, having a very low metabolism they are forced to take the heat directly from the sun. This aspect can have pros and cons, indeed, if on one hand their low metabolism forces them to be inactive during the night, on the other hand they can survive in very dry environment, with poor faunas and flora, because their food need is only around one tenth of that of mammals of the same size.

These animals have also been defined cold-blooded, this because often they have their Tb in the lower and middle portion of the life range and being bradymetabolic animals in response to cold, they cannot increase their metabolism strongly enough to prevent a drop in deep Tb.

The definition cold-blooded can induce to think that their temperature has to be always low, and they remain mandatorily passive to the environmental variations. But, this is not totally true, they can show over some compensatory behaviors (like some reptiles that during the cold day look for sunny places exposing themselves to the sun and staying in contact with the earth) also some real additional thermoregulatory mechanisms (e.g. some reptiles of the iguanid family and also some box turtles can use the wheezing to lose heat when, exposing to the sun, the skin or the Tb increase too much. Another strategy that some poikilotherms adopt when a warm environment is not available or when the food is scarce, they look for a safe place and fall into lethargy).

So rather than the tag poikilotherms these animals are better defined by the label “ectothermic”, namely organisms that take the heat they need from the external environment.

At this point the homeotherms can be considered “endothermic” as they are able to generate the heat they need, even though they use the 80 percent of the energy from their food to get that.

The overlap between poikilotherms and ectotherms and that between homeotherms and endotherms is not complete, since for example some fish species are considered to be facultative endotherms. However, this subtle distinction goes far beyond the scope of this thesis.

Homeotherms are all the animals whose internal temperature varies in very restricted range, despite even notable thermal variations of the external environment or of their internal heat production. The homeothermy implies a fine equilibrium between heat production and loss. These animals are warm-blooded, and they can achieve warm-bloodedness and homeothermy because they can readily generate heat due to a high basal metabolic rate, which can be increased in response to cold. Indeed, they can be defined tachymetabolic and their sustained metabolic rate is 15–50 times higher than that of bradymetabolic animals (Hammond & Diamond, 1997).

The higher metabolic rate that was needed for homeothermy had same consequences: It required a more complex thermoregulation, mainly under the control of the autonomic nervous

system (ANS), and it also required a higher caloric intake (Cerri, 2017). Nevertheless homeothermy was the feature that allowed mammals to spread across practically the entire planet, occupying almost every ecological niche (Grigg et al., 2004).

Normal core Tb in mammals is around 37°C and controlled within a quite narrow range (33.2–38.2°C), although there are normal fluctuations that occur throughout the day (circadian rhythm), throughout a month (menstrual cycle), and throughout a life-time (aging).

Maintenance of mammalian core Tb within a narrow range is an essential homeostatic process to optimize cellular and tissue function. In fact, for example, beyond a Tb of 42°C, cytotoxicity occurs with protein denaturation and impaired DNA synthesis (Lepock, 2003), resulting in end-organ failure and neuronal impairment. Instead, if Tb drops below 27°C (severe hypothermia), the associated neuromuscular, cardiovascular, hematological, and respiratory changes can equally prove fatal (Mallet, 2002). Despite the need for tight regulation of core temperature, humans can survive in the most inhospitable places and can challenge their thermoregulatory capacity in the most extreme ways especially with regards to the cold environments (Tansey & Johnson, 2015).

Indeed, it is important to note that mammal's thermoregulation system is highly asymmetric, as a homeothermic animal's normal Tb is much closer to the deadly temperature of enzyme denaturation than to that of water crystallization (Romanovsky, 2007). Hence, high Tbs are much more dangerous than low ones.

Homeotherms have two possibilities for regulating Tb: the first is based on the variation of heat production and is called "chemical thermoregulation"; the second is based on controlling the amount of heat exchange between the body and the ambient temperature (Ta) and is called "physical thermoregulation".

1.1.1 CHEMICAL THERMOREGULATION

The constancy of the Tb is maintained if the heat loss and production are equivalent.

The heat production is a function of the energetic metabolism, whose efficacy degree is equal or minor than 25 percent (Klinke et al., 2010).

There is an environmental temperature range in which the heat generated from the basal metabolism is sufficient to maintain a physiological Tb: it is called “Thermoneutrality Zone”. Within this range the animal is suffering neither the cold nor the hot. As the temperature decreases or increases, two other characteristic points can be noted:

“The critical inferior temperature” is the value under which heat production starts to linearly increase.

“The critical superior temperature” is the temperature value above which there is an increase of heat production due to the increase of the respiratory and heart activity (Scotto, 2006).

In the human being the thermoneutrality zone is between 27,8 and 30 °C, but this range can vary according several factors, such as the wind speed or the thermal insulation coefficient etc. (Silverthorn et al., 2007).

An homeothermic organism reacts to decreasing Ta, below the thermoneutrality zone, increasing the owner heat production. Chemical thermoregulation presents an immediate response to rise Tb which is the shiver.

Shivering consists of a sequence of involuntary, rapid, and oscillating contractions of skeletal muscle. It stars with single contractions not coordinated and asynchronous of the muscle fibers and only in a second moment the coordinated activation of the single fibers starts inducing the shiver (controlled by the spinal cord). The reason why shivering is thermogenic is because the muscles contract, splitting adenosine triphosphate (ATP) in adenosine diphosphate (ADP), isometrically, namely without varying their amplitude and therefore without develop mechanic work, so that a greater amount of energy coming from ATP goes under heat form. The ATP hydrolysis also increases the muscular concentration of ADP, which stimulates the electrons’ transport system and the oxygen consumption, accelerating the substrates utilization, which, in turn, allows the ADP reconversion in ATP and the concomitant heat dissipation. This physiological mechanism is also defined as “shivering thermogenesis”. In adult human being, shivering, at its peak, can elicit heat production equivalent to five times the basal metabolic rate (Eyolfson et al., 2001).

The shiver is not the only methods that homeotherms can use to produce heat, another possibility, especially for chronic cold exposure, is the chemical thermogenesis, also called the

non-shivering thermogenesis. Two main mechanisms are involved in this other thermogenic method.

The brown adipose tissue (BAT) is an adipose reticular tissue whose function is to generate heat. Compared to the white adipose tissue, it contains several mitochondria whose cytochromes confer it the characteristic brown color. His anatomical distribution is strategic, and, in fact, it is found in proximity with the main blood vessels. In this way the heat generated can be rapidly transferred to the blood and distributed to all the organs. In rodents, the interscapular BAT is the largest depot, with smaller depots in the mediastinum, along the cervical and thoracic aorta, and around the kidney (Giordano et al., 2004). In human beings, BAT is less centralized than in rodents, there are significant depots in supraclavicular, neck, and paraspinal regions (Cypess et al., 2009; Lidell et al., 2013). The thermogenic capacity of the BAT depends on the uncoupling of oxidative phosphorylation, operated by the Uncoupling protein 1 (UCP1) on the internal mitochondrial membrane. The norepinephrine (NE) released by the sympathetic fibers on the brown adipocytes, in consequence of the hypothalamic signal, interacts with β3-adrenergic receptors. This binding causes an intracellular cascade, as shown in figure 1.This cascade starts with the increase of the cyclic AMP (cAMP) which activates the cAMP-dependent protein kinase (PKA), which, in turn, activates different targets, including: i) in the cytoplasm, the Hormone-sensitive lipase, that increases the lipase (cleavage of the triglycerides present in the lipid drops into fatty acids and glycerol); ii) in the nucleus, the cAMP response element-binding protein (CREB) which stimulates the transcription of the UCP1 gene. At this point the fatty acids released from the lipid drops enter the mitochondria and if one part undergoes β-oxidation, to be oxidized and supply electrons to the respiratory chain, another part activates the UCP1. The UCP1 is a channel protein that, once activated, creates a passage of protons. Consequently, the protons, from the intramembrane space, fall into the mitochondrial matrix through the UCP1 and not through ATP synthase. This mechanism is known as uncoupling of oxidative phosphorylation. In this way, the energy of the proton gradient is dispersed as heat, rather than be utilized to form ATP (Scotto, 2006), while the substrate utilization for the production of ATP from ADP, and the related heat-production, is maintained ongoing due to the low ATP levels.

The second system, that interacts in the non-shivering thermogenesis, involves the thyroid hormone.

The thyroid hormone (TH) could be considered as the most important humoral regulator of energy homeostasis, metabolism and thermogenesis in both humans and rodents. It is regulated by the brain via the hypothalamic-pituitary-thyroid (HPT) axis, in which the activation of thyrotropin-releasing hormone (TRH) neurons within the hypothalamus ultimately leads to increased thyroid hormones (Thyroxine-T4, and Triiodothyronine-T3) at peripheral tissues (Fekete & Lechan, 2014). There are several researches showing a central role played by thyroid hormones in non-shivering thermogenesis. For example, it is well known that the cold exposure increases the plasmatic levels of TH, the latter could lead to an increase in oxygen consumption and consequently to heat production. But this happens within a latency period lasting from several hours to days, even if this action then continues for many days.

The thermogenic effects of thyroid hormones are supposed to be particularly related to the UCP1 and BAT activity. Indeed, it seems that both the sympathetic nervous system (SNS) and TH are required for maintenance of core Tb and non-shivering thermogenesis (Silva & Rabelo, 1997). In fact, if hypothyroid rodents are exposed to cold environment, they develop marked hypothermia, but T4 treatment is capable to reverse this through the induction of BAT activity (Carvalho et al., 1991). As already discussed, the expression of UCP1 is necessary for BAT activity, and it has long been known that UCP1 is synergistically regulated by both norepinephrine and T3. In this regard, while T3 and NE each increase UCP1 expression by 2-fold separately, there is a 20-fold induction of UCP1 when both agents are combined (Bianco et al., 1988). It is important to note that while thyroid hormone receptor (TR) isoform β regulates UCP1 expression in BAT, TR isoform α mediates sensitivity to adrenergic simulation (Ribeiro et al., 2001). This shows the specificity of TR isoforms in metabolic regulation, but especially that both the TR isoforms α and β are required for a physiological thermogenic response (Mullur et al., 2014).

What has also been confirmed in different experimental models of hyperthyroidism and hypothyroidism, both in animal models and humans, is that THs can act directly on important metabolically active organs and thus alter obligatory thermogenesis. But this aspect of thermogenesis may also be regulated through the central nervous system (CNS) having an impact on facultative thermogenesis as well (fig. 2) (Herwig et al., 2008; López et al., 2010).

In particular, among the past years, novel complex interactions within the hypothalamus concerning THs and thermogenesis have been revealed mainly in rodents. Most importantly,

the Paraventricular Hypothalamic Nucleus (PVH) contains the TRH neurons, which regulate the HPT axis and sensitively respond to changes in TH status by reducing TRH release into the hypophyseal portal system, which is a system of blood vessels in the microcirculation at the base of the brain, linking the hypothalamus with the anterior pituitary gland (Iwen et al., 2018).

The PVH plays a central role in thermoregulation, receiving neurons input from other central brain regions such as the Preoptic Area (POA) (Larsen et al., 1994). The latter brain area, in fact, responds to peripheral temperature sensors, which reveal changes in environmental temperature and central Tb. Thus, direct heating or cooling of the POA results in a modulation of thermogenesis by changing efferent SNS-signaling (Morrison, 2016). Cooling of the POA has direct effects on the regulation of the HPT. In rats during wakefulness, it induces an increased release of TSH (Martelli et al., 2014). In contrast, i.c.v. injections of T3, resulting in an increased T3 concentration in the POA, causes a dose-dependent decrease in TRH and TSH, remarkably supplemented by a drop in core Tb (Moffett et al., 2013). Finally, the activation as well as the inhibition of the POA γ-aminobutyric acid (GABA)ergic neurons, which project to the dorsomedial (DMH) and the ventromedial (VMH) hypothalamus, powerfully decreased or increased, respectively, core Tb by modifying sympathetic tone to BAT, liver and muscle (Tan et al., 2016; Z. D. Zhao et al., 2017)

1.1.2 PHYSICAL THERMOREGULATION

The other possibility that homeotherms have to regulate Tb is the physical thermoregulation. It concerns the set of those mechanisms that regulate the heat exchanges with the environment, which are essentially based on some well-known physical phenomena, that are:

- Radiation
- Convection
- Evaporation
- Conduction

Radiation is the process by which the surfaces of all the objects constantly emit heat through the electromagnetic energy in the form of photons. Also, the animals emit photons that are absorbed by the environment, but they also absorb photons from it. The photons emitted from

these surfaces rise with the increment of the temperature of the radiant structure. Thus, if the body surface is warmer than the environment, net heat is lost from the body, the rate being directly depend on the temperature difference between the surfaces.

Convection is the process whereby a fluid that comes in contact with a heat source tends to rise and its place is taken by the colder fluid coming from the depth. This happens also for the air; thus, these movements cause the expansion of the rising air, which rarefying cools down, at the same time the falling air heats up. This is what happens also at the level of the body surface. When the Tb is higher than the environmental one, the heat coming from the body heats the air next to the body for conduction, then it moves away. The latter is replaced by cooler air, which in turn follows the same pattern. Convection is always occurring but can be greatly facilitated by external forces such as wind or fans. A human in thermal equilibrium loses by convection around the 42% of the heat produced.

Conduction is the loss or gain of heat by transfer of thermal energy during collisions between adjacent molecules. When a body is in physical contact with another one, the heat passes from the warmer to the cooler body.

Evaporation of water from the skin and membrane lining the respiratory tract is the other major process for loss of body heat. Indeed, in the first three processes, the exchange can occur in both directions, whilst the last one can only appear unidirectionally from the body to the environment, since heat is transferred to the fluid, which evaporates and leaves the body in gaseous form. This mechanism of heat loss exploits the principle according to which to get the water from the liquid to gaseous state it is necessary to provide heat. The latent heat of evaporation is thermal energy necessary to evaporate the water when the temperature does not vary. In humans, the heat loss via evaporation, in basal conditions, is the 20 percent of the total and it is almost completely burnt by the respiratory apparatus, only a small part (one third) depends on the skin. By considering that the heat loss due to other mechanisms (radiation, convection, conduction) is always proportional to Tb – Ta, when the environmental temperature increases and becomes equal or exceeds the Tb, evaporation remains almost the only available mechanism to lose heat (as can be seen from Fig. 3). Since the heat loss occurs on the body surface, it remains to understand how the heat produced in the core is transported in the body surface. A predominant role is played by the blood circulation, which in addition to bringing

the heat from the depths of the organism to the surface, affect its distribution inside the body. This occurs mainly through the mechanisms of vasoconstriction and vasodilatation.

Usually the blood transfers heat from the body core to the environment, which generally is at a lower temperature (but it can also transport the heat in the opposite way according to the thermal gradient). The blood flow through the cutaneous vessel varies with values close to zero when heat conservation is necessary, up to almost one third of the cardiac output when the heat has to be released to the environment. The local control can influence to the same extent the cutaneous blood flow, probably due to vasodilating substances produced by the vascular endothelium, but the primary control factor is represented by the nervous regulation. In fact, the major part of the arterioles is under the control of the SNS (Silverthorn et al., 2007). These vessels are largely controlled by vasoconstrictor sympathetic nerves, whose firing rate is reflexively increased in response to cold and decreased in response to heat. There is also a population of sympathetic neurons to the skin whose neurotransmitters cause active vasodilatation (Vander et al., 2001). Hence, the thermoregulatory control via SNS can modulate the cardiovascular system in two main ways: by modifying the heart rate, and by adjusting the diameter of the vessels. It follows that the exposure to low environmental temperatures induces vasoconstriction in cutaneous blood vessels to preserve heat; meanwhile, there is also an increase in heart rate, to amplify heat transport from thermogenic organs to the whole body. In hot environments, instead, the body has to dissipate heat, which is achieved by increasing cutaneous blood flow and by shutting down thermogenic effectors. Moreover, in these circumstances, a decrease in cardiac frequency has been detected, which is caused by a lower oxygen demand by thermogenic organs.

1.1.3 MODELS OF THERMOREGULATION

There are different theoretical models of thermoregulation. Already from this premise is possibly to understand that, although much has been done, there are still some uncertain notions in this field. In the various studies, the results may largely depend on the experimental conditions, and the techniques or, the animals utilized. Indeed, different animals can adopt different thermoregulatory strategies (e.g. the hibernators), or the diversity can also depend on the size of the animals. Nonetheless, it is important to underline that, in general, the thermoregulatory system in vertebrates is quite similar in the global organization, as all these animals are sensitive to both surface temperature and deep core temperature. Then, this

information arrives to the central neural controller, mainly represented by the hypothalamus, which in the end triggers behavioral and autonomic responses.

Most of the historic concepts of thermoregulation theorized a unified system with a single controller and a unique reference threshold, which is called the set point. The set point theory assumed that thermal information detected by the thermoreceptors in the surface and in the core of the body are integrated by a specific network into a mean Tb, then, another network compares the average Tb with the value of the set point and after that, possibly, generates an error signal, which should induce the thermal effectors to work in a coordinated manner to diminish the difference between the mean temperature and the set point (Vendrik, 1959).

However, in the first versions of this theory there were several problems that were not addressed. Indeed, considering that thermoregulation requires a lot of energy, time and risks, as the costs increase an animal should shift its set point to reduce the costs and maximize the benefits (Angilletta, 2009). Thus, in general, rather than a constant and fixed set point we should expect an adjustable and variable one.

Under extreme circumstances animals can even drastically reduce their set point value, as it is the case of torpor. Both daily and seasonal torpor involves a reduction in the set-point temperature and the sensitivity of the set point (Sunagawa & Takahashi, 2016)

Another situation in which there seems to be an adjustment of the set point is fever. In fact, with fever the Tb is stably over the typical physiological value of each species. Nonetheless, during the feverish episodes the thermoregulatory mechanisms are still working, but the set point value appears to have been moved higher. This can be due to the action of some substances called pyrogens, which can be introduced from the outside, for example deriving from bacterial cells, or can be produced endogenously. The bacterial toxins can act as pyrogens both directly and through the mediated action of the macrophages, which release a cytokine such as interleukin 1 (IL-1). Other examples of endogenous pyrogens are interferon and tumor necrosis factor (TNF). The pyrogens are chaperoned across the blood-brain barrier to reach hypothalamic neurons. It was shown that in the POA, pyrogens can reduce the frequency of action potentials in warm-activated neurons (Boulant, 2006; Pierau et al., 1998), precluding these neurons from activating effectors for heat loss. As a consequence, metabolic heating continues until the hypothalamus reaches a higher set-point value (Angilletta et al., 2019).

In the list of the phenomenon that do not fit with the constant set point theory there is also dehydration. When dehydrated, endothermic animals increase the set point in order to reduce the water needed for evaporative cooling (Cain et al., 2006; Mitchell et al., 2002). Also in this case, the plasticity of the set point likely includes the POA, considering that in this area there are neurons sensitive to osmolarity as well as to temperature (Mckinley et al., 2015). Indeed, in one study, it was shown that a change of osmolarity within the hypothalamus can specifically affect the activity of thermosensitive neurons, sparing the other hypothalamic neurons. McKinley and colleagues hypothesized that the thermosensitive neurons of the POA are inhibited by the neurons of the median preoptic nucleus (MnPO) (McKinley et al., 2018).

Another aspect that can alter the set point is hypoxia. The performance at a high Tb are limited by the oxygen supply, because warmer animals require more oxygen to sustain aerobic metabolism (Gangloff & Telemeco, 2018; Pörtner, 2010). For this reason, endotherms decreased the Tb when exposed to severe hypoxia. When the rats are faced with hypoxia, they decreased their temperature around 35.7 °C within a day, but when they are challenged with the combination of hypoxia and cold, the rats cool down to 34.1 °C in the same time window. Interestingly, they keep a Tb of 37.3 °C when just cold exposed. This means that if the oxygen supply was sufficient, the rats would support the energetic cost of thermogenesis in the cold (Cadena & Tattersall, 2014).

Thus, in line with all this information a new version of the constant set point theory was proposed. Hammel (1968) was one of the early proponents of the adjustability of the set point, even though many other scientists also played important roles in developing this model (Boulant, 2006; Cabanac, 2006). In this version the set-point temperature was converted from a parameter to a variable, which depends on physiological or environmental factors (Fig. 4).

However, also this new version of the set point theory received several criticisms. The main criticism is that there have been difficulties with identifying the set point signal, the integrating network, and the coordinator (Berner & Heller, 1998).

But, about forty years ago, Jürgen Werner had already proposed a different model of thermoregulation, which did not need a set point and was based on the balance of controlling and controlled processes (Werner, 1980). In the following years, scientific evidences started to show that thermoeffectors operate largely independently from each other (Roberts, 1988; Satinoff, 1978). Studies, from Kazuyuki Kanosue's laboratory, have demonstrated that the left

and right pathways of shivering in rats are interconnected in the POA, whereas the pathways for thermoregulatory skin vasomotion are not. The authors concluded that the POA is just an assembly of different neuronal groups working independently, each sending efferent signals to its effector, without neural connections to each other (Kanosue et al., 1998). Another line of research has shown that some effectors can be predominantly driven by surface temperature, others seem to be mainly guided by core Tb (Roberts, 1988). Finally, another study has shown that different thermoeffectors sometimes defend significantly different levels of Tb, (Romanovsky, 2004). All this information and experimental data were difficult to fit into the unified control system, in which all effectors were driven by a unique signal.

Therefore, many researchers began to realize that a complex system does not need a coordinator or a global rule to function. (Partridge & Partridge, 1993). As a matter of fact, for other several physiological parameters, for example blood pressure or plasma pH, there is a general consensus that systems work in a decentralized way, as a group of relatively independent controllers, acting in a shared environment (Partridge, 1982).

The last and current model of thermoregulation, proposed mainly by Romanovsky, leaves the old concept of the feedback loops in place, but removing the single controller and the set point, consequently they turn out to be independent thermoeffector loops. The loops are specific thermoeffector responses, which are driven by Tb detected by thermoreceptors. Whereas, the effectors activity, as result, changes the Tb by sending, in this way, feedback to the receptors (Romanovsky, 2007). Being anatomically distinct, thermoeffector loops operate generally independently, and the coordination of the effectors is achieved mostly due to their dependence on the common regulated variable: the Tb. As the effector activity and other factors (including Ta) changed the Tb, various thermoeffectors turn on and off in a coordinated manner. Hence, the thermoregulation does not need a coordinating network (see figure 5). In conclusion, theoretic studies on feedback control systems have shown that multiple parallel controllers can offer a better and more precise control of a variable than a unified controller (L. Partridge & Partridge, 1993).

1.1.4 THE NEURAL CONTROL OF THERMOREGULATION

In this paragraph, the neural thermoregulatory loops and networks will be described in better details. Below, I will frequently refer to experimental data found in rats, principally because the

thermoregulation system has been explored much more broadly in laboratory rodents than in humans. This is also true because of the neurophysiological techniques utilized in this field of research (Romanovsky, 2018).

The thermoregulation in mammals is under the control of the ANS. The ANS regulates the thermogenesis and the heat loss to maintain a Tb appropriate for the behavior that the animal is currently engaged in. To date, although, there are still some aspects not completely explained, most of the details of the neural pathway of thermoregulation have been described (Cerri, 2017). Illustrating the circuit is useful to differentiate the afferent pathway (the detection of the temperature) and the efferent pathway (the responses to the organs).

1.1.4.1 THE AFFERENT PATHWAY

The afferent pathway follows the pattern known as spino-reticulo-hypothalamic tract. There are two classes of thermal afferent pathways, those activated by cold stimuli and those activated by warming. The Ta is detected mainly by the skin, but thermoreceptors have been found also in the oral cavity and in the upper part of the respiratory airways (Cliff & Green, 1996). Thermoreceptors are transient receptor potential (TRP) channels and there are specific TRP channels for different ranges of temperature (H. Wang & Siemens, 2015). TRPM8 is the most important for detecting the cold stimuli. In fact, its agonists applied to the skin can evoke cold exposure responses (Tajino et al., 2007). Furthermore, TRPM8 knockout mice show deficiencies in cold sensation as well as a significant reduction in injury-induced responsiveness to cooling (Colburn et al., 2007; Dhaka et al., 2007). Another TRP channel which is relevant for the feeling of cold is TRPA1 (Jun Chen, 2015). Instead, the TRPV1 channel is the main candidate for detecting the warm stimuli (Szolcsányi, 2015), but the feeling of warmth is also sensed by the TRPV3 channel (H. Wang & Siemens, 2015).

The cell body of the primary somatosensory neurons containing these TRP channels are located in the dorsal root ganglia. They collect temperature information from broad regions of the skin and send their input to the secondary neurons. The latter are located in the dorsal horn (primarily lamina I) of the spinal cord (Takashima et al., 2007). The response of the secondary neurons to skin cooling is mainly mediated by glutamatergic signals from the TRPM8 channel containing primary neurons, as demonstrated by the fact that both the ablation of the TRPM8 neurons and the blockade of the glutamate receptors in the dorsal horn prevent the activation of cooling

responsive neurons in the dorsal horn. Whereas, the somatosensory TRPV1-containing neurons contribute to the warming activation of dorsal horn neurons, also in this case through a glutamatergic input (Ran et al., 2016).

From the dorsal horn, the secondary neurons project to the lateral parabrachial nucleus (LPB), where the tertiary neurons of the afferent pathway are located. In the LPB there are neurons activated by either warm or cold stimuli (Nakamura & Morrison, 2010). The external lateral subdivision of the LPB (LPBel) contains neurons that are activated by cooling of the skin. The activation of these neurons is required for the induction of responses to cold, such as shivering and BAT thermogenesis (Nakamura & Morrison, 2008a). Whereas, in the dorsal portion of the LPB (LPBd) there are the neurons activated by heat exposure, and a glutamatergic activation of these neurons is essential for the induction of the autonomic responses to heat, such as the inhibition of vasoconstriction and thermogenesis (Nakamura & Morrison, 2010).

The LPB neurons can be considered an important relay in processing the thermal information. Indeed, they send axonal branches to the ventrolateral thalamus, which will then relay the information to the cerebral cortex. This spinothalamic pathway provides the structural substrate for the thermal sensation (Craig, 2002). But this is not necessary for the autonomic responses to the detected thermal information.

In fact, the anatomical substrate for the autonomic control of Tb involves the other axonal branches that the LPB neurons send to the hypothalamus. Indeed, both the LPBel and the LPBd neurons project to the hypothalamus, in particular to the median preoptic area (MnPO) (Nakamura & Morrison, 2010) (see figure 6).

The preoptic area (POA) neurons integrate the thermal afferent information to control the thermoeffectors responses. There are two areas of primary importance at preoptic level: one is more rostral, ventral and medial, which is the Median preoptic nucleus (MnPO) and the other is more caudal, dorsal and lateral that is called the Medial preoptic area (MPA) (Tanaka et al., 2009). In the former, directly thermosensitive neurons have been found. Variations of temperature in this area can evoke a broad set of thermoregulatory responses including both cold and heat defense responses (Carlisle & Laudenslager, 1979; Hayward & Baker, 1968; Mohammed et al., 2018; Satinoff, 1964). Mostly of the MnPO thermosensitive neurons are warm sensitive neurons (WSN), which rise their firing rate as a consequence of an increase in surrounding temperature. About thirty percent of the neurons in the POA are WSN, compared

to cold sensitive neurons that make up less the ten percent of the recorded neurons in the region (Hori et al., 1980; Kelso et al., 1982). Moreover, most of the WSNs are γ-aminobutyric acid (GABA)-ergic neurons. Considering the huge amount of WSNs in the area, it follows that, the main output of the POA is an inhibitory signal to thermogenesis and heat-saving processes (Christopher J. Madden & Morrison, 2019). The neural connections among the POA areas play a crucial role in thermoregulation. On one hand, the MnPo neurons, which receive the thermal information from the cold-activated LPBel neurons, prevent the GABAergic output of the MPA neurons (Morrison & Madden, 2014). On the other hand, the MnPO neurons, receiving the input from the warm-activated LPBd neurons, activate the GABAergic output of the MPA neurons (Nakamura & Morrison, 2010; Tan et al., 2016).

1.1.4.2 THE EFFERENT PATHWAY

The activity of most of the organs involved in thermoregulation is under the control of the ANS, and in particular of the sympathetic branch. A key area in controlling the thermoregulatory sympathetic outflow is the raphe pallidus (RPa), a region in the lower medulla where the sympathetic premotor neurons are located. (Mcallen et al., 1995; Nakamura et al., 2004). The raphe pallidus contains several neuronal populations, such as serotoninergic and GABAergic, but many of them are glutamatergic (Stornetta et al., 2005). Moreover, numerous organs involved in thermoregulation and energy expenditure, for example BAT, thyroid, heart, skeletal muscles etc. (Billig et al., 1999; Cano et al., 2003; Kalsbeek et al., 2000; Standish et al., 1995), have synaptic connections on RPa neurons, further underlining the crucial role of this brain area in the thermoeffector pathways.

There are three main categories of thermal efferent pathways from RPa, which regulate: i) vasomotion (cutaneous vasoconstrictor and vasodilatation); ii) thermogenesis (BAT and shivering); iii) evaporative heat loss (sweating and saliva secretion) (see figure 7).

1.1.4.2.1 Vasomotion

The sympathetic premotor neurons contained in the raphe pallidus area can induce cutaneous vasoconstriction (Blessing et al., 1999). Thus, the warm stimuli, activating the MnPO, in order to be effective has to inhibit the cutaneous vasoconstrictor neurons in the RPa via the activation of the GABAergic neurons in MPA, which directly inhibit the RPa (Nakamura et al., 2002). Conversely, the skin cooling activates the neurons in the MnPO, which, in this case, can directly

activate the cutaneous vasoconstrictor neurons in the RPa (Tanaka et al., 2011). Consequently, the RPa neurons induce cutaneous vasoconstriction through excitatory glutamatergic and serotoninergic projections to preganglionic neurons located in the intermediolateral column of the spinal cord (Ootsuka & Blessing, 2005). The preganglionic cells project to the sympathetic ganglia, which harbor the last neurons of the efferent pathway that directly control effector responses. Additionally, a minor role can be played in this pathway also by the rostral ventrolateral medulla (RVLM), considering that some RVLM neurons projecting to the spinal cord can be inhibited by warming of the POA and contribute to the mediation of the cutaneous vasoconstriction circuit (Ootsuka & Terui, 1997).

1.1.4.2.2 Thermogenesis

Similarly, to what happen for vasomotion, even in the case of the BAT activation the role played by the RPa is fundamental. However, for thermogenesis there is also the crucial mediation of the DMH, which contains thermogenesis promoting neurons as well as RPa. In the presence of warm stimuli there is an inhibitory output from the MPA and from the ventral portion of the lateral preoptic area (vLPO) to the thermogenesis-promoting neurons in the DMH and the RPa (Conceição et al., 2019; Nakamura & Morrison, 2010). On the contrary, during body cooling the afferent input to the MnPO stimulates the inhibitory MnPO neurons that prevent the activation of the inhibitory neuronal population in the MPA (Nakamura & Morrison, 2008b). Thus, the activation of the BAT thermogenesis promoting neurons in the DMH and the RPa occurs thanks to the removal of a tonic inhibition from the MPA, together with an activation of the glutamatergic receptors on the neurons of the DMH. The RPa sympathetic premotor neurons activation, via the glutamatergic input from the DMH, it is followed by the excitatory input from the RPa to the spinal cord, which in the end causes BAT activation. (Madden & Morrison, 2019). The activity of the descending pathway undergoes various modulatory effects at different levels. One of this is played by the orexinergic neurons in the perifornical lateral hypothalamus, that have been shown to project to the medullary raphe and have been reported to modulate BAT thermogenesis (Madden et al., 2012).

Although the thermogenic pathways for BAT activation and for shivering partially overlap, some differences have been reported in particular in their final portion. During warm conditions, the MPA and the vLPO provide inhibitory output to the DMH, preventing the activation of the thermogenesis promoting neurons in the DMH and RPa. Conversely, cooling

has been found to activate the shivering promoting neurons in the DMH, through the removal of the tonic inhibitory input from the POA (Nakamura & Morrison, 2011). In turn, the DMH neurons stimulate the somatic muscle premotor neurons in the RPa. Finally, the input from the latter activates the anterior gamma and alpha motoneurons of the ventral horn of the spinal cord (Tanaka et al., 2006). The activation of these neurons increases muscle tone before shivering and modulates the intensity of shivering (Schäfer & Schäfer, 1973).

1.1.4.2.3 Evaporative heat loss

Sweat is released by eccrine glands, which are distributed in huge amounts over the whole surface of the body. Thus, from the skin the evaporation of sweat permits to transfer the heat to the environment under water vapor. Sweating is mediated by the activation of sympathetic cholinergic fibers (Shibasaki et al., 2006). The POA seems to play an important role in the neural control of sweating circuit, in fact, sweating can be evoked by the local warming of the POA (Magoun et al., 1938). However, in this case the premotor neurons causing sweating are located in the RVMM or parafacial area. The entire pathway is still not completely defined, but the neuronal connection from the GABAergic warm sensitive neurons in the POA to the RVMM is likely to be indirect, and could pass through the lateral periaqueductal grey area (PAG) (Farrell et al., 2013).

Unlike humans and other mammals such as cats, rodents do not sweat, but they exploit the evaporative heat loss using the salivary secretion associated with grooming in order to spread the saliva over the skin surface. The submaxillary and sublingual glands mediate saliva secretion (Stricker & Hainsworth, 1970). The parasympathetic preganglionic neurons for saliva secretion are located in the superior salivary nucleus (Hübschle et al., 2001). It has been found that salivation is reduced by lesions of the lateral hypothalamus (Stricker & Hainsworth, 1970). Thus, even if the entire thermal salivation circuit is not yet completely understood, it is supposed that the POA stimulates the lateral hypothalamic neurons, which in turn activates the superior salivary nucleus (Saper & Loewy, 1980).

1.2 NATURAL TORPOR

As already discussed, poikilotherms, unlike the homeotherms, are not able to maintain a specific Tb despite of the environmental thermal variations. Whereas this is not a huge problem when the Ta is high, it becomes a problem when the Ta is quite low. In this case, it is impossible for

poikilotherms to keep an adequate metabolic activity, and, consequently, they adopt a behavioral strategy, which is called hibernation. It consists in seeking for a dan or a safe refuge and then to became inactive or torpid in order to survive for a rather long time period saving energy by reducing their body metabolism (Scotto, 2006).

A similar strategy is adopted also by homeotherms, in particular, by several mammals and birds. These animals can also be defined as heterothermic animals, because they can apparently switch between homeothermy (with the associated endothermy) and poikilothermy (with the associated ectothermy) by turning thermogenesis off and on (Romanovsky, 2018).

However, between the hibernation of the homeotherms and that of the poikilotherms there are huge differences. The main distinction is about the possibility that the homeotherm animals have to "voluntary" enter and exit from hibernation. Concerning the "voluntary" awakening from the hibernation, this is not possible for poikilotherms, because they are bradymetabolic animals and cannot produce the large amount of heat, which is needed to exit from the hibernation state. Other important differences are that, unlike to what happens to poikilotherms, the hibernation state of the homeotherms is not a passive state and their Tb does not follow the Ta slavishly. In addition, during hibernation intermittent periods of arousal usually occur (Scotto, 2006).

The torpid state in these heterothermic endotherms, which can occur during period of scarcity of resources, is characterized by a controlled reduction of Tb, metabolic rate (MR), and other physiological parameters. The Tb during torpor falls, from the normothermic values around 37 °C, to values between −3 to < 30 °C, and the metabolic rate is, on average, reduced to 5–30% of the basal metabolic rate (Barnes, 1989; Geiser & Ruf, 1995).

Although metabolic rate during torpid period can be only a fraction of that in normothermic animals, regulation of Tb during torpor is not abandoned. In fact, the temperature variations are retained within certain limits, considering the temperature gradient between the body and the environment (Geiser, 2004; Heldmaier et al., 2004).

Inside a wide range of environmental temperature values, the temperature of the torpid animal can reach a value very close to the Ta itself; but for extremely low Ta (below 0 °C), the core temperature remains in the proximity of 0 °C (Arnold et al., 1991; Barnes, 1989). For example, at environmental temperature above 0 °C arctic ground squirrels in the torpid phase of

hibernation will thermoconform, and metabolic rate does not significantly change until external temperature rises above 16 °C. But if the latter falls below 0 °C, the thermogenic metabolism will increase in order to defend the Tb around −0.4 °C (Buck & Barnes, 2000).

However, torpor does not only reduce energy expenditure and temperature, but also provides other benefits: it may help to save energy for long migration in some bird species (Carpenter & Hixon, 1988), it can also play a role in reproduction strategies, by allowing sperm storage in some bats and other mammals, and facilitates fat storage during pregnancy and delays parturition until more favorable periods. Torpor appears to increase the efficiency of energy and nutrient use during development, and can also be considered a water saving strategy; finally, it seems to be associated with a reduction in risk of extinction (Fritz Geiser & Brigham, 2012).

Hibernation and torpor occur in species representing at least 10 mammalian orders (Fritz Geiser, 2004) and 12 avian families (McKechnie & Lovegrove, 2002). Obligate hibernation is expressed even in at least one strepsirrhine primate, Cheirogaleus medius (Dausmann et al., 2004). Looking at the heterogeneous diffusion of the hibernating species in these animal orders, it can be hypothesized that this characteristic trait has been inherited by a common protomammal. Therefore, it is likely that the ability to undergo torpor was then lost in many mammals, but it was maintained in species that could take advantage of energy saving to cope with extreme cold environments and resources shortage. This means that it is plausible that the gene pool required for torpor is still present and conserved in all mammals, including humans, but the regulatory mechanisms are no longer functioning (Cerri, 2017).

There are three main states of spontaneous hypothermia in the homeotherms: hibernation, daily torpor, and estivation. These three conditions are joined by the same physiological basis, as proposed by Heldmaier (2004). If the physiological properties of hibernation, daily torpor and estivation are similar, their classification is simply represented by differences in time, duration, and the extent of physiological inhibition.

1.2.1 HIBERNATION

The word “hibernate” derives from the Latin hibernus, which means “of winter,” referring to the period of year in which hibernation usually occurs. Hibernation seems to be confined to mammals (with the exception of the poorwill, a Caprimulgid bird) (Staples, 2016). The

hibernation can be defined as a physiological state, lasting days or months, in which the metabolic rate is reversibly reduced to about 5% of the basal metabolic rate, but can be also less than 1% compering to the resting metabolic rate in normothermic animals exposed to low environmental temperature. Furthermore, even when the expensive cost of the periodic arousals is considered, the metabolic rate of the hibernator during the hibernation period is still less than 15% of that of the animal that remained normothermic during the course of the winter (Wang, 1978). The metabolic reduction is associated with a decrease also in Tb. Hibernating species usually reduce their Tb to below 10 °C, with a minimum of −3 °C (Fritz Geiser, 2004).

However, hibernators are not in torpid state during the entire hibernation season. In fact, the hibernation period is composed by bouts of torpor, with the controlled decrease of core temperature and metabolic rate, lasting for many days or weeks, and interrupted by arousals and brief normothermic resting periods, generally lasting less than one day (Geiser et al., 1988; Humphries et al., 2003). The arousal is a very rapid process, but it requires a huge amount of energy. It has been calculated that during the arousal phase the metabolic rate of the animal is about six time higher than that in basal condition of euthermia, but it can bring the animal temperature from 3 to 35 °C in less than 3 hours (Scotto, 2006). The role played by these arousals and euthermic periods remains still unknown (Heldmaier et al., 2004).

Hibernators are generally small, and most of them weigh between 10 g and 1 kg, with a median mass of 85 g (F. Geiser & Ruf, 1995). The entire mass range of hibernators, including black bears (Ursus americanus), is from about 5 g to 80 kg. Nonetheless, deep torpor with a deep drop of Tb of more than 10 °C is limited to species weighing less than 10 kg (Fritz Geiser, 2004).

The hibernators can be categorized in two main subclasses: the obligate and the facultative hibernators.

The obligate hibernators follow an endogenous circannual rhythm, which induces them to hibernate each year, usually during the cold season, from the late summer/autumn to late winter/spring, regardless of the environmental conditions. For example, it has been showed that golden malted ground squirrels, born in captivity and housed with constant light and Ta, continue to hibernate each year, in a period corresponding to when the winter would begin in the wild (Pengelley et al., 1976; Pengelley & Fisher, 1963). In addition, during the summer, obligate hibernators do not undergo hibernation, even if they are exposed to winter-like light and Ta. The endogenous circannual rhythm of the obligate hibernators can also be interfered

by the cycle of the food intake and body mass in animals maintained under constant laboratory conditions (Ward & Armitage, 1981). This cycle, indeed, reflects the increase in body mass, before the hibernation, of the wild hibernators, such as the artic ground squirrels, which enhance their body fat to about seven or eight fold (Sheriff et al., 2013), with also an increase in circulating leptin (Florant et al., 2004).

In facultative hibernators, instead, the expression and the various characteristics of hibernation, like duration, Tb reached, and metabolic rate etc., can diverge significantly in the different species, and, in particular, depend primarily on the environmental conditions. Thus, in the facultative hibernators, environmental conditions, such as: the Ta, the rainfall, the resources availability, strongly influence the heterothermy patterns. For example, the Syrian hamster does not seem to have any endogenous hibernation rhythm and can hibernate indifferently at any time of the year if it is exposed to short photoperiod and low Ta (Talaei et al., 2011).

1.2.2 DAILY TORPOR

The daily torpor is another state of spontaneous hypothermia shown by homeotherms. This form of torpor is not as deep as hibernation, in fact, the reduction of core temperature and metabolic rate are on average less severe, besides, compared to hibernation, the daily torpor lasts just for hours, less than 24 hours, rather than days or weeks, and it's usually interrupted by daily feeding and foraging.

In particular, during this pattern of metabolic flexibility the animals reduce their metabolic levels not below the 26% of the basal metabolic rate (Staples, 2016). Instead, the Tb in daily heterotherms, such as small carnivorous marsupials and mice, normally decreases to near 18 °C, even though in some hummingbirds, values lower than 10 °C have been observed. While generally bigger species such as tawny frogmouths or American badgers, the Tb is kept slightly below 30◦C (F. Geiser & Ruf, 1995; Harlow, 1981). This physiological strategy can allow animals to save energy during their period of inactivity, while still permit them foraging during their active period of the circadian cycle (Geiser, 2004). Thus, in general the total energy expenditure, depending on the species, the duration and depth of torpor and duration and intensity of activity, is typically decreased 50-90% on days when daily torpor is used, compared with days when this strategy is not employed (Ellison & Skinner, 1992; Holloway & Geiser, 1995).

Compered to hibernators, in which the seasonal rhythm seems to cause the beginning and the end of the hibernation period, in daily torpor the animals appear to follow more a circadian rhythmicity, rather than a seasonal pattern (Körtner & Geiser, 2000).

Indeed, many daily heterotherms do not show an increase in fat accumulation previous to the season in which torpor is most commonly employed, but they usually enter torpor with a low body mass (Heldmaier & Steinlechner, 1981; Körtner & Geiser, 2000). Moreover, the daily torpor bouts are prevented when the fat storage is mimicked by administration of the leptin (Geiser et al., 1998). When small daily heterotherms are food deprived for several days they can perish, while hibernators in the same condition may survive for months entering torpor. This means that, even during the common torpor season, the animals that use daily torpor are still basing their energy expenditure and uptake on a daily basis (Fritz Geiser, 2004).

Even if in some daily heterotherms the appearance of torpor requires a relatively long period of acclimation to short photoperiods and/or to low Ta, this apparently seasonal daily torpor occurs even when food availability is favorable, and in some species, it is employed regularly to balance energy resources. For example, some hummingbirds, use daily torpor at night to preserve fat stores for next day of migration (Carpenter & Hixon, 1988). Furthermore, the marsupial Mulgara (Dasycercus cristicauda) commonly uses daily torpor during pregnancy period to increase the fat storage in anticipation of the following energetically demanding period of lactation (Geiser & Masters, 1994).

Other differences between the hibernation and the daily torpor are concerning the body size of the animal. On average, daily heterotherms are quite smaller than hibernators, since most of them weigh between 5 and 50g, with a median weight of 19g, and a general range of more or less 2 to 9000g (Geiser & Ruf, 1995).

1.2.3 ESTIVATION

The word estivation derives from the Latin aestas which means summer. In fact, the definition estivation is referred to a kind of torpor in which, the main characteristic, that differentiates this period of spontaneous hypometabolism from hibernation and daily torpor, is that in this case the torpid phase occurs at a high environmental temperature (Wilz & Heldmaier, 2000).

The estivation is a torpid state which can be considered as an energy saving strategy in environmental conditions of dry, high temperature and food as well as water shortage.

Not only many invertebrates can adopt this strategy, but also many vertebrates; for example: fish, amphibians, reptiles, and small mammals. In mammals, estivation occurs in monotremes (for example, echidna, Tachyglossus aculeatus) marsupials (e.g. dunnarts, Sminthopsis) and placentals, mainly bats. Also a tropical primate is able to enter estivation (Dausmann et al., 2004, 2012).

Estivation, in some conditions, can be difficult to recognize based just on the Tb detection, because, obviously, the Tb of these animals cannot be lower than the environmental one. The high summer Ta will lead to a passive increase of Tb during the torpid phase, not too far from the physiological core temperature of the endothermic animal (Canale et al., 2012). In addition, it can also be complicated to discern between estivation and hibernation since some animals can enter estivation at the end of the summer, and prolong the period of metabolic suppression throughout autumn and winter (Geiser & Heldmaier, 1995).

In fact, during estivation the duration of the torpid period can vary a lot. Although it usually lasts around 9-10 months, it can go up to two years in some species. However, in general animals use estivation to survive to the long dry season incompatible with life.

The key elements during estivation are: the accumulation of sufficient water and food resources for the duration of the dormancy period, and at a behavioral level, the finding of a sheltered and hidden place, where animals in estivation can ensure the conservation of water in the body, minimize their exposure to atmospheric agents and hide from predators.

The energetic metabolism of the animals that undergo estivation is primarily entrusted to the aerobic oxidation of the lipids together with the protein catabolism with a small contribution of carbohydrates. The conservation of energy reserves to survive during the dormancy period is essential and the metabolic rate during this period drops by 10-30% compared to the animal's metabolic rate during the rest period (Storey & Storey, 1990). But one of the most important consequences of the reduced metabolism during estivation is the associated decrease in gas exchange, which lend to a reduction in evaporative water loss (Fritz Geiser, 2010), probably a key selective pressure during the evolution of the estivation strategy in the hot and dry environments. In fact, defense against water loss during dormancy is crucial; the water is lost

during breathing and across the body surface, which is why the animal goes into estivation with a high amount of water, which is used to keep the tissues hydrated.

However, it is likely that daily torpor, hibernation and estivation all rely on similar physiological patterns and underlying mechanisms of metabolic suppression and probably they also share a similar neuronal control (Ruf & Geiser, 2015).

1.2.4 NEURAL CONTROL OF TORPOR

Torpor is a complex energy saving strategy, that heterotherms utilize in harsh and stressful circumstances of resources scarcity and extreme environmental temperatures, that are otherwise incompatible with life. Adaptations of animals to life in such stressful environments require changes on several levels, not only physiological but also biochemical and behavioral. Thus, they not only have to decease their Tb and metabolic rate with all the biochemical consequences at the cellular and organs level, but it is also essential for them to prepare their hypometabolic period, for example by storing resources or increase their body fats and even by looking for or building a safe den, to avoid predators and to be protected from weathering. This means that, in order to regulate all these responses and processes, a complex circuitry, able to integrate internal information (such as energy balance, core temperature, energy availability etc.) with external information deriving from the environment (for example, Ta, resources accessibility, possible risks etc.), and in the end modulate metabolism, temperature and behavioral activity should exist.

Although neural circuit that underlines the physiological control of the Tb is starting to become well understood and uncovered, to date, it is still not clear how some animals are capable to bypass these homeostatic mechanisms, in response to extreme environmental conditions to enter in the spontaneous hypothermic and hypometabolic state of torpor (Hrvatin et al., 2020). However, very recent data have begun to point out some neural pathways and brain areas potentially responsible for the torpor onset, highlighting in particular the role played by POA and DMH (Hrvatin et al., 2020; Takahashi et al., 2020).

1.2.4.1 THE AUTONOMIC NERVOUS SYSTEM

The system that has been proposed, more than thirty years ago, as the possible main regulator of the expression of torpor states is the ANS (Twente & Twente, 1978). In fact, the ANS plays

a critical role in the direct and indirect regulation of the metabolic rate. The parasympathetic and sympathetic branches modulate the autonomic output of the central nervous system to the rest of the body, which is the key mechanism in the control of homeostatic processes, like heart and respiratory rate, and oxygen consumption (Shibao et al., 2007). In particular, concerning torpor, it has been hypothesized that the onset of torpor is mediated by the parasympathetic branch, while the arousal from the hypometabolic state by the sympathetic branch (Harris & Milsom, 1995; Milsom et al., 1999). Instead, it is still not clear the role of autonomic nervous system during the period of hibernation. Two main opinions have been suggested. One hypothesis indicates that the parasympathetic branch, to prevent the arousal during the torpid period, actively inhibits the neuronal activity of the sympathetic branch (Twente & Twente, 1978). On the other hand, the alternative theory, which seems to have more consensus, supposes that the modulation of the parasympathetic nervous system vanish during the deep hibernation (Lyman, 1982).

1.2.4.2 HYPOTHALAMUS

One of the brain areas mostly involved in the control of the autonomic nervous system is the hypothalamus. It can regulate the thermoregulation, the energetic balance, neuroendocrine secretion, and the timing of the torpor presentation.

1.2.4.2.1 Suprachiasmatic nucleus

Concerning the circannual timing of hibernation, a central role seems to be played by the suprachiasmatic nucleus (SCN) of the hypothalamus. Indeed, it has been shown that the glucose utilization by the suprachiasmatic nucleus was higher, compared to most of the other brain areas during the torpor bouts, and always in this regard, the expression of the early gene c-fos, an indicator of neural activity, has been reported to increase in the suprachiasmatic nucleus during the arousal from the torpor (Kilduff et al., 1982; O'Hara et al., 1999). Another prove of the key role played by this area in the expression of hibernation is the fact that after an anatomical lesion in the suprachiasmatic nucleus, the circannual rhythm of hibernation and the associated circannual cycle of fats storage and reproductive behavior, resulted altered in ground squirrels (Ruby et al., 1998). Moreover, recent researches show that, thanks to the specific position of the suprachiasmatic nucleus, and to the numerous inputs that it receives from many different brain regions, the activity of the nucleus, his efferences and the torpor circuit, can be influenced

by not only the internal and external information, but also by hormones, such as melatonin. Indeed, an up-regulation of the melatonin receptor Mel1a has been demonstrated during torpor in the suprachiasmatic nucleus (McCarron et al., 2001).

1.2.4.2.2 Dorsomedial hypothalamic nucleus

The suprachiasmatic nucleus efferences project to the sub-paraventricular zone, which is involved in the regulation of the wake-sleep cycle and in thermoregulation, and to the dorsomedial hypothalamic nucleus (DMH). The latter has been receiving great attention in the last years regarding his predominant role in the induction of torpor. In fact, a recent study was carried out with the aim of revealing the neural pathways involved in the onset of torpor in mice (facultative heterotherms) food deprived and exposed to cold Ta (Hitrec et al, 2019).This study was made by combining the analyses of the neural activity marker c-fos and of a retrograde tracer injected into the raphe pallidus at torpor onset, in order to identify all the brain areas activated during the torpor onset and projecting to the raphe pallidus, the key area in the thermogenic outflow, that is supposed to be inhibited to suppress heat production and to allow the heat loss necessary for the entrance into torpor. The main result of this study was the identification of a neural network that is active during torpor onset in mice and possibly inhibits thermogenesis. In particular, two hypothalamic areas showed a particular c-fos expression and directly project to the raphe pallidus. The first one was the PVH, whose activation in rats induced an inhibition of the cold-induced activation of thermogenesis (C. J. Madden & Morrison, 2009). The other one was the DMH, that can be considered an important relay of the thermoregulatory information from superior brain centers to the raphe pallidus. In this regard, a study on mice has shown an inhibitor AcetylCholine (ACh) projection from the DMH to the raphe pallidus, able to inhibit the thermogenesis (Jeong et al., 2015). But even though, DMH neurons activated during torpor seems not to be AChergic, it has been proposed the DMH as the possible brain area responsible for the inhibition of the thermogenesis and the induction of torpor (Hitrec et al., 2019).

Another even more recent study underlined the role of the hypothalamus and especially of the DMH in the torpor onset. In this study of Takahaski et al (2020) the researchers showed that a hypothalamic neuronal population expressing pyroglutamylated RFamide peptide (QRFP), a neuropeptide, located in the anteroventral periventricular nucleus (AVPe) and in the medial preoptic area (MPA), is fundamental in mice for the entrance into torpor. Indeed, the authors

through the chemogenetic activation of this hypothalamic population of neurons were able to induce a long period (more than 24 hours) of hypometabolism. This condition was characterized by a reduction of the Tb concurrently with the temperature of the BAT of the animals, even if thermoregulatory mechanisms seem still to be active. In fact, when the Ta was reduced to 12 °C the mice adopted a more conservative posture, from the heat loss point of view, and exhibited also shivering and an increase in the rate of oxygen consumption (VO2). The other characteristics of the induced torpor were the huge heart rate reduction, the decrease of the respiratory rate, the very low amplitude of the electroencephalogram (EEG), and the low levels of blood glucose, probably due to the decrement of gluconeogenesis as a consequence of the low sympathetic activity. Finally, the animals spontaneously recovered from the induced torpor and did not show any tissue damage. Moreover, the authors indicated the DMH as the main effector brain area for the Q neurons, which are either glutamatergic or GABAergic. Considering that in the study the optogenetic stimulation of fibers of Q neurons located into DMH caused a transient increase of the tail temperature, the authors hypothesized that the GABAergic neurotransmission by Q neurons may inhibit the excitatory circuit between DMH neurons and the RPa. While, at the same time, the glutamatergic Q neurons might excite another subset of DMH neurons to inhibit heat production (Takahashi et al., 2020).

1.2.4.2.3 Preoptic area

Another recent article evidenced the crucial role played by the hypothalamus in the torpor network, in this case focusing on the POA. In this study, the researchers demonstrated that the fasting-induced torpor in mice, is modulated by neurons located in the medial and lateral POA. Thus, through the chemogenetic reactivation of these neurons, which were active during torpor onset, it was possible to obtain a new torpor bout, with a robust decrease in central Tb, locomotor activity and metabolism, even in mice that were not food deprived. In particular, in the anterior and ventral portions of the medial and lateral preoptic area (avMLPA) of the hypothalamus, the neurons expressing the vesicular glutamate transporter 2 (Vglut2) and Adenylate Cyclase Activating Polypeptide 1 (Adcyap1) were identified as the neuronal population regulating torpor. Indeed, the authors found changes in the electrophysiological activity of these neurons at torpor onset, and it seems that both these neurons are necessary for the drastic decrease of the Tb during the torpor bout. Moreover, the activity of these neurons seems to be specific for the expression of torpor, since their chemogenetic silencing had no significant effect on normal homeostatic Tb control, and on its circadian rhythmicity, inducing,

on the contrary, a profound disruption of fasting-induced torpor. In the end, the authors speculated about the possible mechanisms used by these neurons to integrate the huge amount of information, from the internal status and the environmental conditions. They stated that the glutamatergic Adcyap1 neurons in the avMLPA receive information about the decrease of the external temperature. In addition, concerning the internal energy resources, they found that these neurons and the Vglut2+ neurons express leptin receptors, suggesting that the circulating leptin levels could modulate the activity of these neurons. Consequently, in response to reduced energy reserves in fasting mice and during cold exposure, these neurons might be activated and induce torpor onset (Hrvatin et al., 2020).

1.2.4.3 NEUROMODULATORS

All these results indicate that the neural pathway underlining torpor is the main responsible for torpor induction. Furthermore, his systematic reactivation is sufficient to induce the primary behavioral and physiological elements of torpor. Nevertheless, these results cannot exclude a contribution of other chemical mediators, such as hormones and neuromodulators.

1.2.4.3.1 Adenosine

One of the neuromodulators that has received a lot of attention, regarding his potential role in torpor expression, is adenosine. Adenosine is a nucleoside produced by ATP metabolism. It plays a fundamental role in biochemical processes, such as in the transfer of energy (in the transition from ATP to ADP) and in the transduction of the signal, through the cAMP. Adenosine is involved in many physiological processes; it reduces heart rate, increases oxygen perfusion and vasodilatation, and modulates energy balance.

In the central nervous system, the adenosine acts as a neuromodulator. It binds four different receptors, all expressed in the brain, named A1 R, A2a R, A2b R, and A3 R (Fredholm et al., 2011). Adenosine affects the glutamatergic transmission, inhibiting the neurons expressing the different adenosine receptors. Centrally, it has been shown to be involved in wake-sleep regulation (Bjorness et al., 2009), but it seems to be also involved in torpor-related processes.

Indeed, some studies have demonstrated the important role played by adenosine in the induction and maintenance of torpor. The central administration of A1 R antagonist, in Syrian hamsters, artic ground squirrels and mice, can prevent the entrance in torpor, and if administered during

the torpid period, it may induce arousal from torpor (Iliff & Swoap, 2012; Jinka et al., 2011; Tamura et al., 2012). On the contrary, peripheral injection of adenosine causes a torpor bout, bradycardia and a decrease in metabolic rate (Iliff & Swoap, 2012). Moreover, the intracerebroventricular administration of adenosine-A1 receptor agonist, cyclohexyladenosine, in hamsters induces a decrease in Tb similar to that observed in this species during natural hibernation (Shiomi & Tamura, 2000)

In addition, a form of synthetic torpor (see chapter 1.3 for definition) was induced through the intracerebroventricular administration of the A1 R agonist, N6-cyclohexyladenosine (CHA), in rats, a non-hibernating animal. In rats, exposed to 15 °C Ta, the administration of CHA induced a torpor-like state characterized by a drastic reduction in Tb, due to an inhibition of thermogenesis, and by a concomitant decrease in heart rate and EEG amplitude (Tupone et al., 2013).

In another recent study, that tried to clarify the role played by adenosine in torpor regulation, a model of mouse, knockout for all the four types of adenosine receptors was generated. The authors wanted to test whether exogenous administration of adenosine could induce hypothermia, independently from the presence of adenosine receptors, for example through energy depletion. In fact, a gluco-privation in the brain causes hypothermia (Freinkel et al., 1972). The lack of adenosine-induced hypothermia in this model suggests that adenosine produces hypothermia via the adenosine receptors and not via cellular energy depletion. (Xiao et al., 2019). However, in this study, the knockout mice were still able to enter torpor, if food deprived for 24 h, although they showed just a mild hypothermia. It is not clear, however, if this was due to the mice phenotype or because the Ta was not lowered enough.

Despite the hypothermia induced in rats and mice by the administration of adenosine receptor agonists shared some physiological characteristics with natural torpor, other features are pretty different (Silvani et al., 2018). In particular, this state differs from natural torpor under the aspects of cardiovascular and metabolic regulation (Vicent et al., 2017).

1.2.4.3.2 Hibernation protein complex

Another neuromodulator involved in torpor and especially in hibernation is the hibernation protein complex (HPc). This complex of proteins is made by four proteins: HP20, 25 and 27 that create the HP20c complex, which by binding the fourth protein, HP55, in the blood,

constitutes the hibernation protein complex (Kondo & Kondo, 1992). In chipmunks, seasonal variations of the HPc seems to play an important permissive role in torpor.

The kinetic of HPc depends on the circannual rhythm. During the hibernation season, the levels of HPc in the blood seems to decrease, this happens due to the dissociation from the complex of the HP55, the largest protein of the complex, making the HP20c permeable for the central nervous system, with a consequent increase of HP20c in the brain. Even if the role of HP20 in the brain is unknown, it is thought that it can be involved in cellular adaptation to the hibernation period. In fact, the concentration of HP20c increases during the beginning of torpor. Moreover, hibernators that do not enter torpor during the hibernation season do not show any decrease in HPc in plasma and increase of HP20c in the cerebrospinal fluid. Additionally, the intracerebroventricular administration of anti-HPc antibodies promotes arousal (Noriaki Kondo et al., 2006).

Thus, it seems that the HPc, produced in the liver and secreted into blood, transports, following a circannual rhythm, hormonal signals to the brain, which in combination with other signals and information might activate the mechanisms for torpor induction (Drew et al., 2007; Noriaki Kondo et al., 2006).

1.2.5 NEURAL PLASTICITY

The term “neural plasticity” indicates the ability of the nervous system to modify and reorganize itself, in function, connections and structure, as a consequence of either experience or injury. Plasticity is important for neural networks to develop new functional properties, but also to maintain their stability. Moreover, plasticity can occur at different levels of the nervous system. For example, there is the nervous tissue plasticity, neuronal or glial plasticity, synaptic plasticity, and others. In general, plasticity is a crucial element of neural development and physiological functioning of the nervous system, but it is also a response to aging, pathological insults, or challenging environments (Von Bernhardi et al., 2017).

Animals living in environments that can result periodically challenging, for example according to a seasonal cycle, adopt various strategies to survive. Faced with food shortage and extreme Tas, animals can minimize the costs for foraging, for instance by storing food supplies, migrating in search of a more hospitable environment, or undergoing hibernation. Each of these strategies are related with a certain level of neural plasticity (Arendt & Bullmann, 2013).

In fact, it has been reported a huge neural reorganization during the hibernation period. Even though, large scale changes in the nervous system of mammals are not common after animal maturity (that may be a limitation for recovery from injury or illness), hibernation is an exception, showing rapid and reversible neural plasticity, with rates of reorganization of dendritic microstructures and synapses that are among the most dramatic found in nature in adult mammals (Von Der Ohe et al., 2007).

The preservation of cellular integrity and the maintenance of neuronal resting potential are the most energetically demanding processes for the mammalian brain (Du et al., 2008). Thus, the reduction of the metabolism in the whole body, with the consequent decrease of energy availability during hibernation is, inevitably, associated with a drastic reduction of the neuronal activity (Chatfield & Lyman, 1954; Massopust et al., 1965). Indeed, the EEG recording of hibernators during the torpid phases seems to detect almost no brain activity (Krilowicz et al., 1988). Considering that the neuronal activity is an indicator of neuronal connections and their utilization and bearing in mind the main functional principle of the nervous system "use it or lose it", the reduction of neuronal activity is supposed to negatively impact the conservation of neuronal connections (Kavanau, 1997). This is exactly what several researchers have found, a huge and generalized decrease of neuronal connectivity during the hibernation period in numerous brain areas, as well as in various hibernating animals (Hut et al., 2002).

In particular, in hippocampal region a pattern of synaptic regression during the torpid phase followed by reinnervation during arousal has been demonstrated (Arendt et al., 2003; Von Der Ohe et al., 2006, 2007) In all studies, this brain area shows transformation of apical dendrites, which became shorter, less ramified, and present less dendritic spines during torpor compared to the normothermic period. Even if all these transformations reverse and the dendrites and synapses return to their physiological status just two hours after the arousal (Popov et al., 1992).

These reversible modifications imply a cyclical process of partial denervation and re-innervation of the neurons in the hippocampus during hibernation phases. However, also in other brain areas, such as the neocortex and thalamus, the same modifications, in dendritic ramifications, spine amount and synaptic ultrastructure has been found during torpor, with a return to their normal levels and values after arousal (Von Der Ohe et al., 2007; Zhao et al., 2006). This can suggest that these adaptations are a global phenomenon.

The neuronal plasticity observed during hibernation is characterized by cyclic modifications of synaptic vesicle concentration and pre and post-synaptic marker proteins, which detaches from the cytoskeleton, producing a pool of proteins that may be rapidly mobilized to restore the dendritic spine and synapses with the occurrence of arousal and the regained normothermia (Arendt et al., 2003; Strijkstra et al., 2003).

It reasonable to hypothesize that a consequence of the synaptic retraction during hibernation may be the alteration of memory and learning processes. This thought can also be supported by other observations. For example, considering that learning can require the production of new neurons (Gould et al., 1999; Sultan et al., 2010), the analysis of neurogenesis during hibernation in Syrian hamsters indicated a significant decline of neuronal proliferation in the subventricular zone (SVZ) and in the dentate gyrus (DG) during the torpid state (León-Espinosa et al., 2016).

Moreover, other data show that long term potentiation (LTP), a form of neuroplasticity that strengthened synaptic signaling, and that is crucial for the creation of new memories and learning, is impaired at Tas below 15 °C in brain slices of hippocampus in both non-hibernators and hibernating animals (see figure 8) (Hamilton et al., 2017). Even if the brain slices of the latter, when the temperature is 22 °C, show a better ability to develop LTP compared non-hibernators (Spangenberger et al., 1995). Howsoever, these results derived from in vitro studies, where the tetanizing stimulus (multiple single shocks) can easier induce a weak depolarization and allow LTP generation even at low temperature (Krelstein et al., 1990). But, in vivo, the hippocampal conditions during hibernation are supposed to be even less favorable for the LTP generation, because the LTP expression requires not only the glutamate binding to N-methyl-D-aspartate (NMDA) receptors (Nicoll & Malenka, 1999), but the synchronized firing of the neurons in the hippocampus is also necessary (Axmacher et al., 2006). Instead, during the torpor bout EEG synchronization (theta and gamma waves) is absent, since EEG activity is drastically decreased at low brain temperature (Chatfield & Lyman, 1954).

Therefore, to date, a great amount of data has been collected about the effects of hibernation and hypothermia on learning and memory. Many researchers have tested these effects in different species using a broad variety of paradigms. Unfortunately, the results of the studies seem to be rather inconsistent. Thus, while some studies detect an impairment of memory after the hibernation period, others give opposite results. In general, it appears that the effect of hypothermia is paradigm-dependent, with tasks involving the amygdala, like active and passive

avoidance, that are less vulnerable than hippocampus-dependent spatial learning tasks (Arendt & Bullmann, 2013).

In particular, two convincing studies showed contradictory effects of hibernation on memory. The first one, performed on European ground squirrels, demonstrated, after hibernation, impairments in spatial and operative memory tasks, even if social memory appeared to be conserved (Millesi et al., 2001). While, a recent study on Syrian hamsters showed no impairments in a spatial memory tasks after hibernation compared with animals maintained at a warm Ta (Bullmann et al., 2016). These contradictory results can be explained by species-specific differences. Squirrels, for their hibernation period, rely primarily on their body fat reserves, and, usually, enter hibernation in groups in shared dens. On the other hand, hamsters before undergoing torpor, store food in their solitary dens. Thus, from an evolutionary point of view, may be useful for hamsters to preserve spatial memory, while for the squirrels social memory is apparently more important (Bullmann et al., 2016). Additionally, also the time windows in which the measurements were made can explain the inconsistency of the results, amnesia due to hypothermia might only be observed for those memories that have long consolidation times (Arendt & Bullmann, 2013).

1.2.5.1 TAU PROTEIN

Several studies that explored the correlations between the neural plasticity, memory, and torpor, evaluate also the role played in these associated processes by Tau protein. For example, Bullmann and colleagues (2016) revealed that the distribution of the dendritic spine regression was associated with Tau phosphorylation, which was more evident in the dendrites that presented more regression. Thus, the authors speculated that the phosphorylation of Tau and the associated synaptic regression may involve mainly instable and dynamic dendritic spines, sparing the stable spines (Bullmann et al., 2016). In another study, the Tau isoform with three microtubule-binding domains (tau 3R) that is considered a marker of new developing neurons, was found to be associated with the reduction of neurogenesis in the brain of Syrian hamsters during hibernation, while during the arousal it was also found a recovery of Tau 3R expression (León-Espinosa et al., 2016).

Tau is a soluble microtubule-associated protein (MAP) with a low molecular weight. The regulation of Tau protein is determined by the MAPT gene (microtubule-associated protein

tau), on chromosome 17q21.31, with an alternative splicing mechanism by which six isoforms, expressed in the central nervous system, are derived. The six isoforms differ from each other by the presence of three (3R) or four (4R) repeated C-terminal sequences of 31-32 amino acids, coded by exons 9-12; and for the combination with the presence or absence of one or two insertions of 29 amino acids (0N, 1N, 2N), in the N-terminal part, coded by exons 2 and 3 (Arendt et al., 2016).

Based on the amino acid composition of Tau protein and on the functional interactions, 4 domains can be distinguished along the sequence of amino acids: An N-terminal domain, the negatively charged projection that moves away from the surface of the microtubules, to keep them spaced out, thanks to the electrostatic repulsion (Amos, 2004). A region rich in proline, involved in cellular communication. A microtubule binding region, which also regulates the degree of polymerization of the microtubules (Mukrasch et al., 2005). In the end, a C-terminal region that plays a role in regulating Tau's ability to induce the polymerization of microtubules and its interaction with the plasmatic membrane (Reynolds et al., 2008).

In the mature brain, Tau is mainly expressed in neurons and it is preferentially located in axons (Kempf et al., 1996), but it has also been found in the somatodendritic compartments (Tashiro et al., 1997) and in the nucleus associated with nucleoli (Cross et al., 2000; Violet et al., 2014). Based on the aforementioned locations, Tau protein performs various functions, and it is involved in different processes.

In axon, Tau by binding to tubulin promotes the polymerization of the latter, regulates the stability of the microtubules, and determines the spacing between them (Chen et al., 1992). It has also been observed that thanks to the dynamic link with tubulin, Tau is likewise involved in morphogenesis and differentiation, axonal growth, neuronal plasticity and axonal transport mediated by kinesin motor proteins (Dawson et al., 2010; Dixit et al., 2008).

Concerning the localization of Tau in synapses and dendrites, it has been found at both pre and post-synaptic level, where in its hyperphosphorylated form accumulates in Alzheimer's disease (Tai et al., 2012). At synaptic level, Tau has been shown to be directly or indirectly involved, through phosphorylation, in the modulation of the communication of ligand-dependent synaptic receptors, such as muscarinic acetylcholine receptor (mAChR) and NMDA (L. M. Ittner et al., 2010). It is always at the synaptic level, that Tau, phosphorylated by GSK3β, appears to modulate the phenomenon of long-term depression (LTD) (Regan et al., 2015).

Finally, as regards the presence of Tau protein at the nuclear level, it could be involved in nuclear organization and in the protection of DNA (Sjöberg et al., 2006).

1.2.5.2 TAU HYPERPHOSPHORYLATION

The functions of Tau protein in the mature brain are finely regulated by post-translational mechanisms. Among these, the phosphorylation process of a limited number of Serine and Threonine residues is a rapid mechanism for regulating the binding capacity of Tau to microtubules. In general, the phosphorylation induces a reduction of the binding affinity for microtubules, regulating in this way the normal physiological function of this protein in the assembly and stability of microtubules (Crespo-Biel et al., 2012).

A large number of protein kinases, such as GSK-3β and cdk5, and phosphatases, such as: PP1, PP2A, PP2B, PP2C, PP3 and PP5, are implicated in the regulation of the phosphorylation of the Tau protein; the former phosphorylating and the latter dephosphorylating (Arendt et al., 2016) Compared to kinases, phosphatases are more sensitive to temperature changes: hypothermia inhibits phosphatases exponentially, while the activity of kinases is inhibited only linearly (Y. Wang & Mandelkow, 2016).

However, if the degree of Tau protein phosphorylation becomes progressively higher it can reach a state defined of hyperphosphorylation (Crespo-Biel et al., 2012). This state, characterized by the loss of affinity of Tau protein for the microtubules, can induce the association of Tau in paired helical filaments (PHF), which take a β-sheet fold, and represents the structural subunit of neurofibrillary tangles (NFT) and other intracellular aggregates present in the so-called "Tauopathies", like the Alzheimer's disease (Michel Goedert & Spillantini, 2011). The term Tauopathies indicates a group of about twenty neurodegenerative diseases characterized by common key features, the deposit of NFT of phosphorylated Tau protein inside neurons and/or inside glial cells (Arendt et al., 2016).

Although Tau hyperphosphorylation seems to be the basic element of neurodegenerative diseases, the increase in Tau protein phosphorylation is not always harmful. In fact, it has been observed also in physiological conditions without inducing neuronal damages, for example in fetal development (Goedert & Jakes, 1990), hibernation (Stieler et al., 2011) and hypothermia induced by anesthesia (Planel et al., 2007). This may suggest that hyperphosphorylation alone

is not sufficient to determine NFT and neurodegeneration, but that other cofactors should be implicated (Wang & Mandelkow, 2016).

During the torpid phase of hibernation, Tau is highly hyperphosphorylated, how it has been observed in various heterothermic species. However, the presence of PHFs is well tolerated by the organism as, unlike what occurs in neurodegenerative diseases, it is not associated with NFT formation, and also because this hyperphosphorylation is completely reversible, in all the species and brain areas analyzed, with the return of the animal to euthermia (Arendt et al., 2003; Stieler et al., 2011). This Tau hyperphosphorylation during hibernation can be induced by different factors, such as hypothermia, hypometabolism, or hibernation-specific regulation of enzyme kinetics. Each of these factors may contribute to different degrees to Tau hyperphosphorylation (Arendt & Bullmann, 2013).

1.2.5.3 TAU PHOSPHORYLATION AND SYNAPTIC PLASTYCITY

The kinetic of Tau phosphorylation during the hypothermic phase of torpor and the subsequent dephosphorylation with the return to euthermia occur in parallel with the regression and the following synaptic reconnection of the neurons in the brain of hibernators, in particular, in the hippocampal mossy fiber terminals (Arendt et al., 2003). An explanation of this phenomenon may be given by the fact that the phosphorylation of Tau protein, caused by the alteration of enzyme activities of phosphatases and kinases typical of the torpid phase, induces the detachment of Tau from the microtubules, which in turn increases the instability of the microtubules, favoring their dynamic state. This would facilitate the structural changes and the neural plasticity of the mossy fibers during hibernation. This cascade of related processes suggests a link between protein phosphorylation and the synaptic plasticity that appears during hibernation (see Figure 9; Su et al., 2008).

The evolutionary and physiological meaning and function of this associated processes could be a neuroprotective effect. Indeed, it has been shown that the entry and exit from a hypothermic state is accompanied by a phase of hyperexcitability of the neuronal activity in both hibernators and not-hibernating animals. In hippocampal slices the peak of evoked electrical activity appears between 20 and 30 °C during both cooling and rewarming (Hooper et al., 1985). The sensitivity of neuronal activity to temperature variation seems to be mediated by the NMDA receptors (Mcnaughton et al., 1994). Thus, Tau in a hyperphosphorylated state, with a reduced

affinity for microtubules, could be displaced in the dendritic spines where it reduces the synaptic function, plausibly reducing or dislocating the NMDA receptors at the postsynaptic level. According to this hypothesis, Tau hyperphosphorylation could be used during hibernation as a neuroprotective mechanism that prevents neuronal hyperexcitability mediated by NMDA receptors, that would otherwise occur during the gradual cooling of the brain (Arendt & Bullmann, 2013).

In a comparable fashion, hyperphosphorylation of Tau in Alzheimer's disease could be interpreted as a compensatory attempt occurring in the first steps of the progression of the disease (Morris et al., 2011) to suppress excitatory and inhibitory imbalances and neuronal network dysrhythmias (Palop & Mucke, 2010; Roberson et al., 2011). Nonetheless, if this compensatory mechanism lasts too long, it may eventually turn into a pathological trigger, causing NFT and all the other aspects of neurodegeneration that appear in Alzheimer's disease and other Tauopathies (Arendt & Bullmann, 2013).

1.2.6 SLEEP

Sleep is a behavioral state characterized by reversibility, reduced responses to external stimuli, and perceptual isolation; it is associated with several physiological changes that depend on the species and on the sleep phases. In every species studied, sleep propensity is related to the circadian rest-activity cycle and, in humans, the majority of sleep time occurs during the nocturnal hours (Achermann et al., 2017). Sleep cyclically alternates with wakefulness every single day and is, by itself, a cyclical process characterized by the alternation of two phases: non-rapid eye movement (NREM) sleep (also called, synchronized or "slow wave" sleep) and REM sleep (also called, desynchronized or active sleep). In the overall night, in humans sleep duration is between 7 and 8 hours and the NREM accounts for 70-80% of total sleep (Carskadon & Dement, 2011). In different species sleep duration is largely variable, but, in the majority of terrestrial mammals, the proportion between NREM sleep and REM sleep remains quite similar (Siegel, 2010).

During NREM sleep, the EEG becomes typically synchronized, i.e. rich in slow-frequency and high-voltage waves, in contrast to the fast-frequency and low-voltage waves of waking EEG (Brown et al., 2012). In humans, the structure of NREM sleep is further subdivided into three stages (N1-N3, American Academy of Sleep Medicine classification, AASM) (Carskadon &

Dement, 2011), substantially based on the degree of the EEG synchronization. During sleep, the NREM sleep stages and REM sleep occur in a precise order: NREM sleep N1 represents a transition from wakefulness to sleep and represents the first step of EEG synchronization with a predominance of theta activity (4.0-7.0 Hz). Stage N2 is characterized by the appearance of two EEG markers, the "K-complex" (a high voltage negative wave, followed by a slow positive wave) and the "spindle" (a 12-14 Hz oscillation with an increasing and then a decreasing amplitude, lasting around 2 s). The deeper stage of NREM is the N3 one, during which the EEG is rich of high-amplitude activity in the slow delta range (0,5-2.0 Hz). This slow-wave activity (SWA) characterizes deep NREM sleep in all mammals and it is considered to be the result of a cellular phenomenon, called "slow-oscillation", during which cortical neurons oscillate between a hyperpolarized and silent "down-state" and a high-frequency (around 40 Hz) "up-state" (Steriade et al., 2001). Finally, during REM sleep the EEG returns to be desynchronized and is very similar to that observed in wakefulness.

During a normal NREM-REM sleep cycle, N3 is followed by a reverse progression to light NREM sleep stages, and then REM sleep occurs. REM sleep is followed by either an awakening or by light NREM sleep. In the latter case, the whole sequence to N3 and back to S1 and REM sleep usually starts again. In humans, the NREM-REM sleep cycle lasts about 90-100 min (Carskadon & Dement, 2011), but in different species the duration of the sleep cycle reduces apparently in proportion with the decrease in body size and the increase in metabolic activity, and becomes of around 12 minutes in the rat (Siegel, 2010).

NREM sleep, and REM sleep are usually recognized not only on the basis of the EEG rhythms, but also from the presence of specific somatomotor signs. In fact, muscle tone progressively decreases from quiet wakefulness to NREM sleep, and fully disappears during REM sleep, when muscle atonia occurs. Such atonia is interrupted by the phasic occurrence of brief twitches and jerks of limb and eye muscles (from which the term: rapid eye movement sleep). However, the physiological definition and understanding of sleep cannot disregard the assessment of the respiratory, cardiovascular, and metabolic parameters, under the control of the ANS (Parmeggiani, 2005; Zoccoli & Amici, 2020). In fact, NREM sleep is a state of minimal energy expenditure and motor activity, during which physiological regulation is set for the maintenance of body homeostasis. Cardiovascular, respiratory, and thermoregulatory variables are driven at a lower level compared to wakefulness and are kept stable by the ANS. On the contrary, during REM sleep not only the control of postural muscle is lost, but ANS activity is very unstable:

surges in heart rate and blood pressure occur, breathing becomes irregular, and, in particular, thermoregulation is suspended or depressed. This modality of physiological regulation has been defined as “poikilostatic” because it is apparently not aimed at the maintenance of body homeostasis (Parmeggiani, 2005). However, the lack of thermoregulatory response observed during REM sleep seems quite specific and does not depend on a generalized loss of the regulatory capacity of the homeostatic processes, since the hypothalamic regulation of osmolarity has been shown to be conserved (Luppi et al., 2010).

1.2.6.1 SLEEP HOMEOSTASIS

The term homeostasis was proposed about one century ago by Walter B. Cannon and refers to a peculiar steady state of living organisms, which is characterized by the keeping of physiological variables at a rather stable, although not rigid, level.

This term has been subsequently used by sleep researchers in order to describe the tendency of sleeping animals to maintain a sort of average daily amount of sleep by increasing its duration and/or intensity (the so-called sleep rebound) after prolonged wakefulness or to reduce its propensity after excessive sleep (Achermann et al., 2017). However, it is still not clear which is the physiological variable, if any, that is “homeostatically” kept at a steady level by sleep.

The amount of time spent in NREM sleep, which is gained during the sleep rebound is usually lower than the loss occurred during previous sleep deprivation. However, the EEG spectral power in the delta band also increases in different species during the NREM sleep rebound as a function of both the duration and the intensity of prior wakefulness, and these changes roughly parallel an increase in the arousal threshold. On these bases, it is widely accepted that the recovery of NREM sleep substantially occurs by increasing NREM sleep intensity, as indexed by increased SWA (Achermann et al., 2017). Such a homeostatic regulation of NREM sleep in terms of SWA apparently occurs at both a local and a global level. In fact, SWA during NREM sleep is usually higher in frontal than in parieto-occipital EEG derivations, and brain regions which result to be more active during wakefulness develop a larger increase in SWA during the subsequent NREM sleep compared to the less active (Huber et al., 2004).

In various species, differently from NREM sleep, the homeostatic response to REM sleep loss substantially occurs in terms of its amount (Amici et al. 2008). In the rat, following either total sleep or selective REM sleep deprivation a REM sleep rebound is observed during the recovery

period, which allows the animal to fully restore the previous REM sleep loss within four days of recovery (Amici et al., 2008). The recovery is mainly linked to an increase in the frequency of REM episodes rather than their duration (Cerri et al., 2005). In humans, however, the REM sleep rebound after total sleep deprivation seems to be less intense and to be postponed after the SWA rebound in NREM sleep (Achermann et al., 2017)

Interestingly, allometric scaling of the dynamics of REM sleep rebound with body mass in different species suggests that small animals, such as rats, have a lower tolerance to REM sleep loss than large animals such as humans (Amici et al., 2008).

1.2.6.2 SLEEP HOMEOSTASIS AND SYNAPTIC PLASTICITY

The mechanism underlying local and global NREM sleep homeostasis in terms of SWA has been proposed to be that of an increase in cortical synaptic strength during wakefulness which would increases neuronal synchrony during subsequent NREM sleep, leading to more frequent and large EEG slow waves (Tononi & Cirelli, 2003). Indeed, during NREM sleep, SWA may contribute to downscale the strength of cortical synapses and would be beneficial on neuronal efficacy and function, representing a fundamental positive property of sleep on cortical performance (Vyazovskiy et al., 2011). According to this theory, that has been called "synaptic homeostasis hypothesis" (SHY) (Tononi & Cirelli, 2003), one major function of SWA during NREM sleep would be to avoid overloads of synaptic connections at neuronal level, by reducing the density of connections and, therefore, improving their efficiency.

To date, several researches found evidence and confirmations to this theory. For example, in the rat, the expression of excitatory glutamatergic AMPA (α-amino-3-hydroxy-5-methyl-4-isoxazolepropionic acid) receptors at synaptic level resulted to be higher after wakefulness than after sleep (Vyazovskiy et al., 2008). Moreover, in vivo experiments showed that the field excitatory postsynaptic potentials (fEPSPs) are increased during wakefulness and decreased during sleep in cortex and hippocampus of both adult rodents and humans (Huber et al., 2013; Norimoto et al., 2018).

Nevertheless, other studies reported an increase rather than a decrease of the synaptic strength during sleep (Puentes-Mestril & Aton, 2017). Additionally, other experiments found an enhancement of the functional connectivity within the hippocampal cortex neurons, during the NREM sleep following learning (Ognjanovski et al., 2014).

However, the synaptic homeostasis hypothesis does not exclude the possibility of synaptic downregulation in wake or the potentiation of some synapses during sleep, but it rather assumes that the overall balance in total synaptic strength is maintained across a 24-h time scale, with a net increase in synaptic strength in wakefulness and a net decrease across most brain circuits during the sleep (Tononi & Cirelli, 2019).

Indeed, in a recent study using a serial block-face scanning electron microscopy, around 7,000 synapses in the cortex of mice were reconstructed and it was found that the axon-spine interface decreases on average by 18% after 6–8 hours of sleep compared to 6–8 hours of wake. In particular, sleep related synaptic downscaling was found in small and medium size synapses, which represents about 80% of all synapses, although not in the largest synapses (De Vivo et al., 2017).

Thus, it seems that sleep dependent renormalization spare or could even strengthen some synapses or neurons according to certain still unknown principles, that could be the size of the neurons, but the synapses spared might also be those that have been more active during wakefulness or those that result more active during NREM sleep. Additionally, at synaptic level, various molecular compounds could be involved in guiding the downregulation processes, such as Homer1a, Arc, GSK-3ß and other proteins that can likely control the endocytosis of glutamatergic receptors (Tononi & Cirelli, 2019).

A role in synaptic plasticity during NREM sleep may also be played by the phosphorylation of Tau protein.

Indeed, one recent study showed an interesting association between Tau phosphorylation and the wake-sleep cycle. In the cortex of mice, researchers described a negative correlation between the degree of phosphorylation of Tau protein and Tb rhythmicity (Guisle et al., 2020). During wakefulness, when the core temperature is higher, the levels of Tau phosphorylated are low, while during the resting phase, when the central Tb slightly decreases, Tau results to be highly phosphorylated.

Indeed, heat exposure prevented the daily changes in Tau phosphorylation both in the cerebral cortex of mice exposed to an Ta of 34 °C, and also in *in vitro* experiments, when human neuroblastoma cells were incubated at Ta of 37.4 °C, mimicking the core temperature of animals during the waking period (Guisle et al., 2020). Another result that underlines the key

role played by temperature in Tau phosphorylation during sleep is the detection of the inhibition of the PP2A, the main phosphatase of Tau, during the rest period. This is in line with studies showing that the PP2A is more active during wakefulness (Olcese, 2003), and it results to be inhibited, causing increased levels of Tau phosphorylation, by the lowering of Tb (M. Goedert, Jakes, Qi, et al., 1995; Planel et al., 2004).

Additionally, the authors showed that Tau phosphorylation was also prevented by acute sleep deprivation in mice. However, also in this case, the reason seemed to be the temperature, considering that the core temperature of the sleep deprived animals resulted higher than that of sleeping mice (Guisle et al., 2020).

Another recent study seems to be complementary to this one, showing cyclical variations in the presence of extracellular Tau, at the level of the interstitial space in the human brain. In this study, Tau appears to be reduced during sleep, increased during wakefulness, and further increased following sleep deprivation (Holth et al., 2019). However, since Tau at the extracellular level is mainly dephosphorylated (Pooler et al., 2013), there is likely to be an inverse relationship between phosphorylation and secretion into extracellular space, with less secretion of Tau during sleep when the protein is highly phosphorylated, and on the other hand, an increase of extracellular levels of Tau when it is dephosphorylated during wakefulness (Guisle et al., 2020)

The physiological and molecular role played by the Tau protein in the wake-sleep cycle is still unknown, but it is assumed that Tau phosphorylation during sleep might influence the stability of the cytoskeleton and axonal transport. Consequently, this would impact on synaptic plasticity occurring during NREM sleep. In accordance with the synaptic homeostasis hypothesis, this process might consolidate memory and learning (Guisle et al., 2020).

1.2.6.3 SLEEP HOMEOSTASIS AND AROUSAL FROM TORPOR

One aspect that seems apparently complicated to explain through the synaptic homeostasis hypothesis is the occurrence of a strong pressure to sleep soon after the arousal from a torpor bout. In fact, despite the animals exiting from a torpor bout are basically recovering from a period characterized by poor EEG activity, it has been observed that during the euthermic interbout periods, the hibernators spend most of their time sleeping. For example the golden mantled ground squirrels spends 70% of the euthermic intervals asleep (Larkin & Heller, 1999).

This phenomenon has been observed in different species and the EEG characteristics of these sleep periods are similar to those observed in mammals after a prolonged sleep deprivation, i.e. an increase in the intensity of the delta band (Deboer & Tobler, 1994).

Although the significance of post-torpor NREM sleep has not yet been fully elucidated, this phenomenon has been extensively documented in several rodent species, both seasonal hibernating, such as the arctic squirrel (Daan et al., 1991), and animals that exhibit daily torpor, like the Djungarian hamster (Deboer & Tobler, 1994); but also in different species of non-human primates (Blanco et al., 2016; Royo et al., 2019).

However, this phenomenon could be critical to allow us to understand many still unclear aspects related to sleep, hibernation, and their interconnections. For example, it was the main prove against the first theory that tried to correlate torpor and sleep. Indeed, considering the reduction in core temperature and metabolic rate to be common to both torpor and NREM sleep, and the fact that rodents seem to start their torpor bouts during a NREM sleep period, Berger (1984) speculated that the daily torpor and hibernation evolved as an extension of NREM sleep. But obviously, the appearance of the high activity of SWA in NREM sleep immediately after the arousal from torpor bout and the predominance of sleep in most of the following euthermic period confuted this hypothesis (Deboer, 1998). In effect, these observations rather suggest that the torpor period is incompatible with the sleep functions, and consequently the arousals may allow the animals to recover from a period comparable with sleep deprivation (Daan et al., 1991). It was indeed noted that during the torpid period the alternation between NREM sleep and REM sleep disappear from the EEG spectra, which became isoelectric when the brain temperature goes below the 21 °C (Royo et al., 2019).

Moreover, many data have shown that this phenomenon seems homeostatically regulated. In fact, SWA during NREM sleep occurring after the arousal from torpor increases with longer period of torpor based on an exponential saturation curve (Strijkstra & Daan, 1997). This is analogous to the progressive increase in SWA consequent to a prolongation of sleep deprivation (Tobler & Borbély, 1986). Similarly, during the euthermic interval SWA decreases monotonically throughout NREM sleep. This result seems to indicate that the sleep need accumulated during the hibernation bout decreases during post-torpor NREM sleep (Daan et al., 1991; Trachsel et al., 1991). Furthermore, the SWA in ground squirrels resulted also inversely correlated with the brain temperature that the animals reached during the previous

torpor bout (J E Larkin & Heller, 1996). Another observation that indicates the homeostatic nature of this phenomenon is the fact that if a daily heterotherm, in this case the Djungarian hamster, is sleep deprived soon after his arousal from torpor, then the power density of SWA during the recovery period will be higher compared to the SWA occurring in the first hour after arousal from torpor without sleep deprivation (Deboer & Tobler, 2000, 2003). This result was also confirmed applying a selective sleep deprivation for NREM sleep (Palchykova et al., 2002). Additionally, in the same study the authors also showed that during the recovery from both torpor and a period of sleep deprivation, the SWA was higher in the frontal than in the parietal derivation of the EEG. This further highlight that torpor and sleep deprivation have equivalent effects on sleep (Palchykova et al., 2002).

However, other studies showed conflicting results, questioning the homeostatic regulation of the SWA occurring after torpor. In particular, in two experiments the authors sleep deprived ground squirrels, soon after the arousal from a torpor bout, by using two different methods, i.e. the injection of caffeine or the gentle handling of the animals. As a consequence of the sleep deprivation, the expected increase in SWA during the recovery from torpor did not occur (Larkin & Heller, 1998; 1999). Other researchers found differences in the SWA occurring in post-torpor NREM sleep compared to a sleep deprivation recovery. In one study, during the recovery from torpor a reduction in spectral activity in the sigma frequency range (7–14 Hz) was found, which was not observed after sleep deprivation. This means that the SWA following torpor or sleep deprivation seem to be qualitatively different (Strijkstra & Daan, 1998). In another study, the slopes of single slow waves during NREM sleep were shown to be steeper in the first hour after sleep deprivation but not in the first hour after the end of the torpor bout. In addition, the slow-wave slopes decreased progressively within the first 2 hours after sleep deprivation, while a progressive increase in slow-wave slopes occurred during the first 2 hours after the end of the torpor bout. It seems therefore that sleep deprivation and torpor have different effects on cortical network activity, even if they result in an overall similar sleep response in terms of SWA (Vyazovskiy et al., 2017). These findings would indicate that the SWA after arousal from torpor, rather than indicating an homeostatic regulation of NREM sleep, may reflect some neurological processes in the recovery of neural function from a protracted period at low temperature (Larkin & Heller, 1999).

Even if the contradictory results might be the consequences of species-specific differences, for example between hibernators and daily heterotherms or discrepancies in the methodologies

used in the experiments, one hypothesis tried to address all these heterogeneous data assuming that the main role of the SWA after torpor is correlated with an intense synaptogenesis. According to this hypothesis the loss of dendritic complexity and synapses during the hibernation period (Popov & Bocharova, 1992; Strijkstra et al., 2003; Von Der Ohe et al., 2006, 2007), could suggest that the function of periodic arousals is restoration of synapses. The occurrence of the SWA after torpor may be the result of loss of dendrites and synapses in the thalamocortical circuits, which are normally depolarized by the ascending influences from the brainstem causing wakefulness. While sleep onset, on the contrary, is associated with the removal of these ascending activities, resulting in hyperpolarization of thalamocortical neurons, which in turn causes the synchronized bursting activity that generates the slow waves in the cortical EEG (Benington & Craig Heller, 1995). Thus, the loss of synapses during hibernation removing the ascending influences on thalamocortical neurons would lead to a tonic hyperpolarization of the cerebral cortex, which would potentiate the expression of SWA. In the end, as dendrites and synapses are restored, the high SWA would gradually diminish as reported in various studies (Heller & Ruby, 2004).

Although the synaptogenesis hypothesis appears to be a likely explanation for the SWA following arousal from deep torpor in hibernators, like ground squirrels, the picture is less clear when we have to explain the results about species that undergoes shallow or daily torpor.

One hypothesis to account these data suggests that a need for SWA can be built-up even during a relatively short interval of time, in accordance with the huge autonomic and metabolic activation that occurs during the brief period of wakefulness preceding sleep occurrence, after the arousal from torpor (Amici et al., 2014). This hypothesis is supported by the evidence that although 3 days of water deprivation in rats induced a reduction of motor activity and waking, nonetheless a large increase of SWA was detected during the recovery period which followed the restoration to water access. The build-up might be the consequence of 2 hours of strong behavioral activity, which follows water delivery and precedes NREM sleep onset (Martelli et al., 2012). Moreover, another study showed that the intensification of SWA in NREM sleep can occur as a consequence of stressful stimuli increasing the ANS activity (Meerlo et al., 2001). Thus, these results may suggest, in line with the sleep homeostasis hypothesis, that the increased need for NREM sleep soon after a hypothermic bout, can be generated during the brief period of rewarming, associated with a strong ANS activity and synaptogenesis, which ultimately lead

to the need for synaptic renormalization occurring through SWA synaptic downscaling (Amici et al., 2014; Vyazovskiy et al., 2011).

1.2.7 RADIOPROTECTION

The physiological changes and adaptations that occur during natural torpor have different consequences at cellular and biochemical level. Indeed, the decrease in the metabolic rate and the reduction in core Tb are related, for example, to a shift from glycolysis to lipolysis and ketone utilization, an alteration in heart rate control via Ca^{2+} and to strong but reversible alterations in several organs like brain, heart and kidney. These changes would prevent degenerative processes caused by organs inactivity and increase the resistance and tolerance of the tissues to stressful conditions, such as ischemia/reperfusion, hypothermia and also radiation exposure (Choukèr et al., 2019).

Various potentially protective physiological and molecular changes have been observed in hibernators. For example, an increase in anti-apoptotic proteins, or the activation of serine/threonine kinase Akt (Fleck & Carey, 2005) and redox sensitive transcription factor NF-κB (Carey et al., 2000) may serve to resist tissue degradation. In addition, recently it has been reported an increased formation of endogenous H_2S by induction of cystathionine-beta-synthase (CBS) expression during the late phase of torpor and early arousal, which could also have protective effects for call damage (D'alessandro et al., 2016; Talaei, Bouma, et al., 2011). In the brain, the hyperphosphorylation of Tau protein can have a protective effect on neurons, preventing memory loss (Clemens et al., 2009). In the heart, the hibernation-related phenotypes are characterized by changes in Ca^{2+} homeostasis and intense upregulation of antioxidant enzymes (Horii et al., 2018).

It is generally accepted that hibernation increases resistance to stressful conditions. Thus, it is plausible to suppose that natural torpor can be associated also with increased resistance to radiation damages. Several studies provided data in this direction. In fact, in cultured cells, the induction of hypothermia provides protection against radiation-induced DNA damage, including double-strand breaks (DSBs) (Baird et al., 2011; Elmroth et al., 2000b), improves cell survival after radiation (Elmroth et al., 2000a), and protects cells from cell death by apoptosis (Sakurai et al., 2005). The protective effects have been detected independently if hypothermia was applied before, during, or soon after the irradiation (Lisowska et al., 2014). Especially, in

one study using in vitro systems, the mechanisms of acquired resistance related to hypothermia has been investigated. Measuring the survival curves in BJ-hTERT human cells irradiated in hypothermic conditions (at 13 °C, 20 °C and 30 °C), Baird and colleagues (2011) identified a pronounced radioprotective effect when cells were cooled to 13 °C during and 12h after irradiation. Mild hypothermia at 20°C and 30°C also resulted in some radioprotection. Parallel analyses on ex vivo-irradiated human lymphocytes focusing on radiation-induced oxidatively clustered DNA lesions (OCDLs) and phosphorylated H2AX (ɣ-H2AX) revealed partial repair at 13 °C compared to the rapid repair at 37 °C. For both ɣ-H2AX foci and OCDLs, the return of lymphocytes to 37 °C resulted in recovery of normal repair kinetics (Baird et al., 2011). These results seem to suggest that slowly repair of double strand breaks, due to hypothermia, may have beneficial impact on the survival of the cell. Moreover, also localized hypothermia, induced in healthy tissues surrounding tumors, in some pilot studies has been shown to induce a reduction in radiation side effects in patients (Hong et al., 1985; Shah et al., 2000). On the contrary, it is also well known that the hyperthermia has opposite effects on radiation stress, inducing an increase in radiosensitivity, possibly through an impairment of certain DNA repair processes (Oei et al., 2015; Raaphorst et al., 1999). In this regard, hyperthermia has been proposed to be used in association with radiotherapy to increase its efficacy in treating tumors. This alternative approach not only would cause a higher probability of eradicating the tumor, but also lowers normal tissue damage since lower doses of radiation may be sufficient (Spirou et al., 2018). Pre-clinical results have supported the above hypothesis, showing that hyperthermia can significantly improve the outcomes when combined with radiotherapy (Datta et al., 2016; Zagar et al., 2010).

Other studies have focused on the impact of hypoxia on radioresistance. The hypoxia can markedly reduce the extent of radiation-induced cell damage (Cuisnier et al., 2003; Roy et al., 2000) most probably through the suppression of oxygen radicals production, which is the indirect effect of radiation on cells and it could be even more harmful than the direct effect on DNA of the radiation exposure. Indeed, both acute and chronic hypoxia has been shown to be associated with an increased radioresistance in cells (Ma et al., 2013; Tinganelli et al., 2013). Hypoxia is also supposed to be the reason why tumors are more radioresistant compared to healthy cells. In fact, tumors generally live in a hypoxic microenvironment, and the ratio of the doses to induce the same cell killing in hypoxia and aerobic atmosphere (oxygen enhancement ratio, OER) is close to 3 after X-rays (Wilson & Hay, 2011).

Considering all these data and the fact that hibernation is characterized by hypothermia, hypoxia, and hypometabolism, in general, it is reasonable to assume that hibernators can show an increased radioresistance. The studies that extensively evaluated this aspect were performed mostly between 1950s to 1970s. One of the first study about this topic showed that the lethal damage on hibernating marmots exposed to radiation was just postponed after the arousal, so the survival curves observed at this time point were equivalent for animals irradiated during the torpid phase or in euthermic state (Smith & Grenan, 1951). The same pattern of delaying damages was revealed for the ground squirrels (Doull & Dubois, 1953). Instead, an increase in radioresistance, for a wide range of doses, in hibernating ground squirrels (5°C Tb) has been detected when compared to animals in active period (37°C Tb). The normothermic animals exposed to 15 Gy of total body radiation showed a mean survival time of 8 days, while animals in hibernation survived for a mean of 66 days, even if animals irradiated during torpor and immediately after aroused within 2 hours demonstrated the longest survival. The survival advantage decreased to a factor of two at 20 Gy and disappeared by 30 Gy (Musacchia & Barr, 1968). In accordance with this experiment another study showed an increased survival rate in hibernating ground squirrels to a lethal dose of Cobalt-60 gamma radiation and, also in this case, the highest survival rate was found in the hibernating animals that aroused one day after the irradiation (Jaroslow et al., 1969).

Additionally, several physiological and biochemical protective effects have been reported in tissues of hibernating irradiated animals. For example, more resistant protein synthesis in neurons, and less loss of cellular structural integrity. In particular, in ground squirrels irradiated in normothermia, neurons were less radioresistant and recovered slower than cells from animal in torpor, the distinctions were most expressed in CA1 field neurons (Gordon et al., 2006). In another study, it has been observed an increased survival of intestinal crypt cells of ground squirrels if irradiated during hibernation, and the same survival was found also in squirrels irradiated 1 hour after the arousal, when the animals had a Tb similar to the euthermic controls (Jaroslow et al., 1976). Finally, in another experiment the authors observed that the values of functional synthetic activity and the total number of blood and bone marrow cells in ground squirrels, irradiated during the torpid phase, did not differ from those in non-irradiated torpid animals. The damaging effect of radiation exposure at the initial stage of arousal (9.8–11.5°C) is weaker than during the activity period, whereas animals at the late phase of awakening (18–35°C) were more vulnerable to radiation (Karnaukhova et al., 2008).

More recently, a meta-analysis summarizing some of the data about radioprotection due to hypothermia and torpor, from published papers, supported the hypothesis of hibernation increasing radioresistance. Pooling several data from different articles produced a very significant spread in results, but the trend clearly showed the increased survival of squirrels irradiated during hibernation and rats irradiated under hypothermia, with a high protective factor (ratio of LD50 values in hibernation/hypothermia and normal conditions) around 1.4 for both squirrels (hibernators) and rats (non-hibernators) (Cerri et al., 2016).

1.2.7.1 THE MECHANISMS UNDERLYING RADIORESISTANCE

The exact mechanisms underlying radioresistance observed during hibernation in mammals remains unknown. Considering that radioresistance could be ascribed to a broad variety of processes, occurring between the radiation exposure to the final response, it is not surprising that various studies proposed different plausible explanations.

One of the proposed mechanisms for radioprotection is mediated by antioxidants. Indeed, the ionizing radiation (IR) causes damage by energizing water molecules, and this leads to the formation of highly unstable oxygen species, whose obtain stability at the expense of cellular compounds. The damaged cellular components include proteins, lipids, and DNA. Antioxidants can stop this chain reaction by preventing or intercepting the free radicals (Sies, 1997). Thus, antioxidants may play a role in radioprotection in mammals. Hibernators increase the expression and levels of antioxidants in plasma and tissues during the torpid period. In both the Arctic ground squirrel and the ground squirrel, levels of plasma ascorbate are three- to four-fold higher during torpor and they decrease to euthermic levels only during arousal (Drew et al., 1999). Although the decline in plasma levels of ascorbate is associated with an increase of ascorbate in peripheral tissues. This reallocation is supposed to reduce the effects of oxidative stress during reoxygenation of tissues upon arousal (Tøien et al., 2001).

Another aspect that plays a central role in radioprotection is the DNA repair. In mammals the radiation-induced single-strand damages are mainly repaired through two principal DNA repair mechanisms: base excision repair (BER) and nucleotide excision repair (NER). BER repairs the damage involving a single nucleotide, caused by oxidation, alkylation, hydrolysis, or deamination. While NER repairs damage involving strands from 2 to 30 nucleotides long. These include massive helix distortion damage, which cause mutations in a single strand (Cline &

Hanawalt, 2003). Considering that both of these repair mechanisms require an access to the DNA to perform their function, the cells should orchestrate genome remodeling to facilitate these repair processes. But, in the ground squirrel, during torpor the genome undergoes structural modifications that block transcription, making DNA inaccessible, while during interbout arousals the DNA activity resumes for a brief period of time (Biggar & Storey, 2014). If we consider, in addition, that low Tb reached by hibernators would cause a reduction in the rate of biochemical reactions, including those involved in detection, recruitment and performance of enzymes repairing DNA damage, it is reasonable that the interbout arousals are needed to arrange and promote cellular preservation, likely including DNA repair too, that during the torpor is hindered by various factors, such as low Tb and DNA inaccessibility. The importance of arousal for radioresistance may also be supported by the observation that sleep, which as previously described characterizes the interbout arousals, seems to be critical to repair radiation induced DNA damage. It has been observed that sleeping mice, after irradiation, repair DNA damages in the brain more rapidly than sleep deprived animals. Sleep may boost DNA repair for different reasons. It might be that since neurons are more hyperpolarized and fire less during sleep, the latter may basically provide a period with more energy for housekeeping functions, including DNA repair (Bellesi et al., 2016; Mackiewicz et al., 2007). Another reason might be the increase of melatonin associated with NREM sleep (Troynikov et al., 2018). Melatonin is a free radical scavenger, and it can stimulate numerous antioxidant enzymes. Indeed, in a review on 37 studies, all of them showed that exogenous melatonin reduced oxidative stress and inflammation in all tissues analyzed, additionally, melatonin increased survival, after radiation, up to 30 days and protected against radiation enteritis (Zetner et al., 2016). There are various correspondences between this data and arousal. In fact, it is well known that during the arousal from torpor there is an increase in melatonin levels. For example, this increase has been reported in golden hamsters regardless whether they were provoked to arousal during day or night (Vaněček et al., 1984). Similar results were also found in ground squirrels, where melatonin levels were lowest during the state of deep hibernation, and significantly increased in the interbout phase within 1 hour after the arousal (Stanton et al., 1986). Moreover, during the arousal period the animals spend most of their time sleeping.

Another mechanism involved in radioresistance is the balance between pro- and anti-apoptotic pathways. Indeed, if attempts to repair DNA damage fail, then programmable cell death (PCD) pathways are activated. Three are the main PCD types: apoptosis, autophagy, and necrosis

(Pietenpol & Stewart, 2002). There is evidence that hibernators possess adaptive responses anti PCD in order to increase the protection against the stresses of hibernation. Overexpression of anti-apoptotic genes, for example coding for ROS scavengers and heat shock proteins (HSP), have been detected in hibernators (Portt et al., 2011). Also anti-apoptotic Bcl-2 family members have been shown to be upregulated in white adipose tissue in ground squirrels in order to rise cell survival during torpor-arousal cycles (Logan et al., 2016).

Finally, the last documented mechanism that hibernators might use to increase tissues radioresistance involve the cell cycle progression.

There are four stages of cell division cycle: mitotic-phase (M) and an interphase of G1, S, and G2. Cells can escape the cell cycle during G1 to a reversible, quiescent stage (G0). Cell-cycle progression is precisely regulated by the activity of cyclin dependent kinases (Cdk) and their association with cyclins. Thus, the cell-cycle arrest is mediated by Cdk inhibitors (CKI) (Pines, 1995). During hibernation, due to hypometabolism and hypothermia many energetically demanding processes are downregulated; the process of cellular division is among them. Indeed, researches about gastrointestinal radioprotection in hibernators were the first to reveal a cell-cycle stall at the G1-phase during torpor (Jaroslow et al., 1976). The pattern of cyclin and Cdk proteins in liver tissue of ground squirrels, also support arrest in G1 during the beginning of the torpid phase and throughout torpor (Wu & Storey, 2012). The results of another study about bone marrow, always in ground squirrels, indicate hematopoiesis suppression during hibernation (Cooper et al., 2016). Additionally, these two last studies suggested that the arrest at G1/S transition was mediated by upregulation and expression of CKI, specifically p15INK4b and p21CIP1(Cooper et al., 2016; Wu & Storey, 2012). Therefore, it seems that during torpor there is a shift in cell cycle progression that delays proliferation until returning to euthermia. In in this way the DNA division mistakes, usually promoted by stresses, can be reduced.

1.3 SYNTHETIC TORPOR

Hibernation is an evolutionarily well conserved phenomenon, which has been described in many orders of mammals. The wide distribution of hibernators in phylogeny could suggest that it is an ancestral character, and therefore the genetic predisposition for survival in a state of hypometabolism should be preserved in almost all mammals, but only a part of them has maintained also the ability to activate these genes in harsh environmental conditions. This

considerations may consequently suggest that it is possible to induce a hypothermic and hypometabolic state in all mammals (Cerri, 2017).

Although the mechanisms underlying the natural torpor are not yet entirely clarified, several studies have investigated, both in heterothermic species and in species that do not spontaneously exhibit torpor, the possibility of inducing a "synthetic" torpor (ST), i.e. a condition characterized by the reversible downregulation of normal physiological functions such as the regulation of Tb and metabolism.

1.3.1 POSSIBLE APPLICATIONS

The reason why the researchers are increasingly interested in inducing torpor artificially, in species of mammals that naturally do not exhibit this complex physiological behavior, stems from the possible applications, therapeutic and others, that a condition of reduced Tb and reduced metabolism could have in humans.

Concerning the medical applications, a condition of hypothermia is advantageous in all those situations where the oxygen and metabolic demands of the whole body or a specific organ exceed its availability. For example, in case of cerebral stroke and myocardial infarction, an hypometabolic state could expand the time window needed to allow the reperfusion of the organs, while in conditions such as trauma, surgery, sepsis and generalized hypoxia it could protect against cell damage (Cerri, 2017).

To date, in the clinical practice, therapeutic hypothermia is induced in two main ways. The first method is based on a common peripheral cooling. Instead, the second option entails a central cooling, using intravascular catheters, cold fluids infusions and external body circulation. Nonetheless, since both of these methods basically induce an exogenous hypothermia, the neural control of thermoregulation is activated by the drop in core temperature, and, therefore, in order to maintain euthermia the body activates thermogenic responses and prevents heat loss responses, leading to sympathetic activation, tachycardia, shivering, and vasoconstriction (MacLaren et al., 2014; Polderman, 2004). As a consequence of these homeostatic responses there will be an increase in glucose, cortisol and catecholamine levels, and in protein and fat consumption, also causing an increment of oxygen consumption (Frank et al., 2003). The final result of this physiological activity is the increase in metabolic rate that actually is the direct opposite of what is desirable to achieve through the induction of therapeutic hypothermia,

which as we said, is implemented in situations where oxygen and glucose demands cannot be satisfied.

Currently, to limit this problem only mild hypothermia (32-34 °C) can be safely induced in clinical practice. Nonetheless, to completely overcome the problem, a way to induce a form of endogenous hypothermia should be found. If it acted on the CNS, it would provide an active reduction of Tb and metabolism, allowing a deeper hypothermia without the side effects deriving from thermogenic stimulation to occur.

Another reason to work on possible forms of synthetic torpor is to produce living models for the possible study of some pathologies, and to deepen the knowledge of physiological adaptations that occur during hibernation, whose understanding could lead to the development of new therapeutic strategies. Some of the peculiar characteristics of torpor that could have clinical interest are: the reversible hyperphosphorylation of Tau protein, the strong and extended neural plasticity, the absence of muscle atrophy despite a prolonged inactivity, as well as the metabolic and immunological adaptations, and, last but not least, radioresistance.

Concerning radioresistance, this aspect could have two main applications: in cancer patients that undergo radiotherapy, the induced synthetic torpor may protect the rest of the body from radiation, minimizing the collateral effects of radiation exposure. Another application could be the long-distance space exploration. Indeed, the astronauts are exposed to cosmic radiations, which limit the time that they can spend in space travel. The induction of synthetic torpor would not only have a radioprotective effect, but it would also decrease food amount required for survival, prevent the problems related to microgravity exposition for a long time period, as well as the psychological issues that could derive from sharing a small space with other people, such as the cabin fever (Cerri, 2017).

1.3.2 VARIOUS STRATEGIES TO INDUCE SYNTHETIC TORPOR

The physiological mechanisms that can be manipulated to induce a reduction of metabolism are mainly two: reduce the use or production of the energy substrate ATP, by intervening on the mechanisms that regulate cellular metabolism, or act at the level of the CNS modifying the central control of thermoregulation (Griko & Regan, 2018).

Different strategies have been used in order to mimic most of the natural features of the torpor occurring in hibernating species, but principally we can group all of them in two main categories: the strategies that involved the use at systemic level of various molecules, such as 5'-AMP, neuropeptide Y, 2-deoxy-D-glucose, and hydrogen sulphide and those that act directly on the CNS to alter the central control of metabolism.

1.3.2.1 HYDROGEN SULPHIDE (H_2S)

Considering that the central characteristic of torpor is an active reduction of metabolic rate, and consequently of oxygen consumption (Heldmaier et al., 2004), the activity of mitochondria has received great attention in the research of strategies to induce synthetic torpor (Mathers et al., 2017). In fact, by the inhibition of mitochondrial activity, ATP production is decreased and the metabolism too.

Among the molecules utilized in the attempt to induce an inhibition of mitochondrial activity, the hydrogen sulphide (H_2S) has been shown to be efficient. It is an endogenous molecule involved in signaling in CNS and the cardiovascular system. It also acts as a reversible inhibitor of mitochondrial complex IV (cytochrome c oxidase) essential for the last phase of oxidative phosphorylation and therefore for the production of ATP. Hydrogen sulphide competes with O_2 to bind cytochrome-c oxidase, and, as a result, it produces a decrease in cellular oxygen consumption and a reversible inhibition of cellular metabolism. It has also been found implicated in the activation of anti-apoptotic systems and antioxidant mechanisms (Calvert et al., 2010).

One study on mice showed that exposure to gaseous H_2S produced a decrease in cellular metabolism and Tb. After exposure, the metabolism dropped by 90% and the Tb reached a minimum of 15 ° C. Six hours after exposure to H_2S, the mouse slowly warmed up and cellular metabolism and Tb returned to normal values (Blackstone et al., 2005). Administration of H_2S to other, larger types of animals has reported inconsistent results.

H_2S was less effective in inducing synthetic torpor in other species: it induced a modest drop in the metabolic rate and Tb in rats (Lou et al., 2008), but failed to induce metabolic suppression in piglets (Li et al., 2008), pigs (Drabek et al., 2011) and sheep (Haouzi et al., 2008). One explanation of the lack of hypometabolism in larger animals is that the hypometabolic effects

of H_2S could not be the result of direct inhibition of the mitochondria but the activation of the hypoxic pathways from the carotid body (Dirkes et al., 2015).

1.3.2.2 3-IODOTHYRONAMINE (T_1AM)

3-Iodiothyamine (T_1AM) is a substance derived from the thyroid hormone and it is an agonist of the G protein-coupled receptor TAAR1. Its physiological role is not completely known, but its injection into the mouse has led to a decrease in Tb and heart rate, while in the Djungarian hamsters it has reduced the metabolic rate.

However, the hypothermia induced by T_1AM administration is less pronounced, with Tb settling at 33 ° C in hamsters and 30 °C in mice, than the hypothermia occurring during natural torpor in these species. Another difference with the natural torpor is that following the T_1AM injections, the drop of Tb is faster, while after the torpid phase the increase of the temperature is slower (Braulke et al., 2008; Scanlan et al., 2004).

The administration of T_1AM can induce several days of synthetic torpor in the mouse, following an experimental protocol that provides the administration of a fat diet for four weeks before the experiment, and repeated intraperitoneal injections of T_1AM (Ju et al., 2011).

1.3.2.3 2-DEOXY-D-GLUCOSE (2-DG)

2-deoxy-D-glucose (2-DG) is a non-metabolizable analog of glucose, that, due to its inhibitory effect of glycolysis, can be used to pharmacologically induce a condition of glycoprivation. 2-DG has been used in several studies aimed at investigating its effectiveness in inducing a torpor-like condition. It has been reported to cause a drop in Tb below 30 °C when injected in Siberian hamsters (Dark et al., 1994).

Interestingly, the pharmacological induction of lipoprivation, through the administration of β-oxidation inhibitors of fatty acids, such as mercaptoacetate, did not provoke any hypothermic effect. Suggesting that it is the availability of glucose, and not that of fatty acids, that has a critical role in torpor induction (Chi et al., 2017).

1.3.2.4 NEUROPEPTIDE Y (NPY)

Neuropeptide Y (NPY) is a common neurotransmitter and a strong orexigenic agent. It can induce a decrease in metabolic rate in mice (Walker & Romsos, 1993). Intracerebroventricular administration of NPY in the Siberian hamster has proven to be sufficient to induce hypothermia (Paul et al., 2005). In the rat, instead, the central administration of NPY does not cause a torpor-like state, but causes a very small drop in Tb of 1-3 ° C (Székely et al., 2005).

1.3.2.5 5’-ADENOSINE MONOPHOSPHATE (5'-AMP)

5'-adenosine monophosphate (5'-AMP) is a metabolite of ATP hydrolysis and has been proposed as a possible inducer of synthetic torpor in mice. In conditions of fasting and constant darkness, the intraperitoneal administration of 5'-AMP induced a torpor-like state in the mouse, with an important and sudden bradycardia (Tao et al., 2011).

There are two main hypotheses that may explain the pharmacological effects of 5'-AMP: 5'-AMP can be dephosphorylated producing adenosine, which activates the adenosine receptors and may lead to a reduction in cardiac performance through A1 receptors, and consequently to a reduction in Tb (Swoap et al., 2007). The other hypothesis assumes that absorption of 5'-AMP leads to the activation of the AMP protein kinase (AMPK), a key enzyme involved in the regulation of metabolism.

A recent study testing the 5'-AMP on mice knockout for all the four adenosine receptors subtypes revealed that a partial hypothermic effect was still presented in these animals (Xiao et al., 2019), indicating that probably the action of 5'-AMP on the adenosine receptors is not the only underlying mechanism and both of the hypothesis on the pharmacological effects of 5'-AMP may be true.

However, the attempt to use 5'-AMP in non-hibernating animals did not work completely. The administration of 5'AMP in the rat induced only a modest state of hypothermia and has produced many metabolic and cardiovascular problems (Zhang et al., 2009).

1.3.2.6 ACTIVATION OF CENTRAL ADENOSINE A1 RECEPTORS

Adenosine is a nucleoside that has inhibitory neuromodulating characteristics and it can act as signaling molecule. The presence of adenosine affects excitable tissues, in particular in the heart

and the brain, where the adenosine receptors are particularly present, and induces vasodilation, acting as a co-factor in regulation of energy homeostasis.

In hamsters, the intracerebroventricular administration of CHA, a A1-receptor agonist, causes a drop in Tb (Tamura et al., 2005); similar results have been found in arctic ground squirrels (Olson et al., 2013).

The effects of CHA have also been tested in a non-hibernating mammal, the rat, through its i.c.v. administration in animals kept at Ta 15 ° C. It has been shown that CHA injection induced a reduction in Tb, to about 28 °C, and in heart rate, which is lowered to about 200 bpm, accompanied by a decrease in the amplitude of the EEG.

The effectiveness of this procedure seems to depend on the inhibition of the activation mechanisms of thermogenesis in response to cold; in this process, the neurons present in the NTS play an important role, which guide the inhibition of the activity of brown adipose tissue and shivering thermogenesis. It is likely that CHA binds to inhibitory A1AR receptors of a GABA-ergic neurons, removing an inhibitory drive to the sympatho-inhibitory activity of the NTS, ultimately activating that branch (Tupone et al., 2013).

1.3.2.7 INHIBITION OF THE RAPHE PALLIDUS

Raphe Pallidus is located in the caudal portion of the brainstem, at the level of the ventromedial medullary area (RVMM). It plays a central role in regulating thermogenic responses, controlling the activation of both thermogenesis at the level of brown adipose tissue and shivering, and the increase in heart rate and vasoconstriction in response to cold exposure (Morrison & Nakamura, 2011).

Considering the central role played by this area in thermogenesis, it was hypothesized that the inhibition of this area could induce hypothermia. In 2013, Cerri and colleagues inhibited this brain area in rats kept at Ta 15 °C in a condition of constant darkness and subjected to a high fat diet, microinjecting for 6 times (1/h) muscimol, a GABAA agonist. The result was an important drop in brain temperature (with a minimum of 22 ° C), heart rate (from 440 bpm to around 200 bpm) and a reduction in EEG power. The injections resulted in a significant peripheral vasodilation while the average blood pressure did not change, and no major cardiac arrhythmias were observed (Cerri et al., 2013).

Considering all the changes in cardiovascular system, EEG, and behavior, it seems that the inhibition of the RPa is the best strategy to induce a synthetic torpor with all the main characteristics proper of the natural torpor. It is also confirmed by the fact that, in natural torpor in mice, neurons within RPa, during the torpid phase, have been found inactive, as indicated by the absence of the immunohistochemical staining for cfos in this brain area (Hitrec et al., 2019).

A further proof, also useful from the translational point of view, derive from another experiment made on pig, where the injection of GABAzine a GABA-A antagonist in the RPa caused an increase in heart rate, systolic and diastolic arterial pressure, and end-tidal CO2. All these modifications were reversed by the injection in the same area of the GABA-A agonist muscimol (Zucchelli et al., 2020).

1.3.3 NEURAL PLASTICITY

As we have already mentioned before, the induction of a state of synthetic torpor is particularly interesting and useful for the study of many clinical conditions that could benefit of the physiological adaptations normally occurring in natural torpor and hypothetically simulated by synthetic torpor. One example of these clinical conditions are the Tauopathies. In this case, the development of a valid model of synthetic torpor would allow to analyze not only the mechanisms that guide the hyperphosphorylation and dephosphorylation processes of Tau protein, but also their consequences in non-hibernating mammals.

In one study, through the production of a state of suspended animation induced by the Raphe Pallidus inhibition procedure developed by Cerri and colleagues (2013) and illustrated above, these phosphorylation and dephosphorylation patterns similar to that existing in episodes of natural torpor were observed in rats, a non-hibernating animal.

During the time course of the ST procedure, 19 brain areas were immunohistochemically analyzed, using two different antibodies: AT8 and Tau-1. AT8 recognizes phosphorylated Tau at the level of Ser202 / Thr205 residues, and it has been used as a marker of phosphorylated Tau, while Tau1 recognizes Tau when it is not phosphorylated between residues 189 and 207 and highlights the presence of dephosphorylated Tau (Luppi et al., 2019). The experimental conditions explored were: i) control, after the injection of saline; ii) N30, between the second and third injection of muscimol, when Tb reached the level of 30°C; iii) N, in which animals were sacrificed 1 h after the last injection of muscimol, when Tb reached the nadir of

hypothermia; iv) ER, early recovery; in which animal were sacrificed when Tb reached 35.5◦C during the rewarming after ST; v) R6, in which animals were sacrificed 6 h after ER (during this 6-h period animals sleep intensely); vi) finally, R38, in which animals were sacrificed 38 h after ER. Similarly, to what occurs in natural torpor, an increase in AT8 and a specular decrease in Tau-1 were shown upon reaching a Tb of 30°C. At the nadir of hypothermia, the peak of AT8 was reached in the majority of the brain areas analyzed and it was accompanied by the disappearance of Tau-1. In R6, AT8 was significantly reduced and in R38 it had almost completely disappeared. However, Tau-1 even at 38 hours after arousal showed values still low compared to the control condition, suggesting that Tau dephosphorylation was still only partial in spite of the absence of AT8 immunoreactivity (representative images in fig. 10).

The analysis of these data suggests that the induction and reversibility of a widespread phosphorylated Tau accumulation can occur also in the brain of a non-hibernating mammal, following the induction of synthetic torpor. Thus, this model allowed to reveal that the resolution of hyperphosphorylated Tau appears to be actively regulated, and the physiological mechanism involved in this process can sustain an apparently protective neuronal response to extreme conditions, which may instead lead to neurodegeneration when particular intensities and durations are exceeded (Luppi et al., 2019).

1.3.4 SLEEP

Concerning the debate on the homeostatic aspect of the sleep rebound which follows natural torpor, useful information derived from the analysis of the synthetic torpor model. Indeed, it is interesting to note that also in a study of induction of synthetic torpor in the rat, by means of the protocol already exposed (Cerri et al., 2013), a post-torpor sleep rebound was observed which appeared to be similar to that observed in natural torpor.

During the torpid phase induced by muscimol injections in the RPa, the state of consciousness remained unclassifiable according to standard criteria, and clearly classifiable sleep states returned only with the recovery of euthermia, and in particular when a Tb of 35 °C was reached. Soon after the arousal, as it happens in natural torpor, the animals fell asleep and a large increase in SWA was detected during a state which appeared to be NREM sleep (Cerri et al., 2013).

However, during the rewarming phase animals were divided in two groups. In one case the Ta during their awakening was settled at 28 °C, in another group the Ta was set at 37 °C during

the first hour of the rewarming and then moved to 28°C. Interestingly, in accordance with the hypothesis that the thermogenic effort during the arousal define the magnitude of delta waves, the group of animals that during the awakening phase was exposed to a higher Ta (37 °C) developed a smaller increase in delta power, possibly as a consequence of a lower activation of the sympathetic pathways during the rewarming. This led Amici and colleagues (2014) to propose that sleep pressure occurring soon after torpor would be a consequence of the intense, even if brief, activity experienced by the animal during the arousal phase to reach euthermia. This, in fact, may cause a neural hyperactivity that would require a neural renormalization via synapses downregulation (Tononi & Cirelli, 2014).

Interestingly, the rebound of REM sleep which followed the synthetic torpor bout, although present, was not large enough to compensate for the REM sleep loss during the hypothermic period. Apparently, however, it was large enough to compensate for the REM sleep loss observed during the rewarming phase, independently from the exposure, during the rewarming, to either Ta 28°C or Ta 37°C (Cerri et al., 2013).

1.3.5 RADIOPROTECTION

There are only two studies that evaluated radioresistance in models of synthetic torpor.

The first one was made in 1959 by Kuskin and colleagues, the purpose of this study was to evaluate the protective effect of the lytic cocktails and refrigeration, alone or in combination, in mice exposed to a lethal dose of whole-body x-irradiation.

Mice were divided into nine groups of about 120 each. The individual mice in each group were given an intraperitoneal injection of one of the drugs listed below, or one of two lytic cocktails, or a physiological saline solution. After that, about half of them remained in an environment at normal room temperature (22 °C) before irradiation, whereas the other half was placed in a freezer (-10 °C) until their rectal temperatures reached 20-23 °C. The drugs used were: Hydergine, chlorpromazine HCl, promethazine HCl, urethane, reserpine Pod. Two lytic cocktails were used: Hydergine mixture, which consisted of Hydergine, promethazine and urethane; and a chlorpromazine mixture, which consisted of chlorpromazine, promethazine, and urethane.

The results indicated that hypothermia immediately before radiation exposure caused a significant improvement in the chances of survival. Hypothermia, but not the drug administered, is the most important factor, how shown by the fact that in the refrigerated groups, the differences in survival rate between controls (not pre-treatment with drugs) and groups which were pre-treated with drugs was not statistically significant. The only effect of the drugs was to reduce the time needed to reach a core temperature of 20°C in the refrigerated group, maybe inhibiting the thermogenic responses (Kuskin et al., 1959).

The other study that evaluated radioresistance in artificial torpor is more recent (Ghosh et al., 2017). Authors used adenosine monophosphate (AMP) to trigger an hypometabolic state for a duration of 6 hours, 1–3 hours after lethal total body irradiation (8 Gy). This condition protected mice from radiation-induced lethality, and the effect was shown to be mediated by persistent hypothermia.

Moreover, authors also showed that the AMP-induced hypometabolic state reduced radiation-induced oxidative DNA damage and loss of hematopoietic stem cells (HSPCs). These effects seem to be mediated by the increase in interleukin-6 and interleukin-10 levels and by the shift towards an anti-inflammatory milieu that could be responsible for the augmented survival HSCs in the bone marrow, leading to effective hematopoietic recovery and increased survival (Ghosh et al., 2017).

2. AIMS

This thesis aimed at investigating the neurophysiological, molecular, and pathophysiological aspects of a model of synthetic torpor induced in a non-hibernator, the rat, by the inhibition of the RPa, a key brainstem thermoregulatory area. In fact, the local repeated administration of the GABA-A agonist muscimol in the RPa has been shown to induce a reversible inhibition of thermogenesis, leading to a progressive decrease in central Tb (down to approximately 20 °C when animals are kept a Ta 15°C), and to a concomitant inhibition of any behavioral activity, with a concomitant depression of the EEG activity (Cerri et al., 2013).

This model of synthetic torpor was used for three different studies aimed at expanding the knowledge on the functional changes occurring during and after synthetic torpor with a translational aim. A better understanding of these changes may lead to the standardization of safe procedures to be also used in humans and to the implementation of new therapeutic strategies.

The first experiment (EXPERIMENT I) aimed at investigating the changes in phosphorylation of the Tau protein in the spinal cord of rats at different time points during and after synthetic torpor. Tau is involved in the functional physiological regulation of the microtubule system, and through its phosphorylation/dephosphorylation processes plays a central role in the neural plasticity. Recently, the dysregulation of Tau phosphorylation has been intensively studied for its role in several neurodegenerative diseases, commonly defined as Tauopathies. It has been suggested that the pathologic neuronal death is triggered by the accumulation of hyper-phosphorylated Tau protein, both in the brain and in the spinal cord (Crespo-Biel et al., 2012; Guo et al., 2016). Interestingly, a transient and reversible accumulation of hyper-phosphorylated Tau was also described in some physiological conditions, such as during natural torpor in hibernating mammals, and more recently in the brain of rats, a non-hibernating species, induced into synthetic torpor (Luppi et al., 2019). Since the mechanisms underlying these changes in Tau are unknown, this study aims to broad the frame of knowledge about this phenomenon evaluating it also at spinal cord level, to better elucidate the underlying processes that induce the reversible accumulation of hyper-phosphorylated Tau in the central nervous system, without causing neurodegeneration. Since Tauopathies are thought to be in close relationship with neuroinflammation (Nilson et al., 2017), the microglia activation in the spinal cord was also assessed.

The second experiment (EXPERIMENT II) aimed at assessing the role of sleep which follows a period of synthetic torpor in the rat. Torpor is typically followed by a long bout of NREM sleep, with an intense delta activity (Deboer & Tobler, 1994), the physiological role of which is still widely debated: increased delta activity typically occurs during the sleep rebound which follows sleep deprivation. However some authors suggest that this process is not ascribable to a homeostatic regulation of sleep, since in some hibernators the suppression of the sleep rebound which follows the arousal from torpor apparently abolishes the sleep need, and the delta rebound is not postponed (Larkin & Heller, 1999). More recently, a study has shown that the increase in delta activity occurs also soon after synthetic torpor (Cerri et al., 2013). In light of the fact that NREM sleep plays a key role in neural plasticity, and that the arousal from torpor is associated with the dephosphorylation of Tau protein, a process which is also strongly related to neural plasticity, this experiment aimed at investigating the possible relationships between these phenomena. In particular, this experiment aimed at investigating: i) whether the increase in delta activity was postponed in rats in which the sleep bout which followed the exit from synthetic torpor was suppressed by gentle handling the animal; ii) the role of sleep in the process of Tau dephosphorylation after synthetic torpor by comparing the degree of phosphorylation in sleep deprived animals and animals which were left undisturbed following the return to euthermia.

The third experiment (EXPERIMENT III) aimed at evaluating the possible radioprotective effect of synthetic torpor and the underlying molecular mechanisms developed in hypothermic rats irradiated with X-rays. Some hibernators and facultative heterotherms, such as squirrels, hamsters, and mice (Cerri et al., 2016), can survive higher doses of radiation during torpid period compared to the euthermic period, due to unknown mechanisms. The possibility to mimic the radioresistance observed during natural torpor would be of great relevance in several fields, although, to date, it is unknown whether synthetic torpor in non-hibernating animals can be radioprotective. If this was the case, the induction of a condition of synthetic torpor in human subjects could be useful to change the radiotherapy approach in cancer patients and could also be useful for future long-term interplanetary travels: besides the advantage of reducing the metabolic rate and thus energy demands, torpor could be extremely valuable for space exploration in virtue of the increased radioprotection against cosmic radiation, that as of now is the biggest showstopper for interplanetary travels. The purpose of this study was to evaluate

whether synthetic torpor had radioprotective properties, by studying the histopathological and molecular characteristics of normothermic and hypothermic rats exposed to 3 Gy X-rays.

3. MATERIAL AND METHODS

All the experiments were performed in accordance with the DL 26/2014 and the European Union Directive 2010/63/EU, under the supervision of the Central Veterinary Service of the University of Bologna, after the approval of the National Health Authority (decrees 779/2017-PR; 112/2018-PR; 262/2020-PR). All possible efforts were made to minimize the number of animals used and their pain and distress.

3.1 EXPERIMENT I

3.1.1 ANIMALS

Experiments were performed on 17 Sprague-Dawley rats (Charles River), weighting approximately 201-225g. After their arrival, animals were acclimated for one week to standard laboratory conditions: light-dark cycle (LD cycle) 12h:12h (L 9:00-21:00) with ad libitum access to food (4RF21 diet, Mucedola, Settimo Milanese, Italy) and water, and Ta of 24 ± 0.5°C, light intensity of 150 lux at cage level. During the adaptation period, animals were housed in groups of two rats, in plexiglass cages (Techniplast) containing dust-free wood shavings; and the bedding was changed every two days.

3.1.2 PREOPERATIVE PROCEDURES

Hypothalamic temperature (Thy) was measured through resin insulated thermistors (B10KA303N, NTC Thermometrix) of 0.3 mm diameter. The thermistors were previously inserted in a 21 G needle soldered to a 2-pin connector; insulated with electrode resin. The day before the surgery, thermistors were calibrated to evaluate their sensibility and linearity; to obtain the calibration, the end of the thermistor was introduced in a heated bath set at a temperature of 37°C, measured with a mercury thermometer (scale 34 °C - 42 °C), and was connected to the same amplifier in direct current used during the experimental day. The impedance was then measured at three different temperatures (37.0, 38.0, 39.0°C), and the three values were interpolated.

As for the thermistors, the electrodes for the EEG were prepared in advance: two copper wires (length 2 mm, diameter 0.3) covered by an insulating layer were suitably stripped for 1 mm at the ends, and soldered to the ends of two pins connected to a connector by tin soldering. During

the surgery two knots were made at the free ends of the threads, to avoid any damage to the dura mater during insertion through the cranial theca.

Cannulas for Raphe Pallidus injections were obtained from Bilaney Consultants GmbH and were disinfected with 70% alcohol solution prior to use.

3.1.3 SURGERY

Before each surgical session, animals were administered with the pre-anesthetic Diazepam (Valium Roche, 5 mg / Kg intramuscular) and after sedation was obtained, they were anaesthetized with an intraperitoneal injection of Ketavet (Ketamine -HCl, Parke-Davis, 100 mg / Kg). After confirming the surgical plane of anesthesia by the absence of blink and toe-pinch reflexes, the trichotomy of the skull was carried out using a small animal shaver. The exposed skin was disinfected with iodine solution to avoid bacterial contamination of the surgical field. The animal was then positioned on a stereotaxic frame (Kopf instruments), with the aid of a transverse support bar for the jaw (muzzle blocking bar, 4 mm) and two ear bars inserted gently in the external auditory meatus, in order to maintain the head firm; the scalp was incised in the midline from the frontal bone to the nuchal muscles with a surgical sterile blade. The periosteum was removed, and the cranium surface was cleaned, making the cranial sutures clearly visible. Using a 0.5 mm of diameter drill tip, four holes in the cranium were made, two on the left and right frontal bones (in antero-lateral position), and two on the left and right parietal bones (in postero-lateral position), to implant four stainless steel screws to ensure all the inserted probes in place. Another hole of the same dimensions was made close to bregma and above the right anterior hypothalamus to insert the calibrated thermistor to record deep brain temperature. After that, 1 hole on the parietal bone (4mm Anterior Posterior (AP), 2mm Lateral Latero (LL) from bregma) and 1 hole on the frontal bone (-3mm AP, 2mm LL from bregma) for implantation of registering and reference electrode for the EEG measurement were made. In the end, 1 hole in the occipital bone for the insertion of a guide microcannula (C315G-SPC, Plastics One; external gauge of the guide cannula: 0.46 mm; extension of the internal cannula from the pedestal: +3.5 mm; external caliber of the internal cannula: 0.20 mm) suitable for the administration of solutions at the RPa level (from -9.7 mm to -14 mm AP; 0 mm LL; -9.5 DV from bregma). The craniotomy was made following the coordinates of “The Rat Brain in Stereotaxic Coordinates” (Paxinos & Watson, 2007) (Fig. 11).

A functional test was performed during the surgery in order to verify the correct positioning of the guide cannula. GABA-A agonist muscimol (100nl 1mM) was injected, and the tail temperature was monitored via a thermistor positioned on the skin surface of the tail. Since the inhibition of Raphe Pallidus neurons causes massive vasodilation (Blessing & Nalivaiko, 2001), the positioning was presumed correct if a clear increase in tail surface temperature was detected within 5 minutes from muscimol injection. In absence of any physiological response, the DV and LL coordinates were adjusted and the test repeated. Correct positioning was always achieved within the second attempt. When the cannula was assessed to be in the right position, it was fixed with dental resin (ResPal), covering the whole surgical field, incorporating the thermistor, the EEG electrodes, and the screws.

At the end of the surgical procedure wide-spectrum antibiotics (benzathine benzylpenicillin, 12.500.000 U.I., dihydrostreptomycin sulphate 5 g/100 mL, Rubrocillina Veterinaria, Intervet—1 mL/kg) were injected to prevent any postoperative infections and 5 ml of physiological solution were administered subcutaneously for the rehydration of the animal. The post-operative pain was prevented by the administration of an analgesic (Rimadyl - Carprofen 5mg/ml, subcutaneously). After the surgery, each animal was individually housed to prevent injuries caused by other animals in the presence of surgical implants. However, during the week of post-operative recovery, the operated animals maintained visual and olfactory contact with the other rats to mitigate the effects of isolation. During the whole week after surgery the animals were kept under close observation by an operator and the veterinary doctors of the Centralized Veterinary Service. The animal's pain, distress or suffering symptoms were constantly monitored using the Humane End Point (HEP) criteria. Animals that displayed some degree of suffering symptoms were administered, as needed, with 5mg/kg of Rimadyl (Carprofen 5mg/ml, Pfizer).

3.1.4 EXPERIMENTAL SET-UP

After recovery from surgery, three days before the experimental session, animals were moved to the recording cages, where they were connected to the instrumentation used to record physiological parameters. The experimental cages were positioned in a thermoregulated and sound-attenuated box, which consists of a modified freezer that allows fine control of the Ta by means of a thermostat connected to the freezer compressor and to an electric stove (1500 W) positioned inside it. The thermostat activates the compressor or stove respectively whenever

the temperature differs from that set by the operator. The modified freezer box was also equipped with a ventilation system, a black and white video system (Philips) for monitoring the animal's behavior, an illumination system consisting of optical fibers (100 lux) controlled by a timer, each box can contain a maximum of two recording cages, each instrumented with a rotating swivel, connected to the external amplifiers, positioned on a tilting arm above the cage, that allows the animal to move freely during the experiment.

Three days before the experiment, the EEG connector and the thermistor of the animals were connected to the swivels with copper wires, to acquire baseline of Thy and EEG activity. Data were recorded (EEG and Thy), amplified (mod. Grass 7P511L, Astro-Med Inc, West Warwick (RI), USA) and filtered with a high pass and low pass filter with the following values for each bioelectric signal: EEG 0.3 Hz / 30 Hz and Thy 0.5 Hz (for the high pass), and finally converted from analog to digital (12-bit analog-digital, CED Micro MK 1401 II) to allow the storing on a digital hard drive with a sampling rate of 500 Hz for the EEG and 50 Hz for Thy. EEG signal was subjected to a spectral analysis every second using the Fourier transform algorithm (FFT). In this way, the power density values for the Delta (0.75-4 Hz) Theta (5.5-9 Hz) and Sigma (11-16 Hz) bands were obtained.

During the adaptation and the experimental period rats were exposed to a moderately below thermoneutral Ta (15°C), constant darkness and were fed a high-fat diet (35% fats, Mucedola), all environmental conditions known to facilitate the occurrence of a torpor in hibernators (Cerri et al., 2013).

3.1.5 EXPERIMENTAL PLAN

Animals were randomly assigned to six different experimental groups and were sacrificed at different times following the injection of either muscimol or artificial cerebrospinal fluid (aCSF) (first injection at 11.00h). An illustrative scheme of the protocol is shown in Fig. 12. The experimental groups were the following:

1) Control (C); injected with aCSF (N=3) and culled at around 17.00h, to match the experimental time of the N nadir condition.

2) Nadir 30 °C (N30); culled at around 12.00h-13.00h, between the second and third injection of muscimol, when Thy reached the level of 30 °C (N=3).

3) Nadir (N); culled 1h after the last injection, at 17.00h, when brain temperature reached the nadir of hypothermia (N=3; Thy= 22.1±1.4°C mean ± SEM).

4) Early-recovery (ER); culled around 19.00h (2h after Ta was increased from 15°C to 28°C) when brain temperature reached 35.5 °C after synthetic torpor; at this specific central temperature, animals began to show clear signs of sleep at the EEG level (N=3).

5) Recovery 6 hours (R6); culled around 01.00h, 6 hours after ER (N=3).

6) Recovery 38 hours (R38); culled at around 09.00h of the third day, 38 hours after ER (N=2).

3.1.6 MICROINJECTIONS

The microinjection apparatus has been developed in our laboratory and consists of: i) a Teflon tube, 1 meter long and with a constant diameter along its entire length (DI0.2mm, FEP-Tubing 4001005 10X1m Microbiotech / se AB, Stockholm, Sweden), ii) two watertight connectors that connect one end of the tube with the internal cannula (fitted to implanted guide cannula) and the other with a Hamilton syringe (5 µl, Hamilton Company, Bonaduz, Switzerland). Before each experimental session, the tube and cannula are filled with the substance to be injected (muscimol or aCSF), while the syringe is filled with mineral oil and hydrophobic dye. The interface created between the dye and the oil allows the operator to verify, by using a stereoscopic microscope and a centimeter suitably positioned under the tube, drug movement in the tube and to control the injected volume. The prepared syringe is placed on an infusion pump (Harvard Apparatus), with the infusion rate set at 0.3 µl/min, positioned outside the registration box so as not to disturb the animals during the injection (Fig. 13).

3.1.7 PERFUSION

According to the experimental plan, animals under general anesthesia were transcardially perfused with 200 ml of saline solution (0.9% NaCl, weight / volume) followed by an equal amount of paraformaldehyde 4% (weight / volume) (Sigma-Aldrich, St Louis, MO, USA) in phosphate buffer (0.1 M, pH 7.4) solution. In this procedure, a peristaltic pump was used, connected to a perfusion needle (16 G), loaded before perfusion with saline solution, subsequently replaced by 4% paraformaldehyde. After verifying the anesthesia plane, a thoracotomy was performed to expose the heart, followed by the insertion of the perfusion

needle into the aorta. Subsequently, the needle was fixed with a hemostatic clamp and the peristaltic pump was switched on, and a cut was made at the level of the right atrium of the heart to allow the excess liquid drainage. Having ascertained the successful removal of the blood by verifying the discoloration of the liver and limbs, saline solution was replaced with paraformaldehyde to fix the organs. At the end of the procedure the spinal cord was extracted, post-fixed for an hour and a half in paraformaldehyde, immersed in a 30% sucrose solution with NaN_3 and kept at 4 ° C overnight.

3.1.8 IMMUNOHISTOCHEMISTRY

Spinal cords were cut with a cryostat (Reichert-Jung, 2800 Frogocut-N), set at a temperature of - 22 ° C, in 35 μm coronal sections, for subsequent immunohistochemical analysis. Prior to cutting, any residues of meninges were removed from the samples and a first rough cut of the spinal cord was made at cervicothoracic lumbar level with a brain blocker (PA 001 Rat Brain Blocker, David Kopf Instruments). The samples were then mounted on the cryostat cutting base with an embedding medium (Killik, Bio Optica Milano s.p.a). Slices were then washed in a 10 mM phosphate buffered saline (PBS) and stored in a cryoprotective solution at a temperature of -70 ° C until used for immunohistochemical analysis.

The immunohistochemical procedure was aimed to assess the presence of the following antigens: The Tau in the phosphorylated and not-phosphorylated isoforms and NeuN, a neuronal soma marker that helps in the anatomical identification of the sections. To evaluate different spinal cord regions, for each animal we used 10 slices from the cervicothoracic and lumbar region respectively (Fig. 14). Slices were rinsed twice in PBS and then incubated for 2 hours in Antibody Dilution Solution (ADS) made with normal donkey serum (Sigma-Aldrich, St Louis, MO, USA). Afterwards, all slices were incubated overnight with the following primary antibodies:

i) monoclonal rabbit Anti-NeuN (Merck-Millipore; 1:400 dilution), a neuronal soma marker.

ii) monoclonal mouse Anti-AT8 (Thermo Fisher; 1:400 dilution), marker of the phospho-[Ser202/Thr205]-Tau protein. As control for the AT8 detection, the same procedure was carried out using the monoclonal mouse Anti-Tau-1 (Merck-Millipore; 1:400). This primary antibody detects Tau protein when it has no phosphorylation between residues from 189 to 207.

Slices were then rinsed twice in PBS with 0.3% (v/v) Triton X-100. To mark the conjugated primary antibodies, the sections were moved in a second incubation solution made with secondary antibodies conjugated with fluorochromes in ADS for 2 hours. The following secondary antibodies were used:

i) Donkey Anti-rabbit IgG conjugated with Alexa-488 (Thermo Fisher).

ii) Donkey Anti-mouse IgG conjugated with Alexa-594 (Thermo Fisher). This secondary antibody was used for both the Anti-AT8 and the Anti-Tau-1.

Both secondary antibodies were diluted at 1:500. After the 2-hour incubation, paying attention not to expose the sections to bright light to avoid fluorescence fading, the sections were once again rinsed in PBS 10mM, and mounted by free floating technique on glass slides pre-treated to allow better adhesion of the sections (Superfrost Plus, Thermo Scientific Menzel). Slides were left to air-dry overnight and then covered with the coverslips and an anti-fading agent (Prolong-Diamond Antifade, Invitrogen). The slides were then placed in a slide holder box kept at 4 ° C.

Further immunohistochemical analyses were performed to assess the presence of the Glycogen-synthase kinase-3-β (GSK3-β), considered to be the main kinase responsible for the phosphorylation of Tau protein. GSK3-β is inactive when phosphorylated at Ser9, thus preventing the phosphorylation of Tau (Frame et al., 2001). Its involvement in the Tau phosphorylation processes has been evaluated in this experiment by quantifying the expression of phospho-[Ser9] -GSK3-β.

A discrete sample of sections was stained for phospho-[Ser9]-GSK3-β, with a specific rabbit primary antibody (Sigma-Aldrich; 1:200 dilution), and marked with Donkey anti-rabbit IgG conjugated with Alexa-488 (Thermo Fisher; 1:500 dilution).

Furthermore, the regulation of GSK3-β activity in motor neurons of the spinal cord was also studied, running a double staining experiment on those samples stained for P-GSK3-β: specifically, an additional staining for choline-acetil transferase (ChAT) with a specific goat primary antibody (Merk-Millipore; 1:300 dilution), and marked with Donkey anti-goat IgG conjugated with Alexa-555 (Thermo Fisher; 1:500 dilution) was carried out. Procedure steps were the same as described earlier.

Moreover, since Tauopathies appear closely related to neuroinflammation (Nilson et al., 2017; Ransohoff, 2016), suggesting a role played by immune system and in particular microglia in the Tau phosphorylation processes (Davies et al., 2017), we also assessed the microglia activation during the experiment.

Microglia was specifically stained with the rabbit polyclonal Anti-Iba1 antibody (Wako Chemicals; 1:800 dilution) and the secondary antibody Anti-rabbit IgG conjugated with Alexa-488 (Thermo Fisher; 1:500 dilution). The procedure was the same as previously described.

3.1.9 IMAGE ACQUISITION AND ANALYSIS

Images were acquired with a Nikon Eclipse 80i microscope, connected to an image acquisition camera (Nikon Digital Sight DS-Vi1), at 100x magnification (200x for the microglia staining).

Among the collected sections, per each rat, those in best conditions were chosen for image acquisition. Three pictures per single section were taken, both for cervicothoracic and lumbar level, as follows (fig. 14):

i) framing one hemi-ventral part, including the ventral horn (VH)

ii) framing one hemi-central part, including the central canal (Central)

iii) framing one hemi-dorsal part, including the dorsal horn (DH).

The visual recognition of these structures was possible through the observation of NeuN staining (Alexa-488) of the whole section and comparing it with the atlas. Distinguishing the different levels of the spinal cord was possible by roughly evaluating the white to gray matter ratio, being clearly smaller in cervicothoracic sections (Paxinos & Watson, 2007).

Each microscopic field was acquired in two separate pictures that were distinct according to the fluorochrome used, in order to have NeuN (Alexa-488) for the anatomical identification and AT8 or Tau-1 (Alexa-594) for the Tau isoforms staining for each picture taken. In addition, to create digital pictures that best reproduce the variations of staining intensity observed for AT8 and Tau-1 at the microscope oculars, the exposure time of the camera was manually regulated. This fine regulation of the exposure time was necessary to avoid automatic compensations of

the camera that may interfere with the subsequent evaluation of the staining intensity. All other camera settings were left unchanged.

The analysis was carried out with a qualitative approach, two operators blindly and independently evaluated the fluorescence intensity corresponding to the AT8 and Tau-1 in the structures of interest. The estimation was given while observing pictures on a computer monitor (using Windows Photo Viewer) and scoring the intensity on a scale of 5 levels, using the following criteria:

i) "-" complete absence of the signal

ii) "+" weak signal intensity

iii) "++" intermediate signal intensity

iv) "+++" high staining signal

v) "++++" maximum signal strength

The final score was obtained by averaging the scores given by the two experimenters and averaging the two spinal cord levels considered, and all the animals belonging to the same experimental condition.

Staining for P-GSK3-β/ChAT was qualitative and carried on two samples from a single rat per experimental condition.

Microglial activation is characterized by measurable morphological changes (Banati, 2002; Davies et al., 2017), in our experiment the activation level of microglia was measured following established morphometric parameters:

i) Soma area

ii) Arborization area

iii) Morphological index (MI): soma area/arborization area ratio

iv) Microglial density (counting the number of cells in every picture taken)

v) Nearest neighbor distance.

Measurements were carried on using Image Pro Analyzer 7.0 (Media Cybernetics) with the inbuilt calibration function.

3.1.10 STATISTICAL ANALYSIS

Tau staining was analyzed on two levels: i) "gross analysis", considering the scores of all the structures analyzed as one value; ii) "fine analysis" considering separately the three frames examined. We used the non-parametric Kruskal-Wallis test and, only if the null hypothesis was rejected, pairwise comparisons were carried out using the non-parametric Mann-Whitney test in the following evaluations: i) all the experimental conditions vs. C; ii) R6 vs. ER; iii) R6 vs. R38. Significance level was preset at $p<0.05$ for all comparisons.

For microglial activation levels, the statistical analysis was carried out with a one-way ANOVA, considering only C, N, R6 and R38 experimental groups and independently for VH and DH of the spinal cord. Where ANOVA comparison was significant, the following post-hoc comparisons were carried on with the modified t-test (t*), with α level opportunely modified following the sequential Bonferroni method: i) all the experimental conditions vs. C; ii) R6 vs. N; iii) R38 vs. N. Significance level was preset at $p<0.05$ for all comparisons.

No statistical analysis was performed for P-GSK3-β/ChAT, intended as merely qualitative data.

All the statistical analyses were performed using IBM SPSS Statistics 21.0 version.

3.2 EXPERIMENT II

This experiment was designed to investigate two aspects of torpor: in particular, the first part of the experiment was focused on the electrophysiological characterization of sleep following synthetic torpor, while the second was focused on the neuromolecular aspects implicated in the recovery and sleep processes following synthetic torpor.

3.2.1 ANIMALS

12 Sprague-Dawley rats (Charles River) were used for the first part of the experiment, and 17 for the second part, the latter involved some already published data (Di Cristoforo, 2017, *Ph.D. thesis*) but the numerosity of the experimental groups has been increased, in particular a new

experimental condition of sleep deprivation has been added. Further, also the whole Tau-1 analysis was an original work of this thesis. The housing conditions of the animals were the same as described for the experiment I.

3.2.2 PREOPERATIVE PROCEDURES

Nuchal Electromyography (nuEMG) electrodes were built from pairs of stainless-steel wires, (mod. AS 632, Cooner Wire Inc., Chatsworth (CA), USA) covered with an insulating polyethylene sheath, 8 cm long (nuEMG), 3 mm of insulating sheath at the ends and 2 mm of sheath at half the length of the wire have been removed to allow signal transmission.

3.2.3 SURGERY

All rats underwent the same surgical procedures described in the experiment I, in addition to that, the 12 rats used for the first part of this experiment were also implanted for registration of nuchal muscle activity, to aid sleep scoring.

Nuchal muscles were exposed and by means of a suture needle, nuchal electrodes were inserted into the muscles and made to slide up to bring the central part, without any sheathing, in direct contact with muscle tissue. After that, the electrode wires were brought out subcutaneously from the cut on the skin surface above the skull, where the two ends of each wire were joined and connected to a two-pin connector. After completing all the surgical procedures (see experiment I), connectors for EEG and nuEMG, the guide cannula, the thermistor, and the screws were finally fixed on the skull with a self-curing acrylic resin (ResPal). At the end of the surgery animals received the post-operative treatments as experiment I.

3.2.4 EXPERIMENTAL SET-UP

In addition to the experimental set-up used for the experiment I, in this experiment the bioelectric signal recorded by the nuchal electrodes was amplified (mod. Grass 7P511L, Astro-Med Inc, West Warwick (RI), USA) and filtered with a high pass and low pass filter respectively of 10 Hz / 3000 Hz, converted from analog to digital (12-bit analog-digital, CED Micro MK 1401 II) and saved on a digital hard drive with a sampling rate of 1KHz.

3.2.5 EXPERIMENTAL PLAN

After one week of post-surgery recovery, animals were assigned to the different experimental groups (fig. 15).

The experimental plan of the first part of this experiment included the following 2 experimental conditions:

i) Recovery 6 hours with sleep deprivation (R6 SD); following synthetic torpor, as soon as the brain temperature reached 35,5 °C and clear signs of sleep were observed in the EEG activity, animals were sleep deprived by gentle handling (Franken et al., 1991) for 6 hours (N=6).

ii) Data were compared with a set of data of animals in Recovery 6 hours condition (R6); in which following synthetic torpor, as soon as the brain temperature reached 35,5 °C, animals were left to sleep and recover undisturbed from this point for 6 hours (N=6). Data of the R6 group were taken from (Cerri et al., 2013).

For this part of the experiment the neural activity of these animals had to be recorded for 3 consecutive days in total, one day of baseline, the day of the experimental protocol and the day after, thus only at the end of the third day of recording the animals were sacrificed.

For the second part of the experiment the following experimental conditions were used:

i) Control (C); in this condition animals were injected with aCSF in the raphe pallidus and sacrificed at around 17.00 h (N=3).

ii) Early recovery (ER); animals were sacrificed at around 19.00 h when, after synthetic torpor, the brain temperature reached 35.5 °C (N = 4).

iii) Recovery 6 hours (R6); following synthetic torpor, as soon as the brain temperature reached 35,5 °C, animals were left to sleep and recover undisturbed from this point for 6 hours (N=5).

iv) Recovery 6 hours with sleep deprivation (R6 SD); following synthetic torpor, as soon as the brain temperature reached 35,5 °C and clear signs of sleep were observed in the EEG activity, animals were sleep deprived by gentle handling (Franken et al., 1991) for 6 hours (N=5).

Unlike the first part of the experiment, for this second part the animals were sacrificed by intracardiac perfusion immediately after the experimental protocol, i.e. after 6 hours of recovery in R6 and R6 SD, around 17:00h for the control group and around 19:00 h for the early recovery group.

3.2.6 SIGNAL RECORDING AND DATA ANALYSIS

For the first part of the experiment the EEG power spectrum was calculated from a 4 s long 1 s sliding window. EEG total power and power bands Delta (0.75-4 Hz) Theta (5.5-9 Hz) e Sigma (11-16 Hz) were normalized to the mean value (100%) of the baseline recording of Day 1. The scoring of the sleep stages was performed visually by an operator (1 second of resolution), using a script for Spike2 (sleep score). Standard criteria based on EEG, nuEMG, and brain temperature signals were used to score wake, NREM sleep, and REM sleep (Cerri et al., 2005; Franken et al., 1991). The time for the minimal duration of a single wake–sleep episode was considered 8 seconds for NREM sleep and REM sleep, and 4 seconds for Wake.

3.2.7 IMMUNOHISTOCHEMISTRY

In the second part of this experiment, after the experimental procedures animals were perfused (see experiment I) the brain was extracted and post-fixed for an hour and a half in paraformaldehyde 4% and then kept in a 30% sucrose solution with NaN3 at 4 ° C until the day of cutting.

Before cutting, any residues of meninges, peripheral nerves and areas not of interest for immunohistochemical analysis were removed, after that a first rough cut of the brain was made at the level of the median eminence with the help of a brain blocker (PA 001 Rat Brain Blocker, David Kopf Instruments). Afterwards, the samples were positioned on the cryostat cutting base using an embedding medium (Killik, Bio Optica Milano s.p.a) for the subsequent cutting, through which coronal sections of 35 μm were obtained. During the cutting operation, the slices were collected in rotation in 6 different wells to obtain different samples of brain sets, all equal. At the end of the procedure, the slices obtained were washed in a 10 mM PBS and stored in a cryoprotective solution at -70 ° C until the start of the immunohistochemical protocol.

The same immunohistochemical procedures of experiment I were used to detect the presence of Tau protein in the phosphorylated and not-phosphorylated isoforms and the neuronal marker

NeuN, but in this case on brain slides. The main analysis focused on the phosphorylated Tau detected with the antibody Anti-AT8 (Thermo Fisher; 1:400 dilution), marker of the phospho-[Ser202/Thr205]-Tau protein. The data was obtained from 4 animals in R6 condition, 5 in R6 SD, 2 in control, and 4 in ER group. In addition, data about the antibody Anti-Tau-1 (Merck-Millipore; 1:400), marker of Tau not phosphorylated between residues from 189 to 207, was obtained from: 3 brain sets of animals in R6 SD condition, 2 brain sets of animals in R6 condition and 3 in control group.

3.2.8 IMAGE ACQUISITION AND ANALYSIS

The same apparatus of image acquisition of experiment I was used. 19 brain areas were analyzed (Fig. 16) characterized by different functions and belonging to different anatomical structures in a caudal to rostral direction: nucleus ambiguus (Amb); dorsal motor nucleus of the vagus nerve (dMV); nucleus of the solitary tract (NTS); raphe pallidus (RPa); locus coeruleus (LC); lateral parabrachial nucleus (LPB); ventrolateral part of the periaqueductal grey matter (VLPAG); medial mammillary nucleus (MM); lateral hypothalamus (LH); arcuate nucleus of the hypothalamus (Arc); dorsomedial nucleus of the hypothalamus (DMH); paraventricular nucleus of the hypothalamus (PVH); ventrolateral preoptic nucleus (VLPO); median preoptic nucleus of the hypothalamus (MnPO); paraventricular nucleus of the thalamus (PV); cerebellum cortex (Cb-Cx); CA3 field of the hippocampus (CA3); perirhinal cortex (PRh); parietal cortex (P-Cx). A summary of the characteristics and function of each area is displayed in Fig. 17.

The analysis of the images obtained was carried out with the same criteria used for experiment I.

3.2.9 STATISTICAL ANALYSIS

For the first part of this experiment, all values are reported as mean ± S.E.M. The statistical analysis was developed using SPSS 21.0, a two-way ANOVA test was used for repeated measurements. The post-hoc comparisons were made by means of a modified t-test, with significance set at $p<0.05$.

For the second part of the experiment, the statistical analysis was carried out in two steps: i) gross analysis, where all the brain areas were considered as a single structure; ii) fine analysis,

in which each structure was analyzed individually, by means of the Mann-Whitney nonparametric test, for both AT8 and Tau-1 staining all the experimental conditions were compared with R6 SD. Significance level was preset at $p<0.05$ for all comparisons.

3.3 EXPERIMENT III

3.3.1 ANIMALS

This experiment was conducted on 10 male Sprague-Dawley rats (Charles River), weighing 250–300 g. The housing conditions were the same as previously described.

3.3.2 EXPERIMENTAL PLAN

Animals underwent the same surgical procedures described for experiment I, and following the post-operative period of recovery, 48 hours before the experimental procedure of induction of synthetic torpor, animals were moved to the experimental cages and their thermistors were wired to the swivels, in order to acquire baseline brain temperature.

For this study, animals were divided in two experimental groups (fig. 18):

i) Hypothermia (N = 5): Animals from this group were injected with the GABA-A agonist muscimol (1 mM) within the Raphe Pallidus (RPa). Starting from 07:00 h, each rat had one injection per hour of 100 nL. All animals entered synthetic torpor rapidly after the first injection and maintained such condition until the end of the experiment.

ii) Control (N = 5): In this experimental condition animals were injected with aCSF within the RPa. Each animal, matching the hypothermic group injections, received, starting from 07:00 h, one injection per hour (100 nL).

In order to reduce as much as possible any environmental difference, animals underwent the experiment in couples: each animal from the Hypothermia group underwent the procedure on the same experimental day as its corresponding Control. After 4 hours from the first injection, at 11:00 h, each animal of the experimental couple of the day was moved to a transportable thermoregulated and sound attenuated radiotransparent custom-made box, which had a ventilatory system and the Ta set at 15 °C. Inside these boxes the animals were transported to the Department of Nuclear Medicine, Sant'Orsola Hospital, to be irradiated with X-rays. After

about 15 minutes long irradiation, animals were returned to the experimental cages. After 4 hours from the irradiation, they received a lethal dose of anesthetic (500 µl of Ketavet) and several organs were collected for histological and molecular assays, the complete list is showed in fig. 19.

3.2.3 RADIATION DATA

The transportable boxes containing the animals were irradiated from above, one at a time, using an X-ray tube operating at 180 kV, producing a uniform radiation field throughout the region where the animal was located, administering a dose of 3 Gy total body, with a dose of 23 cGy/min. The use of a radiochromic film, placed below the demarcated area in which the animal was located, allowed an accurate estimate of the distribution and the gradients of the absorbed dose (fig. 20).

3.2.4 HISTOLOGICAL ANALYSIS

The whole organs or fractions dissected for the histological analysis were fixed in 4% paraformaldehyde overnight at 4 °C. After 24 hours, samples were washed in PBS (10mM) to eliminate excess fixative and stored in 70% ethanol. Following the complete dehydration of the tissues by treating them with increasing concentrations of alcohols up to absolute ethanol, the samples were clarified through incubation in xylene for 30 minutes, to optimize the subsequent embedding in paraffin. The latter was warmed up, using a thermostatic stove set at 58 °C, to allow its melting and therefore the inclusion of the samples; after 6 hours of incubation the samples were embedded in paraffin blocks and left to solidify. Subsequently, the microtome cut was made and cross sections of 7 µm were obtained, then stained with hematoxylin-eosin to show general morphology. This staining involved two dyes in succession: Hematoxylin colors negatively charged cellular components, such as nucleic acids, membrane proteins and cell membranes, in violet blue. These components are called basophils and are found mainly at the level of the nucleus, which therefore assumes a blue color. Eosin, on the other hand, stains positively charged components in pinkish red, such as many cellular proteins, mitochondrial proteins, collagen fibers. These components are called eosinophils or acidophiles and cause a pinkish coloration of all the remaining cellular areas, the cytoplasm, and extracellular substances. However, since the histological dyes are soluble in water, before the staining, the sections were deparaffinized in xylene, rehydrated in descending alcohol series, from absolute

ethanol to 50% alcohol and finally in water, and then stained by placing the sections in a solution of Mayer's hematoxylin for about 10 minutes; followed by washing in source water and the staining of the cytoplasm by incubation in a 0.25% eosin solution. Finally, after removing the excess dye by washing in 75% ethanol, sections were dehydrated again, clarified in xylene and mounted on glass slides with DPX mounting media. Thus, on the slides obtained, the cytohistological evaluation was performed under an optical microscope.

These histological analyses were carried out at the Department of Science and Technology, Parthenope University of Naples.

3.2.5 GENE EXPRESSION

From each organ designated for molecular analysis, small tissue fragments were obtained and collected in Eppendorf tubes containing 600 µl of the RNA later (Ambion), a tissue storage reagent that stabilizes and protects cellular RNA, in order to postpone the processing of the samples without compromising the quality and quantity of the RNA itself. After a few minutes at room temperature to facilitate the penetration of the reagent into the tissue, the samples were stored at -70 °C pending subsequent analyses.

To date this analysis has only been carried out on liver and testicle tissues. On the liver, the gene expression was assessed by a Custom RT2 Profiler PCR Arrays from Qiagen. 13 genes were profiled on 1 array in a biological triplicate. Each array also included a panel to control genomic DNA contamination (GDC), first strand synthesis (RTC), and the real-time PCR efficiency (PPC). To have an overview of the cell functions, a heterogeneous group of genes involved in different pathways of cell metabolism, regulation of clock genes and DNA damage were considered.

In testicles the gene expression was assessed by a DNA Damage Signaling RT2 Profiler PCR Arrays from Qiagen. 84 genes were profiled on 3 arrays in a biological triplicate. As for the liver, the arrays contain a panel of controls for genomic DNA contamination (GDC), first strand synthesis (RTC) and the real-time PCR efficiency (PPC).

The procedures used were the following: mature RNA was isolated from tissues using an RNA extraction kit (QiagenRNeasy Plus Micro Kit, Hilden, Germany), and its quality was verified using a spectrophotometer (NanoDrop™ 2000 Spectrophotometer, Thermofisher). 1000 ng of

extracted RNA was used for the reverse transcription, the latter was performed using a cDNA conversion kit (Qiagen QuantiTect Reverse Transcription Kit, Hilden, Germany). For the liver analysis, the cDNA in combination with a fluorescent interlayer (RT2 SYBR® Green qPCR Mastermix) was used on a Custom RT2 Profiler PCR Array. For the testicles, the cDNA, always in combination RT2 SYBR® Green qPCR Mastermix, was used on a real-time RT2 Profiler PCR Array (QIAGEN, Cat. no. PARN-029Z). The CT (cycle threshold) values obtained and normalized were exported to an Excel file and a table was created, then uploaded to web portal for data analysis and graphing (http://www.qiagen.com/geneglobe). Samples extracted from animals irradiated in normothermia were assigned to the control group, while samples of animals irradiated in synthetic torpor were assigned to the experimental group. CT values were normalized based on a manual selection of reference genes. The relative quantification of the target genes was obtained according to the delta-delta CT method, which provides: i) the delta CT calculated between the gene of interest (GOI) and an average of housekeeping genes (HKG); ii) the calculation of the delta-delta CT given by the comparison between the delta CT of the experimental group and the delta CT of the control group; iii) finally the calculation of the fold change, using the 2^(delta-delta CT) formula. The quantification allows the evaluation of the differential expression of a transcript in the two different experimental conditions.

The gene expression analyses were carried out at TIFPA, Trento Institute for Fundamentals Physics and Applications, Istituto Nazionale Fisica Nucleare.

3.2.6 STATISTICAL ANALYSIS

P values were calculated based on a Student's t-test of the replicate 2^(-Delta CT) values for each gene in the control group and experimental group. Gene expression data are presented with a Volcano Plot scheme. The volcano plot combines a p-value statistical test with the fold regulation change facilitating identification of genes with both large and small expression changes that are statistically significant ($p<0.05$).

4. RESULTS

4.1 EXPERIMENT I

4.1.1 AT8 AND TAU-1

Since no differences were observed among the two anatomical levels of the spinal cord, all the statistical analyses were carried out by combining the data from the cervicothoracic and lumbar level. An overview of the results is displayed in figure 22.

The "gross" analysis was performed to obtain an overview of the Tau phosphorylation pattern in the whole spinal cord, the immunoreactivity was significantly higher for AT8 ($p<0.001$), and lower for Tau-1 ($p<0.001$) in N compared to C. Additionally, only for AT8, staining intensity was significantly lower in R6, compared to C ($p<0.001$), ER ($p<0.001$), and R38 ($p<0.001$).

The "fine" analysis was carried out by considering the dorsal horn (DH), central canal (Central), and ventral horn (VH) as separate structures, and revealed that AT8 immunoreactivity was significantly higher in N compared to C in Central ($p=0,004$) and DH ($p=0.006$), but, surprisingly, it was not in VH ($P=0,418$). Only in DH, AT8 staining was significantly higher ($p=0,014$) in N30 vs C. For the R6 condition, differences in AT8 immunoreactivity were as follow: staining was significantly lower than C (VH: $p=0,006$; Central: $p=0,002$; DH: $p<0.001$), ER (VH: $P=0,006$; Central: $p=0,001$; DH: $p<0.001$), and R38 (VH: $p<0.001$; Central: $p<0.001$; DH: $p=0,002$).

Tau-1 immunoreactivity was significantly lower in N compared to C for all the three structures analyzed (VH: $p=0,002$; Central: $p<0.001$; DH: $p<0.001$). Only in VH, R6 was significantly lower than C ($p=0,017$), ER ($p=0,012$), and R38 ($p=0,049$).

Exemplificative images of immunohistochemistry for the dorsal and ventral horn are shown in figures 22 and 23.

4.1.2 P-GSK3-β

Staining for the isoform of GSK3β phosphorylated on serine 9 (the inactive form of GSK3β) showed positive cells only within the VH (see figure 24), while no staining was found in the DH or in the area of the central canal. Qualitative results from the double-staining experiment,

where the P-GSK3-β was stained in combination with cholinergic neurons (ChAT), showed a very frequent co-localization of the two antigens, as represented in figure 25.

4.1.3 MICROGLIA

Analysis of the microglia morphology, performed with the intent of verifying the possible activation of a neuro-inflammatory response, potentially implicated in the process of phosphorylation and dephosphorylation of the Tau protein, showed very few statistically significant differences in the various structures and conditions analyzed (fig. 26). In particular, only the morphological index (MI) was significantly lower (indicating a resting phenotype of the microglia) in N compared to C ($p=0,006$) and R38 ($p<0.001$): both differences were limited to the DH ($F_{3,36}=2,904$; $p=0,048$). No statistically significant differences were found for all other morphometric parameters examined.

An illustrative image of the immunoreactivity of Iba-1 is shown in figure 27.

4.2 EXPERIMENT II

4.2.1 ELECTROENCEPHALOGRAPHIC ANALYSIS

The comparison between the amount of NREM sleep and the power in the delta band of the EEG in rats which were left undisturbed for 6-h period after the arousal from synthetic torpor (fig. 28), and rats which were sleep deprived by gentle handling (fig. 29), is shown in Fig. 30. Data for animals which were left undisturbed were taken from (Cerri et al., 2013). Sleep deprived animals showed a large increase in delta power at the beginning of the recovery period which followed sleep deprivation (281±13%), that was significantly higher ($p<0.05$) than that observed in the control group (237±19%) .

4.2.2 AT8 AND TAU-1

4.2.2.1 GROSS ANALYSIS

This first step of the Tau phosphorylation analysis compared the experimental condition of recovery with sleep deprivation vs. all other experimental groups, considering the 19 brain structures together as a whole. Regarding the AT8 staining intensity, as described in the table

of figure 31 and displayed in the exemplificative figures 32-33, the results showed that staining levels in R6 SD were significantly lower than those found in R6, ER, and C ($p<0.001$ for each comparison).

Concerning Tau-1 staining intensity, which is shown in table of figure 31 and in the exemplificative figures 34-35, the differences detected were partially complementary to those found for AT8. In detail, staining scores in R6 SD were significantly higher than those in R6 ($p<0.01$). Whereas no substantial differences were observed between R6 SD and C.

4.2.2.2 FINE ANALYSIS

Concerning the fine analysis for AT8 and Tau-1 staining, significant variations were detected in many of the neural structures analyzed (fig. 31), since the results were quite heterogenous in the different structures, for clarity, these data will be described separately per experimental condition.

R6: In this experimental condition, statistically significant higher AT8 staining scores compared to R6 SD were observed in six structures: RPa ($p=0.017$), MM ($p<0,01$), Arc ($p=0.012$), DMH ($p= 0.041$), VLPO ($p=0.041$), and MnPO ($p= 0.041$).

The figure 31 shows that the staining intensity of Tau-1 in R6 was, instead, lower than that found in R6 SD for the following structures: Amb ($p=0.01$), NTS ($p<0.01$), dMV ($p=<0.01$), RPa ($p<0.01$), LC ($p=0.01$), VLPAG ($p=0.02$), Cb-Cx ($p=0.02$), MM ($p<0.01$), LH ($p=0.04$), PV ($p=0.02$), VLPO ($p<0.01$), MnPO ($p=0.01$), CA3 ($p=0.02$), PRh ($p=0.05$).

ER: In the samples of animals belonging to the early recovery condition the staining intensity of AT8 was higher compared to R6 SD for almost all brain structures, except for the PV and P-Cx. In particular, Amb ($p<0.01$), NTS ($p<0.01$), dMV ($p=0.01$), RPa ($p<0.01$), LC ($p<0.01$), LPB ($p<0.01$), VLPAG ($p=0.02$), Cb-Cx ($p<0.01$), MM ($p<0.01$), LH ($p<0.01$), Arc ($p<0.01$), DMH ($p<0.01$), PVH ($p<0.01$), VLPO ($p<0.01$), MnPO ($p<0.01$), CA3 ($p<0.01$), PRh ($p=0.01$).

C: Results from the control group, regarding the AT8 staining intensity, showed higher intensity levels compared to R6 SD in only four brain structures: RPa ($p=0.03$), LC ($p=0.046$), LH ($p<0.01$), CA3 ($p<0.01$).

The statistical comparison between C and R6 SD for the intensity of Tau-1 staining revealed a heterogenous pattern, that is probably the reason why the gross analysis did not reveal any statistically significant difference between these two conditions. Indeed, the fine analysis showed higher scores in the control condition in four brain structures: Amb ($p=0.03$), NTS ($p<0.01$), dMV ($p=0.02$), RPa ($p<0.01$). On the other hand, the analysis also revealed lower staining intensity in C compared to R6 SD in four other brain areas: LH ($p<0.01$), Arc ($p=0.01$), MnPO ($p=0.02$), PRh ($p=0.03$).

4.3 EXPERIMENT III

Animals from the hypothermic experimental group showed a consistent decrease in Thy reaching the nadir just before the irradiation, as reported in figure 36 (Hypothermia, Thy: 22.2 ± 1.1; Control, Thy: 37.54 ± 0.24).

4.3.1 HISTOLOGICAL ANALYSIS

Part of the organs collected from rats induced into synthetic torpor and from the normothermic group were intended for histological analysis, in order to evaluate their tissue organization and cell morphology following radiation exposure. These analyses are still ongoing, but to effectively test the experimental hypothesis, the first organs analyzed are among those most sensitive to radiation damage: liver, testicle, kidney, and small intestine.

4.3.1.1 LIVER

The qualitative analysis of the liver showed that hepatic tissues of normothermic animals were affected by the irradiation, whereas the state of synthetic torpor seemed provide a degree of protection from radiation damage. Indeed, in light microscopy normothermic rats showed altered hepatocytes morphology, where tissue appeared disorganized, with cells visibly altered both at the cytoplasm level, which seemed less dense and intensely vacuolized, and at the level of the nucleus, which appeared shrunken with irregular shape, condensed chromatin and less distinct nucleoli (fig. 37, A-B). Vice versa, the liver of hypothermic animals showed a classic organization in lobes and lobules, hepatocytes preserved their morphology with a dense cytoplasm, the nuclei appeared rounded and one or more nucleoli were visible in them (fig. 37, C-D). Moreover, in the liver of hypothermic animals, an abundance of erythrocytes was present (indicated by arrows, fig. 37 C-D).

4.3.1.2 TESTICLE

The analysis on the cross sections of seminiferous tubules of testis revealed alterations on the cell stratification and differentiation in normothermic animals. Internal organization of the tubules was irregular, the junctions between the germinal cells was altered and, in some spots completely lost, also the normal cell stratification was lost, a sign of alteration in the gametogenesis process (fig. 38 A-B). All these alterations were not present in the testicle tissue of hypothermic animals, where the internal structures were almost comparable to the normal organization, and cell stratification was preserved (fig. 38 C-D).

4.3.1.3 KIDNEY

Similarly, as for the tissues above, the histological analysis on the cross sections of the kidney cortex showed cytohistological differences between the two experimental conditions. In this case, the irradiation in the normothermic rats seemed to induce edema and an expansion of the tubular lumen (fig. 39 A-C-E), while these effects were not detected in the tissues of the rats induced in synthetic torpor, in which there was, instead, an increase of erythrocytes (fig. 39 B-D-F).

4.3.1.4 SMALL INTESTINE

The histological observation of the intestine from the normothermic rats revealed disorganization and alteration of the mucous membrane of the intestinal villi and of the lamina propria, at the this level there was a condition of edema with related lymphocytic infiltrate, indicating an inflammatory state (fig 40 A-B), pathological effects that were not found in the small intestine of hypothermic animals, which showed a less impaired morphology (fig. 40 C-D).

4.3.2 GENE EXPRESSION

The difference in expression of each gene in the two experimental groups was derived from the fold change (FC). If the fold change value is greater than one, the observed data indicates a gene up-regulation; conversely, values lower than one indicate a downregulation. To date, two organs have been used for the gene expression analysis: the liver and the testicle.

4.3.2.1 LIVER

Of the 13 genes analyzed in the liver samples, three genes were significantly downregulated in the hypothermic animals compared with the normothermic rats: ATM (Ataxia telangiectasia mutated homolog; human) (Fold regulation: −2.90; p = 0.02), Pfkb (Phosphofructokinase, platelet) (Fold regulation: −2.73; p =0.02) and Pde1α (Phosphodiesterase1A, calmodulin-dependent) (Fold regulation: −2.80; p =0.01) (fig. 41). ATM is of particular interest, since it is involved in repairing DNA double strand breaks. The lower expression of this gene in the hypothermic animals could indicate that less damage was induced by radiation exposure in these animals. There was also an up-regulated gene, the nuclear factor of interleukin 3 (NFIL3, FC = 2.35), which, however, did not reach statistical significance.

4.3.2.2 TESTICLE

A more extensive analysis of gene expression was carried out on the testis. Hypothermic rats showed a downregulation of many genes involved in the DNA damage signaling. Of the 84 genes analyzed, 7 genes were significantly downregulated in the group of animals induced into synthetic torpor: Bbc3 (Bcl-2 binding component 3) (fold regulation: −5.49; p=0.01), Fancg (Fanconi anemia, complementation group G) (fold regulation: −1.58; p=0.04), Mbd4 (Methyl-CpG binding domain protein 4) (fold regulation: −1.79; p=0.04), Mgmt (O-6-methylguanine-DNA methyltransferase) (fold regulation: −1.84; p = 0.04), Pcna (Proliferating cell nuclear antigen) (fold regulation: −1.74; p=0.02), Ppm1d (Protein phosphatase 1D magnesium-dependent, delta isoform) (fold regulation: −1.67; p=0.003), Rad18 (RAD18 homolog; S. cerevisiae) (fold regulation: −1.66; p=0.03) (fig. 42).

5. DISCUSSION

5.1 EXPERIMENT I

The growing interest in the induction of a safe synthetic torpor condition in non-hibernating species derived from the possible applications, therapeutic and others, that a state of reduced Tb and decreased metabolism could have, from a translational point of view, in humans. In fact, a condition of hypothermia and hypometabolism is advantageous in all those circumstances where the oxygen and metabolic demands of one or more organs exceed their availability. For example, in case of cerebral stroke and myocardial infarction, an hypometabolic state could expand the time window needed to allow the reperfusion of organs, while in conditions such as trauma, surgery, sepsis and generalized hypoxia conditions it may protect against cell damage (Cerri, 2017). Up to now, only mild hypothermia (32-34 °C) can be safely induced in clinical practice, since being an exogenous and forced hypothermia it has several side effects, which could be overcome if, instead, an endogenous hypothermic state could be induced.

Beyond the most immediate clinical applications, another reason to work on the development of synthetic torpor models is to produce a living model for the study of many physiological adaptations that occur during natural hibernation, whose understanding could lead to the implementation of new therapeutic strategies. Some of the most interesting and peculiar characteristics of torpor that could have clinical relevance are: the reversible hyperphosphorylation of the Tau protein, the strong and extended neural plasticity, and the radioresistance.

The reversibility of the hyperphosphorylated Tau protein is a very interesting topic for explicative potentialities in the field of Tauopathies. Indeed, it has been shown that during their torpid period the brain of hibernators undergoes a massive phosphorylation of the Tau protein, but few hours after the arousal from torpor, physiological levels of Tau are restored (Arendt et al., 2003; Stieler et al., 2011). While in the case of Tauopathies the hyperphosphorylation of Tau is irreversible and leads to the NFT formation, and consequently to the neuronal death, not only in the brain but also at spinal cord level (Arendt et al., 2016; Guo et al., 2016) Therefore, the possibility to comprehend the mechanisms underlying the Tau dephosphorylation in hibernators could have beneficial repercussions for neurodegenerative diseases. Recently, a study showed that even in non-hibernating animals the induction of a synthetic torpor state, through the inhibition of the raphe pallidus, caused a reversible hyperphosphorylation of the Tau protein (Luppi et al., 2019).

Thus, in this study, using the same protocol to induce synthetic torpor, we aimed to broad the frame of knowledge about this phenomenon, evaluating if it also occurs at the spinal cord level, with the final intention to better elucidate which mechanism is responsible for the reversible accumulation of hyper-phosphorylated Tau in the central nervous system, avoiding neurodegeneration. Regarding this, since Tauopathies appear closely related to neuroinflammation (Nilson et al., 2017), we also assessed the microglia activation in the spinal cord during the experiment.

The results of this experiment show that, likewise to what was observed in the brain (Luppi et al., 2019), the induction of synthetic torpor in rats caused a reversible accumulation of hyperphosphorylated Tau even in the spinal cord. Nonetheless, different phosphorylation patterns have been observed within the spinal cord. In particular, the statistically significant increase of AT8 immunoreactivity in DH and central part during nadir was not detected in the ventral horn. Nevertheless, a significant decrease of Tau-1 immunoreactivity during the hypothermic period was observed in both the DH and the VH. Hence, in the VH a reduction of the non-phosphorylated form of Tau occurred in the absence of a reciprocal increase of the Ser202/Thr205-phosphorylated one (Malia et al., 2016).

These results may indicate that Tau protein is phosphorylated on different positions in VH and DH, moreover, neurons of the VH, may promote phosphorylation of Tau protein during synthetic torpor in positions not recognized by the monoclonal AT8 antibodies, at least considering the first 6 hours after the hypothermia. As noticed also in the aforementioned study focused on the brain Tau phosphorylation (Luppi et al., 2019), the possibility that a phosphorylation occurs on the only Threonine-205 position of Tau protein may explain the pattern observed in VH, indeed, considering that AT8 binds Tau only if it is phosphorylated at both serine 202 and threonine 205 (Goedert, Jakes, & Vanmechelen, 1995), the Tau phosphorylated only in threonine 205 is not enough for AT8 immunoreactivity, but is enough to depresses Tau-1 binding. This is also intriguing, since this phosphorylated form of Tau resulted protective against neurodegeneration (Ittner et al., 2016), but further experiments are needed to verify this possibility.

In this experiment, we also wanted to try to outline at least part of the mechanism underlining these results, by staining the spinal cord slices also for Phospho-Ser9-GSK3-β (P-GSK3-β), the inactive form of this kinase (Grimes & Jope, 2001). GSK3-β is the most important kinase

phosphorylating Tau protein (Planel et al., 2001; Wang & Mandelkow, 2016). In the present experiment, in line with the AT8 results, the staining for P-GSK3-β was positive during the hypothermic period for most of the motor-neurons in the VH, while no staining was observed within the DH. This may be interpreted as a biochemically regulated process of inhibition on the GSK3-β, which may lead to an only "partial" phosphorylation of Tau protein in VH, not involving all the positions necessary for the recognition by the AT8 antibody (Malia et al., 2016).

Moreover, the comparison of the present results with those observed in the brain of the same animals (Luppi et al., 2019) points out the existence of a different kinetic of Tau phosphorylation and dephosphorylation also during the recovery period. In fact, in this condition, while in the brain the disappearance of AT8 immunoreactivity was not complemented by the reappearance of Tau-1 (Luppi et al., 2019), in the spinal cord the normalization of Tau-1 staining levels was complete in all the areas analyzed, and independently from the degree of Tau phosphorylation during the hypothermic period. Therefore, while in the brain during the recovery period Tau dephosphorylation was detected, but was, apparently, "incomplete", in the spinal cord the return of Tau-1 immunoreactivity to baseline levels during the recovery period indicates a complete and/or faster dephosphorylation process.

In this experiment we also examined the microglia activation within the spinal cord, in order to evaluate its possible role in the Tau phosphorylation/dephosphorylation processes, but in general our morphometric measurements showed no significant changes. Small changes are shown in the morphological index (MI) parameter (Baldy et al., 2018), that evolves toward smaller value and variability during synthetic torpor and the following recovery. A low value of MI means higher ramified cells, a sign of resting phenotype of microglia cells (Graeber & Streit, 2010). This clearly show that synthetic torpor, while inducing dramatic Tau phosphorylation, does not trigger any neuroinflammatory response within the spinal cord, that is, instead, considered an important factor in neurodegenerative diseases (Nilson et al., 2017; Ransohoff, 2016). Moreover, this is somehow different from what observed in the brain (Luppi et al., 2019), where apparently a transient gliosis was shown during the synthetic torpor, rapidly recovered with the returned euthermia after synthetic torpor. Even though, as specified on the paper, those data were preliminary and still incomplete (Luppi et al., 2019).

In conclusion, despite the discrepancies found between the brain and spinal cord results, mostly explained by the existence of different regulatory mechanisms of Tau kinases and phosphatases in those areas of the central nervous system, the general reversibility of Tau hyperphosphorylation during synthetic torpor found in the spinal cord, as well as in the brain (Luppi et al., 2019), suggests that, in specific circumstances, also a non-hibernating mammal is able to reverse a huge accumulation of Tau phosphorylated. This may indicate the presence of a physiological mechanism, never described before, that can contrast the accumulation of phosphorylated Tau before the development of neurodegeneration, whose comprehension may represent a possible new approach helping to contrast Tauopathies.

5.2 EXPERIMENT II

The second experiment evaluated the role of sleep following a period of synthetic torpor in the rat. Indeed, during the euthermic interbout periods hibernators spend most of the time sleeping. For example, the golden mantled ground squirrels spends 70% of the euthermic intervals asleep (Larkin & Heller, 1999). This phenomenon has been observed in different species and the EEG characteristics of these sleep periods are similar to those observed in mammals after sleep deprivation (Achermann et al., 2017), since an increase in both NREM sleep amount and delta power proportionally to the duration of the torpor bout were observed (Deboer & Tobler, 1994).

Nonetheless, various studies have questioned the existence of a homeostatic regulation of the NREM sleep after torpor, considering the fact that in some natural hibernators, if they are sleep deprived soon after the arousal, the sleep bout is not postponed and the increase in delta power disappears (Larkin & Heller, 1998; 1999). More recently, however a study has shown that an increase in delta activity also occurs soon after the exit from synthetic torpor (Cerri et al., 2013).

For this reason, we decided to test whether the increase in delta activity was maintained in rats following 6 hours of sleep deprivation soon after the exit from an episode of synthetic torpor.

The result of the first part of this experiment about sleep and synthetic torpor revealed that the sleep bout was postponed in sleep deprived animals and that the intensity of delta power in the sleep bout which followed sleep deprivation was larger than that occurring soon after the torpor bout in undisturbed animals. In other words, apparently, not only the sleep bout was postponed, but the size of the sleep rebound was enhanced by sleep deprivation.

This results are in line with data showing an increase in delta power during NREM sleep in the hibernator when the animal is sleep deprived soon after the return to euthermia (Deboer & Tobler, 2000, 2003). Therefore, the delta rebound, which immediately follows a torpor-like condition, would not be the consequence of a nonspecific reactivation of cortical activity, but the expression of a real sleep need and suggests the presence of a homeostatic regulation of sleep after a torpid period.

The hypothesis that seems to better account this result suggests that a need for NREM sleep can be built-up even during the brief period of awakening from torpor which precedes sleep occurrence, considering that this period is not only associated with a huge autonomic and metabolic activation leading to a quick increase in Tb, but also with a large synaptogenesis (Amici et al., 2014). Consequently, this strong autonomic and neural activity may cause a need for synaptic renormalization, occurring through SWA synaptic downscaling, as proposed by the synaptic homeostasis hypothesis (Vyazovskiy et al., 2011; Tononi & Cirelli, 2003). Indeed, in our experiment the sleep deprivation soon after torpor had increased and sustained the autonomic activity underlying the process of rewarming. Consistently with these results, and in accordance with the hypothesis that the thermogenic effort during the arousal from torpor may define the magnitude of SWA, in the experiment performed by Cerri and colleagues (2013), a larger increase in delta power after arousal from synthetic torpor, was observed in the group of animals that during the awakening phase was exposed to Ta of 28 °C than in the group exposed during the arousal phase at Ta of 37°C. Possibly, as a consequence of the higher sympathetic activation required to reach euthermia.

The second part of this experiment was more focused on the investigation of the possible relations between sleep and Tau dephosphorylation after the arousal from synthetic torpor. Considering that the animals after torpor spend most of their time sleeping, and this is true in both natural torpor (Larkin & Heller, 1999) and synthetic torpor (Cerri et al., 2013), and taking into consideration that the period after a torpid interval is associated in natural (Arendt et al., 2015) and synthetic torpor (Luppi et al., 2019) with a strong dephosphorylation of the Tau protein, in this experiment we aimed to evaluate the role played by sleep in the process of Tau dephosphorylation after synthetic torpor, basically by comparing sleep deprived animals with those left undisturbed following the return to euthermia.

The results of this study not only indicate that sleep deprivation did not impede the dephosphorylation of Tau protein, but, actually, animals that were sleep deprived for 6 hours after arousal from synthetic torpor showed a statistically significant reduction of the hyperphosphorylated Tau compared to the animals that normally recovered after reaching the euthermia from synthetic torpor. This result was also confirmed by the assessment of the Tau-1 staining levels, which revealed that sleep deprived animals had higher levels of dephosphorylated Tau compared to animals that normally recovered. Furthermore, Tau-1 immunoreactivity in the sleep deprived group was not statistically different from that of the control group, indicating an apparent complete restoration of the dephosphorylated Tau isoform.

The enhancement of Tau dephosphorylation that we observed in the sleep deprived rats is in line with recent researches that showed an increase of Tau phosphorylation during sleep. In particular, one study showed that, in mice, during the waking period, when the core temperature is higher, the levels of phosphorylated Tau are low, while during the resting phase, when the central Tb slightly decreases, Tau results more largely phosphorylated. The authors attributed these changes to the variation of Tb. Indeed, heat exposure prevented the daily changes in Tau phosphorylation in the cerebral cortex of mice exposed to Ta 34 °C. Another result underlining the key role played by temperature in Tau phosphorylation during sleep was the detection of the inhibition of PP2A, the main phosphatase of Tau, during the rest period. Indeed, when PP2A is inhibited by lowering the temperature, it causes increased levels of phosphorylated Tau (M. Goedert, Jakes, Qi, et al., 1995; Planel et al., 2004). Always in line with the results of our experiment, authors showed that Tau phosphorylation was prevented by acute sleep deprivation in mice. However, also in this case, the reason seems to be related to the temperature, considering that the core temperature of the sleep deprived animals resulted to be higher than that of the sleeping mice (Guisle et al., 2020). The increase in core temperature as a consequence of sleep deprivation by gentle handling has also been described in rats (Franken et al., 1992).

Another recent study seems to be complementary to this one. Showing that Tau in the interstitial space in the human brain appears to be reduced during sleep, increased during wakefulness, and further increased following sleep deprivation (Holth et al., 2019). However, since Tau at the extracellular level is mainly dephosphorylated (Pooler et al., 2013), there is likely to be an inverse relationship between phosphorylation and secretion into the extracellular space (Guisle et al., 2020).

A possible interpretation that could account for all these findings is related to the synaptic homeostasis hypothesis. In fact, this hypothesis asserts that during NREM sleep there is a renormalization of the synaptic connections that are enhanced by wakefulness, by removing some synapses and sparing others. Tononi and Cirelli (2019) suggested among the possible compound having a role in guiding the downregulation processes the GSK-3ß. In fact, the induction of LTP causes a GSK-3ß phosphorylation at Serine 9, which inhibits its activity and prevents the induction of long-term depression in the same synapses (Peineau et al., 2007). Furthermore, in rats, levels of phosphorylated GSK-3ß are higher during wakefulness than during sleep (Vyazovskiy et al., 2008). Thus, the phosphorylation of GSK-3ß could be a mechanism to tag synapses that are reinforced during wakefulness and protect them from weakening during the following sleep period.

At the light of what has been reported, it is possible to speculate that if the inactive form of GSK-3ß prevents the weakening of synapses reinforced during wakefulness, the active form of GSK-3ß, that is the main kinase of Tau protein, could induce the downscaling of other synapses through the phosphorylation of Tau protein, that by influencing the stability of the cytoskeleton and axonal transport may induce the synaptic plasticity processes occurring during NREM sleep. Moreover, according to data presented by Guisle and coll. (2020), the reduction of brain temperature occurring during NREM sleep could be the cause of the increased Tau phosphorylation during sleep, due to the inhibition of the PPF2, but this Tau phosphorylation would occur only in synapses where the GSK-3ß is not inactivated, protecting in this way some synapses and allowing the remodeling of others. However, this is just a speculative hypothesis that should be experimentally verified. For example, in order to test the role of temperature on these processes of neural plasticity would be interesting, soon after the animals reach the euthermia following synthetic torpor, to divide the rats in different groups were they are allowed to sleep at a different Ta (e.g. 34, 26, and 15 °C) in order to dissociate the occurrence of sleep by the brain temperature levels during NREM sleep, that should be higher in animals sleeping at a higher Ta.

Another possible explanation for our results involves melatonin. Indeed, it is well known that the arousal from a torpid period in hibernators is associated with a peak of melatonin (Vaněček et al., 1984). Furthermore, melatonin has been largely studied for its effects on the reduction of Tau phosphorylation and accumulation (Das et al., 2020). Thus, it is reasonable to suppose that

by sleep depriving the animals, their melatonin peak has been maintained throughout the sleep deprivation, facilitating Tau dephosphorylation.

In conclusion, with this experiment we supported the hypothesis of an homeostatic nature for sleep occurring soon after synthetic torpor, which, however, seems not be indispensable for the process of dephosphorylation of Tau protein to occur, while sleep deprivation seems to enhance this process. Further studies are needed to test the mechanism underlying this finding, that could have great potentialities in the understanding of the relations between sleep, neural plasticity, Tau protein, and Tb.

5.3 EXPERIMENT III

Radioresistance is another interesting characteristic of natural torpor that is worth studying and deepening considering the clinical relevance that this feature might have in a translational perspective. Indeed, if radioresistance were also observed in synthetic torpor, there could be two main applications: in cancer patients that undergo radiotherapy, the induction of a torpor like state may protect the rest of the body from radiation, minimizing the collateral effects of radiation exposure. Another application could be the long-distance space exploration. Indeed, the astronauts are exposed to cosmic radiations, which as of now is the biggest showstopper for interplanetary travel (Cerri, 2017).

Concerning natural torpor, several studies over the years have evaluated the radioresistance in hibernators. For example, in ground squirrels during their torpid period (5°C Tb) an increase in radioresistance has been detected by comparing them with animals in active period (37°C Tb). The normothermic animals exposed to 15 Gy of total body radiation showed a mean survival time of 8 days, while the animals in hibernation survived for a mean of 66 days. (Musacchia & Barr, 1968). In accordance with this experiment, another study showed an increased survival rate in hibernating ground squirrels to a lethal dose of Cobalt-60 gamma radiation (Jaroslow et al., 1969). More recently a meta-analysis, summarizing some of the data from published papers about radioprotection due to hypothermia and torpor, respectively in rats and squirrels, supported the hypothesis that hibernation increases radioresistance (Cerri et al., 2016).

Thus, the purpose of this study was to evaluate whether the same radioprotective effects can be offered also by synthetic torpor, exposing to 3Gy X-rays normothermic and hypothermic rats,

the latter induced into synthetic torpor, pharmacologically inhibiting the RPa, and studying the histopathological and molecular characteristics of both groups.

The histological and molecular results of this experiments seem to confirm a significant protection to ionizing radiation damage induced by synthetic torpor in non-hibernating animals. In particular, the histological analyses of liver, testicle, kidney, and small intestine belonging to the hypothermic irradiated rats showed a phenotype comparable to that present in normal conditions; vice versa, the tissues of the normothermic irradiated rats appeared to be disorganized and morphologically altered, and this suggests not only the radioprotective effect of synthetic torpor but also that the radiation dosage was high enough to induce visible damage after a short time (4 hours).

After that we have investigated the molecular mechanisms underlying the increased radioresistance and we found downregulation of ATM and several other genes involved in the DNA damage signaling in hypothermic animals. In particular, the downregulation of the ATM gene in irradiated and hypothermic animals compared to controls is particularly interesting. In fact, following DNA double strand breaks (like those induced by radiation), ATM operates a phosphorylation of the serine residues of the p53 protein. This modification decreases the affinity of p53 for its physiological inhibitor and at the same time increases its affinity for its nuclear targets: in this way, p53 can migrate in the nucleus and induce, if the damage is repairable, a blockade of the cellular cycle and DNA repair; conversely, if the damage cannot be repaired, cell apoptosis is promoted (Khosravi et al., 1999; Maya et al., 2001).

Our result is in line with the last hypotheses about the mechanism responsible for radioresistance in torpor. In fact, rather than to a simple reduction of cell proliferation, the cause of radioresistance seems to be related to a different DNA repair response. For example, cells irradiated at 37 C exhibit significantly faster double-strand break repair than that occurs at 20 °C or 13 °C; however, following low temperature irradiation the cells continue to show greater survival, a sign of the fact that these alterations do not negatively impact the life of the cell, and that the damage is repaired more slowly, but probably more effectively (Baird et al., 2011). A strong confirmation to this hypothesis is the study of Ghosh and colleagues (2017), that shows how radioprotective effects can be obtained by inducing hypothermia within three hours after the radiation exposure. Such results apparently rule out other hypotheses that torpor-induced

radioprotection can be caused by reducing cell proliferation or by decreasing tissues oxygenation, even though these aspects may still play a role.

However, it is doubtful that the radioprotective effect can simply be explained by hypothermia. In fact, the observed radioresistance in human peripheral blood lymphocytes at low temperature has been associated to increased ATM activation (Lisowska et al., 2018). On the other hand, the pharmacological inhibition of ATM significantly reduces the radiosensitivity of unstimulated human lymphocytes (Heylmann et al., 2018). Thus, the effect of synthetic torpor seems to be more similar to the pharmacological inhibition of ATM than to the simple hypothermia.

Finally, it is important to underline that although a decrease in gene expression occurs in synthetic torpor, the downregulation observed in the group of hypothermic animals is not general. In fact, in the liver the Nfil3 gene is upregulated, among the multiple functions performed, it plays a role in the negative regulation of the circadian rhythm, through the repression of the transcriptional activity of PER1 and PER2, members of the family of Period genes and fundamental for maintaining the circadian rhythm (Cowell, 2002). Its upregulation may indicate an adaptation of the clock to the reduced metabolism.

In conclusion, this is the first study that reports measurement of toxicity and gene expression in animals exposed to ionizing radiation under synthetic torpor, showing for the first time that the radioresistance found in natural torpor is maintained even with synthetic torpor induced in non-hibernating animals, such as rats. The molecular causes of this phenomenon are still to be clarified, but it is reasonable to think that they involve a specific response of DNA repair mechanism.

5.4 CONCLUSIONS AND FUTURE PERSPECTIVES

The growing interest in the research field for the induction of a synthetic torpor state in non-hibernating species derives from all the possible applications that it may have in a translational perspective. The clinical applications would be numerous, but beyond that, another reason to work in this field is to produce a living model for the study of many physiological adaptations that occur during natural hibernation, the deeper comprehension of which could lead to the implementation of new therapeutic strategies, as in the case of: the reversible

hyperphosphorylation of the Tau protein, the strong and extended neural plasticity, and the radioresistance.

In this dissertation all the aforementioned aspects have been studied. In the first experiment, the general reversibility of Tau hyperphosphorylation during synthetic torpor was reported in the spinal cord, confirming that, in specific circumstances, also a non-hibernating mammal is able to reverse a large accumulation of phosphorylated Tau. In the second experiment, the homeostatic nature of sleep regulation soon after synthetic torpor has been shown, together with the finding of an enhancement of Tau dephosphorylation by the sleep deprivation soon after a synthetic torpor bout. Finally, in the last experiment, the radioresistance of non-hibernating animals induced into synthetic torpor was assessed, reporting a consistent radioprotective effect of the hypothermic state against ionized radiation damage.

All these experiments reveal various explicative potentialities in the scientific field and suggest future possible applications of synthetic torpor models. In particular, in the first experiment, in which the phosphorylation and dephosphorylation mechanisms and kinetics of the Tau protein in the spinal cord was studied, the rationale was widening the knowledge about the Tau-related processes, which are so important in the Tauopathies. It is for this reason that in our laboratory we also worked in other experiments aimed at analyzing the Tau-related processes (even in the enteric nervous system), in the perspective of exploring the possible differences in the phosphorylation and dephosphorylation dynamics of the Tau protein in various areas and tissues. The unveiling of specific characteristics and proprieties in these processes in each area of the nervous system, may lead to the understanding of factors explaining the reversibility of Tau phosphorylation and maybe to the possibility, in the future, to be able to act on them.

In this regard, the second experiment presented in this thesis give us an important feedback on these aspects. Indeed, the finding that sleep deprivation strengthens rather than prevents the dephosphorylation of Tau protein in the brain of rats after synthetic torpor, leads to hypothesize that sleep deprivation favors this process by prolonging the sympathetic activation and/or the melatonin peak normally occurring during the exit from torpor. For this reason, we are also working on experiments aimed at exploring the possible association between melatonin and catecholamines during the exit from synthetic torpor in either the presence or the absence of sleep. A possible clinical application of these studies could be a treatment for Tauopathies that takes in consideration the administration of a combination of melatonin and SNS stimulating

agents. In this respect, there are already some studies evaluating the therapeutic properties of melatonin in the neurodegenerative diseases, even if the effects of melatonin alone on the cognitive degeneration seem to be scarce (Cardinali, 2019; Y. Y. Wang et al., 2017). Always in a very speculative way, we can also hypothesize other clinical applications, such as a possible treatment for Tauopathies characterized by several sessions of hypothermia induction in order to likely enhance Tau dephosphorylation mechanisms during the rewarming phase.

Finally, the possible medical applications of the last experiment of this thesis are much more concrete. In fact, the results of this experiment, demonstrating the radioprotective effect of the torpor like state in non-hibernating animals, open multiple doors at translational level. First of all, in the radiotherapy field, where the induction of a torpor like state in cancer patients who have to undergo a treatment with ionizing radiations may have radioprotective effects on healthy tissues surrounding the tumor. Furthermore, another possible declination of these findings could be the treatment of the acute radiation syndrome, which is a set of symptoms caused by accidental exposure to high amounts of ionizing radiation, in a short period of time (Donnelly et al., 2010). In order to test the feasibility of synthetic torpor for this clinical application, and in line with the findings by Ghosh and colleagues, showing that the radiation-protection effect is present even if the animal is induced in torpor after irradiation (Ghosh et al., 2017), we are also working on an experiment aimed at evaluating the protective effects of synthetic torpor induced soon after rat irradiation with x-rays. Finally, a further future perspective of the third experiment could be that concerning long-distance space exploration. Indeed, it is well known that astronauts are exposed to cosmic radiations, which represent a huge limitation to the time that they can spend in space travel. Unfortunately, to date it doesn't exist an efficient way to shield spacecrafts (Cerri, 2017). Thus, synthetic torpor by potentially protecting astronauts from ionizing radiation could be beneficial also in the space travels field. However, of course, many other studies are needed to test all these hypothetic applications.

6. FIGURES

Figure 1. Brown adipose tissue activation

The intracellular cascade starts with the β adrenergic receptors (β-AR) in brown adipocytes that are stimulated by the sympathetic nervous system (SNS) induced-release of norepinephrine (NE). These G-protein coupled receptors then activate adenylate cyclase (AC), inducing an increase in cAMP, which in turn activates protein kinase A (PKA). PKA acutely increases lipolysis by the activation of adipocyte triglyceride lipase (ATGL), hormone-sensitive lipase (HSL) and monoacylglycerol lipase (MGL), which hydrolyze the triacylglycerides to release free fatty acids (FFA) that will enter the mitochondria and will eventually be used for heat production by uncoupling protein 1 (UCP1) in the electron transport chain. The chronic effect of PKA activation increases the expression of thermogenic related genes.

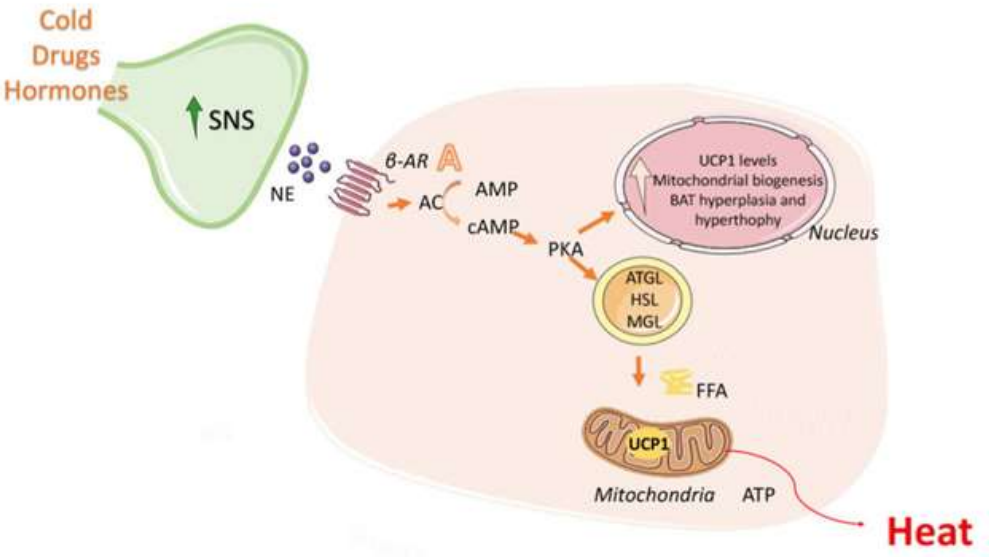

Modified from: (Seoane-Collazo et al., 2020).

Figure 2. Neuromodulations and metabolic adaptions to cold exposure

Interactions between hypothalamic nuclei, following neurohumoral signaling and resulting effects on relevant organs and tissues for metabolism are shown. Solid lines indicate scientifically consolidated effects while more recently described interactions are represented by dotted lines. ARC, arcuate nucleus; BAT, brown adipose tissue; DMH, dorsomedial hypothalamus; HPT, hypothalamic-pituitary-thyroid; NA, noradrenaline; POA, preoptic area; PVH, paraventricular nucleus of the hypothalamus; SNS, sympathetic nervous system; TRH, TSH-releasing hormone; TSH, thyroid-stimulating hormone; T3, triiodothyronine; T4, thyroxine; VMH, ventromedial hypothalamus; WAT, white adipose tissue.

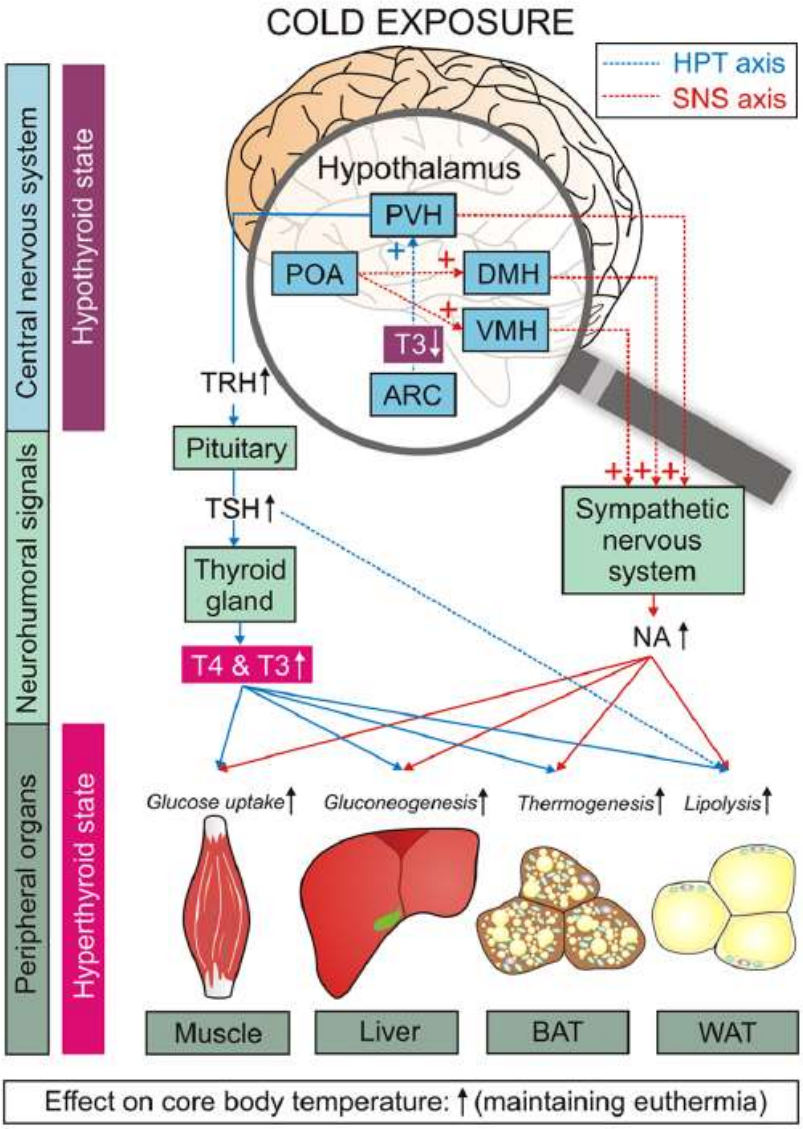

From: (Iwen et al., 2018)

Figure 3. Heat production and heat loss

Heat loss and production of a male subject (age, 33 years; body mass, 67 kg; height, 168 cm) at different calorimeter temperatures. The heat loss by conductance (through feet to the floor) is minimal in a standing person and not shown in the figure.

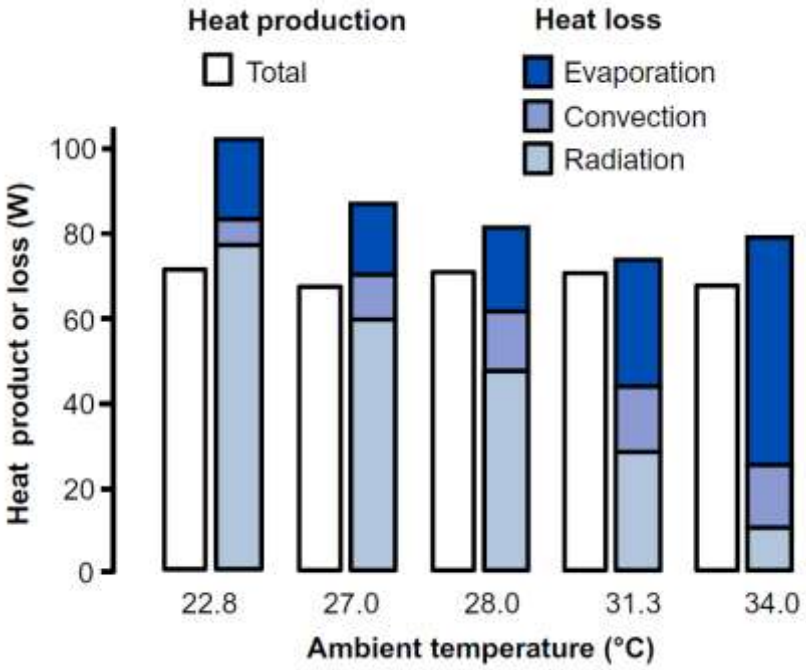

From: (Romanovsky, 2018).

Figure 4. Set-point model of thermoregulation

Illustrative scheme of the historic concept of the unified thermoregulation system, with a single controller. For simplicity, only four effectors are presented: two cold (C1 and C2, in blue) and two warm defense pathways (H1 and H2, in red). According to this model, information about Tb is integrated into preoptic anterior hypothalamus, where the Tb is compared with a set point temperature, as consequence of this comparison there will be an activation or inhibition of the effectors, mediated by a coordinator.

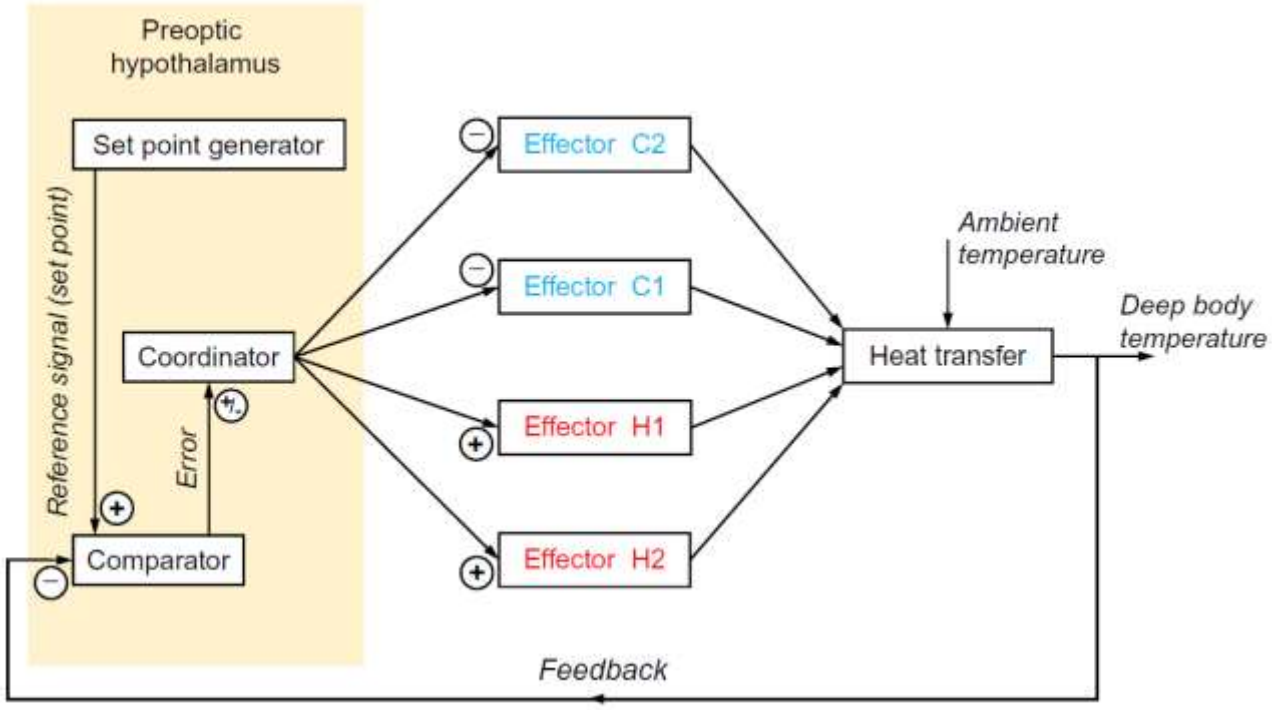

From: (Romanovsky, 2018)

Figure 5. Independent loops model of thermoregulation

Illustrative scheme of thermoregulation with multiple independent controllers. For simplicity, each effector is displayed as controlled by a single warm-sensitive neuron with a specific threshold for central Tb. Thermoeffector loops are completely independent of each other, nonetheless, they function in a coordinated fashion sharing a common feedback, that is the Tb.

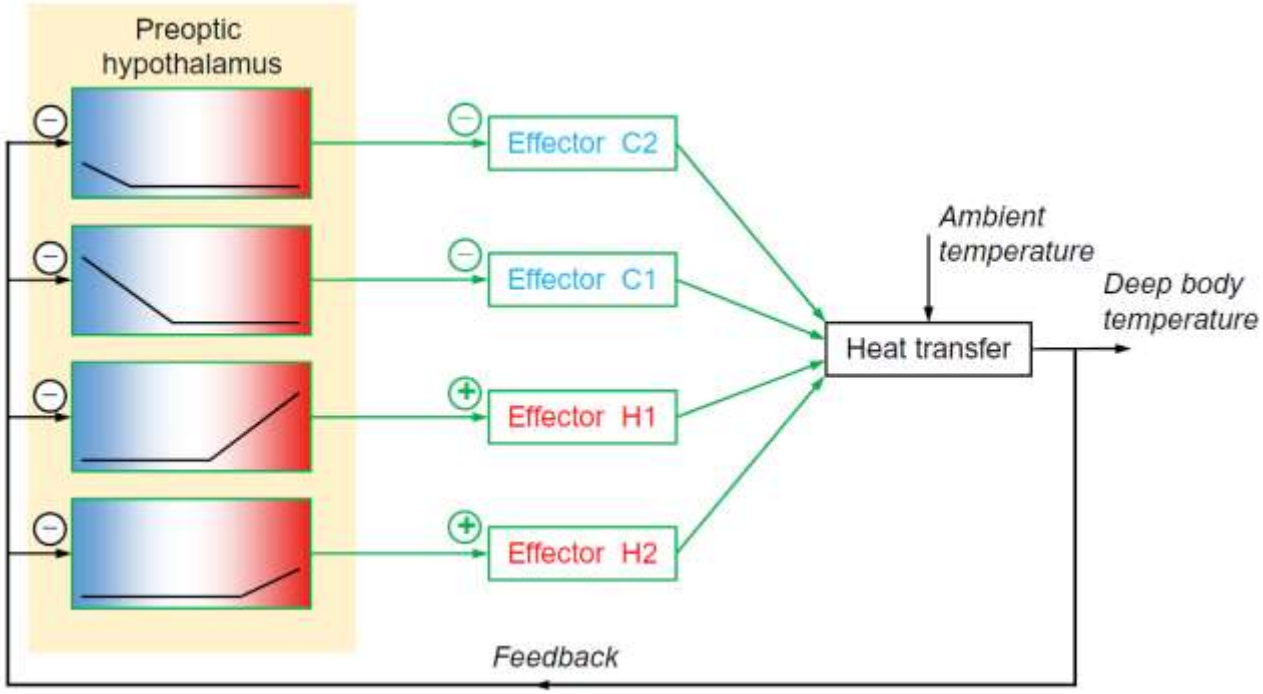

From: (Romanovsky, 2018)

Figure 6. Model of the thermoregulatory afferent pathways

Afferent pathways from the periphery to the preoptic area. Dashed lines indicate pathways that have not been conclusively studied. DH, dorsal horn; DRG, dorsal root ganglia; Dyn, dynorphin; GLU, glutamate; LPBd, dorsal lateral parabrachial nucleus; LPBel, external lateral parabrachial nucleus; MnPO, median preoptic nucleus; MPA, medial preoptic area; TRPM8, transient receptor potential subfamily M member 8; TRPV1, transient receptor potential vanilloid 1; NTS, nucleus tractus solitarius; vLPO, ventral portion of the lateral preoptic area.

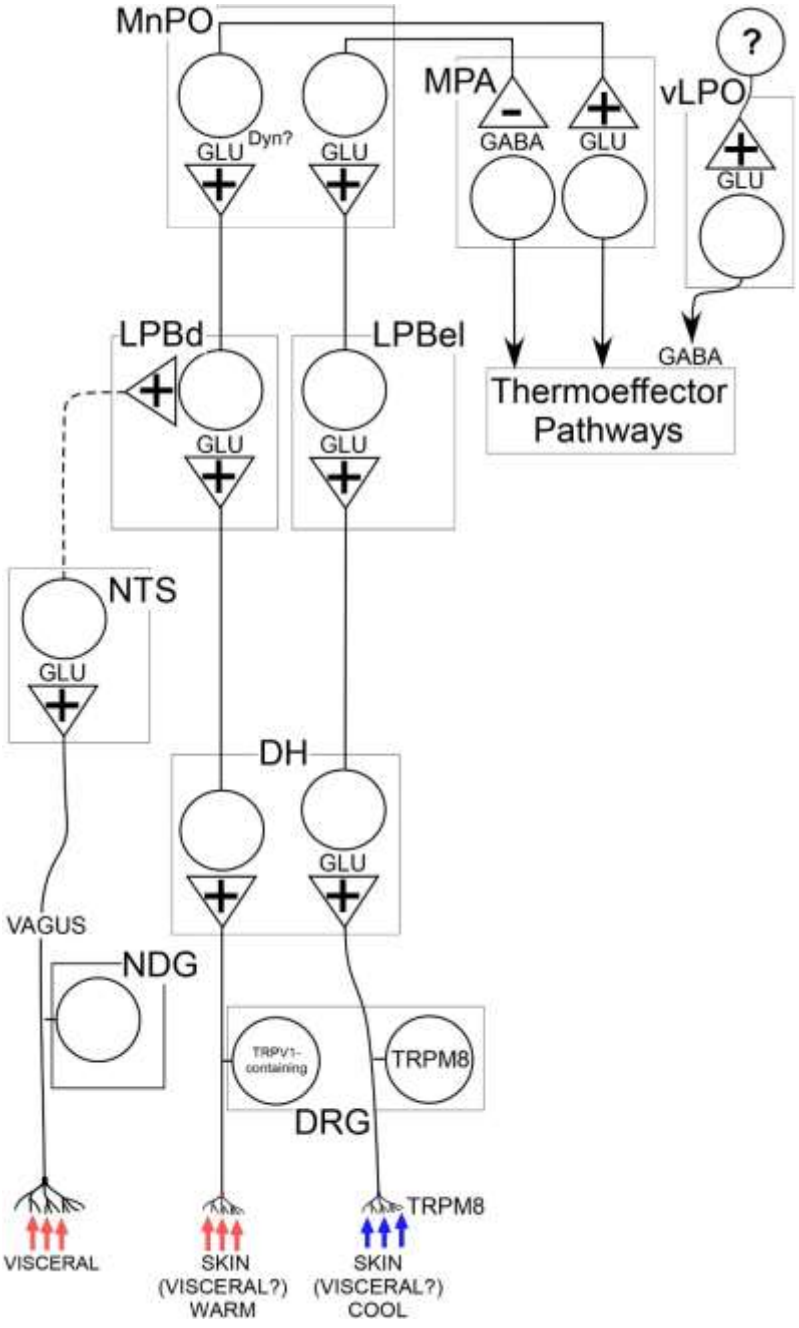

From: (Madden & Morrison, 2019)

Figure 7. Model of thermoregulatory efferent pathways

Efferent pathways for thermogenesis, vasomotion, and evaporative heat loss. Dashed lines indicate pathways that have not been conclusively studied. 5HT, 5-hydroxytryptamine (serotonin); α, alpha motor neuron; Ach, acetylcholine; BAT, brown adipose tissue; CVC, cutaneous vasoconstriction; DMH, dorsomedial hypothalamus; γ, gamma motor neuron; GABA, gamma aminobutyric acid; GLU, glutamate; IML, intermediolateral cell column; LH, lateral hypothalamus; MnPO, median preoptic nucleus; MPA, medial preoptic area; NE, norepinephrine; PG, parasympathetic ganglion cell; RPa, raphe pallidus area; RVLM, rostral ventrolateral medulla; SG, sympathetic ganglion cell; SSN, superior salivatory nucleus; VH, ventral horn; vLPO, ventral portion of the lateral preoptic area.

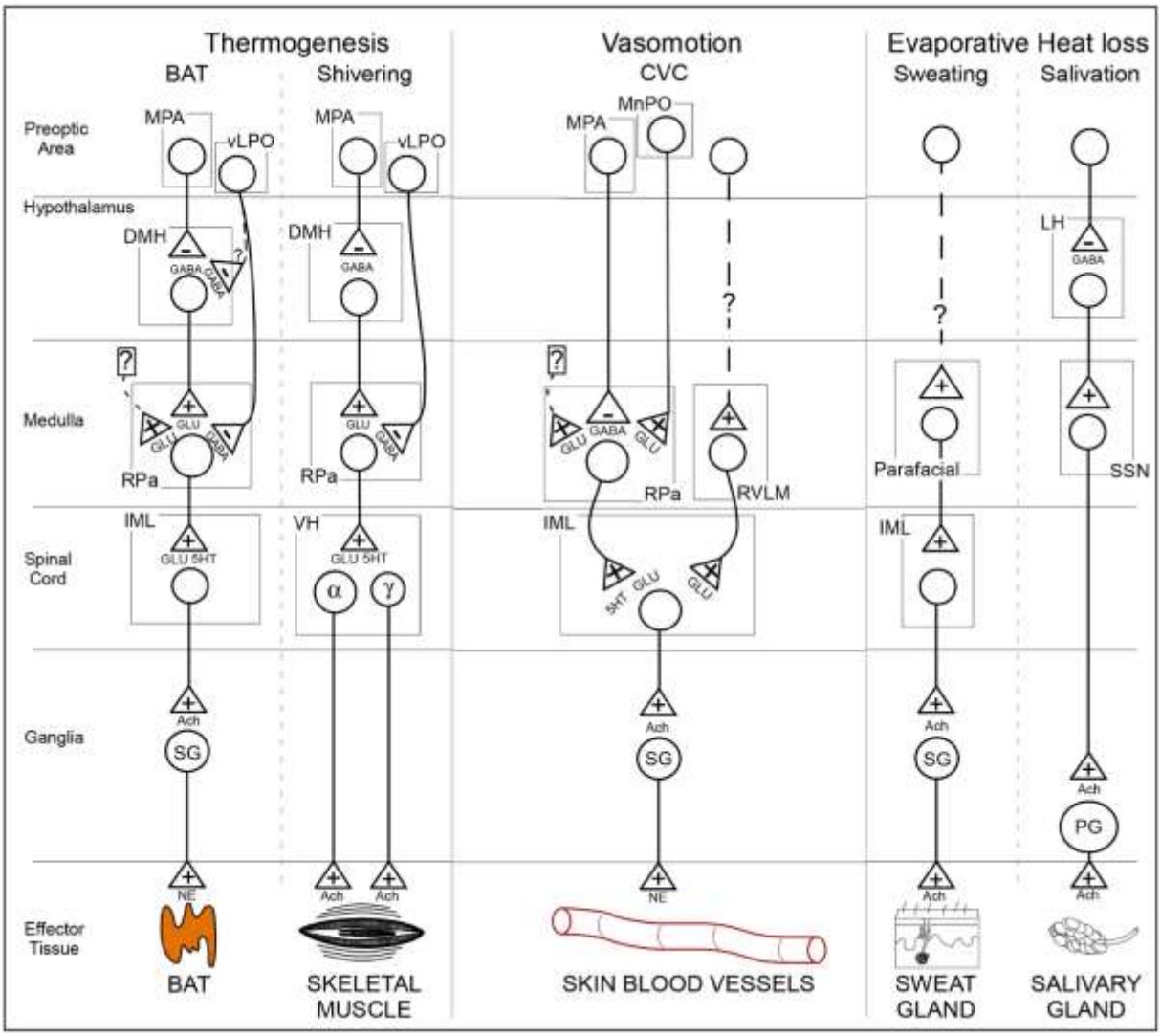

Modified from: (Madden & Morrison, 2019)

Figure 8. The physiological profile of CA1 pyramidal neurons

Panel a The physiological profile displays the temperature dependence of features of CA1 pyramidal neurons. The neuron cannot generate LTP below 21 °C, even though action potentials can be generated at all temperatures, as well as Histamine (HA) responsiveness.

Panel b CA1 pyramidal neurons function might change in a temperature-dependent way: above 21 °C these neurons can be involved in memory formation, while below 21 °C they can control the torpor bout. Histamine enhancement of CA1 pyramidal cell excitability could lead to an inhibition of the ascending arousal system and prolongation of torpor. HH Hamster in hibernation (torpor) at 6 ± 2 °C and short photoperiod (8:16 LD); SH Hamster housed at 22 ± 2 °C and long photoperiod (14:10 LD); WH Non-hibernating hamster housed at 6 ± 2 °C and short photoperiod (8:16 LD).

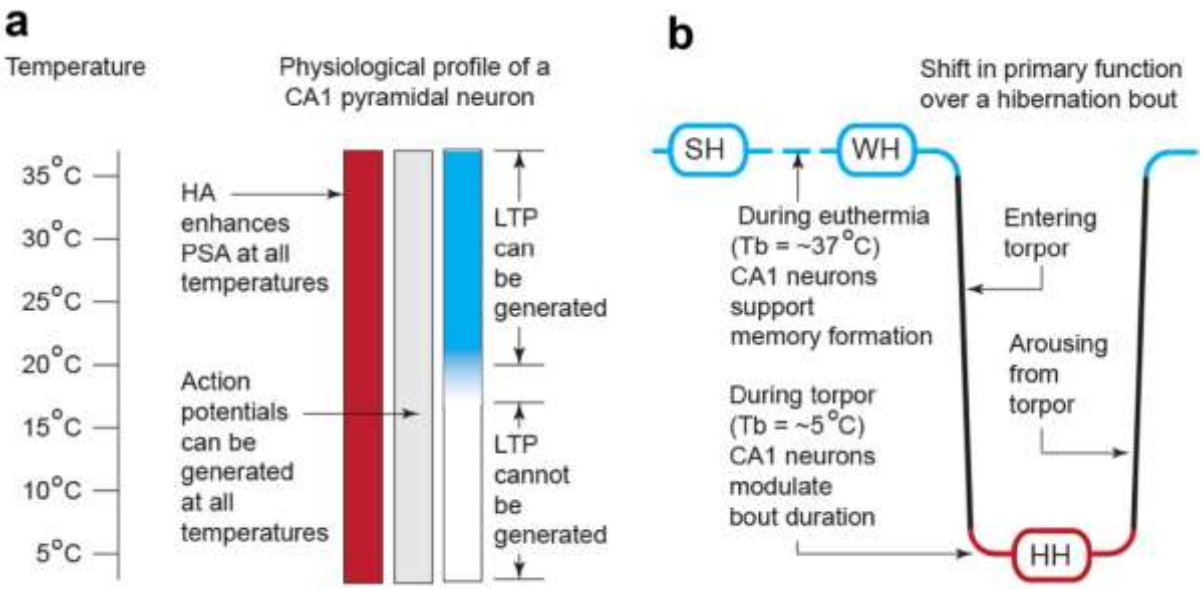

From: (Hamilton et al., 2017)

Figure 9. Cyclical changes in the hippocampal mossy fiber system during hibernation

Repeated disappearance and reappearance of synaptophysin in mossy fiber terminals (stratum lucidum) corresponds to phosphorylation and dephosphorylation of Tau protein in postsynaptic CA3 pyramidal neurons (stratum pyramidale) (the red color over the soma of pyramidal neurons indicates hyperphosphorylated Tau, stained with AT8 antibody).

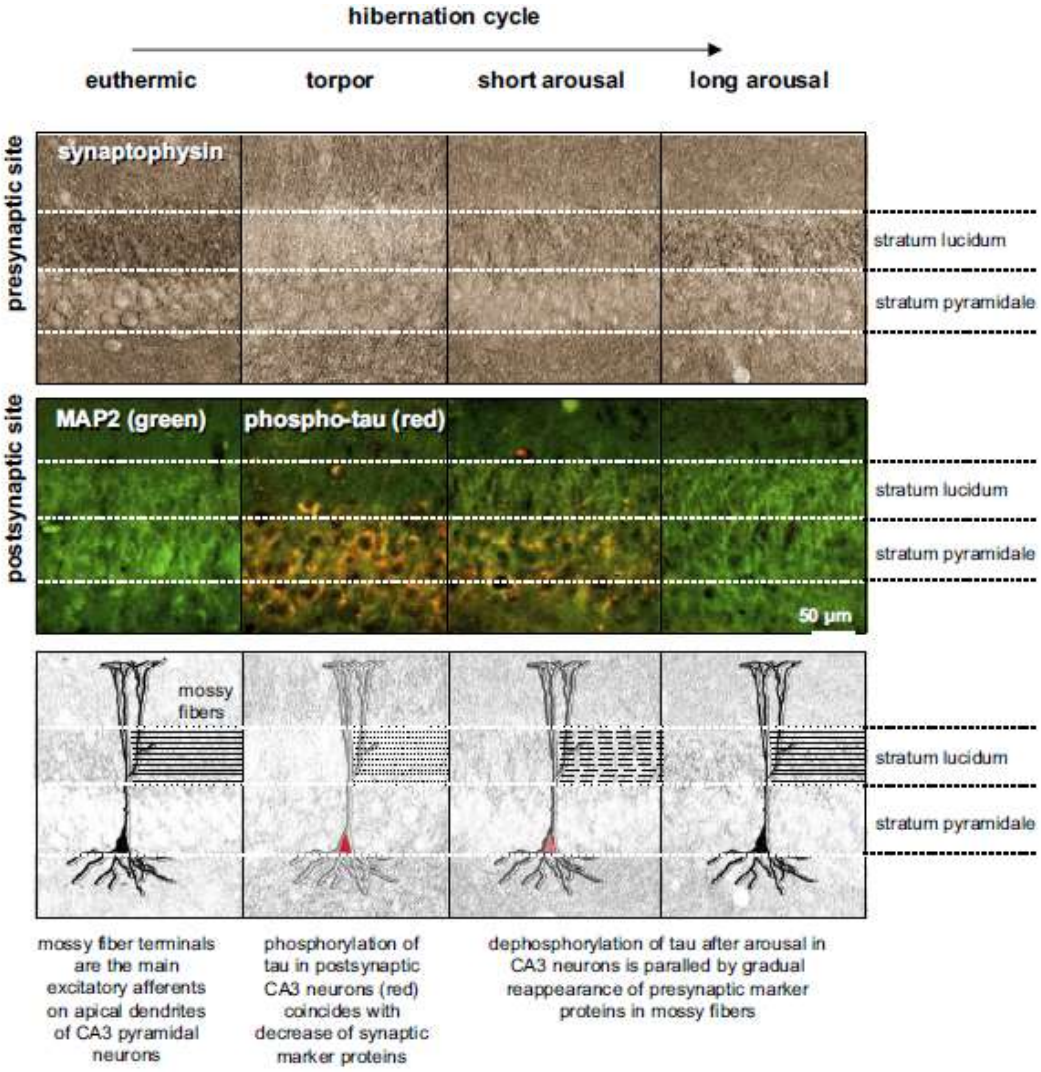

Modified from: (Arendt & Bullmann, 2013)

Figure 10. Representative pictures of NeuN, AT8 and Tau-1 staining

Panel a shows the CA3 field of the hippocampus. Left column represents NeuN staining (neuronal maker). Right column represents the same corresponding field depicted in the left column but stained for AT8 (phosphorylated Tau). C, control; N, nadir; R38, recovery 38 h. (calibration bar: 100 μm)

Panel b shows the paraventricular nucleus of the hypothalamus (PVH). Left column represents NeuN staining (neuronal maker). Right column represents the same corresponding field depicted in the left column but stained for Tau-1 (non-phosphorylated Tau). C, control; N, nadir of hypothermia; R38, samples taken 38 h after 35.5°C brain temperature was reached. 3V, third ventricle. (calibration bar: 100 μm)

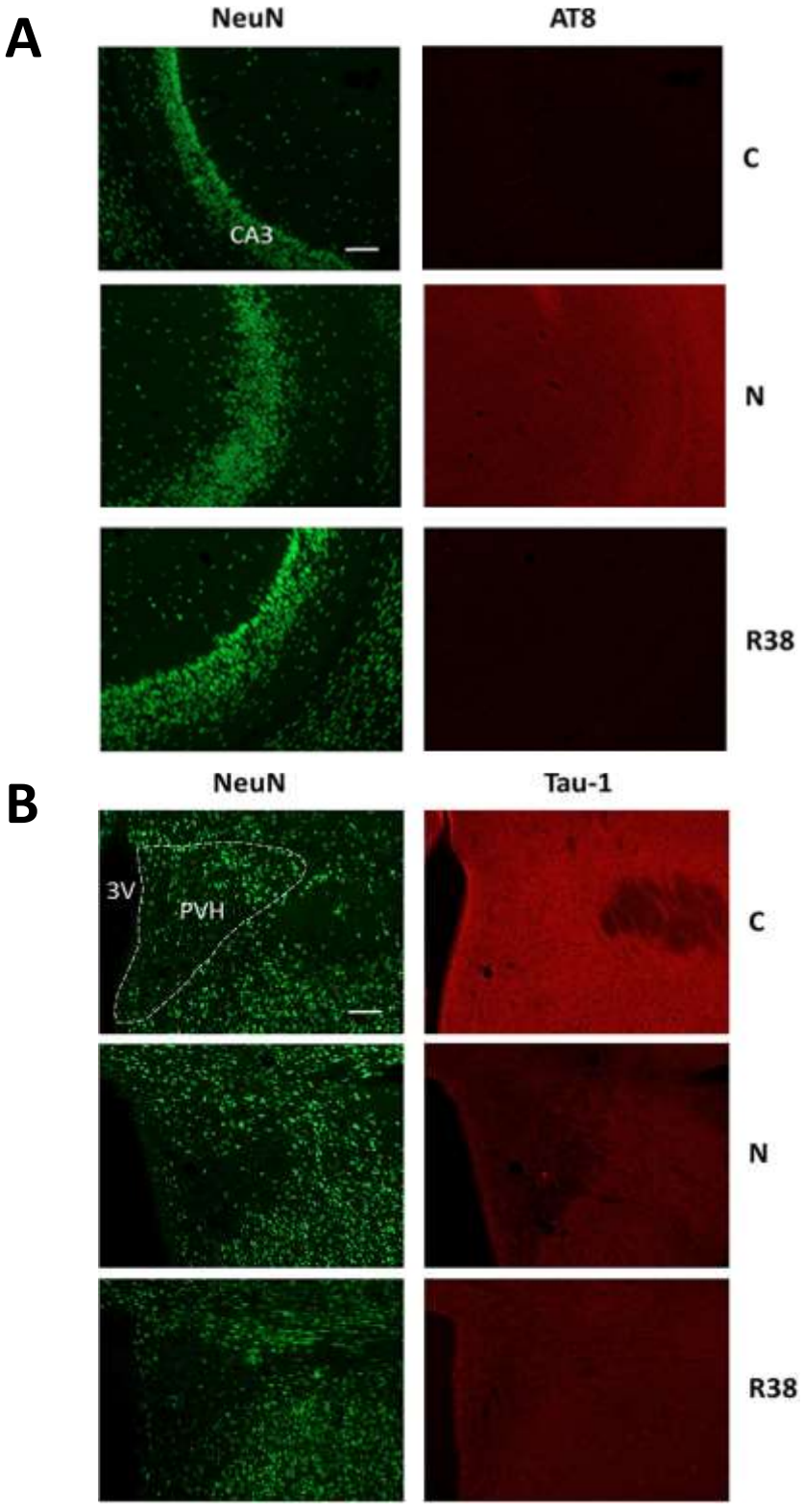

Modified from: (Luppi et al., 2019)

Figure 11. Experiment I: Surgical procedure

The upper figure is a representation of a rat skull: the blue symbol on the occipital bone is the superficial spot where the guide cannula was inserted during the surgery through a craniotomy. The four grey dots represent the sites of placement of the screws to hold the implant, the green dot indicates the placement of the hypothalamic thermistor, and the red squares the placement of the EEG electrodes. The coronal section below shows the target (raphe pallidus) of the microcannula.

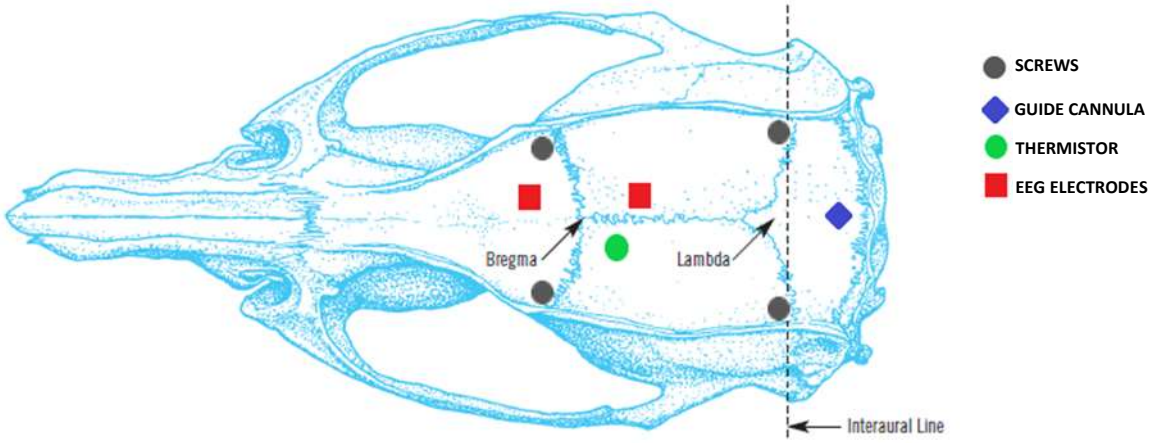

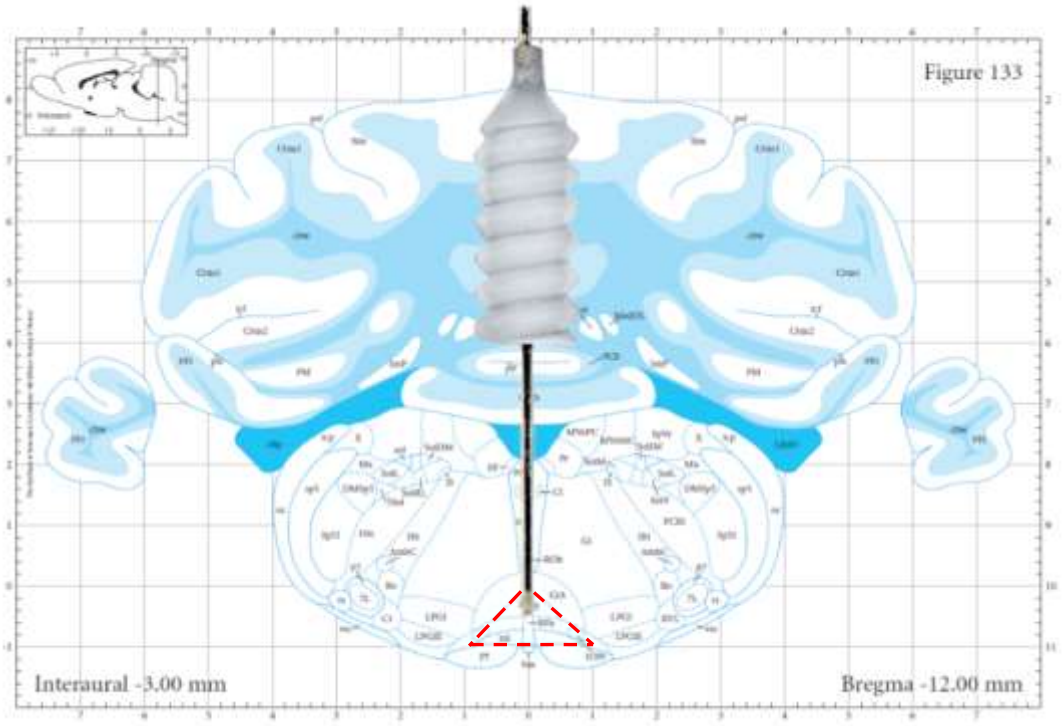

Modified from: (Paxinos & Watson, 2007)

Figure 12. Experiment I: Experimental plan

Animals were randomly assigned to six different experimental groups and were sacrificed at different times following the injection of either muscimol or aCSF. The experimental groups were the following: i) Control (C); injected with aCSF (N=3) and sacrificed at around 17.00h; ii) Nadir 30 °C (N30); sacrificed at around 12.00h-13.00h, between the second and third injection of muscimol, when Thy reached the level of 30 °C (N=3); iii) Nadir (N); sacrificed 1h after the last injection, at 17.00h, when brain temperature reached the nadir of hypothermia (N=3); iv) Early-recovery (ER); sacrificed at around 19.00h when brain temperature reached 35.5 °C after the synthetic torpor (N=3); v) Recovery 6 hours (R6); sacrificed at around 01.00h, 6 hours after ER (N=3); vi) Recovery 38 hours (R38); sacrificed at around 09.00h of the third day, 38 hours after ER (N=2).

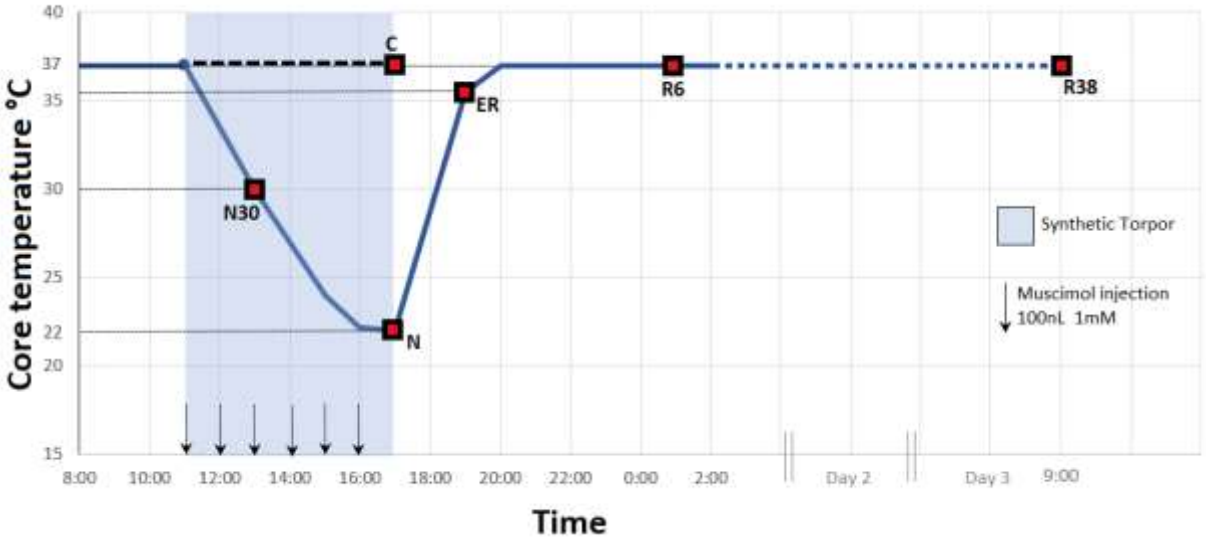
Core temperature °C
40
37
35
30
25
22
20
15
C
ER
R6
R38
N30
N
Synthetic Torpor
Muscimol injection
100nL 1mM
8:00
10:00
12:00
14:00
16:00
18:00
20:00
22:00
0:00
2:00
Day 2
Day 3
9:00
Time

Figure 13. Experiment I: Microinjection apparatus in the free-behaving rat

Representative scheme of the microinjection apparatus in the free-behaving rat. The rat is placed inside a cage, which is located in a sound-attenuated and thermoregulated box. The environmental conditions in the box are continuous darkness and Ta set at 15 °C. The cage is equipped with a swing arm that transmits the bioelectric signals recorded in the animals to the set-up, while allowing the free movement of the animal. Animals are injected with minimal disturbance, evaluating the correct drug delivery by observing the oil-liquid interface (pushing the drug) moving under the microscope, located outside the cage.

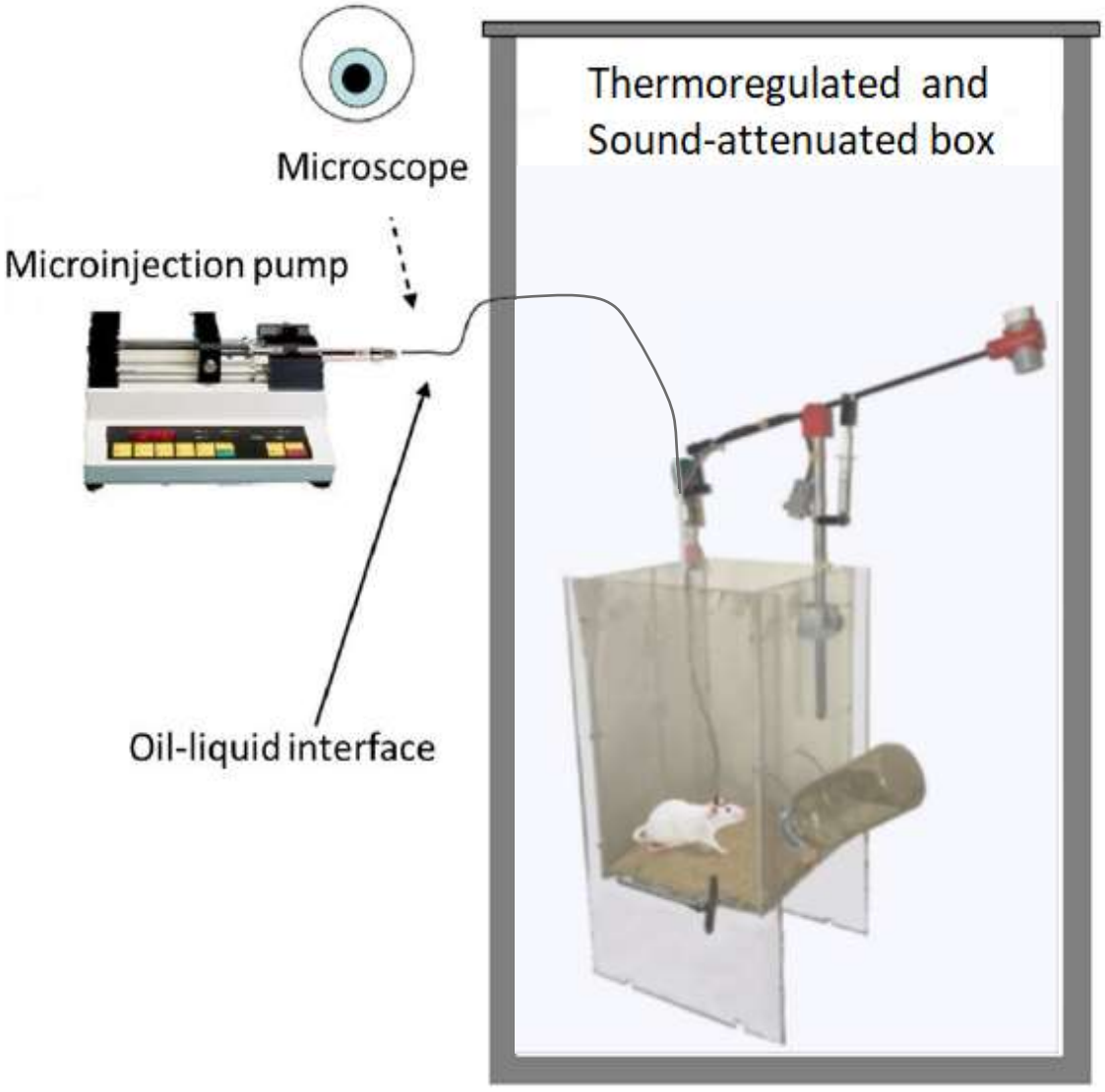
Thermoregulated and
Sound-attenuated box
Microscope
Microinjection pump
Oil-liquid interface

Figure 14. Experiment I: Anatomical areas of interest

Three pictures from a single slice were taken, for cervicothoracic and lumbar levels, as indicated by dotted squares: i) framing one hemi-ventral part, including the ventral horn (VH); ii) framing one hemi-central part, including the central canal (Central); iii) framing one hemi-dorsal part, including the dorsal horn (DH).

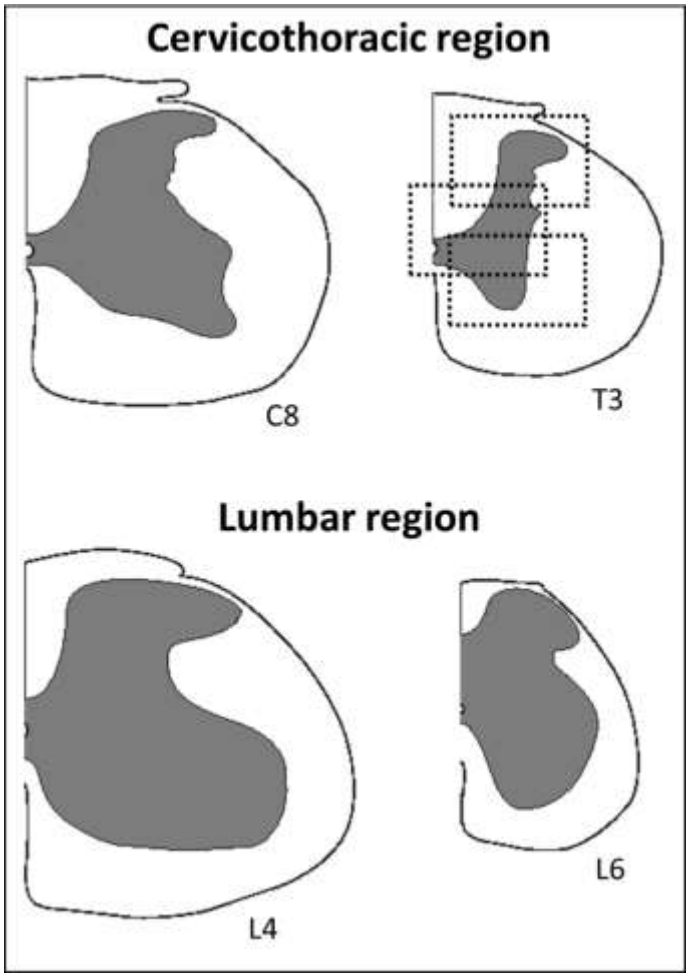
Cervicothoracic region
C8
T3
Lumbar region
L4
L6

Figure 15. Experiment II: Experimental plan

Panel a represents the experimental plan of the first part of experiment II. Two experimental conditions were used in this part: i) Recovery 6 hours with sleep deprivation (R6 SD); following synthetic torpor, as soon as the brain temperature reached 35,5 °C and clear signs of sleep were observed in the EEG activity, animals were sleep deprived by gentle handling for 6 hours (N=6); ii) Recovery 6 hours condition (R6); in which following synthetic torpor, as soon as the brain temperature reached 35,5 °C, animals were left to sleep and recover undisturbed from this point for 6 hours (N=6). Data of the R6 group were taken from (Cerri et al., 2013).

Panel b illustrates the experimental plan of the second part of the experiment, the following experimental conditions were used: i) Control (C); in this condition animals were injected with aCSF in the raphe pallidus and sacrificed at around 17.00 h (N=3); ii) Early recovery (ER); animals were sacrificed at around 19.00 h when, after synthetic torpor, the brain temperature reached 35.5 °C (N = 4); iii) Recovery 6 hours (R6); following synthetic torpor, as soon as the brain temperature reached 35,5 °C, animals were left to sleep and recover undisturbed from this point for 6 hours (N=5); iv) Recovery 6 hours with sleep deprivation (R6 SD); following synthetic torpor, as soon as the brain temperature reached 35,5 °C and clear signs of sleep were observed in the EEG activity, animals were sleep deprived by gentle handling for 6 hours (N=5).

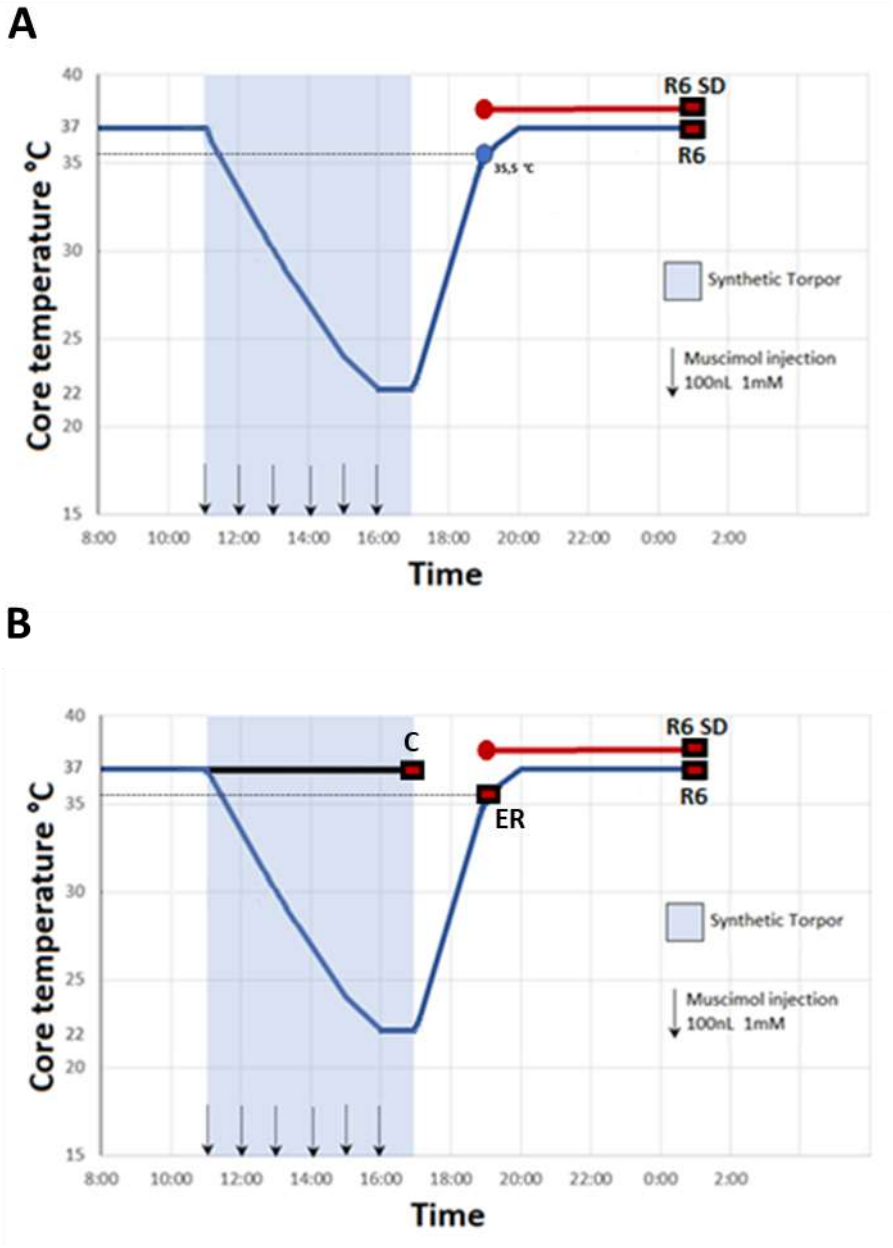
A
Core temperature °C
40
37
35
30
25
22
20
15
8:00
10:00
12:00
14:00
16:00
18:00
20:00
22:00
0:00
2:00
Time
R6 SD
R6
35,5 °C
Synthetic Torpor
Muscimol injection
100nL 1mM
B
Core temperature °C
Time
C
ER
R6 SD
R6
Synthetic Torpor
Muscimol injection
100nL 1mM

Figure 16. Experiment II: Schematic representation of analyzed brain areas

Bregma level is reported on each panel. Panel A: Amb, nucleus ambiguus; NTS, nucleus of the solitary tract; dMV, dorsal motor nucleus of the vagus nerve; RPa, raphe pallidus; py, pyramidal tract. Panel B: LC, locus coeruleus. Panel C: LPB, lateral parabrachial nucleus; mCP, middle cerebellar peduncle. Panel D: VLPAG, ventrolateral part of the periaqueductal gray matter; Aq, Sylvius aqueduct. Panel E: MM, medial mammillary nuclei; 3V, third ventricle. Panel F: LH, lateral hypothalamus; Arc, arcuate nucleus of the hypothalamus; DMH, dorsomedial nucleus of the hypothalamus; PV, paraventricular nucleus of the thalamus; CA3, field CA3 of the hippocampus; PRh, perirhinal cortex; P-Cx, parietal cortex. Panel G: PVH, paraventricular nucleus of the hypothalamus; ot, optic tract. Panel H: VLPO, ventrolateral preoptic nucleus; MnPO, median preoptic nucleus of the hypothalamus; ac, anterior commissure.

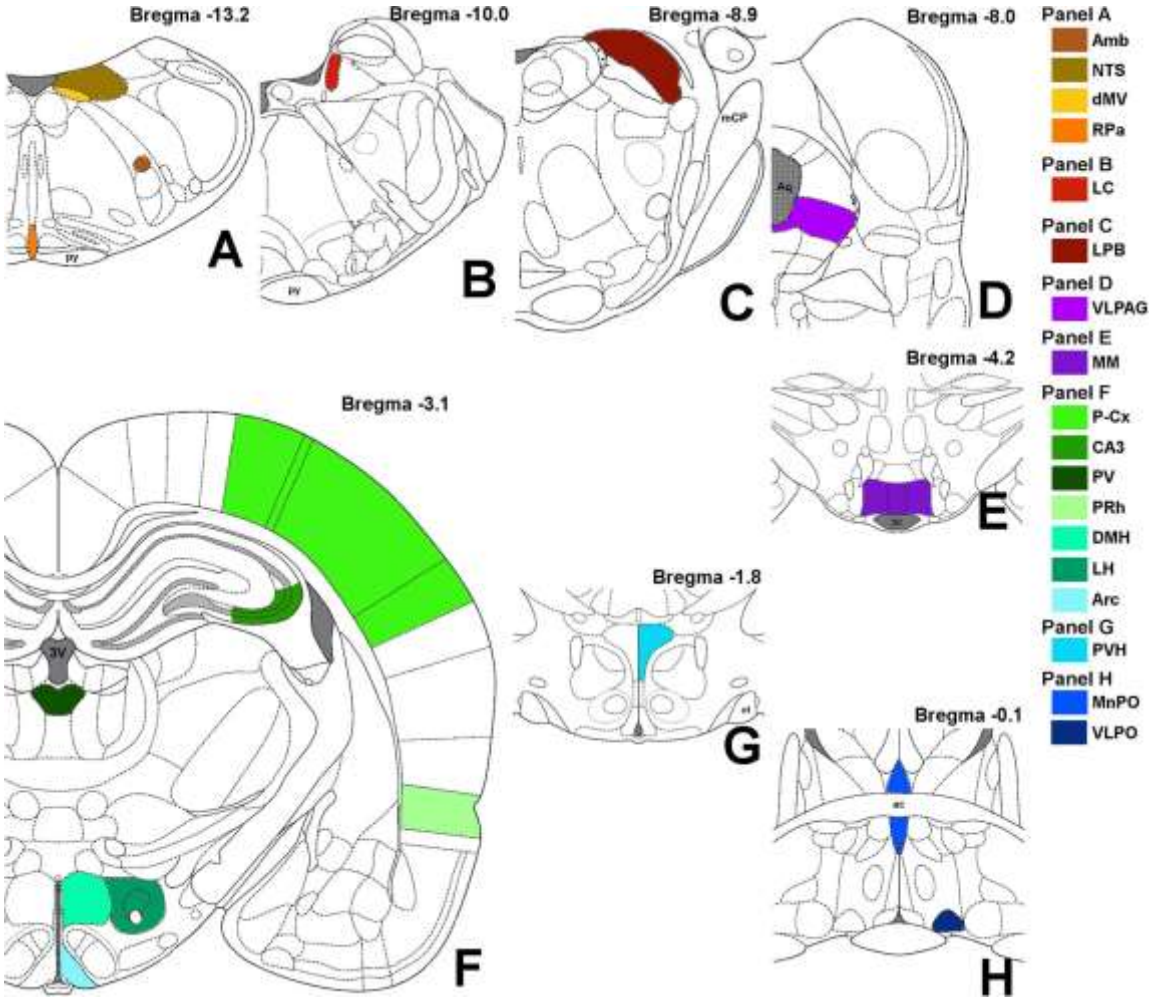

From: (Luppi et al., 2019)

Figure 17. Experiment II: Analyzed neural structures and their function

Analyzed brain structures, caudal to rostral, are shown, with abbreviations, bregma level, abbreviations as reported in the atlas (Paxinos & Watson, 2007), known function, and reference panel in the Figure 16. Structures directly involved in thermoregulation are shown in bold.

Brain structure		Abbreviation	Bregma level*	Abbreviation(s) as in Paxinos and Watson (2007)*	Functional involvement	Panel in Figure 16
Medulla	Nucleus ambiguus	Amb	−13/−13,5	AmbSC	Autonomic function – Parasympathetic	A
	Dorsal motor nucleus of the vagus nerve	dMV	−13/−13,5	10N	Autonomic function – Parasympathetic	A
	Nucleus of the solitary tract	NTS	−13/−13,5	SolI; sol; SolC; SolIM; SolCe; SolL; SolDL; SolM; SolV; SolVL; Psol	Visceral sensory integration – Central autonomic regulation	A
	Raphe pallidus	**Rpa**	−13/−13,5	Rpa	**Thermoregulation**	A
Pons	Locus coeruleus	LC	−9,6/−10,1	LC	Behavioral state control	B
	Lateral parabrachial nucleus	**LPB**	−8,9/−9,2	LPBD; LPBCr; LPBE; LPBV; LPBI; LPBC	Central autonomic regulation – **Thermoregulation**	C
Midbrain	Ventrolateral part of the periaqueductal gray matter	VLPAG	−8,0/−8,5	VLPAG	Central autonomic regulation – Behavioral state control	D
Hypothalamus	Medial mammillary nucleus	MM	−4,2/−4,4	MnM; MM	Memory formation and consolidation	E
	Lateral hypothalamus	LH	−3,0/−3,4	PeFLH; PeF	Behavioral state control – Regulation of body metabolism	F
	Arcuate nucleus	Arc	−3,0/−3,4	ArcD; ArcM; ArcL	Regulation of body metabolism	F
	Dorsomedial nucleus	**DMH**	−3,0/−3,4	DMC; DMD; DMV	**Thermoregulation**	F
	Paraventricular nucleus	**PVH**	−1,6/−1,9	PaMM; PaMP; PaV; PaDC; PaLM	Central autonomic regulation – Osmoregulation-**Thermoregulation**	G
	Ventrolateral preoptic nucleus	**VLPO**	−0,0/−0,6	VLPO	Behavioral State Control – **Thermoregulation**	H
	Median preoptic nucleus of the hypothalamus	**MnPO**	−0,1/−0,2	MnPO	Central autonomic regulation – Behavioral State Control – Osmoregulation-**Thermoregulation**	H
Thalamus	Paraventricular nucleus	PV	−3,0/−3,4	PVP	Central autonomic regulation	F
Cerebellum	Cerebellar cortex	Cb-Cx	−11,5/−13,5	General sample picture from cortical layers	Motor functions –Learning – Lack of Tau phosphorylation in tauopathies	n.s.
Hippocampus	CA3 field	CA3	−3,0/−3,4	CA3; SLu; Rad	Memory formation and consolidation – Well studied for assessing Tau phosphorylation in hibernators	F
Brain Cortex	Perirhinal cortex	PRh	−3,0/−3,4	PRh	Memory formation and consolidation – Recognition of environmental stimuli	F
	Parietal cortex	P-Cx	−3,0/−3,4	Broadly covering primary somatosensory cortex (S1Tr; S1DZ; S1BF; S1ULp)	Sample of neocortex – Sensory integration – Well studied for assessing Tau phosphorylation in hibernators	F

Modified from: (Luppi et al., 2019)

Figure 18. Experiment III: Experimental plan

After one week of post-operative recovery, rats were moved to the experimental box and exposed to a lower Ta (15 °C) 48 h prior to the experiment. At 07:00 of the experimental day, rats were randomly assigned to one of the experimental groups: Hypothermia (N = 5) (Group 1), animals underwent multiple microinjections one per hour of the GABA-A agonist muscimol (1mM) within the RPa. While Control (N = 5) (Group 2) were injected with aCSF. Four hours after the first injection, animals underwent a 3 Gy X-rays radiation exposure and were returned to the experimental box for additional four hours. At 16:00, all animals were euthanized, and organs were collected.

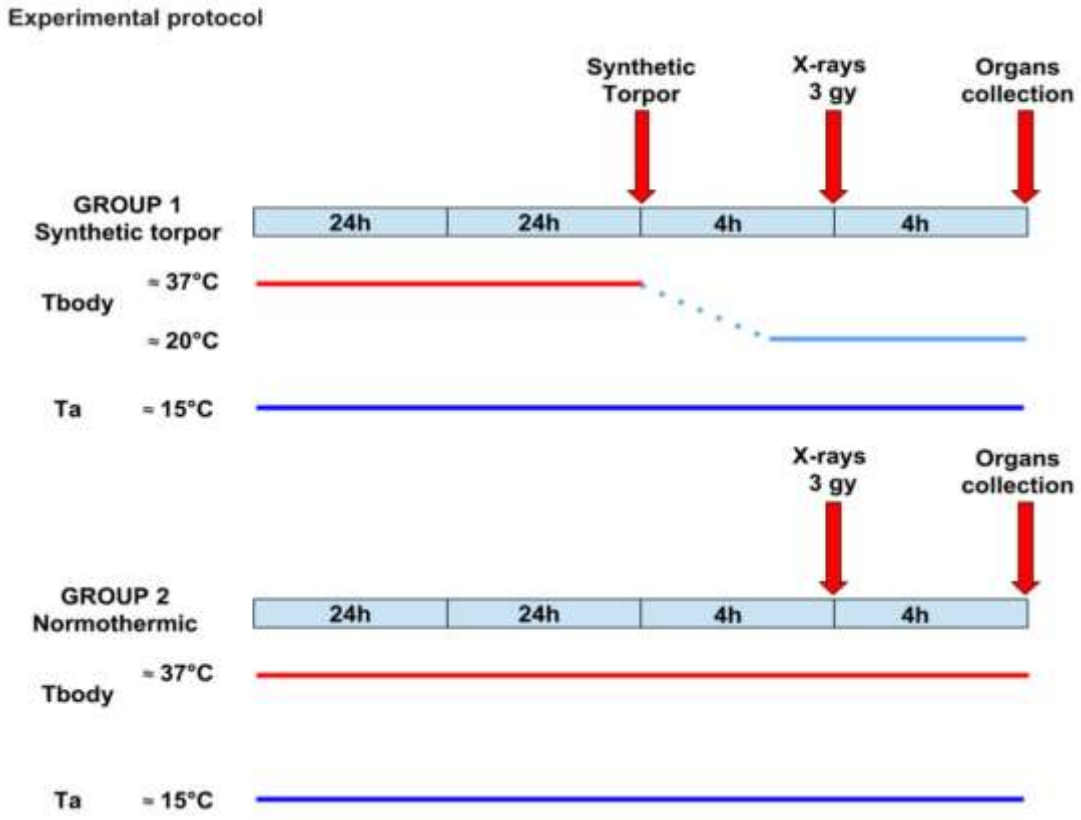

From: (Tinganelli et al., 2019)

Figure 19. Experiment III: List of collected organs

Summary table of organs collected and intended for three different types of analysis: histological evaluation, evaluation of gene expression and laser capturing. For the laser capturing only dorsal skin, ventral skin and small intestine were collected. Once removed, they were placed for a few minutes in later RNA, dried, and then transversely arranged in cryomold plastic molds (Tissue-Tek Cryomold Molds) containing O.C.T. (Optical Cutting Temperature compound, Scigen, USA). The mold was then immersed in a solution, refrigerated in dry ice, of 2-methylbutane (Sigma-Aldrich, St Louis, MO, USA). Finally, samples were stored at a temperature of -70 °C pending subsequent analyses. The laser capturing analysis has not yet been carried out. For other analyses see Material and methods of experiment III.

COLLECTED ORGANS	HISTOLOGY	GENE EXPRESSION	LASER CAPTURING
DORSAL SKIN	X	X	X
VENTRAL SKIN	X	X	X
MUSCLE	X	X	
TESTICLE	X	X	
PROSTATE	X	X	
LIVER	X	X	
KIDNEY	X	X	
INTESTINE	X	X	X
SPLEEN	X	X	
HEART	X	X	
BRAIN	X		

Figure 20. Experiment III: Exit dose in an irradiated rat

Exit dose measured with a radiochromic film positioned under one irradiated animal. Entrance dose can be evaluated from the percentage depth dose curves and the animal thickness. The radiochromic film is composed by two-dimensional dosimeters, formed by layers of transparent material made up of polymers which, if exposed to radiation, polarize and increase the optical density of the film proportionally to the absorbed dose, allowing a precise estimate.

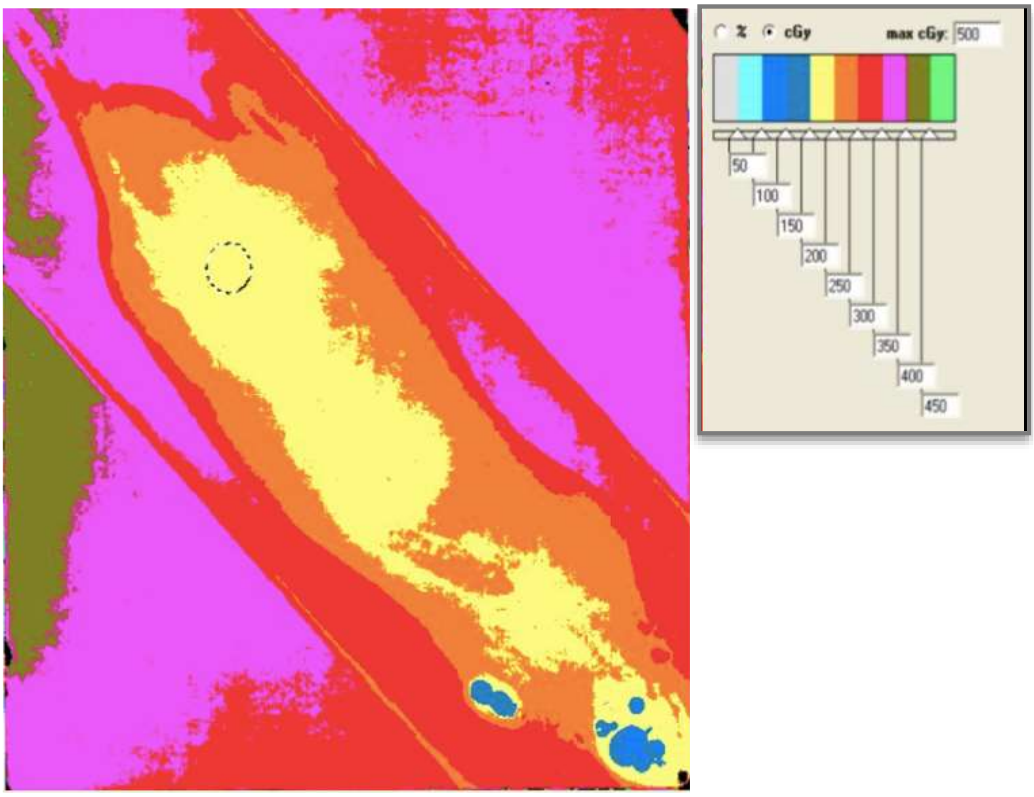

Modified from: (Tinganelli et al., 2019)

Figure 21. Experiment I: Table of AT8 and Tau-1 staining levels

AT8 (phosphorylated Tau protein) and Tau-1 (non-phosphorylated Tau protein) staining intensities. VH: ventral horn; Central: central part of the hemicoronal section of the spinal cord; DH: dorsal horn. Control (C); Nadir 30 °C (N30); Nadir (N); Early-recovery (ER); Recovery 6 hours (R6); Recovery 38 hours (R38). * vs. C; # R6 vs. ER; § R6 vs. R38. ($p<0.05$)

AT8	C	N30	N *	ER	R6 *#§	R38
VH	+	+	+	+	- *#§	+
Central	+	+	++ *	+	- *#§	+
DH	+	++ *	++ *	+	- *#§	+
Tau-1	C	N30	N *	ER	R6	R38
VH	++	++	+ *	++	+ *#§	++
Central	++	+++	+ *	+++	++	++
DH	+++	+++	+ *	+++	+++	+++

Figure 22. Experiment I: Representative pictures of NeuN, AT8, and Tau-1 staining in dorsal horn

Examples of staining for NeuN (green, Alexa-488) and AT8 (red, Alexa-594) the first two columns on the left or NeuN and Tau-1 (red, Alexa-594;) the two columns on the right, for all the experimental conditions. From top to bottom: Control (C); Nadir 30 °C (N30); Nadir (N); Early-recovery (ER); Recovery 6 hours (R6); Recovery 38 hours (R38).

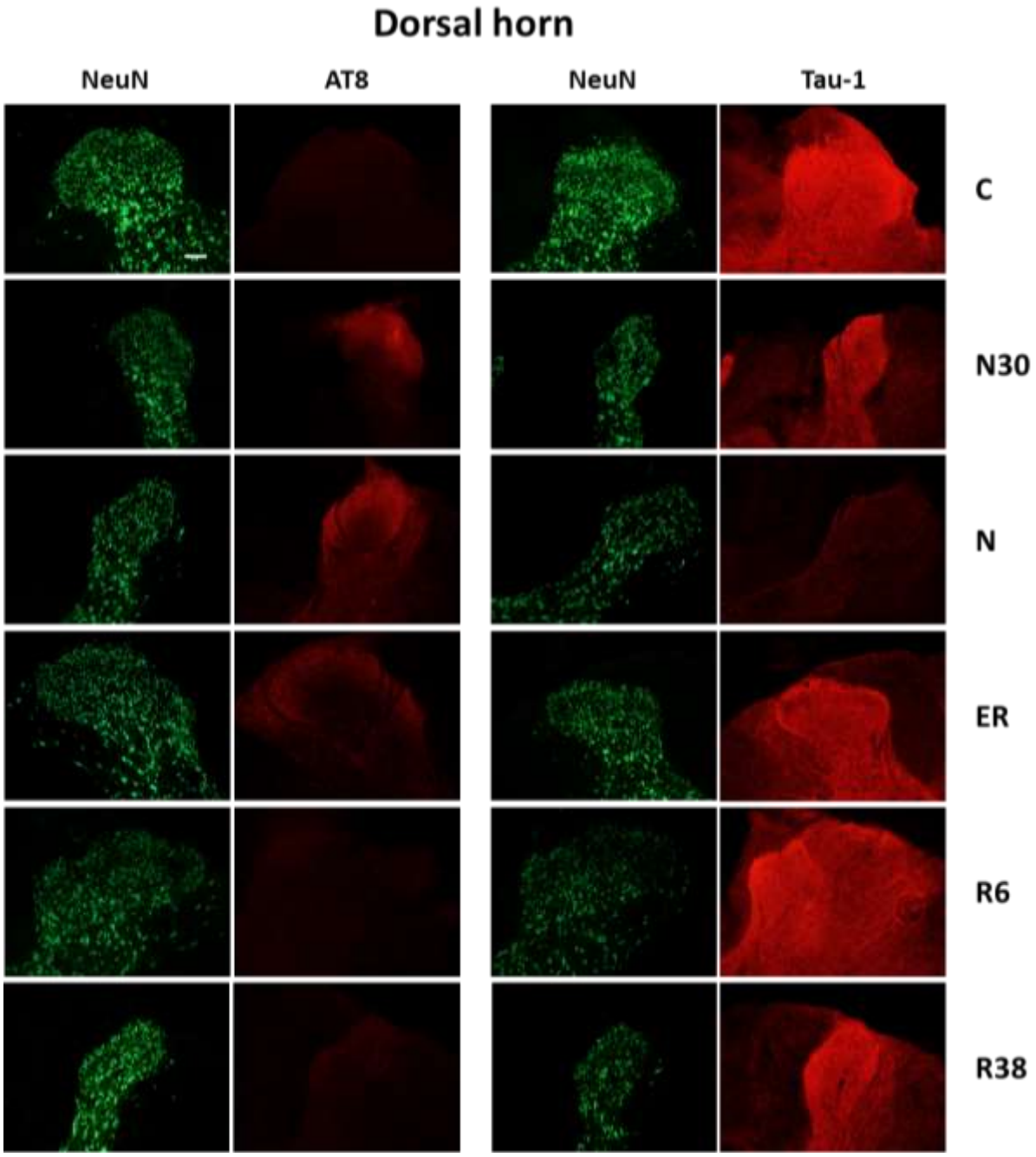
Dorsal horn
NeuN
AT8
NeuN
Tau-1
C
N30
N
ER
R6
R38

Figure 23. Experiment I: Representative pictures of NeuN, AT8, and Tau-1 staining in ventral horn

Examples of staining for NeuN (green, Alexa-488) and AT8 (red, Alexa-594) the first two columns on the left or NeuN and Tau-1 (red, Alexa-594;) the two columns on the right, for all the experimental conditions. From top to bottom: Control (C); Nadir 30 °C (N30); Nadir (N); Early-recovery (ER); Recovery 6 hours (R6); Recovery 38 hours (R38).

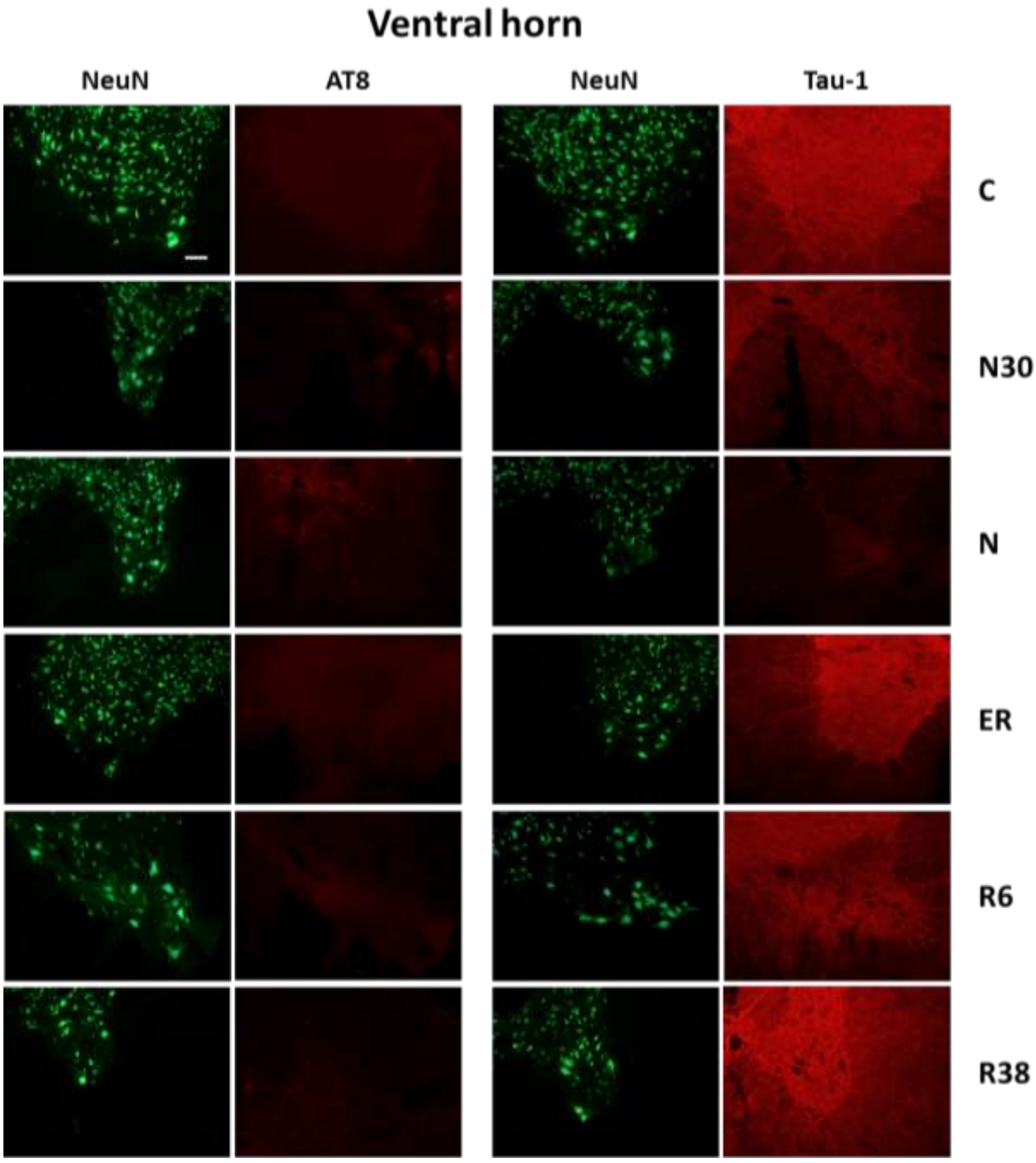
Ventral horn
NeuN
AT8
NeuN
Tau-1
C
N30
N
ER
R6
R38

Figure 24. Experiment I: illustrative comparison between ventral and dorsal horn for P(9)-GSK3β staining

Examples of staining for P(9)-GSK3β (green, Alexa-488) are shown. In the column on the left the staining in the ventral horn, while in the right column the staining of the dorsal horn. Control (C); Nadir 30 °C (N30); Nadir (N); Early-recovery (ER); Recovery 6 hours (R6).

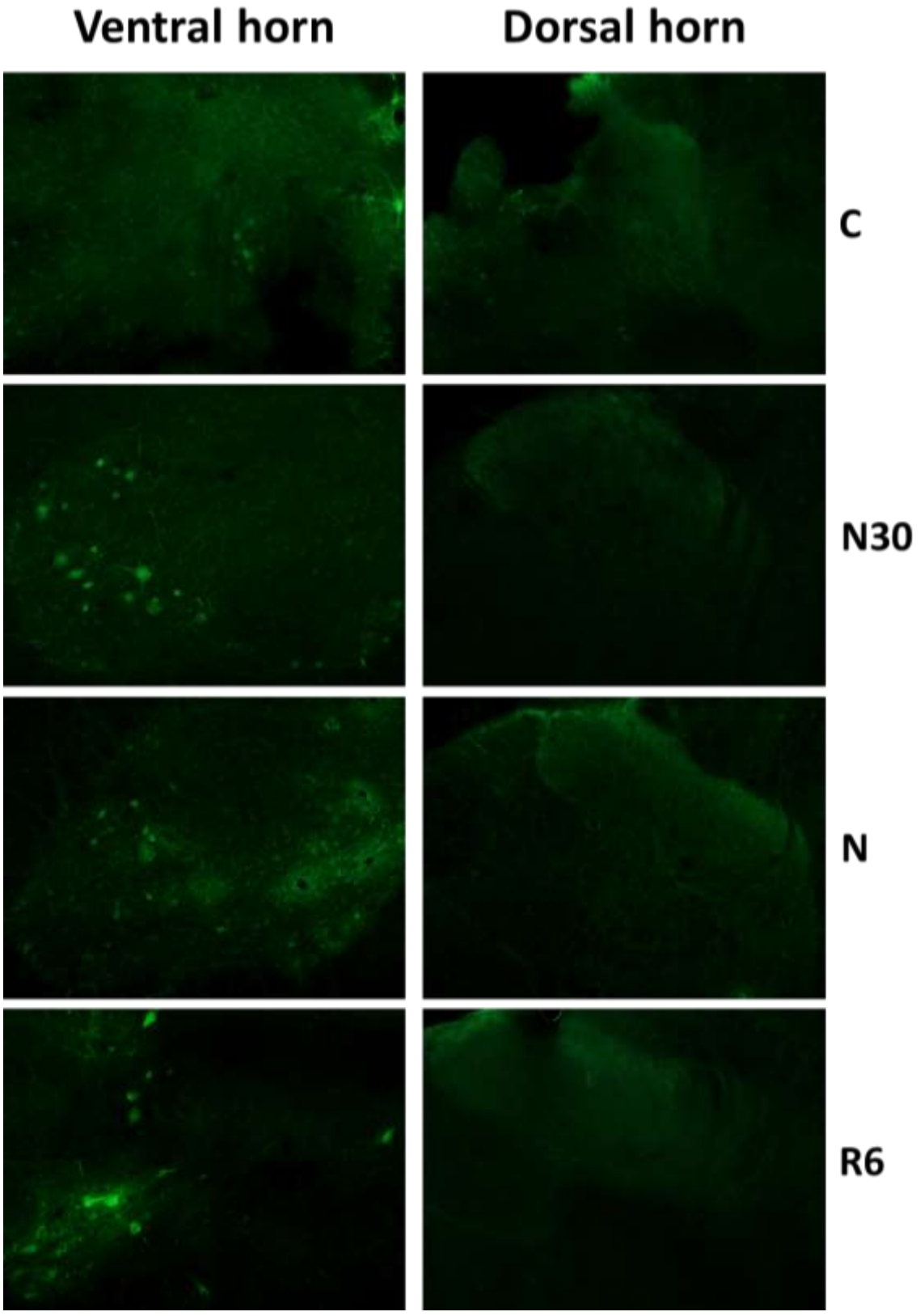
Ventral horn
Dorsal horn
C
N30
N
R6

Figure 25. Experiment I: Representative pictures of P(9)-GSK3β and ChAT double staining in ventral horn

Example of staining for P(9)-GSK3β (green, Alexa-488), image on the left, and ChAT (orange, Alexa-555), image in the middle, in the ventral horn of the spinal cord. The last image on the right represents a merge of the first two. This qualitative analysis was performed in order to evaluate the regulation of GSK3-β activity in motor neurons of the spinal cord.

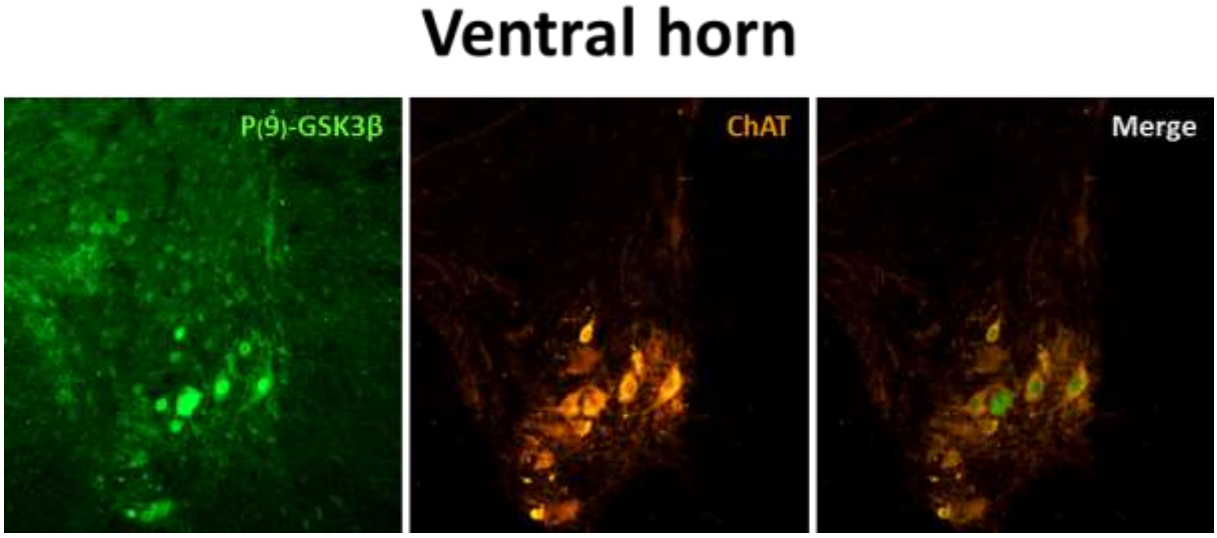
Ventral horn
P(9)-GSK3β
ChAT
Merge

Figure 26. Experiment I: Morphometric parameters for the microglia analysis

Morphometric parameters for the microglia analysis are shown as mean ± s.e.m. This analysis was carried out both in ventral and dorsal horns for the following experimental conditions: Control (C); Nadir (N); Recovery 6 hours (R6); Recovery 38 hours (R38). SA: soma area; AA: arborization area; MI: morphological index (SA/AA); Nnd: nearest neighbor distance; VH: ventral horn; DH: dorsal horn. * vs. C; § vs. N. ($p<0.05$)

	C		N		R6		R38	
	VH	DH	VH	DH	VH	DH	VH	DH
Cell count	76,1 ± 10,3	70,9 ± 7,2	60,5 ± 9,0	58,3 ± 5,3	63,3 ± 8,3	72,5 ± 3,5	59,8 ± 3,1	68,3 ± 7,1
SA (μm^2)	46,7 ± 1,3	48,6 ± 2,7	43,5 ± 2,3	40,9 ± 2,6	46,7 ± 4,6	51,8 ± 3,2	46,6 ± 4,0	46,7 ± 3,0
AA (μm^2)	826,1 ± 270,9	722,7 ± 210,6	608,2 ± 41,4	595,5 ± 29,0	534,8 ± 54,1	663,4 ± 70,7	501,2 ± 36,5	589,3 ± 101,5
MI	0,155 ± 0,047	0,150 ± 0,040	0,082 ± 0,004	0,076* ± 0,005	0,107 ± 0,014	0,096 ± 0,008	0,107 ± 0,011	0,100[§] ± 0,013
Nnd (µm)	41,1 ± 4,1	46,0 ± 4,0	43,9 ± 2,4	42,1 ± 2,0	46,0 ± 1,9	43,3 ± 2,2	40,8 ± 2,5	37,9 ± 3,0

Figure 27. Experiment I: Representative pictures of Iba1 staining in ventral and dorsal horns

Examples of staining for Iba1 (Alexa-488) in ventral (column on the left) and dorsal (column on the right) horns of the spinal cord. From top to bottom: Control (C); Nadir (N); Recovery 6 hours (R6); Recovery 38 hours (R38).

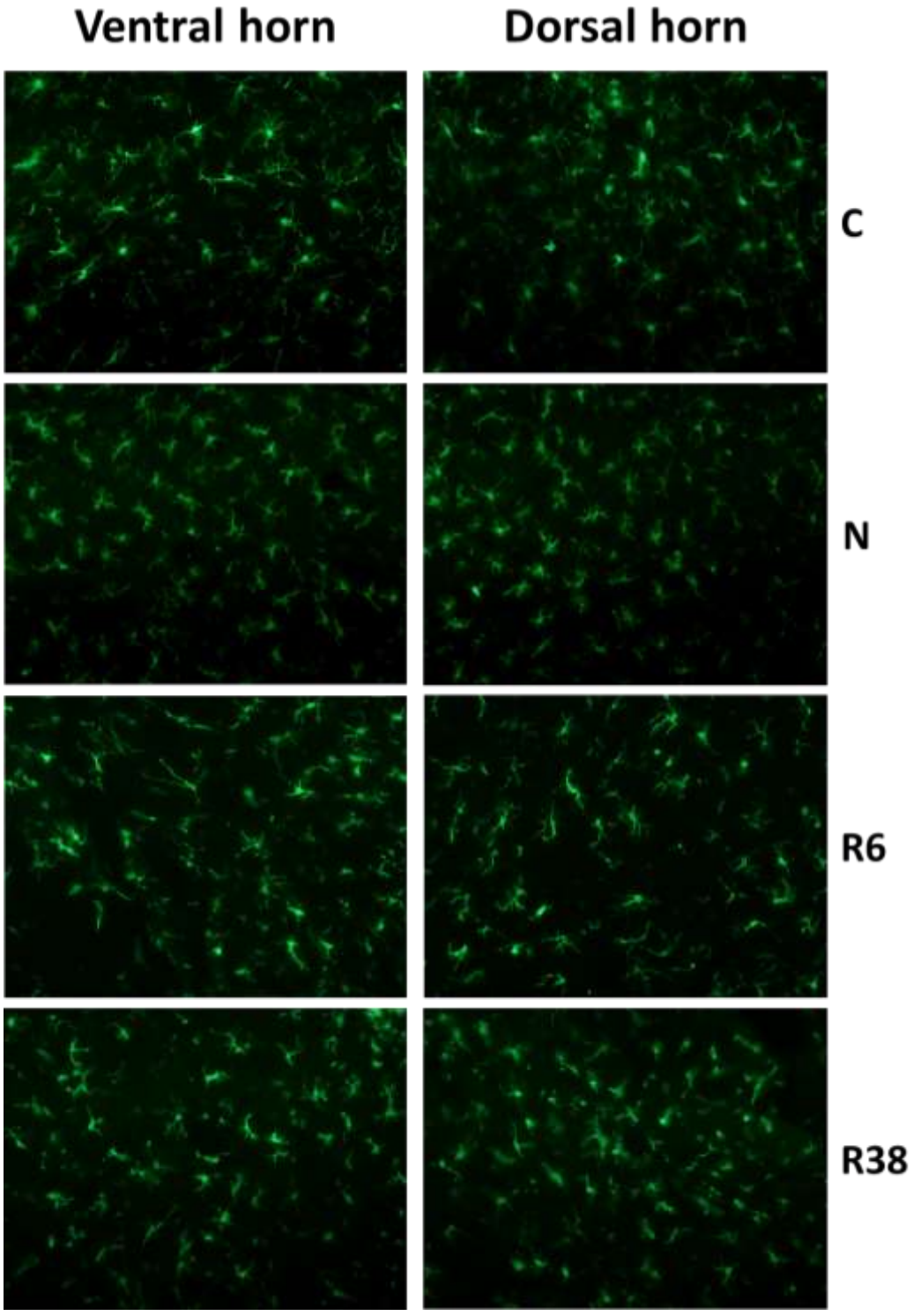
Ventral horn
Dorsal horn
C
N
R6
R38

Figure 28. Experiment II: Delta power and NREM sleep in the R6 experimental condition

Delta power in NREM sleep (% of the average baseline levels in the baseline) and NREM sleep amount (% of each time interval) are shown with a 30-min resolution for the animals in the R6 experimental condition (Data from Cerri et al. 2013). In the bottom part the experimental plan of this part of experiment II is reported.

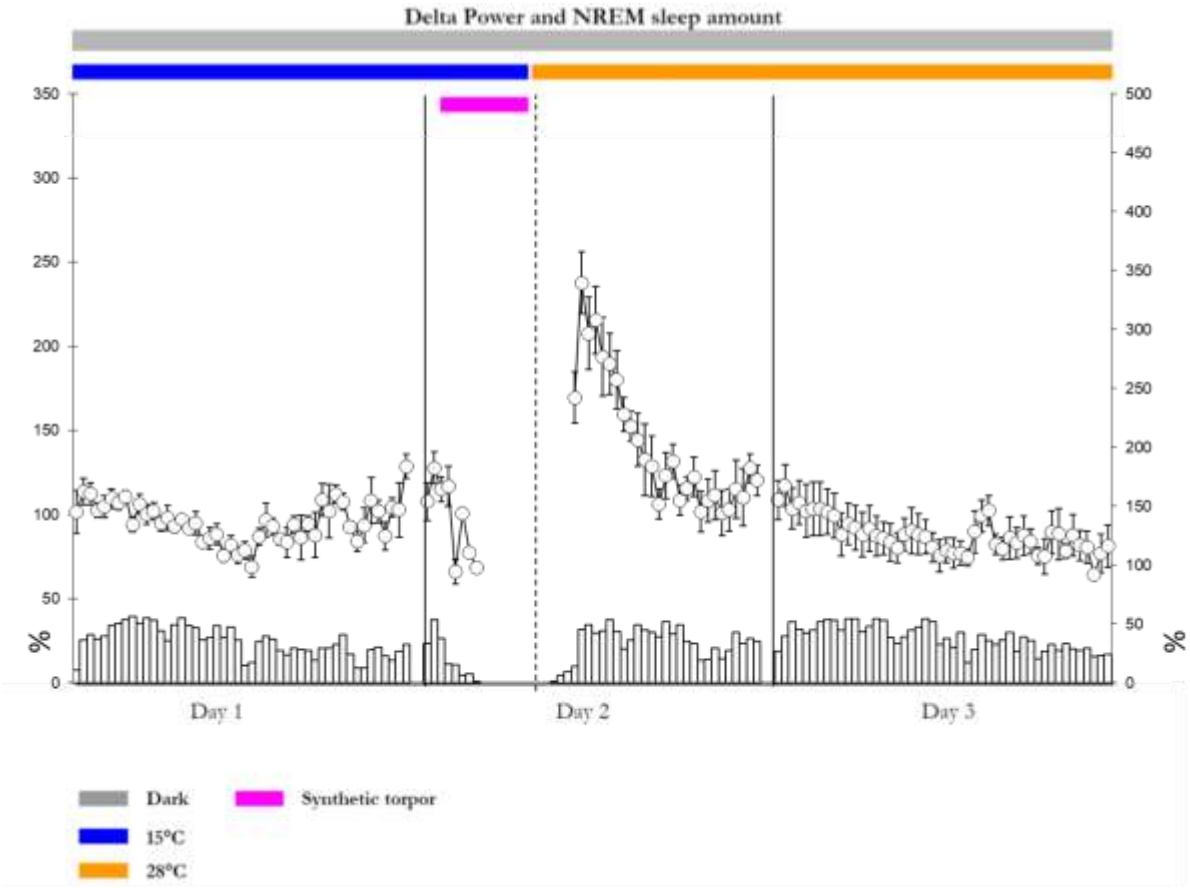
Delta Power and NREM sleep amount
350
300
250
200
150
100
50
0
%
500
450
400
350
300
250
200
150
100
50
0
%
Day 1
Day 2
Day 3
Dark
Synthetic torpor
15°C
28°C

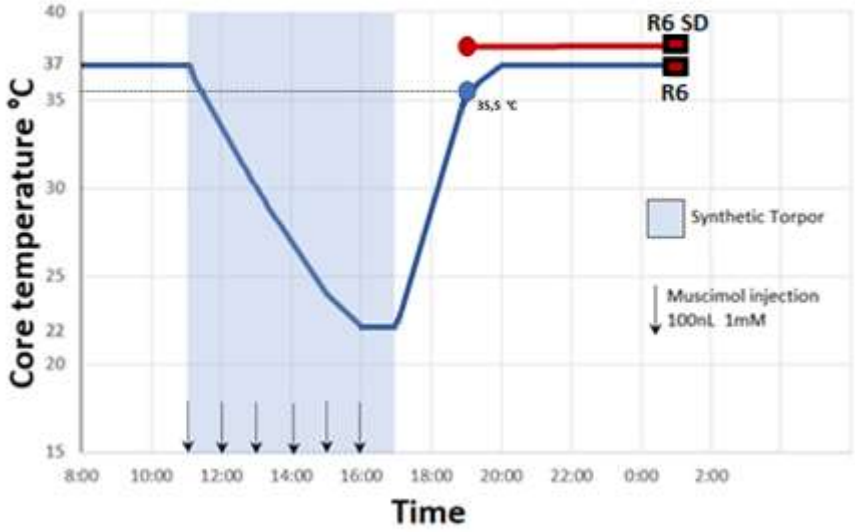
Core temperature °C
40
37
35
30
25
22
20
15
8:00
10:00
12:00
14:00
16:00
18:00
20:00
22:00
0:00
2:00
Time
R6 SD
R6
35,5 °C
Synthetic Torpor
Muscimol injection
100nL 1mM

Figure 29. Experiment II: Delta power and NREM sleep in the R6 SD experimental condition

Delta power in NREM sleep (% of the average baseline levels in the baseline) and NREM sleep amount (% of each time interval) are shown with a 30-min resolution for animals of the R6 SD experimental condition. In the bottom part the experimental plan of this part of experiment II is reported.

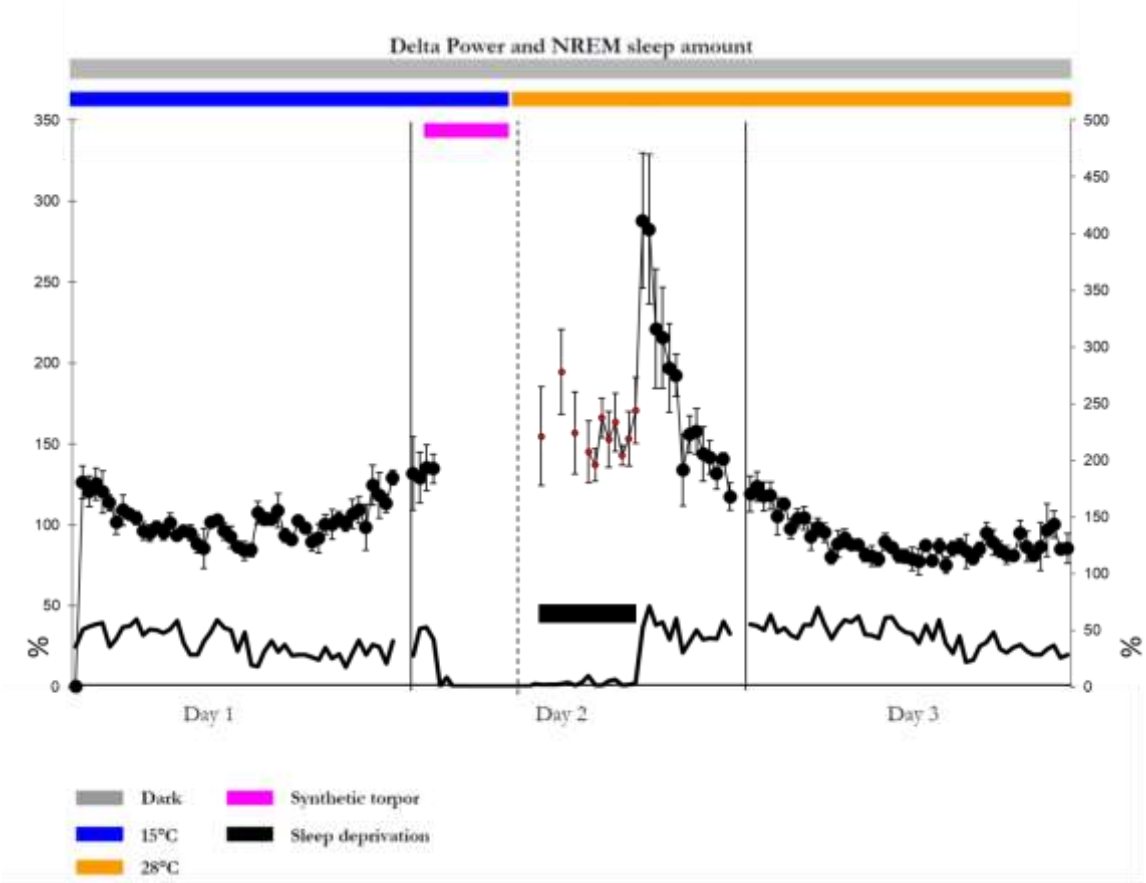
Delta Power and NREM sleep amount
350
300
250
200
150
100
50
0
%
500
450
400
350
300
250
200
150
100
50
0
%
Day 1
Day 2
Day 3
Dark
15°C
28°C
Synthetic torpor
Sleep deprivation

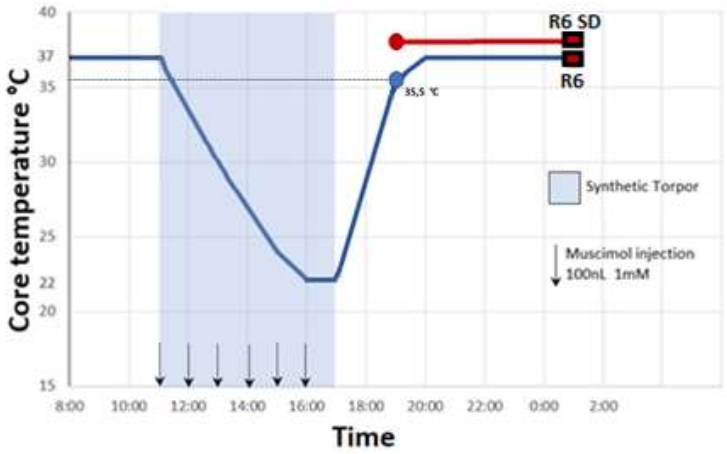
Core temperature °C
40
37
35
30
25
22
20
15
8:00
10:00
12:00
14:00
16:00
18:00
20:00
22:00
0:00
2:00
Time
R6 SD
R6
35,5 °C
Synthetic Torpor
Muscimol injection
100nL 1mM

Figure 30. Experiment II: Delta power and NREM sleep in the R6 and R6 SD experimental conditions

Delta power in NREM sleep (% of the average baseline levels in the baseline) and NREM sleep amount (% of each time interval) are shown with a 30-min resolution for animals of the R6 and R6 SD experimental conditions. The increase in Delta power was significantly larger in R6 SD (281±13%) compared to R6 (237±19%). * vs. R6 ($p<0.05$)

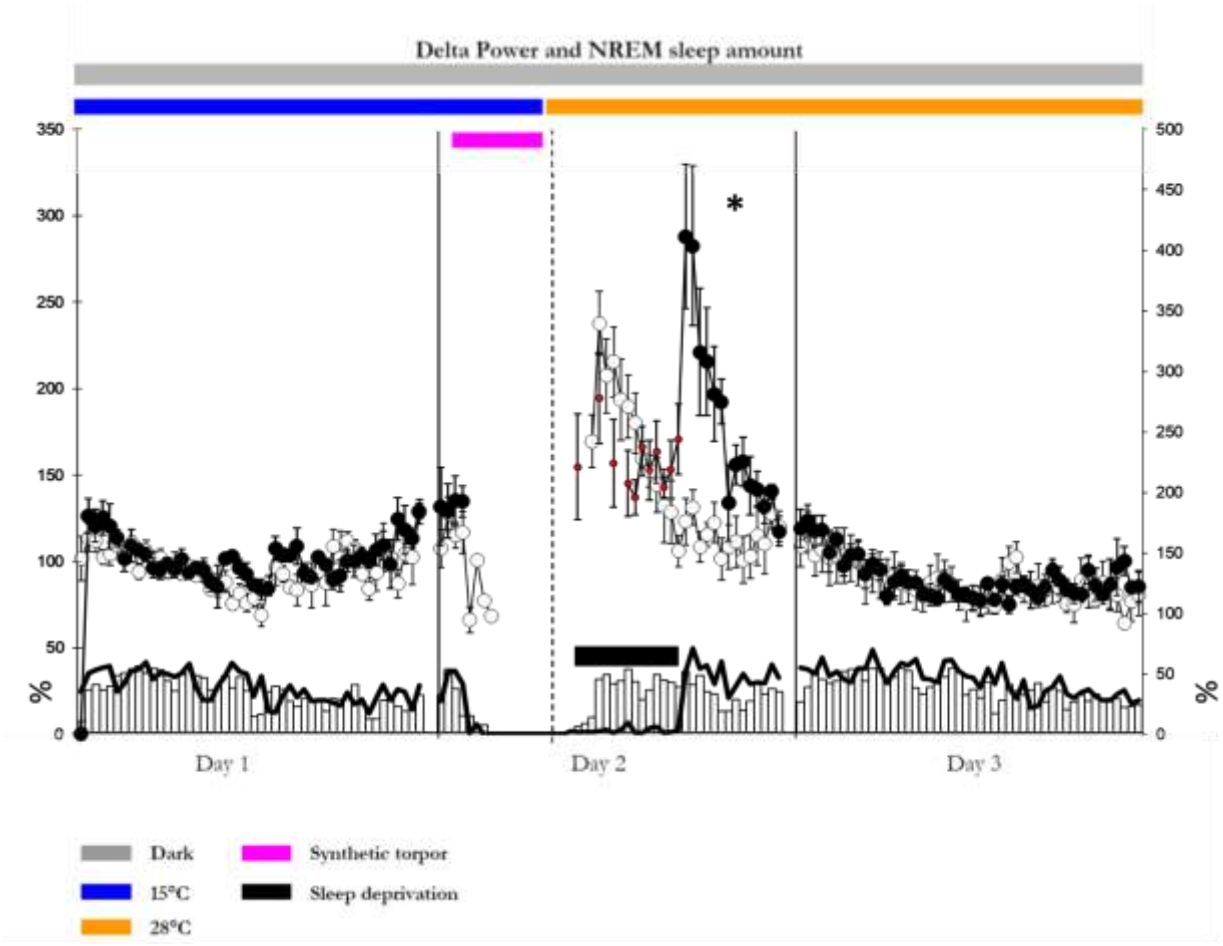
Delta Power and NREM sleep amount
350
300
250
200
150
100
50
0
%
500
450
400
350
300
250
200
150
100
50
0
%
*
Day 1
Day 2
Day 3
Dark
15°C
28°C
Synthetic torpor
Sleep deprivation

Figure 31. Experiment II: Table of AT8 and Tau-1 staining intensities

Panel a represents the method used to encode the average evaluations of the various experimental conditions into symbols to be represented graphically. *Panel b* shows the intensity of the AT8 staining for all the brain areas analyzed (lines) in the different experimental conditions (columns): Control (C); Early-recovery (ER); Recovery 6 hours (R6); Recovery 6 hours with sleep deprivation (R6 SD). *Panel c* shows the intensity of the Tau-1 staining for all the brain areas analyzed (lines) in the different experimental conditions (columns): Control (C); Recovery 6 hours (R6); Recovery 6 hours with sleep deprivation (R6 SD). * vs. R6 SD ($p<0.05$)

A

0 - 0.24	0	-
0.25 - 0.74	0.5	-/+
0.75 - 1.24	1	+
1.25 - 1.74	1.5	+/+
1.75 - 2.24	2	++
2.25 - 2.74	2.5	++/+
2.75 - 3.24	3	+++
3.25 - 3.74	3.5	+++/+
3.75 - 4	4	++++

B

	AT8			
	C*	ER*	R6*	R6 SD
Amb	-/+	+*	-/+	-/+
NTS	-/+	++*	-	-/+
dMV	-/+	+/+*	-/+	-/+
RPa	++*	++/+*	+/+*	+
LC	-/+*	+*	-	-
LPB	-	+/+*	-	-
VLPAG	-/+	+*	-	-/+
Cb-Cx	-	+/+*	-	-
MM	-	+/+*	-/+*	-
LH	-/+*	+/+*	-	-
Arc	-/+	++/+*	+*	-/+
DMH	-	+/+*	-/+*	-
PVH	-	++*	-	-
PV	-	-/+	-	-
VLPO	-	+/+*	-/+*	-
MnPO	-	+/+*	-/+*	-
CA3	-/+*	+/+*	-	-
PRh	-	-/+*	-	-
P-Cx	-/+	+	-	+

C

	TAU-1		
	C	R6*	R6 SD
Amb	+/+*	+*	++/+
NTS	++*	+*	+++
dMV	+/+*	+*	++/+
RPa	+*	-*	+++/+
LC	++	-/+*	++
LPB	+/+	+	++
VLPAG	+++	-/+*	++/+
Cb-Cx	+/+	+*	++/+
MM	++/+	-/+*	++/+
LH	+++*	+*	++
Arc	+++*	++/+	++/+
DMH	++/+	+	+/+
PVH	+++	+/+	++
PV	++/+	+*	++
VLPO	++/+	+*	+++
MnPO	+++*	-/+*	++
CA3	++	+*	++/+
PRh	+++/+*	+/+*	++/+
P-Cx	++/+	+/+	++/+

Figure 32. Experiment II: Representative pictures of NeuN and AT8 staining in ventrolateral preoptic nucleus (VLPO)

Example of staining for NeuN (green, Alexa-488, left column) and AT8 (red, Alexa-594, right column) in ventrolateral preoptic nucleus (VLPO), in the different experimental conditions: Control (C); Early-recovery (ER); Recovery 6 hours (R6); Recovery 6 hours with sleep deprivation (R6 SD). The right panel shows the atlas positioning in a coronal section of the VLPO, obtained from "The Rat Brain in Stereotaxic Coordinates" (Paxinos & Watson, 2007).

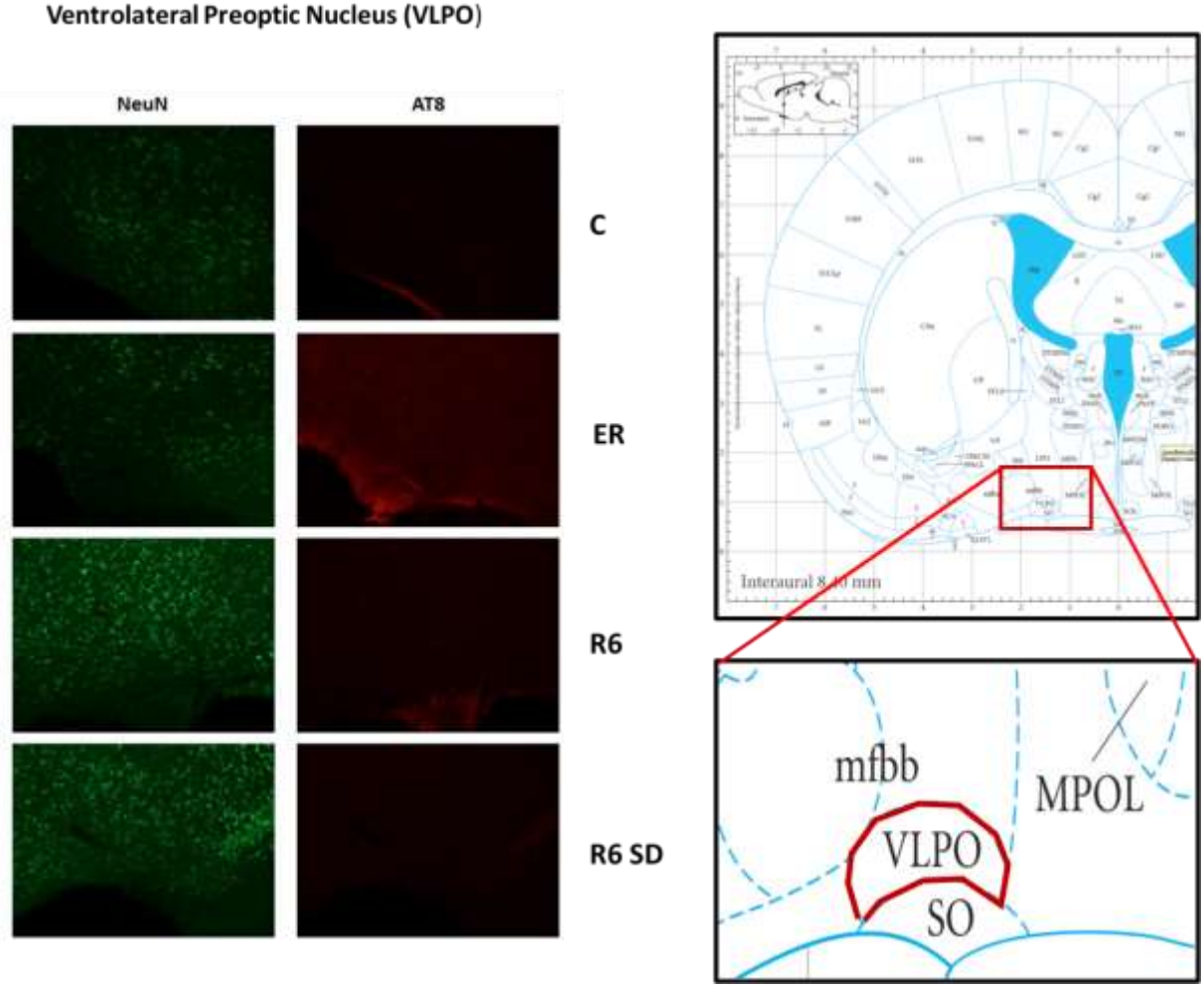
Ventrolateral Preoptic Nucleus (VLPO)
NeuN
AT8
C
ER
R6
R6 SD
Interaural 8.40 mm
mfbb
MPOL
VLPO
SO

Figure 33. Experiment II: Representative pictures of NeuN and AT8 staining in median preoptic nucleus of the hypothalamus (MnPO)

Example of staining for NeuN (green, Alexa-488, left column) and AT8 (red, Alexa-594, right column) in median preoptic nucleus of the hypothalamus (MnPO), in the different experimental conditions: Control (C); Early-recovery (ER); Recovery 6 hours (R6); Recovery 6 hours with sleep deprivation (R6 SD). The right panel shows the atlas positioning in a coronal section of the MnPO, obtained from "The Rat Brain in Stereotaxic Coordinates" (Paxinos & Watson, 2007).

Median Preoptic Nucleus of Hypothalamus (MnPO)

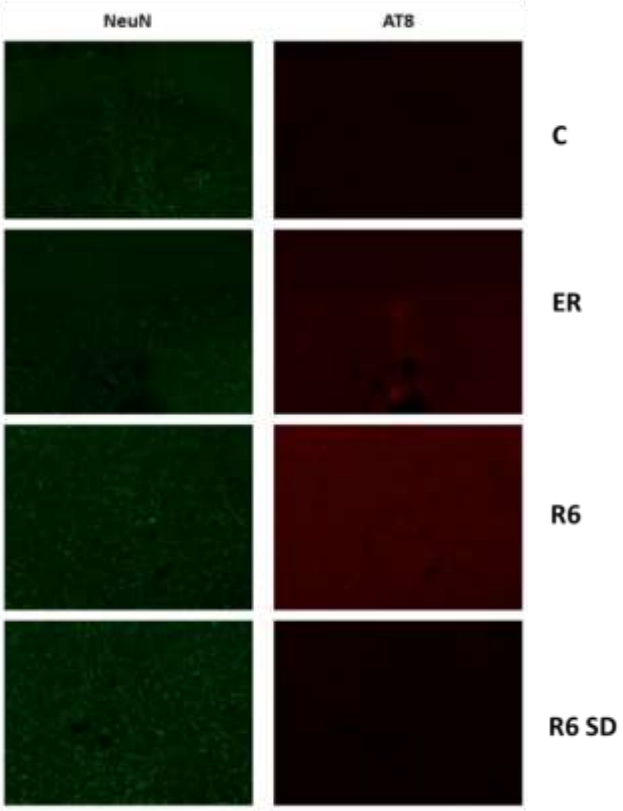

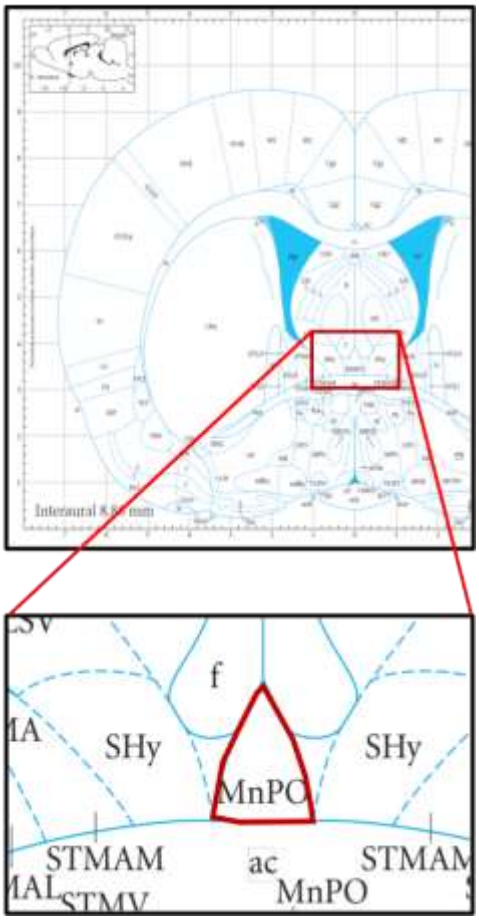

Figure 34. Experiment II: Representative pictures of NeuN and Tau-1 staining in ventrolateral preoptic nucleus (VLPO)

Example of staining for NeuN (green, Alexa-488, left column) and Tau-1 (red, Alexa-594, right column) in ventrolateral preoptic nucleus (VLPO), in the different experimental conditions: Control (C); Recovery 6 hours (R6); Recovery 6 hours with sleep deprivation (R6 SD). The right panel shows the atlas positioning in a coronal section of the VLPO, obtained from "The Rat Brain in Stereotaxic Coordinates" (Paxinos & Watson, 2007).

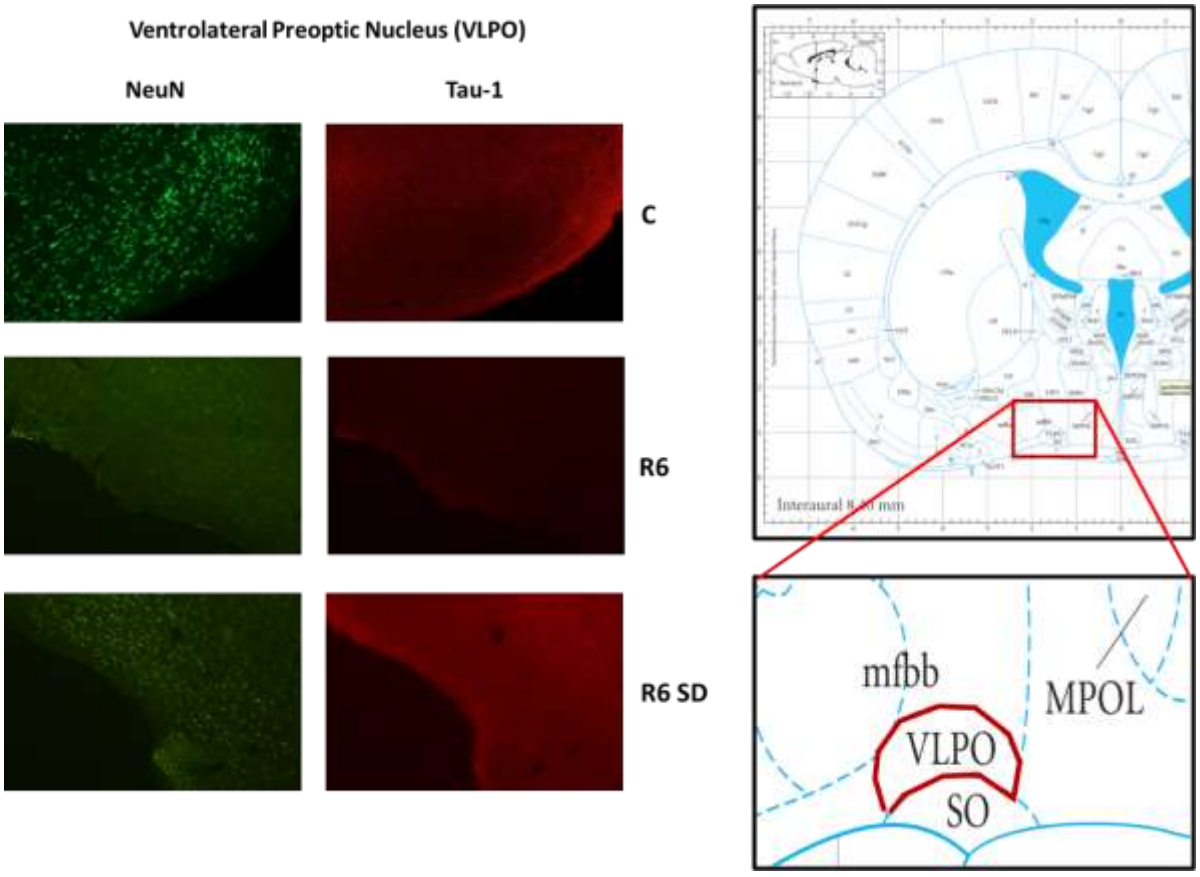
Ventrolateral Preoptic Nucleus (VLPO)
NeuN
Tau-1
C
R6
R6 SD
mfbb
MPOL
VLPO
SO

Figure 35. Experiment II: Representative pictures of NeuN and Tau-1 staining in raphe pallidus (RPa)

Example of staining for NeuN (green, Alexa-488, left column) and Tau-1 (red, Alexa-594, right column) in raphe pallidus (RPa), in the different experimental conditions: Control (C); Recovery 6 hours (R6); Recovery 6 hours with sleep deprivation (R6 SD). The right panel shows the atlas positioning in a coronal section of the RPa, obtained from "The Rat Brain in Stereotaxic Coordinates" (Paxinos & Watson, 2007).

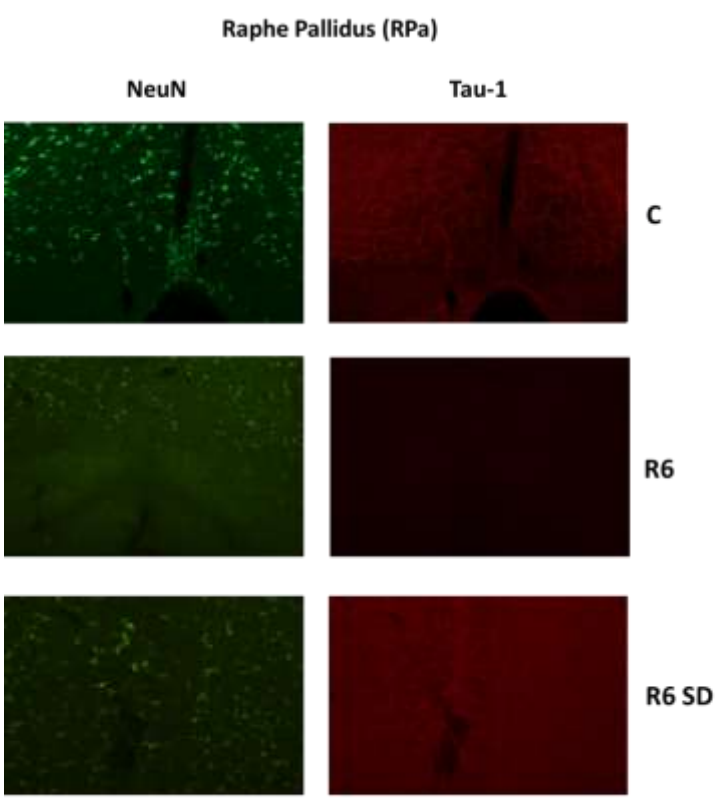
Raphe Pallidus (RPa)
NeuN
Tau-1
C
R6
R6 SD

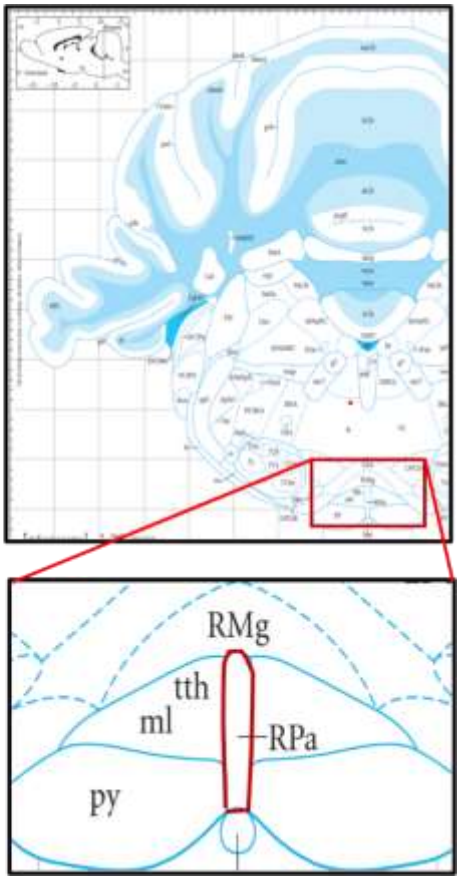
RMg
tth
ml
RPa
py

Figure 36. Experiment III: Brain temperature and irradiation time

Mean value ± SEM every 30 min of the brain temperature, recorded during the experimental day. Brain temperature was recorded by means of a thermistor, surgically implanted in the Lateral Hypothalamus. Empty dots: Control (N = 5), filled dots: Hypothermia (N = 5).

Brain temperature during synthetic torpor.

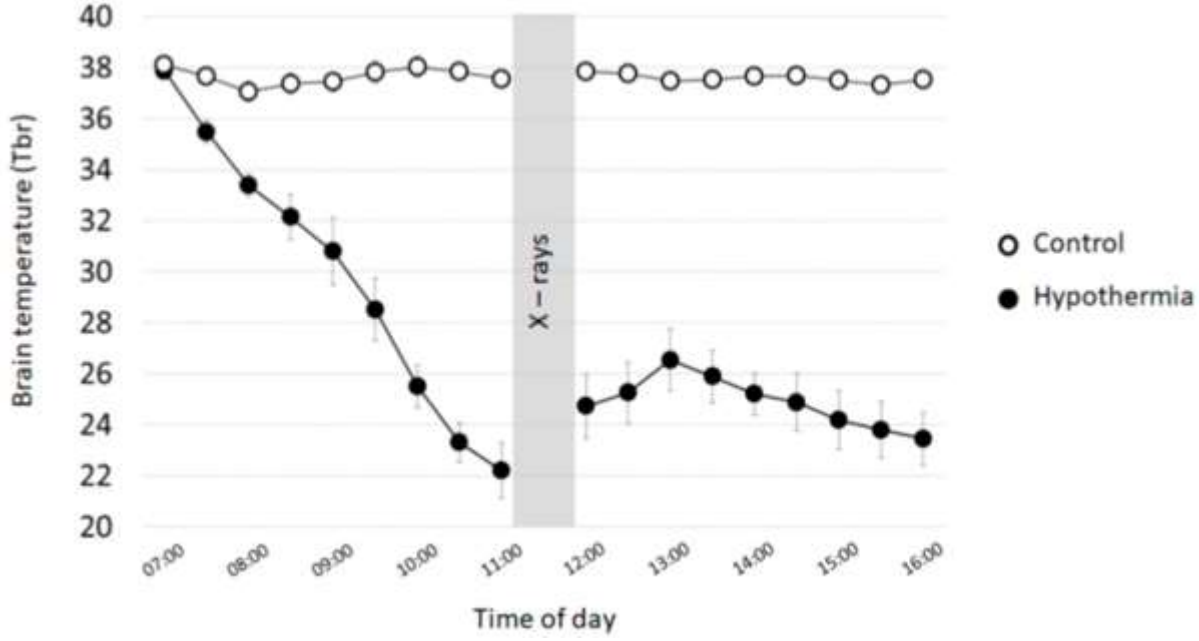

Figure 37. Experiment III: Morphology of the hepatic tissue

Hepatic tissue morphology after hematoxylin-eosin staining in irradiated normothermic (A-B) and hypothermic liver (C-D). The radiation damage in normothermic conditions is visibly greater compared to the effects detected after irradiation in synthetic torpor. Alteration and disorganization in the hepatic parenchyma were observed in A and B, vacuolization and shrunken nuclei with irregular shape and chromatin condensation (A-B, arrows) were identified in the hepatocytes. The morphology and the organization of hepatic parenchyma irradiated during synthetic torpor (C-D) seems comparable to the normal organization of the liver tissue. In this condition hepatocytes show a dense cytoplasm, round nuclei with dispersed chromatin. Scale bars = 20 μm.

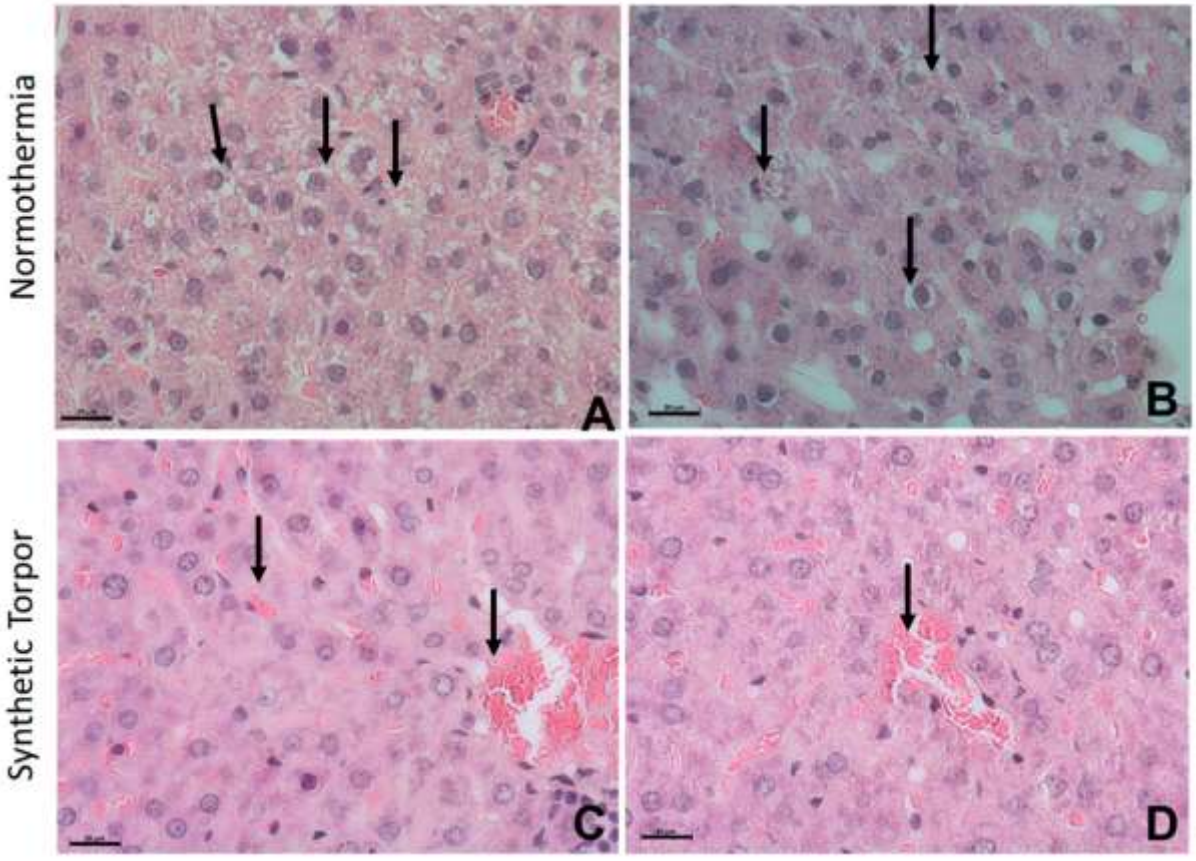
Normothermia
Synthetic Torpor
A
B
C
D

Figure 38. Experiment III: Morphology of the testicle

Morphology of sections of seminiferous tubules, after hematoxylin-eosin staining, in irradiated normothermic testis (A-B) and in testis irradiated during synthetic torpor (C-D). Alteration on the differentiation and cells stratification were found in the testis of normothermic rats (A-B), in particular disorganization of the germinal cells and of their junctions was present. These effects were not detected in the testis tissue of the rats induced into synthetic torpor, in which the structures could be comparable to normal conditions (C-D).

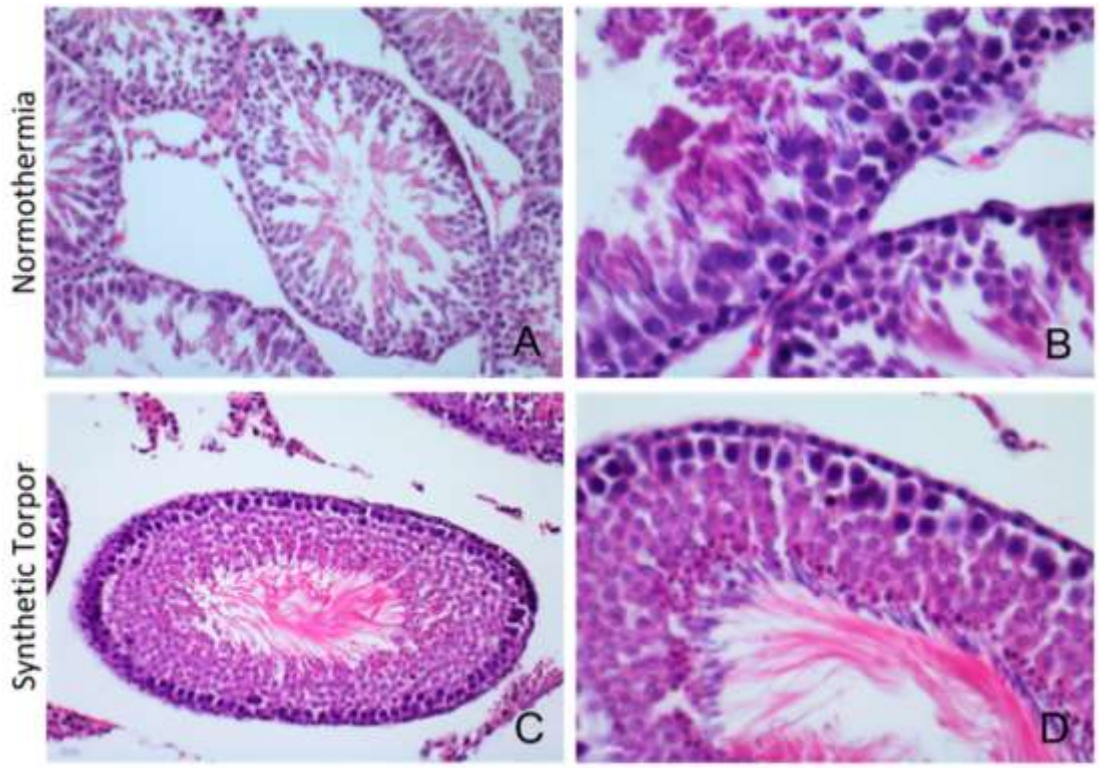
Normothermia
Synthetic Torpor
A
B
C
D

Figure 39. Experiment III: Morphology of the kidney

The figure shows six panels, three for each experimental condition, showing the cross sections of the kidney cortex, at increasing magnification (from top to bottom). Compared to the hypothermic animal (B-D-F), the cells of the animal irradiated under normothermic conditions appear vacuolized, while the tubules have a markedly dilated lumen (A-C-E).

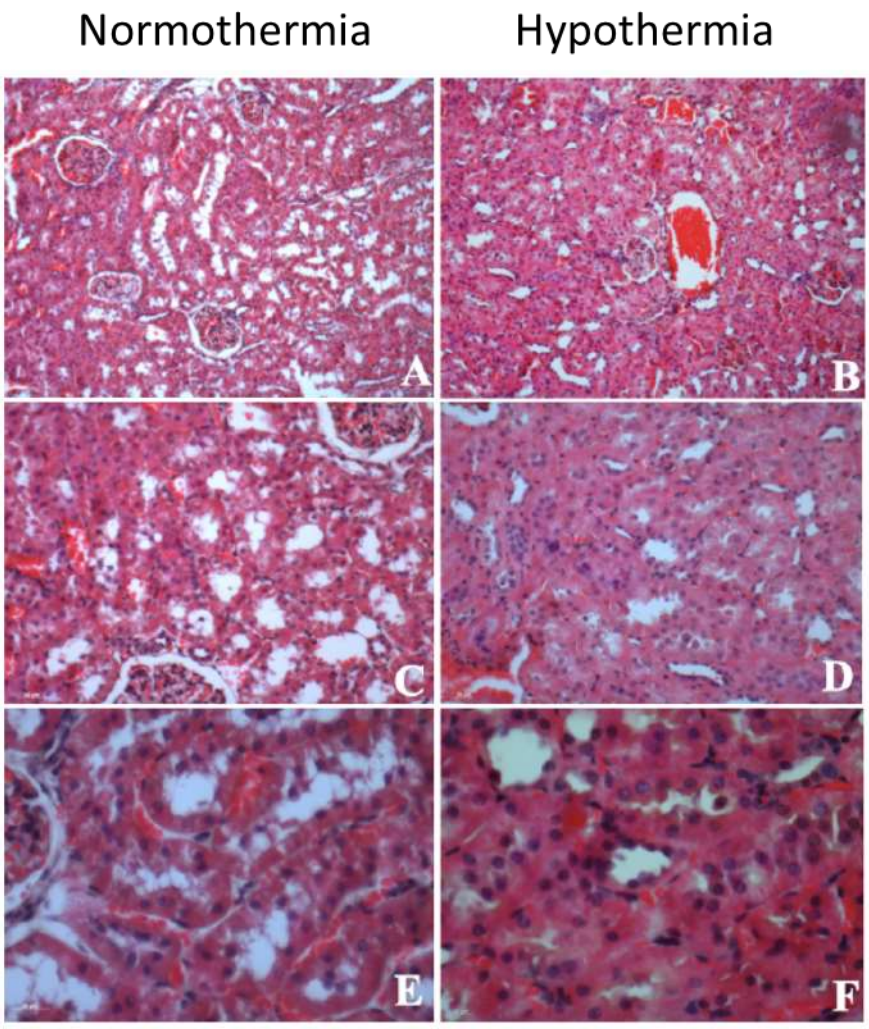
Normothermia
Hypothermia
A
B
C
D
E
F

Figure 40. Experiment III: Morphology of the small intestine

Transverse sections of small intestine. Disorganization and alteration of the mucous membrane and intestinal villi in the rat irradiated in normothermic conditions (A-B) compared to the more regular one of hypothermic rats (C-D) is evident. A-B also show an inflammatory process at the level of the lamina propria with visible lymphocyte infiltrate (boxes, A-B).

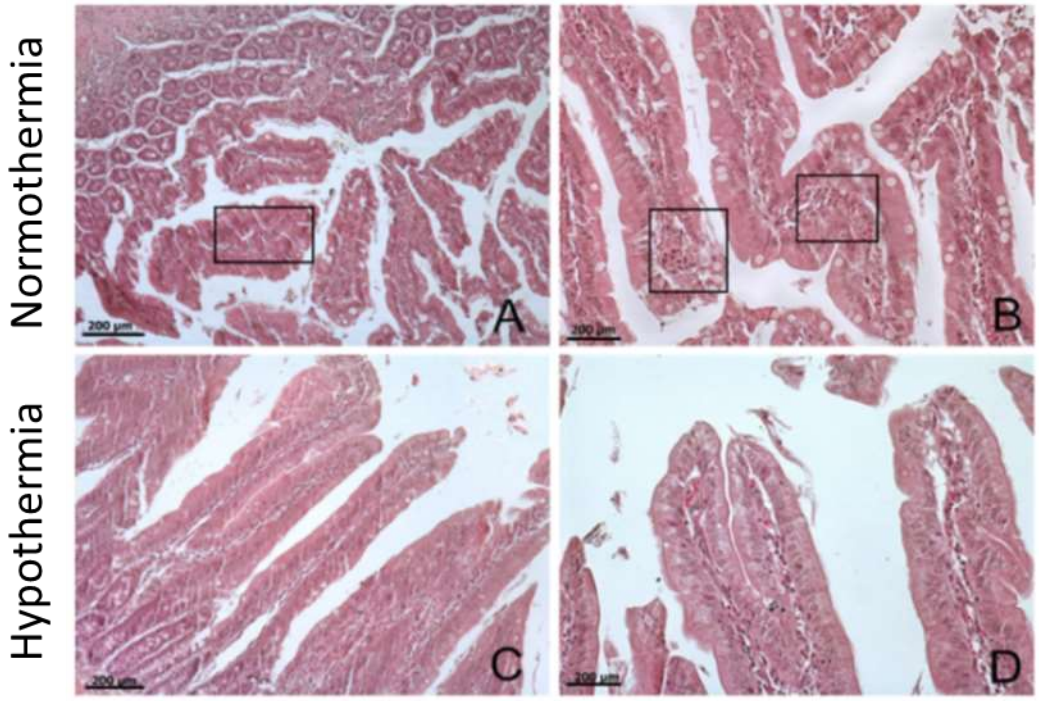
Normothermia
Hypothermia
A
B
C
D

Figure 41. Experiment III: Gene expression analysis in the liver

Volcano plot representing the expression of the analyzed genes in the liver (normothermic vs hypothermic animals) 4 h after a total body irradiation (X-rays, 3Gy) expressed as normalized fold change. In green: downregulated genes (to the left of the left dashed line). In red: upregulated genes (to the right of the right dashed line). Dots above the solid horizontal line are significantly different between the two groups.

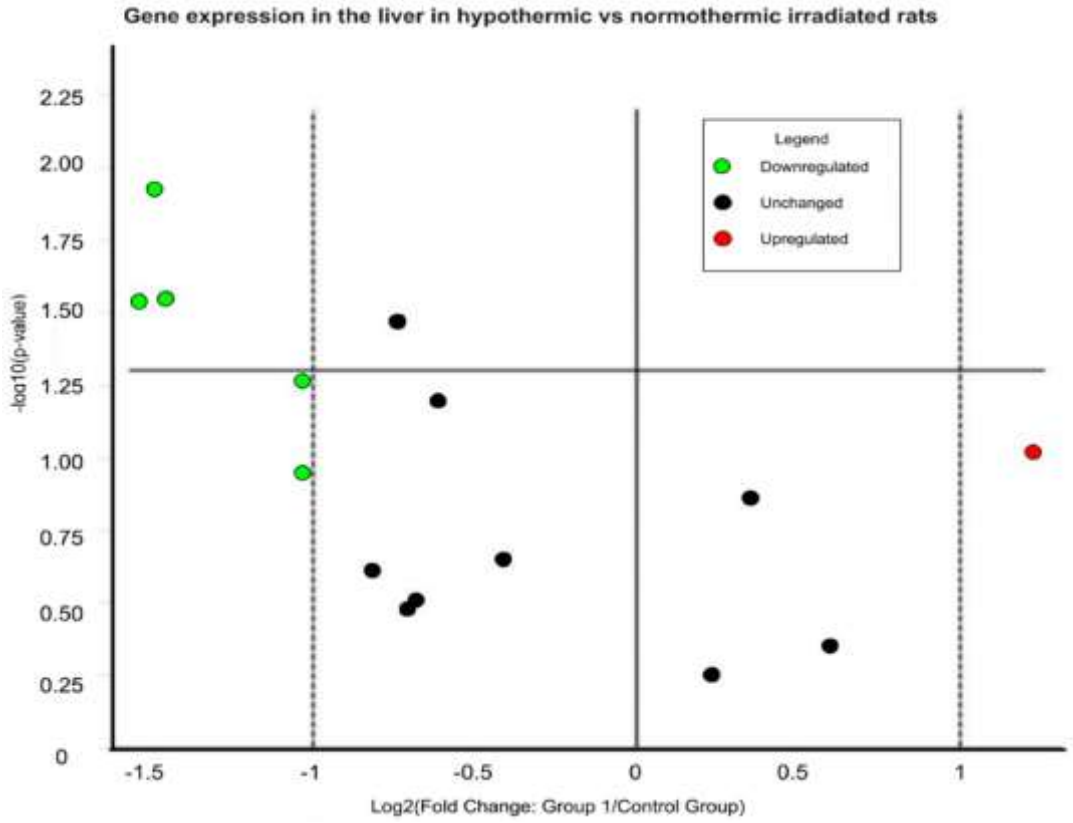
Gene expression in the liver in hypothermic vs normothermic irradiated rats
Legend
Downregulated
Unchanged
Upregulated
-log10(p-value)
2.25
2.00
1.75
1.50
1.25
1.00
0.75
0.50
0.25
0
-1.5
-1
-0.5
0
0.5
1
Log2(Fold Change: Group 1/Control Group)

Figure 42. Experiment III: Gene expression analysis in the testicle

Volcano plot representation of the analyzed genes expression in the testicle (normothermic rat testis vs hypothermic rat testis) 4 h after a total body irradiation (X-rays, 3Gy) expressed as normalized fold change. In green: downregulated genes (to the left of the dashed line). Dots above the solid horizontal line are significantly different between the two groups.

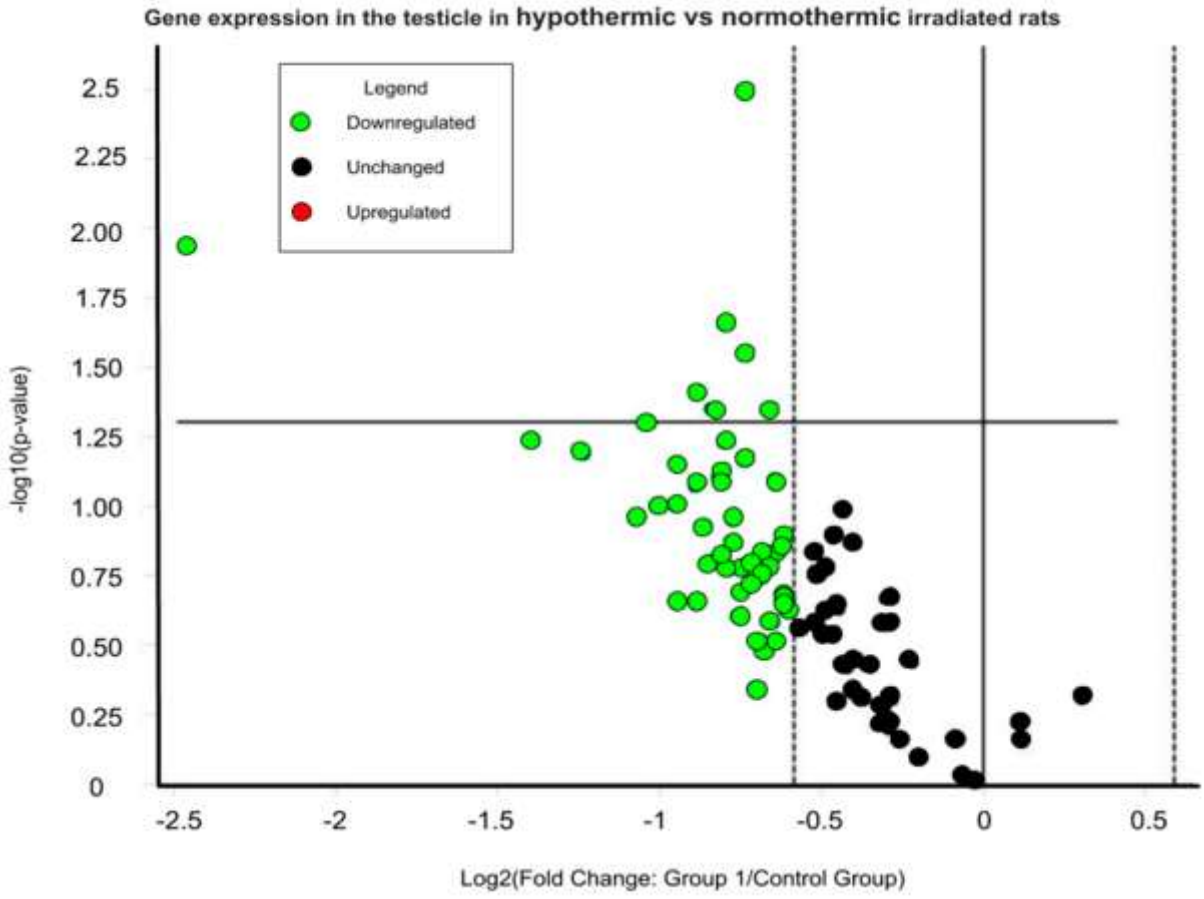
Gene expression in the testicle in hypothermic vs normothermic irradiated rats
Legend
Downregulated
Unchanged
Upregulated
2.5
2.25
2.00
1.75
1.50
1.25
1.00
0.75
0.50
0.25
0
-log10(p-value)
-2.5
-2
-1.5
-1
-0.5
0
0.5
Log2(Fold Change: Group 1/Control Group)

7. REFERENCES

Achermann, P., Borbély, A., Kryger, M., & Roth, T. (2017). *Sleep homeostasis and models of sleep regulation*. https://www.zora.uzh.ch/id/eprint/124066/

Alessia Di Cristoforo. (2017). Aspetti cellulari e sistemici dell'attivazione e dell'inibizione dei neuroni del Raphe Pallidus, [Dissertation thesis], Alma Mater Studiorum Università di Bologna. Dottorato di ricerca in Scienze biomediche, 29 Ciclo. doi.10.6092/unibo/amsdottorato/8162.

Amici, R., Bastianini, S., Berteotti, C., Cerri, M., Del Vecchio, F., Lo Martire, V., Luppi, M., Perez, E., Silvani, A., Zamboni, G., & Zoccoli, G. (2014). Sleep and bodily functions: The physiological interplay between body homeostasis and sleep homeostasis. *Archives Italiennes de Biologie*, *152*(2–3), 66–78. https://doi.org/10.12871/000298292014232

Amici, R., Cerri, M., Ocampo-Garcés, A., Baracchi, F., Dentico, D., Jones, C. A., Luppi, M., Perez, E., Parmeggiani, P. L., & Zamboni, G. (2008). Cold exposure and sleep in the rat: REM sleep homeostasis and body size. *Sleep*, *31*(5), 708–715. https://doi.org/10.1093/sleep/31.5.708

Amos, L. A. (2004). Microtubule structure and its stabilisation. In *Organic and Biomolecular Chemistry* (Vol. 2, Issue 15, pp. 2153–2160). https://doi.org/10.1039/b403634d

Angilletta, M. J. (2009). Thermal Adaptation: A Theoretical and Empirical Synthesis. In *Thermal Adaptation: A Theoretical and Empirical Synthesis*. https://doi.org/10.1093/acprof:oso/9780198570875.001.1

Angilletta, M. J., Youngblood, J. P., Neel, L. K., & VandenBrooks, J. M. (2019). The neuroscience of adaptive thermoregulation. In *Neuroscience Letters* (Vol. 692, pp. 127–136). Elsevier Ireland Ltd. https://doi.org/10.1016/j.neulet.2018.10.046

Arendt, T., & Bullmann, T. (2013). Neuronal plasticity in hibernation and the proposed role of the microtubule-associated protein tau as a “master switch” regulating synaptic gain in neuronal networks. In *American Journal of Physiology - Regulatory Integrative and Comparative Physiology* (Vol. 305, Issue 5). https://doi.org/10.1152/ajpregu.00117.2013

Arendt, T., Stieler, J., & Holzer, M. (2015). Brain hypometabolism triggers PHF-like phosphorylation of tau, a major hallmark of Alzheimer’s disease pathology. In *Journal of*

Neural Transmission (Vol. 122, Issue 4, pp. 531–539). Springer-Verlag Wien. https://doi.org/10.1007/s00702-014-1342-8

Arendt, T., Stieler, J., Strijkstra, A. M., Hut, R. A., Rüdiger, J., Van der Zee, E. A., Harkany, T., Holzer, M., & Härtig, W. (2003). Reversible paired helical filament-like phosphorylation of tau is an adaptive process associated with neuronal plasticity in hibernating animals. *Journal of Neuroscience*, *23*(18), 6972–6981. https://doi.org/10.1523/jneurosci.23-18-06972.2003

Arendt, T., Stieler, J. T., & Holzer, M. (2016). Tau and tauopathies. In *Brain Research Bulletin* (Vol. 126, pp. 238–292). https://doi.org/10.1016/j.brainresbull.2016.08.018

Arnold, W., Heldmaier, G., Ortmann, S., Pohl, H., Ruf, T., & Steinlechner, S. (1991). Ambient temperatures in hibernacula and their energetic consequences for alpine marmots Marmota marmota. *Journal of Thermal Biology*, *16*(4), 223–226. https://doi.org/10.1016/0306-4565(91)90029-2

Axmacher, N., Mormann, F., Fernández, G., Elger, C. E., & Fell, J. (2006). Memory formation by neuronal synchronization. In *Brain Research Reviews* (Vol. 52, Issue 1, pp. 170–182). https://doi.org/10.1016/j.brainresrev.2006.01.007

Baird, B. J., Dickey, J. S., Nakamura, A. J., Redon, C. E., Parekh, P., Griko, Y. V., Aziz, K., Georgakilas, A. G., Bonner, W. M., & Martin, O. A. (2011). Hypothermia postpones DNA damage repair in irradiated cells and protects against cell killing. *Mutation Research - Fundamental and Molecular Mechanisms of Mutagenesis*, *711*(1–2), 142–149. https://doi.org/10.1016/j.mrfmmm.2010.12.006

Baldy, C., Fournier, S., Boisjoly-Villeneuve, S., Tremblay, M. È., & Kinkead, R. (2018). The influence of sex and neonatal stress on medullary microglia in rat pups. *Experimental Physiology*, *103*(9), 1192–1199. https://doi.org/10.1113/EP087088

Banati, R. B. (2002). Visualising microglial activation in vivo. In *GLIA* (Vol. 40, Issue 2, pp. 206–217). John Wiley & Sons, Ltd. https://doi.org/10.1002/glia.10144

Barnes, B. M. (1989). Freeze avoidance in a mammal: Body temperatures below 0°C in an arctic hibernator. *Science*, *244*(4912), 1593–1595.

https://doi.org/10.1126/science.2740905

Bellesi, M., Bushey, D., Chini, M., Tononi, G., & Cirelli, C. (2016). Contribution of sleep to the repair of neuronal DNA double-strand breaks: Evidence from flies and mice. *Scientific Reports*, *6*. https://doi.org/10.1038/srep36804

Benington, J. H., & Craig Heller, H. (1995). Restoration of brain energy metabolism as the function of sleep. In *Progress in Neurobiology* (Vol. 45, Issue 4, pp. 347–360). https://doi.org/10.1016/0301-0082(94)00057-O

Berger, R. J. (1984). Slow wave sleep, shallow torpor and hibernation: Homologous states of diminished metabolism and body temperature. *Biological Psychology*, *19*(3–4), 305–326. https://doi.org/10.1016/0301-0511(84)90045-0

Berner, N. J., & Heller, H. C. (1998). Does the preoptic anterior hypothalamus receive thermoafferent information? *American Journal of Physiology - Regulatory Integrative and Comparative Physiology*, *274*(1 43-1). https://doi.org/10.1152/ajpregu.1998.274.1.r9

Bianco, A. C., Sheng, X., & Silva, J. E. (1988).. *Triiodothyronine Amplifies Norepinephrine Stimulation of Uncoupling Protein Gene Transcription by a Mechanism Not Requiring Protein Synthesis. The journal of biological chemistry* (Vol. 263, Issue 34).

Biggar, Y., & Storey, K. B. (2014). Global DNA modifications suppress transcription in brown adipose tissue during hibernation. *Cryobiology*, *69*(2), 333–338. https://doi.org/10.1016/j.cryobiol.2014.08.008

Billig, I., Foris, J. M., Card, J. P., & Yates, B. J. (1999). Transneuronal tracing of neural pathways controlling an abdominal muscle, rectus abdominis, in the ferret. *Brain Research*, *820*(1–2), 31–44. https://doi.org/10.1016/S0006-8993(98)01320-1

Bjorness, T. E., Kelly, C. L., Gao, T., Poffenberger, V., & Greene, R. W. (2009). Control and function of the homeostatic sleep response by adenosine A 1 receptors. *Journal of Neuroscience*, *29*(5), 1267–1276. https://doi.org/10.1523/JNEUROSCI.2942-08.2009

Blackstone, E., Morrison, M., & Roth, M. B. (2005). H2S induces a suspended animation-like state in mice. *Science*, *308*(5721), 518. https://doi.org/10.1126/science.1108581

Blanco, M. B., Dausmann, K. H., Faherty, S. L., Klopfer, P., Krystal, A. D., Schopler, R., & Yoder, A. D. (2016). Hibernation in a primate: Does sleep occur? *Royal Society Open Science*, *3*(8). https://doi.org/10.1098/rsos.160282

Blessing, W. W., & Nalivaiko, E. (2001). Raphe magnus/pallidus neurons regulate tail but not mesenteric arterial blood flow in rats. *Neuroscience*, *105*(4), 923–929. https://doi.org/10.1016/S0306-4522(01)00251-2

Blessing, W. W., Yu, Y. H., & Nalivaiko, E. (1999). Raphe pallidus and parapyramidal neurons regulate ear pinna vascular conductance in the rabbit. *Neuroscience Letters*, *270*(1), 33–36. https://doi.org/10.1016/S0304-3940(99)00459-0

Boulant, J. A. (2006). Neuronal basis of Hammel's model for set-point thermoregulation. In *Journal of Applied Physiology* (Vol. 100, Issue 4, pp. 1347–1354). American Physiological Society. https://doi.org/10.1152/japplphysiol.01064.2005

Braulke, L. J., Klingenspor, · M, Debarber, · A, Tobias, · S C, Grandy, · D K, Scanlan, · T S, & Heldmaier, · G. (2008). 3-Iodothyronamine: a novel hormone controlling the balance between glucose and lipid utilisation. *J Comp Physiol B*, *178*, 167–177. https://doi.org/10.1007/s00360-007-0208-x

Brown, R. E., Basheer, R., McKenna, J. T., Strecker, R. E., & McCarley, R. W. (2012). Control of sleep and wakefulness. In *Physiological Reviews* (Vol. 92, Issue 3, pp. 1087–1187). https://doi.org/10.1152/physrev.00032.2011

Buck, C. L., & Barnes, B. M. (2000). Effects of ambient temperature on metabolic rate, respiratory quotient, and torpor in an arctic hibernator. *American Journal of Physiology - Regulatory Integrative and Comparative Physiology*, *279*(1 48-1). https://doi.org/10.1152/ajpregu.2000.279.1.r255

Bullmann, T., Seeger, G., Stieler, J., Hanics, J., Reimann, K., Kretzschmann, T. P., Hilbrich, I., Holzer, M., Alpár, A., & Arendt, T. (2016). Tau phosphorylation-associated spine regression does not impair hippocampal-dependent memory in hibernating golden hamsters. *Hippocampus*, *26*(3), 301–318. https://doi.org/10.1002/hipo.22522

Cabanac, M. (2006). Adjustable set point: to honor Harold T. Hammel. *Journal of Applied*

Physiology, *100*(4), 1338–1346. https://doi.org/10.1152/japplphysiol.01021.2005

Cadena, V., & Tattersall, G. J. (2014). Body temperature regulation during acclimation to cold and hypoxia in rats. *Journal of Thermal Biology*, *46*, 56–64. https://doi.org/10.1016/j.jtherbio.2014.10.007

Cain, J. W., Krausman, P. R., Rosenstock, S. S., & Turner, J. C. (2006). Mechanisms of Thermoregulation and Water Balance in Desert Ungulates. *Wildlife Society Bulletin*, *34*(3), 570–581. https://doi.org/10.2193/0091-7648(2006)34[570:motawb]2.0.co;2

Calvert, J. W., Coetzee, W. A., & Lefer, D. J. (2010). Novel insights into hydrogen sulfide-mediated cytoprotection. In *Antioxidants and Redox Signaling* (Vol. 12, Issue 10, pp. 1203–1217). https://doi.org/10.1089/ars.2009.2882

Canale, C. I., Levesque, D. L., & Lovegrove, B. (2012). Living in a Seasonal World Striped Mouse Population Dynamics View project disputes in the construction industry and its avoidance View project. *Springer*, 29–40. https://doi.org/10.1007/978-3-642-28678-0_3

Cano, G., Passerin, A. M., Schiltz, J. C., Card, J. P., Morrison, S. F., & Sved, A. F. (2003). Anatomical substrates for the central control of sympathetic outflow to interscapular adipose tissue during cold exposure. *Journal of Comparative Neurology*, *460*(3), 303–326. https://doi.org/10.1002/cne.10643

Cardinali, D. P. (2019). Melatonin: Clinical perspectives in neurodegeneration. In *Frontiers in Endocrinology* (Vol. 10, Issue JULY). Frontiers Media S.A. https://doi.org/10.3389/fendo.2019.00480

Carey, H. V, Frank, C. L., & Seifert, J. P. (2000). Hibernation induces oxidative stress and activation of NF-κB in ground squirrel intestine. *Journal of Comparative Physiology - B Biochemical, Systemic, and Environmental Physiology*, *170*(7), 551–559. https://doi.org/10.1007/s003600000135

Carlisle, H. J., & Laudenslager, M. L. (1979). Observations on the thermoregulatory effects of preoptic warming in rats. *Physiology and Behavior*, *23*(4), 723–732. https://doi.org/10.1016/0031-9384(79)90166-5

Carpenter, F. L., & Hixon, M. A. (1988). A New Function for Torpor: Fat Conservation in a

Wild Migrant Hummingbird. *The Condor*, *90*(2), 373–378. https://doi.org/10.2307/1368565

Carskadon, M. A., & Dement, W. C. (2011). Normal Human Sleep : An Overview. *Principles and Practice of Sleep Medicine: Fifth Edition*, 1602–1609. https://doi.org/10.1016/B978-1-4160-6645-3.00141-9

Carvalho, S. D., Kimura, E. T., Bianco, A. C., & Enrique Silva, J. (1991). Central role of brown adipose tissue thyroxine 5'-deiodinase on thyroid hormone-dependent thermogenic response to cold. *Endocrinology*, *128*(4), 2149–2159. https://doi.org/10.1210/endo-128-4-2149

Cerri, M. (2017). The Central Control of Energy Expenditure: Exploiting Torpor for Medical Applications. *Annual Review of Physiology*, *79*(1), 167–186. https://doi.org/10.1146/annurev-physiol-022516-034133

Cerri, M., Mastrotto, M., Tupone, D., Martelli, D., Luppi, M., Perez, E., Zamboni, G., & Amici, R. (2013). The inhibition of neurons in the central nervous pathways for thermoregulatory cold defense induces a suspended animation state in the rat. *Journal of Neuroscience*, *33*(7), 2984–2993. https://doi.org/10.1523/JNEUROSCI.3596-12.2013

Cerri, M., Ocampo-Garces, A., Amici, R., Baracchi, F., Capitani, P., Jones, C. A., Luppi, M., Perez, E., Parmeggiani, P. L., & Zamboni, G. (2005a). Cold exposure and sleep in the rat: Effects on sleep architecture and the electroencephalogram. *Sleep*, *28*(6), 694–705. https://doi.org/10.1093/sleep/28.6.694

Cerri, M., Tinganelli, W., Negrini, M., Helm, A., Scifoni, E., Tommasino, F., Sioli, M., Zoccoli, A., & Durante, M. (2016). Hibernation for space travel: Impact on radioprotection. *Life Sciences in Space Research*, *11*, 1–9. https://doi.org/10.1016/j.lssr.2016.09.001

Chatfield, P. O., & Lyman, C. P. (1954). Subcortical electrical activity in the golden hamster during arousal from hibernation. *Electroencephalography and Clinical Neurophysiology*, *6*(C), 403–408. https://doi.org/10.1016/0013-4694(54)90054-1

Chen, J, Kanai, Y., Cowan, N. J., & Hirokawa, N. (1992). Projection domains of MAP2 and

tau determine spacings between microtubules in dendrites and axons. *Nature*, *360*(6405), 674–677. https://doi.org/10.1038/360674a0

Chen, Jun. (2015). The evolutionary divergence of TRPA1 channel: heat-sensitive, cold-sensitive and temperature-insensitive. In *Temperature* (Vol. 2, Issue 2, pp. 158–159). Routledge. https://doi.org/10.1080/23328940.2014.998903

Chi, Q.-S., Li, X.-J., & Wang, D.-H. (2017). *2-Deoxy-D-glucose, not mercaptoacetate, induces a reversible reduction of body temperature in male desert hamsters (Phodopus roborovskii)*. https://doi.org/10.1016/j.jtherbio.2017.11.011

Choukèr, A., Bereiter-Hahn, J., Singer, D., & Heldmaier, G. (2019). Hibernating astronauts—science or fiction? In *Pflugers Archiv European Journal of Physiology* (Vol. 471, Issue 6, pp. 819–828). Springer Verlag. https://doi.org/10.1007/s00424-018-2244-7

Clemens, L. E., Heldmaier, G., & Exner, C. (2009). Keep cool: Memory is retained during hibernation in Alpine marmots. *Physiology and Behavior*, *98*(1–2), 78–84. https://doi.org/10.1016/j.physbeh.2009.04.013

Cliff, M. A., & Green, B. G. (1996). Sensitization and desensitization to capsaicin and menthol in the oral cavity: Interactions and individual differences. *Physiology and Behavior*, *59*(3), 487–494. https://doi.org/10.1016/0031-9384(95)02089-6

Cline, S. D., & Hanawalt, P. C. (2003). Who's on first in the cellular response to dna damage? Excision repair. *Nature reviews | molecular cell biology*, *4*, 6–7. https://doi.org/10.1038/nrm1101

Colburn, R. W., Lubin, M. Lou, Stone, D. J., Wang, Y., Lawrence, D., D'Andrea, M. R. R., Brandt, M. R., Liu, Y., Flores, C. M., & Qin, N. (2007). Attenuated Cold Sensitivity in TRPM8 Null Mice. *Neuron*, *54*(3), 379–386. https://doi.org/10.1016/j.neuron.2007.04.017

Conceição, E. P. S., Madden, C. J., & Morrison, S. F. (2019). Neurons in the rat ventral lateral preoptic area are essential for the warm-evoked inhibition of brown adipose tissue and shivering thermogenesis. *Acta Physiologica*, *225*(4). https://doi.org/10.1111/apha.13213

Cooper, S. T., Sell, S. S., Fahrenkrog, M., Wilkinson, K., Howard, D. R., Bergen, H., Cruz,

E., Cash, S. E., Andrews, M. T., & Hampton, M. (2016). Effects of hibernation on bone marrow transcriptome in thirteen-lined ground squirrels. *Physiological Genomics*, *48*(7), 513–525. https://doi.org/10.1152/physiolgenomics.00120.2015

Cowell, I. G. (2002). E4BP4/NFIL3, a PAR-related bZIP factor with many roles. *BioEssays*, *24*(11), 1023–1029. https://doi.org/10.1002/bies.10176

Craig, A. D. (2002). How do you feel? Interoception: The sense of the physiological condition of the body. *Nature Reviews Neuroscience*, *3*(8), 655–666. https://doi.org/10.1038/nrn894

Crespo-Biel, N., Theunis, C., & Leuven, F. Van. (2012). Protein Tau: Prime Cause of Synaptic and Neuronal Degeneration in Alzheimer's Disease. *International Journal of Alzheimer's Disease*, *2012*. https://doi.org/10.1155/2012/251426

Cross, D. C., Muñoz, J. P., Hernández, P., & Maccioni, R. B. (2000). Nuclear and cytoplasmic tau proteins from human nonneuronal cells share common structural and functional features with brain tau. *Journal of Cellular Biochemistry*, *78*(2), 305–317. https://doi.org/10.1002/(SICI)1097-4644(20000801)78:2<305::AID-JCB12>3.0.CO;2-W

Cuisnier, O., Serduc, R., Lavieille, J. P., Longuet, M., Reyt, E., & Riva, C. (2003). Chronic hypoxia protects against gamma-irradiation-induced apoptosis by inducing bcl-2 up-regulation and inhibiting mitochondrial translocation and conformational change of bax protein. *International Journal of Oncology*, *23*(4), 1033–1041. https://doi.org/10.3892/ijo.23.4.1033

Cypess, A. M., Lehman, S., Williams, G., Tal, I., Rodman, D., Goldfine, A. B., Kuo, F. C., Palmer, E. L., Tseng, Y. H., Doria, A., Kolodny, G. M., & Kahn, C. R. (2009). Identification and importance of brown adipose tissue in adult humans. *New England Journal of Medicine*, *360*(15), 1509–1517. https://doi.org/10.1056/NEJMoa0810780

D'alessandro, A., Nemkov, T., Bogren, L. K., Martin, S. L., & Hansen, K. C. (2016). Comfortably Numb and Back: Plasma Metabolomics Reveals Biochemical Adaptations in the Hibernating 13-Lined Ground Squirrel. *ACS Publications*, *16*(2), 958–969. https://doi.org/10.1021/acs.jproteome.6b00884

Daan, S., Barnes, B. M., & Strijkstra, A. M. (1991). Warming up for sleep? - Ground squirrels sleep during arousals from hibernation. *Neuroscience Letters*, *128*(2), 265–268. https://doi.org/10.1016/0304-3940(91)90276-Y

Dark, J., Miller, D. R., & Zucker, I. (1994). Reduced glucose availability induces torpor in Siberian hamsters. *American Journal of Physiology - Regulatory Integrative and Comparative Physiology*, *267*(2 36-2). https://doi.org/10.1152/ajpregu.1994.267.2.r496

Das, R., Balmik, A. A., & Chinnathambi, S. (2020). Effect of Melatonin on Tau aggregation and Tau-mediated cell surface morphology. *International Journal of Biological Macromolecules*, *152*, 30–39. https://doi.org/10.1016/j.ijbiomac.2020.01.296

Datta, N. R., Rogers, S., Ordóñez, S. G., Puric, E., & Bodis, S. (2016). Hyperthermia and radiotherapy in the management of head and neck cancers: A systematic review and meta-analysis. In *International Journal of Hyperthermia* (Vol. 32, Issue 1, pp. 31–40). https://doi.org/10.3109/02656736.2015.1099746

Dausmann, K. H., Glos, J., Ganzhorn, J. U., & Heldmaier, G. (2004). Hibernation in a tropical primate. *Nature*, *429*(6994), 825–826. https://doi.org/10.1038/429825a

Dausmann, K. H., Nowack, J., Kobbe, S., & Mzilikazi, N. (2012). Afrotropical Heterothermy: A Continuum of Possibilities. In *Living in a Seasonal World* (pp. 13–27). Springer Berlin Heidelberg. https://doi.org/10.1007/978-3-642-28678-0_2

Davies, D. S., Ma, J., Jegathees, T., & Goldsbury, C. (2017). Microglia show altered morphology and reduced arborization in human brain during aging and Alzheimer's disease. *Brain Pathology*, *27*(6), 795–808. https://doi.org/10.1111/bpa.12456

Dawson, H. N., Cantillana, V., Jansen, M., Wang, H., Vitek, M. P., Wilcock, D. M., Lynch, J. R., & Laskowitz, D. T. (2010). Loss of tau elicits axonal degeneration in a mouse model of Alzheimer's disease. *Neuroscience*, *169*(1), 516–531. https://doi.org/10.1016/j.neuroscience.2010.04.037

De Vivo, L., Bellesi, M., Marshall, W., Bushong, E. A., Ellisman, M. H., Tononi, G., & Cirelli, C. (2017). Ultrastructural evidence for synaptic scaling across the wake/sleep cycle. *Science*, *355*(6324), 507–510. https://doi.org/10.1126/science.aah5982

Deboer, T. (1998). Brain temperature dependent changes in the electroencephalogram power spectrum of humans and animals. *Journal of Sleep Research*, *7*(4), 254–262. https://doi.org/10.1046/j.1365-2869.1998.00125.x

Deboer, T., & Tobler, I. (1994). Sleep EEG after daily torpor in the Djungarian hamster: similarity to the effects of sleep deprivation. *Neuroscience Letters*, *166*(1), 35–38. https://doi.org/10.1016/0304-3940(94)90834-6

Deboer, T., & Tobler, I. (2000). Slow waves in the sleep electroencephalogram after daily torpor are homeostatically regulated. *NeuroReport*, *11*(4), 881–885. https://doi.org/10.1097/00001756-200003200-00044

Deboer, T., & Tobler, I. (2003). Sleep regulation in the Djungarian hamster: Comparison of the dynamics leading to the slow-wave activity increase after sleep deprivation and daily torpor. *Sleep*, *26*(5), 567–572. https://doi.org/10.1093/sleep/26.5.567

Dhaka, A., Murray, A. N., Mathur, J., Earley, T. J., Petrus, M. J., & Patapoutian, A. (2007). TRPM8 Is Required for Cold Sensation in Mice. *Neuron*, *54*(3), 371–378. https://doi.org/10.1016/j.neuron.2007.02.024

Dirkes, M. C., Milstein, D. M. J., Heger, M., & van Gulik, T. M. (2015). Absence of Hydrogen Sulfide-Induced Hypometabolism in Pigs: A Mechanistic Explanation in Relation to Small Nonhibernating Mammals. *European Surgical Research*, *54*(3–4), 178–191. https://doi.org/10.1159/000369795

Dixit, R., Ross, J. L., Goldman, Y. E., & Holzbaur, E. L. F. (2008). Differential regulation of dynein and kinesin motor proteins by tau. *Science*, *319*(5866), 1086–1089. https://doi.org/10.1126/science.1152993

Donnelly, E. H., Nemhauser, J. B., Smith, J. M., Kazzi, Z. N., Farfán, E. B., Chang, A. S., & Naeem, S. F. (2010). Acute radiation syndrome: Assessment and management. In *Southern Medical Journal* (Vol. 103, Issue 6, pp. 541–546). South Med J. https://doi.org/10.1097/SMJ.0b013e3181ddd571

Doull, J., & Dubois, K. P. (1953). Influence of Hibernation on Survival Time and Weight Loss of X-Irradiated Ground Squirrels. *Proceedings of the Society for Experimental*

Biology and Medicine, *84*(2), 367–370. https://doi.org/10.3181/00379727-84-20647

Drabek, T., Kochanek, P. M., Stezoski, J., Wu, X., Bayr, H., Morhard, R. C., Stezoski, S. W., & Tisherman, S. A. (2011). Intravenous hydrogen sulfide does not induce hypothermia or improve survival from hemorrhagic shock in pigs. *Shock*, *35*(1), 67–73. https://doi.org/10.1097/SHK.0b013e3181e86f49

Drew, K. L., Buck, C. L., Barnes, B. M., Christian, S. L., Rasley, B. T., & Harris, M. B. (2007). Central nervous system regulation of mammalian hibernation: Implications for metabolic suppression and ischemia tolerance. In *Journal of Neurochemistry* (Vol. 102, Issue 6, pp. 1713–1726). https://doi.org/10.1111/j.1471-4159.2007.04675.x

Drew, K. L., Osborne, P. G., Frerichs, K. U., Hu, Y., Koren, R. E., Hallenbeck, J. M., & Rice, M. E. (1999). Ascorbate and glutathione regulation in hibernating ground squirrels. *Brain Research*, *851*(1–2), 1–8. https://doi.org/10.1016/S0006-8993(99)01969-1

Du, F., Zhu, X. H., Zhang, Y., Friedman, M., Zhang, N., Uğurbil, K., & Chen, W. (2008). Tightly coupled brain activity and cerebral ATP metabolic rate. *Proceedings of the National Academy of Sciences of the United States of America*, *105*(17), 6409–6414. https://doi.org/10.1073/pnas.0710766105

Ellison, G. T. H., & Skinner, J. D. (1992). The influence of ambient temperature on spontaneous daily torpor in pouched mice (Saccostomus campestris: Rodentia-cricetidae) from Southern Africa. *Journal of Thermal Biology*, *17*(1), 25–31. https://doi.org/10.1016/0306-4565(92)90016-9

Elmroth, K., Nygren, J., Erkell, L. J., & Hultborn, R. (2000a). Effect of hypothermic irradiation of the growth characteristics of two human cell lines. *Anticancer Research*, *20*(5 B), 3429–3433. https://europepmc.org/article/med/11131644

Elmroth, K., Nygren, J., Erkell, L. J., & Hultborn, R. (2000b). Radiation-induced double-strand breaks in mammalian DNA: Influence of temperature and DMSO. *International Journal of Radiation Biology*, *76*(11), 1501–1508. https://doi.org/10.1080/09553000050176261

Eyolfson, D. A., Tikuisis, P., Xu, X., Weseen, G., & Giesbrecht, G. G. (2001). Measurement

and prediction of peak shivering intensity in humans. *European Journal of Applied Physiology*, *84*(1–2), 100–106. https://doi.org/10.1007/s004210000329

Farrell, M. J., Trevaks, D., Taylor, N. A. S., & McAllen, R. M. (2013). Brain stem representation of thermal and psychogenic sweating in humans. *American Journal of Physiology - Regulatory Integrative and Comparative Physiology*, *304*(10). https://doi.org/10.1152/ajpregu.00041.2013

Fekete, C., & Lechan, R. M. (2014). Central regulation of hypothalamic-pituitary-thyroid axis under physiological and pathophysiological conditions. In *Endocrine Reviews* (Vol. 35, Issue 2, pp. 159–194). Endocrine Society. https://doi.org/10.1210/er.2013-1087

Fleck, C. C., & Carey, H. V. (2005). Modulation of apoptotic pathways in intestinal mucosa during hibernation. *American Journal of Physiology - Regulatory Integrative and Comparative Physiology*, *289*(2 58-2). https://doi.org/10.1152/ajpregu.00100.2005

Florant, G. L., Porst, H., Peiffer, A., Hudachek, S. F., Pittman, C., Summers, S. A., Rajala, M. W., & Scherer, P. E. (2004). Fat-cell mass, serum leptin and adiponectin changes during weight gain and loss in yellow-bellied marmots (Marmota flaviventris). *Journal of Comparative Physiology B: Biochemical, Systemic, and Environmental Physiology*, *174*(8), 633–639. https://doi.org/10.1007/s00360-004-0454-0

Frame, S., Cohen, P., & Biondi, R. M. (2001). A common phosphate binding site explains the unique substrate specificity of GSK3 and its inactivation by phosphorylation. *Molecular Cell*, *7*(6), 1321–1327. https://doi.org/10.1016/S1097-2765(01)00253-2

Frank, S. M., Satitpunwaycha, P., Bruce, S. R., Herscovitch, P., & Goldstein, D. S. (2003). Increased myocardial perfusion and sympathoadrenal activation during mild core hypothermia in awake humans. In *Clinical Science* (Vol. 104). https://portlandpress.com/clinsci/article-pdf/104/5/503/433681/cs1040503.pdf

Franken, P., Dijk, D. J., Tobler, I., & Borbely, A. A. (1991). Sleep deprivation in rats: Effects on EEG power spectra, vigilance states, and cortical temperature. *American Journal of Physiology - Regulatory Integrative and Comparative Physiology*, *261*(1 30-1). https://doi.org/10.1152/ajpregu.1991.261.1.r198

Franken, Paul, Tobler, I., & Borbély, A. A. (1992). Sleep and Waking Have a Major Effect on the 24-Hr Rhythm of Cortical Temperature in the Rat. *Journal of Biological Rhythms*, *7*(4), 341–352. https://doi.org/10.1177/074873049200700407

Fredholm, B. B., IJzerman, A. P., Jacobson, K. A., Linden, J., & Müller, C. E. (2011). International union of basic and clinical pharmacology. LXXXI. Nomenclature and classification of adenosine receptors - An update. In *Pharmacological Reviews* (Vol. 63, Issue 1, pp. 1–34). American Society for Pharmacology and Experimental Therapeutics. https://doi.org/10.1124/pr.110.003285

Freinkel, N., Metzger, B. E., Harris, E., Robinson, S., & Mager, M. (1972). The Hypothermia of Hypoglycemia: Studies with 2-Deoxy-D-Glucose in Normal Human Subjects and Mice. *New England Journal of Medicine*, *287*(17), 841–845. https://doi.org/10.1056/NEJM197210262871702

Gangloff, E. J., & Telemeco, R. S. (2018). High temperature, oxygen, and performance: Insights from reptiles and amphibians. *Integrative and Comparative Biology*, *58*(1), 9–24. https://doi.org/10.1093/icb/icy005

Geiser F., Heldmaier, G. (1995). The impact of dietary fats, photoperiod, temperature and season on morphological variables, torpor patterns, and brown adipose tissue fatty acid composition of hamsters, Phodopus sungorus. In *J Comp Phys B* (Vol. 165). Springer-Verlag. https://doi.org/10.1007/BF00387311

Geiser, F., & Ruf, T. (1995). Hibernation versus daily torpor in mammals and birds: Physiological variables and classification of torpor patterns. *Physiological Zoology*, *68*(6), 935–966. https://doi.org/10.1086/physzool.68.6.30163788

Geiser, Fritz. (2004). Metabolic Rate and Body Temperature Reduction During Hibernation and Daily Torpor. *Annual Review of Physiology*, *66*(1), 239–274. https://doi.org/10.1146/annurev.physiol.66.032102.115105

Geiser, Fritz. (2010). Aestivation in Mammals and Birds Effects of dietary fats on torpor expression and body lipid composition View project Energetics and thermoregulation in desert hamsters View project. *Springer*, *49*, 95–111. https://doi.org/10.1007/978-3-642-02421-4_5

Geiser, Fritz, & Brigham, R. M. (2012). The Other Functions of Torpor. In *Living in a Seasonal World* (pp. 109–121). Springer Berlin Heidelberg. https://doi.org/10.1007/978-3-642-28678-0_10

Geiser, Fritz, Kenagy, G. J., & Geiser, F. (1988). Torpor Duration in Relation to Temperature and Metabolism in Hibernating Ground Squirrels. *Journals.Uchicago.Edu*, *61*(5), 442–449. https://doi.org/10.1086/physzool.61.5.30161266

Geiser, Fritz, Körtner, G., & Schmidt, I. (1998). Leptin increases energy expenditure of a marsupial by inhibition of daily torpor. *American Journal of Physiology - Regulatory Integrative and Comparative Physiology*, *275*(5 44-5). https://doi.org/10.1152/ajpregu.1998.275.5.r1627

Geiser, Fritz, & Masters, P. (1994). Torpor in relation to reproduction in the mulgara, Dasycercus cristicauda (Dasyuridae: Marsupialia). *Journal of Thermal Biology*, *19*(1), 33–40. https://doi.org/10.1016/0306-4565(94)90007-8

Ghosh, S., Indracanti, N., Joshi, J., Ray, J., & Indraganti, P. K. (2017). Pharmacologically induced reversible hypometabolic state mitigates radiation induced lethality in mice. *Scientific Reports*, *7*(1), 1–14. https://doi.org/10.1038/s41598-017-15002-7

Giordano, A., Frontini, A., Castellucci, M., & Cinti, S. (2004). Presence and distribution of cholinergic nerves in rat mediastinal brown adipose tissue. *Journal of Histochemistry and Cytochemistry*, *52*(7), 923–930. https://doi.org/10.1369/jhc.3A6246.2004

Goedert, M., & Jakes, R. (1990). Expression of separate isoforms of human tau protein: correlation with the tau pattern in brain and effects on tubulin polymerization. *The EMBO Journal*, *9*(13), 4225–4230. https://doi.org/10.1002/j.1460-2075.1990.tb07870.x

Goedert, M., Jakes, R., Qi, Z., Wang, J. H., & Cohen, P. (1995). Protein Phosphatase 2A Is the Major Enzyme in Brain that Dephosphorylates τ Protein Phosphorylated by Proline-Directed Protein Kinases or Cyclic AMP-Dependent Protein Kinase. *Journal of Neurochemistry*, *65*(6), 2804–2807. https://doi.org/10.1046/j.1471-4159.1995.65062804.x

Goedert, M., Jakes, R., & Vanmechelen, E. (1995). Monoclonal antibody AT8 recognises tau

protein phosphorylated at both serine 202 and threonine 205. *Neuroscience Letters*, *189*(3), 167–170. https://doi.org/10.1016/0304-3940(95)11484-E

Goedert, Michel, & Spillantini, M. G. (2011). Pathogenesis of the tauopathies. *Journal of Molecular Neuroscience*, *45*(3), 425–431. https://doi.org/10.1007/s12031-011-9593-4

Gordon, R. I., Ignat'ev, D. A., Mel'nikova, E. V, Rogachevskaĭ, V. V, Kraev, I. V, & Khutsian, S. S. (2006). [Influence of ionizing radiation on the condition of the protein-synthesizing system in ground squirrel brain neurons at different functional states]. *Biofizika*, *51*(2), 316–323. http://www.ncbi.nlm.nih.gov/pubmed/16637340

Gould, E., Beylin, A., Tanapat, P., Reeves, A., & Shors, T. J. (1999). Learning enhances adult neurogenesis in the hippocampal formation. *Nature Neuroscience*, *2*(3), 260–265. https://doi.org/10.1038/6365

Graeber, M. B., & Streit, W. J. (2010). Microglia: biology and pathology. *Springer*, *119*(1), 89–105. https://doi.org/10.1007/s00401-009-0622-0

Grigg, G. C., Beard, L. A., & Augee, M. L. (2004). The evolution of endothermy and its diversity in mammals and birds. *Physiological and Biochemical Zoology*, *77*(6), 982–997. https://doi.org/10.1086/425188

Griko, Y., & Regan, M. D. (2018). Synthetic torpor: A method for safely and practically transporting experimental animals aboard spaceflight missions to deep space. *Life Sciences in Space Research*, *16*, 101–107. https://doi.org/10.1016/j.lssr.2018.01.002

Grimes, C. A., & Jope, R. S. (2001). The multifaceted roles of glycogen synthase kinase 3β in cellular signaling. *Progress in Neurobiology*, *65*(4), 391–426. https://doi.org/10.1016/S0301-0082(01)00011-9

Guisle, I., Gratuze, M., Petry, S., Morin, F., Keraudren, R., Whittington, R. A., Hébert, S. S., Mongrain, V., & Planel, E. (2020). Circadian and sleep/wake-dependent variations in tau phosphorylation are driven by temperature. *SLEEPJ*, *2020*(4), 1–12. https://doi.org/10.1093/sleep/zsz266

Guo, Y., Wang, L., Zhu, M., Zhang, H., Hu, Y., Han, Z., Liu, J., Zhao, W., & Wang, D. (2016). Detection of hyperphosphorylated tau protein and α-synuclein in spinal cord of

patients with Alzheimer's disease. *Neuropsychiatric Disease and Treatment*, *12*, 445–452. https://doi.org/10.2147/NDT.S90735

Hamilton, J. S., Sat, ·, Chau, M., Malins, K. J., Ibanez, G. G., Horowitz, J. M., Horwitz, B. A., Van Breukelen, F., & Utz, J. C. (2017). Syrian hamster neuroplasticity mechanisms fail as temperature declines to 15 °C, but histaminergic neuromodulation persists. *Journal of Comparative Physiology B*, *187*, 779–791. https://doi.org/10.1007/s00360-017-1078-5

Hammond, K. A., & Diamond, J. (1997). Maximal sustained energy budgets in humans and animals. In *Nature* (Vol. 386, Issue 6624, pp. 457–462). Nature Publishing Group. https://doi.org/10.1038/386457a0

Haouzi, P., Notet, V., Chenuel, B., Chalon, B., Sponne, I., Ogier, V., & Bihain, B. (2008). H2S induced hypometabolism in mice is missing in sedated sheep. *Respiratory Physiology and Neurobiology*, *160*(1), 109–115. https://doi.org/10.1016/j.resp.2007.09.001

Harlow, H. J. (1981). Torpor and Other Physiological Adaptations of the Badger (Taxidea taxus) to Cold Environments. *Physiological Zoology*, *54*(3), 267–275. https://doi.org/10.1086/physzool.54.3.30159941

Harris, M. B., & Milsom, W. K. (1995). Parasympathetic influence on heart rate in euthermic and hibernating ground squirrels. In *Journal of Experimental Biology* (Vol. 198, Issue 4). https://jeb.biologists.org/content/198/4/931.short

Hayward, J. N., & Baker, M. A. (1968). Diuretic and thermoregulatory responses to preoptic cooling in the monkey. *The American Journal of Physiology*, *214*(4), 843–850. https://doi.org/10.1152/ajplegacy.1968.214.4.843

Heldmaier, G., Ortmann, S., & Elvert, R. (2004). Natural hypometabolism during hibernation and daily torpor in mammals. *Respiratory Physiology and Neurobiology*, *141*(3), 317–329. https://doi.org/10.1016/j.resp.2004.03.014

Heldmaier, G., & Steinlechner, S. (1981). Seasonal pattern and energetics of short daily torpor in the Djungarian hamster, Phodopus sungorus. *Oecologia*, *48*(2), 265–270.

https://doi.org/10.1007/BF00347975

Heller, H. C., & Ruby, N. F. (2004). Sleep and Circadian Rhythms in Mammalian Torpor. *Annual Review of Physiology*, *66*(1), 275–289. https://doi.org/10.1146/annurev.physiol.66.032102.115313

Herwig, A., Ross, A. W., Nilaweera, K. N., Morgan, P. J., & Barrett, P. (2008). Hypothalamic thyroid hormone in energy balance regulation. In *Obesity Facts* (Vol. 1, Issue 2, pp. 71–79). Obes Facts. https://doi.org/10.1159/000123428

Heylmann, D., Badura, J., Becker, H., Fahrer, J., & Kaina, B. (2018). Sensitivity of CD3/CD28-stimulated versus non-stimulated lymphocytes to ionizing radiation and genotoxic anticancer drugs: key role of ATM in the differential radiation response. *Cell Death and Disease*, *9*(11). https://doi.org/10.1038/s41419-018-1095-7

Hitrec, T., Luppi, M., Bastianini, S., Squarcio, F., Berteotti, C., Lo Martire, V., Martelli, D., Occhinegro, A., Tupone, D., Zoccoli, G., Amici, R., & Cerri, M. (2019). Neural control of fasting-induced torpor in mice. *Scientific Reports*, *9*(1), 1–12. https://doi.org/10.1038/s41598-019-51841-2

Holloway, J. C., & Geiser, F. (1995). Influence of torpor on daily energy expenditure of the dasyurid marsupial Sminthopsis crassicaudata. *Comparative Biochemistry and Physiology -- Part A: Physiology*, *112*(1), 59–66. https://doi.org/10.1016/0300-9629(95)00089-P

Holth, J. K., Fritschi, S. K., Wang, C., Pedersen, N. P., Cirrito, J. R., Mahan, T. E., Finn, M. B., Manis, M., Geerling, J. C., Fuller, P. M., Lucey, B. P., & Holtzman, D. M. (2019). The sleep-wake cycle regulates brain interstitial fluid tau in mice and CSF tau in humans. *Science*, *363*(6429), 80–884. https://doi.org/10.1126/science.aav2546

Hong, S. S., Ogawa, Y., Higano, S., Nakamura, M., & Hoshino, F. (1985). [Radioprotective effect of local hypothermia]. *Gan No Rinsho. Japan Journal of Cancer Clinics*, *31*(7), 854–860. http://www.ncbi.nlm.nih.gov/pubmed/4032761

Hooper, D. C., Martin, S. M., & Horowitz, J. M. (1985). Temperature effects on evoked potentials of hippocampal slices from euthermic chipmunks, hamsters and rats. *Journal*

of Thermal Biology, *10*(1), 35–40. https://doi.org/10.1016/0306-4565(85)90008-7

Hori, T., Nakashima, T., Hori, N., & Kiyohara, T. (1980). Thermo-sensitive neurons in hypothalamic tissue slices in vitro. *Brain Research*, *186*(1), 203–207. https://doi.org/10.1016/0006-8993(80)90266-8

Horii, Y., Shiina, T., & Shimizu, Y. (2018). The mechanism enabling hibernation in mammals. In *Advances in Experimental Medicine and Biology* (Vol. 1081, pp. 45–60). Springer New York LLC. https://doi.org/10.1007/978-981-13-1244-1_3

Hrvatin, S., Sun, S., Wilcox, O. F., Yao, H., Lavin-Peter, A. J., Cicconet, M., Assad, E. G., Palmer, M. E., Aronson, S., Banks, A. S., Griffith, E. C., & Greenberg, M. E. (2020). Neurons that regulate mouse torpor. *Nature*. https://doi.org/10.1038/s41586-020-2387-5

Huber, R., Ghilardi, M. F., Massimini, M., & Tononi, G. (2004). Local sleep and learning. *Nature*, *430*(6995), 78–81. https://doi.org/10.1038/nature02663

Huber, R., Mäki, H., Rosanova, M., Casarotto, S., Canali, P., Casali, A. G., Tononi, G., & Massimini, M. (2013). Human cortical excitability increases with time awake. *Cerebral Cortex*, *23*(2), 332–338. https://doi.org/10.1093/cercor/bhs014

Hübschle, T., Mathai, M. L., McKinley, M. J., & Oldfield, B. J. (2001). Multisynaptic neuronal pathways from the submandibular and sublingual glands to the lamina terminalis in the rat: A model for the role of the lamina terminalis in the control of osmo- and thermoregulatory behaviour. *Clinical and Experimental Pharmacology and Physiology*, *28*(7), 558–569. https://doi.org/10.1046/j.1440-1681.2001.03487.x

Humphries, M. M., Thomas, D. W., & Kramer, D. L. (2003). The role of energy availability in mammalian hibernation: A cost-benefit approach. *Physiological and Biochemical Zoology*, *76*(2), 165–179. https://doi.org/10.1086/367950

Hut, R. A., Van der Zee, E. A., Jansen, K., Gerkema, M. P., & Daan, S. (2002). Gradual reappearance of post-hibernation circadian rhythmicity correlates with numbers of vasopressin-containing neurons in the suprachiasmatic nuclei of European ground squirrels. *Journal of Comparative Physiology B: Biochemical, Systemic, and Environmental Physiology*, *172*(1), 59–70. https://doi.org/10.1007/s003600100227

Iliff, B. W., & Swoap, S. J. (2012). Central adenosine receptor signaling is necessary for daily torpor in mice. *American Journal of Physiology-Regulatory, Integrative and Comparative Physiology*, *303*(5), R477–R484. https://doi.org/10.1152/ajpregu.00081.2012

Ittner, A., Chua, S. W., Bertz, J., Volkerling, A., Van Der Hoven, J., Gladbach, A., Przybyla, M., Bi, M., Van Hummel, A., Stevens, C. H., Ippati, S., Suh, L. S., Macmillan, A., Sutherland, G., Kril, J. J., Silva, A. P. G., Mackay, J., Poljak, A., Delerue, F., … Ittner, L. M. (2016). Site-specific phosphorylation of tau inhibits amyloid-β toxicity in Alzheimer's mice. *Science*, *354*(6314), 904–908. https://doi.org/10.1126/science.aah6205

Ittner, L. M., Ke, Y. D., Delerue, F., Bi, M., Gladbach, A., van Eersel, J., Wölfing, H., Chieng, B. C., Christie, M. J., Napier, I. A., Eckert, A., Staufenbiel, M., Hardeman, E., & Götz, J. (2010). Dendritic function of tau mediates amyloid-β toxicity in alzheimer's disease mouse models. *Cell*, *142*(3), 387–397. https://doi.org/10.1016/j.cell.2010.06.036

Iwen, K. A., Oelkrug, R., & Brabant, G. (2018). Effects of thyroid hormones on thermogenesis and energy partitioning. In *Journal of Molecular Endocrinology* (Vol. 60, Issue 3, pp. R157–R170). BioScientifica Ltd. https://doi.org/10.1530/JME-17-0319

Jaroslow, B. N., Fry, R. J. M., Suhrbier, K. M., & Sallese, A. R. (1976). Radiosensitivity of Ileum Crypt Cells in Hibernating, Arousing, and Awake Ground Squirrels (Citellus tridecemlineatus). *Radiation Research*, *66*(3), 566. https://doi.org/10.2307/3574460

Jaroslow, B. N., Smith, D. E., Williams, M., & Tyler, S. A. (1969). Survival of Hibernating Ground Squirrels (Citellus tridecemlineatus) after Single and Fractionated Doses of Cobalt-60 Gamma Radiation. *Radiation Research*, *38*(2), 379. https://doi.org/10.2307/3572780

Jeong, J. H., Lee, D. K., Blouet, C., Ruiz, H. H., Buettner, C., Chua, S., Schwartz, G. J., & Jo, Y. H. (2015). Cholinergic neurons in the dorsomedial hypothalamus regulate mouse brown adipose tissue metabolism. *Molecular Metabolism*, *4*(6), 483–492. https://doi.org/10.1016/j.molmet.2015.03.006

Jinka, T. R., Tøien, O., & Drew, K. L. (2011). Season primes the brain in an arctic hibernator

to facilitate entrance into torpor mediated by adenosine A1 receptors. *Journal of Neuroscience*, *31*(30), 10752–10758. https://doi.org/10.1523/JNEUROSCI.1240-11.2011

Ju, H., So, H., Ha, K., Park, K., Lee, J. W., Chung, C. M., & Choi, I. (2011). Sustained torpidity following multi-dose administration of 3-iodothyronamine in mice. *Journal of Cellular Physiology*, *226*(4), 853–858. https://doi.org/10.1002/jcp.22573

Kalsbeek, A., Fliers, E., Franke, A. N., Wortel, J., & Buijs, R. M. (2000). Functional connections between the suprachiasmatic nucleus and the thyroid gland as revealed by lesioning and viral tracing techniques in the rat. *Endocrinology*, *141*(10), 3832–3841. https://doi.org/10.1210/endo.141.10.7709

Kanosue, K., Hosono, T., Zhang, Y. H., & Chen, X. M. (1998). Neuronal networks controlling thermoregulatory effectors. In *Progress in Brain Research* (Vol. 115, pp. 49–62). Elsevier B.V. https://doi.org/10.1016/s0079-6123(08)62029-4

Karnaukhova, N. A., Sergievich, L. A., Ignat'ev, D. A., & Karnaukhov, V. N. (2008). Effect of ionizing radiation on the synthetic activity of blood system cells in ground squirrels in different physiological states of animals. *Biofizika*, *53*(1), 113–122. https://pubmed.ncbi.nlm.nih.gov/18488510/

Kavanau, J. L. (1997). Memory, sleep and the evolution of mechanisms of synaptic efficacy maintenance. *Neuroscience*, *79*(1), 7–44. https://doi.org/10.1016/S0306-4522(96)00610-0

Kelso, S. R., Perlmutter, M. N., & Boulant, J. A. (1982). Thermosensitive single-unit activity of in vitro hypothalamic slices. *American Journal of Physiology - Regulatory Integrative and Comparative Physiology*, *11*(1). https://doi.org/10.1152/ajpregu.1982.242.1.r77

Kempf, M., Clement, A., Faissner, A., Lee, G., & Brandt, R. (1996). Tau binds to the distal axon early in development of polarity in a microtubule- and microfilament-dependent manner. *Journal of Neuroscience*, *16*(18), 5583–5592. https://doi.org/10.1523/jneurosci.16-18-05583.1996

Khosravi, R., Maya, R., Gottlieb, T., Oren, M., Shiloh, Y., & Shkedy, D. (1999). Rapid ATM-dependent phosphorylation of MDM2 precedes p53 accumulation in response to DNA

damage. *Proceedings of the National Academy of Sciences of the United States of America*, *96*(26), 14973–14977. https://doi.org/10.1073/pnas.96.26.14973

Kilduff, T. S., Sharp, F. R., & Heller, H. C. (1982). [14C]2-deoxyglucose uptake in ground squirrel brain during hibernation. *Journal of Neuroscience*, *2*(2), 143–157. https://doi.org/10.1523/jneurosci.02-02-00143.1982

Klinke, R., Pape, H.-C., Silbernagl, S., Bauer, C., Brenner, B., Korbmacher, C., Ten Bruggencate, G., Kuschinsky, W., Dieringer, N., Meßlinger, K., Draguhn, A., Oberleithner, H., Ehmke, H., Eysel, U., Scheid, P., Gaehtgens, P., Schrader, J., Gekle, M., Schröder, H., … Kirsch, K. (2010). *Fisiologia II edizione a cura di*. http://www.edises.it

Kondo, N., & Kondo, J. (1992). Identification of novel blood proteins specific for mammalian hibernation. *Journal of Biological Chemistry*, *267*(1), 473–478.

Kondo, Noriaki, Sekijima, T., Kondo, J., Takamatsu, N., Tohya, K., & Ohtsu, T. (2006). Circannual Control of Hibernation by HP Complex in the Brain. *Cell*, *125*(1), 161–172. https://doi.org/10.1016/j.cell.2006.03.017

Körtner, G., & Geiser, F. (2000). The temporal organization of daily torpor and hibernation: Circadian and circannual rhythms. In *Chronobiology International* (Vol. 17, Issue 2, pp. 103–128). Taylor & Francis. https://doi.org/10.1081/CBI-100101036

Krelstein, M. S., Thomas, M. P., & Horowitz, J. M. (1990). Thermal effects on long-term potentiation in the hamster hippocampus. *Brain Research*, *520*(1–2), 115–122. https://doi.org/10.1016/0006-8993(90)91696-E

Krilowicz, B. L., Glotzbach, S. F., & Heller, H. C. (1988). Neuronal activity during sleep and complete bouts of hibernation. *American Journal of Physiology - Regulatory Integrative and Comparative Physiology*, *255*(6). https://doi.org/10.1152/ajpregu.1988.255.6.r1008

Kuskin, S. M., Wang, S. C., & Rugh, R. (1959). Protective effect of artificially induced hibernation against lethal doses of whole body x-irradiation in CF male mice. *The American Journal of Physiology*, *196*(6), 1211–1213. https://doi.org/10.1152/ajplegacy.1959.196.6.1211

Larkin, J. E., & Heller, C. H. (1998). The disappearing slow wave activity of hibernators. *Sleep Research Online : SRO*, *1*(2), 96–101. https://www.ncbi.nlm.nih.gov/pubmed/11382864

Larkin, J E, & Heller, H. C. (1996). Temperature sensitivity of sleep homeostasis during hibernation in the golden-mantled ground squirrel. *American Journal of Physiology - Regulatory Integrative and Comparative Physiology*, *270*(4 39-4). https://doi.org/10.1152/ajpregu.1996.270.4.r777

Larkin, Jennie E., & Heller, H. C. (1999). Sleep after arousal from hibernation is not homeostatically regulated. *American Journal of Physiology - Regulatory Integrative and Comparative Physiology*, *276*(2 45-2), 522–529. https://doi.org/10.1152/ajpregu.1999.276.2.r522

Larsen, P. J., Hay-Schmidt, A., & Mikkelsen, J. D. (1994). Efferent connections from the lateral hypothalamic region and the lateral preoptic area to the hypothalamic paraventricular nucleus of the rat. *The Journal of Comparative Neurology*, *342*(2), 299–319. https://doi.org/10.1002/cne.903420211

León-Espinosa, G., García, E., Gómez-Pinedo, U., Hernández, F., DeFelipe, J., & Ávila, J. (2016). Decreased adult neurogenesis in hibernating Syrian hamster. *Neuroscience*, *333*, 181–192. https://doi.org/10.1016/j.neuroscience.2016.07.016

Lepock, J. R. (2003). Cellular effects of hyperthermia: Relevance to the minimum dose for thermal damage. *International Journal of Hyperthermia*, *19*(3), 252–266. https://doi.org/10.1080/0265673031000065042

Li, J., Zhang, G., Cai, S., & Redington, A. N. (2008). Effect of inhaled hydrogen sulfide on metabolic responses in anesthetized, paralyzed, and mechanically ventilated piglets. *Pediatric Critical Care Medicine*, *9*(1), 110–112. https://doi.org/10.1097/01.PCC.0000298639.08519.0C

Lidell, M. E., Betz, M. J., Leinhard, O. D., Heglind, M., Elander, L., Slawik, M., Mussack, T., Nilsson, D., Romu, T., Nuutila, P., Virtanen, K. A., Beuschlein, F., Persson, A., Borga, M., & Enerbäck, S. (2013). Evidence for two types of brown adipose tissue in humans. *Nature Medicine*, *19*(5), 631–634. https://doi.org/10.1038/nm.3017

Lisowska, H., Brehwens, K., Zölzer, F., Wegierek-Ciuk, A., Czub, J., Lankoff, A., Haghdoost, S., & Wojcik, A. (2014). Effect of hypothermia on radiation-induced micronuclei and delay of cell cycle progression in TK6 cells. *International Journal of Radiation Biology*, *90*(4), 318–324. https://doi.org/10.3109/09553002.2014.887233

Lisowska, H., Cheng, L., Sollazzo, A., Lundholm, L., Wegierek-Ciuk, A., Sommer, S., Lankoff, A., & Wojcik, A. (2018). Hypothermia modulates the DNA damage response to ionizing radiation in human peripheral blood lymphocytes. *International Journal of Radiation Biology*, *94*(6), 551–557. https://doi.org/10.1080/09553002.2018.1466206

Logan, S. M., Luu, B. E., & Storey, K. B. (2016). Turn down genes for WAT? Activation of anti-apoptosis pathways protects white adipose tissue in metabolically depressed thirteen-lined ground squirrels. *Molecular and Cellular Biochemistry*, *416*(1–2), 47–62. https://doi.org/10.1007/s11010-016-2695-0

López, M., Varela, L., Vázquez, M. J., Rodríguez-Cuenca, S., González, C. R., Velagapudi, V. R., Morgan, D. A., Schoenmakers, E., Agassandian, K., Lage, R., De Morentin, P. B. M., Tovar, S., Nogueiras, R., Carling, D., Lelliott, C., Gallego, R., OreŠič, M., Chatterjee, K., Saha, A. K., … Vidal-Puig, A. (2010). Hypothalamic AMPK and fatty acid metabolism mediate thyroid regulation of energy balance. *Nature Medicine*, *16*(9), 1001–1008. https://doi.org/10.1038/nm.2207

Lou, L. X., Geng, B., Du, J. B., & Tang, C. S. (2008). Hydrogen sulphide-induced hypothermia attenuates stress-related ulceration in rats. *Clinical and Experimental Pharmacology and Physiology*, *35*(2), 223–228. https://doi.org/10.1111/j.1440-1681.2007.04812.x

Luppi, M., Hitrec, T., Di Cristoforo, A., Squarcio, F., Stanzani, A., Occhinegro, A., Chiavetta, P., Tupone, D., Zamboni, G., Amici, R., & Cerri, M. (2019). Phosphorylation and Dephosphorylation of Tau Protein During Synthetic Torpor. *Frontiers in Neuroanatomy*, *13*, 57. https://doi.org/10.3389/fnana.2019.00057

Luppi, M., Martelli, D., Amici, R., Baracchi, F., Cerri, M., Dentico, D., Perez, E., & Zamboni, G. (2010). Hypothalamic osmoregulation is maintained across the wake-sleep cycle in the rat: Osmoregulation and sleep. *Journal of Sleep Research*, *19*(3), 394–399.

https://doi.org/10.1111/j.1365-2869.2009.00810.x

Lyman. (1982). The hibernating state, Recent theories of hibernation. *Mammals and Birds. Academic Press, New York,*.

M.L. Mallet. (2002). Pathophysiology of accidental hypothermia. *QJM - Monthly Journal of the Association of Physicians*, *95*(12), 775–785. https://doi.org/10.1093/qjmed/95.12.775

Ma, N.-Y., Tinganelli, W., Maier, A., Durante, M., & Kraft-Weyrather, W. (2013). *Influence of chronic hypoxia and radiation quality on cell survival*. https://doi.org/10.1093/jrr/rrs135

Mackiewicz, M., Shockley, K. R., Romer, M. A., Galante, R. J., Zimmerman, J. E., Naidoo, N., Baldwin, D. A., Jensen, S. T., Churchill, G. A., & Pack, A. I. (2007). Macromolecule biosynthesis: A key function of sleep. *Physiological Genomics*, *31*(3), 441–457. https://doi.org/10.1152/physiolgenomics.00275.2006

MacLaren, R., Gallagher, J., Shin, J., Varnado, S., & Nguyen, L. (2014). Assessment of Adverse Events and Predictors of Neurological Recovery After Therapeutic Hypothermia. *Annals of Pharmacotherapy*, *48*(1), 17–25. https://doi.org/10.1177/1060028013511228

Madden, C. J., & Morrison, S. F. (2009). Neurons in the paraventricular nucleus of the hypothalamus inhibit sympathetic outflow to brown adipose tissue. *American Journal of Physiology - Regulatory Integrative and Comparative Physiology*, *296*(3). https://doi.org/10.1152/ajpregu.91007.2008

Madden, Christopher J., & Morrison, S. F. (2019). Central nervous system circuits that control body temperature. *Neuroscience Letters*, *696*, 225–232. https://doi.org/10.1016/j.neulet.2018.11.027

Magoun, H. W., Harrison, F., Brobeck, J. R., & Ranson, S. W. (1938). Activation of heat loss mechanisms by local heating of the brain. *Journal of Neurophysiology*, *1*(2), 101–114. https://doi.org/10.1152/jn.1938.1.2.101

Malia, T. J., Teplyakov, A., Ernst, R., Wu, S.-J., Lacy, E. R., Liu, X., Vandermeeren, M., Mercken, M., Luo, J., Sweet, R. W., & Gilliland, G. L. (2016). Epitope mapping and

structural basis for the recognition of phosphorylated tau by the anti-tau antibody AT8. *Proteins: Structure, Function, and Bioinformatics*, *84*(4), 427–434. https://doi.org/10.1002/prot.24988

Martelli, D., Luppi, M., Cerri, M., Tupone, D., Mastrotto, M., Perez, E., Zamboni, G., & Amici, R. (2014). The direct cooling of the preoptic-hypothalamic area elicits the release of thyroid stimulating hormone during wakefulness but not during REM sleep. *PLoS ONE*, *9*(2). https://doi.org/10.1371/journal.pone.0087793

Martelli, D., Luppi, M., Cerri, M., Tupone, D., Perez, E., Zamboni, G., & Amici, R. (2012). Waking and Sleeping following Water Deprivation in the Rat. *PLoS ONE*, *7*(9). https://doi.org/10.1371/journal.pone.0046116

Massopust, L. C., Wolin, L. R., & Meder, J. (1965). Spontaneous electrical activity of the brain in hibernators and nonhibernators during hypothermia. *Experimental Neurology*, *12*(1), 25–32. https://doi.org/10.1016/0014-4886(65)90096-8

Mathers, K. E., Mcfarlane, S. V, Zhao, L., & Staples, J. F. (2017). Regulation of mitochondrial metabolism during hibernation by reversible suppression of electron transport system enzymes. *Journal of Comparative Physiology B*, *187*, 227–234. https://doi.org/10.1007/s00360-016-1022-0

Maya, R., Balass, M., Kim, S. T., Shkedy, D., Martinez Leal, J. F., Shifman, O., Moas, M., Buschmann, T., Ronai, Z., Shiloh, Y., Kastan, M. B., Katzir, E., & Oren, M. (2001). ATM-dependent phosphorylation of Mdm2 on serine 395: Role in p53 activation by DNA damage. *Genes and Development*, *15*(9), 1067–1077. https://doi.org/10.1101/gad.886901

Mcallen, R. M., May, C. N., & Shafton, A. D. (1995). Functional anatomy of sympathetic premotor cell groups in the medulla. *Clinical and Experimental Hypertension*, *17*(1–2), 209–221. https://doi.org/10.3109/10641969509087066

McCarron, R. M., Sieckmann, D. G., Yu, E. Z., Frerichs, K., & Hallenbeck, J. M. (2001). Hibernation , a state of natural tolerance to profound reduction in organ blood flow and oxygen delivery capacity. In *Molecular Mechanisms of Metabolic Arrest: Life in Limbo* (pp. 23–42).

McKechnie, A. E., & Lovegrove, B. G. (2002). Avian Facultative Hypothermic Responses: A Review. *The Condor*, *104*(4), 705–724. https://doi.org/10.1093/CONDOR/104.4.705

McKinley, M. J., Martelli, D., Pennington, G. L., Trevaks, D., & McAllen, R. M. (2018). Integrating competing demands of osmoregulatory and thermoregulatory homeostasis. In *Physiology* (Vol. 33, Issue 3, pp. 170–181). American Physiological Society. https://doi.org/10.1152/physiol.00037.2017

Mckinley, M. J., Yao, S. T., Uschakov, A., McAllen, R. M., Rundgren, M., & Martelli, D. (2015). The median preoptic nucleus: Front and centre for the regulation of body fluid, sodium, temperature, sleep and cardiovascular homeostasis. In *Acta Physiologica* (Vol. 214, Issue 1, pp. 8–32). Blackwell Publishing Ltd. https://doi.org/10.1111/apha.12487

Mcnaughton, B. L., Shen, J., Rao, G., Fostert, T. C., & Barnes, C. A. (1994). Persistent increase of hippocampal presynaptic axon excitability after repetitive electrical stimulation: Dependence on N-methyl-D-aspartate receptor activity, nitric-oxide synthase, and temperature (quantal analysis/long-term potentiation/neurophysiology). In *Neurobiology* (Vol. 91). https://www.pnas.org/content/91/11/4830.short

Meerlo, P., De Bruin, E. A., Strijkstra, A. M., & Daan, S. (2001). A social conflict increases EEG slow-wave activity during subsequent sleep. *Physiology and Behavior*, *73*(3), 331–335. https://doi.org/10.1016/S0031-9384(01)00451-6

Millesi, E., Prossinger, H., Dittami, J. P., & Fieder, M. (2001). Hibernation effects on memory in European ground squirrels (Spermophilus citellus). *Journal of Biological Rhythms*, *16*(3), 264–271. https://doi.org/10.1177/074873040101600309

Milsom, W. K., Zimmer, M. B., & Harris, M. B. (1999). Regulation of cardiac rhythm in hibernating mammals. In *Comparative Biochemistry and Physiology - A Molecular and Integrative Physiology* (Vol. 124, Issue 4, pp. 383–391). Elsevier Inc. https://doi.org/10.1016/S1095-6433(99)00130-0

Mitchell, D., Maloney, S. K., Jessen, C., Laburn, H. P., Kamerman, P. R., Mitchell, G., & Fuller, A. (2002). Adaptive heterothermy and selective brain cooling in arid-zone mammals. *Comparative Biochemistry and Physiology - B Biochemistry and Molecular Biology*, *131*(4), 571–585. https://doi.org/10.1016/S1096-4959(02)00012-X

Moffett, S. X., Giannopoulos, P. F., James, T. D., & Martin, J. V. (2013). Effects of acute microinjections of thyroid hormone to the preoptic region of hypothyroid adult male rats on sleep, motor activity and body temperature. *Brain Research*, *1516*, 55–65. https://doi.org/10.1016/j.brainres.2013.04.017

Mohammed, M., Madden, C. J., Burchiel, K. J., & Morrison, S. F. (2018). Preoptic area cooling increases the sympathetic outflow to brown adipose tissue and brown adipose tissue thermogenesis. *American Journal of Physiology - Regulatory Integrative and Comparative Physiology*, *315*(4), R609–R618. https://doi.org/10.1152/ajpregu.00113.2018

Morris, M., Maeda, S., Vossel, K., & Mucke, L. (2011). The Many Faces of Tau. In *Neuron* (Vol. 70, Issue 3, pp. 410–426). Cell Press. https://doi.org/10.1016/j.neuron.2011.04.009

Morrison, S. F. (2016). Central neural control of thermoregulation and brown adipose tissue. In *Autonomic Neuroscience: Basic and Clinical* (Vol. 196, pp. 14–24). Elsevier B.V. https://doi.org/10.1016/j.autneu.2016.02.010

Morrison, S. F., & Madden, C. J. (2014). Central nervous system regulation of brown adipose tissue. *Comprehensive Physiology*, *4*(4), 1677–1713. https://doi.org/10.1002/cphy.c140013

Morrison, S. F., & Nakamura, K. (2011). Central neural pathways for thermoregulation. *Frontiers in Bioscience*, *16*(1), 74–104. https://doi.org/10.2741/3677

Mukrasch, M. D., Biernat, J., Von Bergen, M., Griesinger, C., Mandelkow, E., & Zweckstetter, M. (2005). Sites of tau important for aggregation populate β-structure and bind to microtubules and polyanions. *Journal of Biological Chemistry*, *280*(26), 24978–24986. https://doi.org/10.1074/jbc.M501565200

Mullur, R., Liu, Y. Y., & Brent, G. A. (2014). Thyroid hormone regulation of metabolism. *Physiological Reviews*, *94*(2), 355–382. https://doi.org/10.1152/physrev.00030.2013

Musacchia, X. J., & Barr, R. E. (1968). Survival of Whole-Body-Irradiated Hibernating and Active Ground Squirrels; Citellus tridecemlineatus. *Radiation Research*, *33*(2), 348. https://doi.org/10.2307/3572485

Nakamura, K., Matsumura, K., Hübschle, T., Nakamura, Y., Hioki, H., Fujiyama, F., Boldogköi, Z., König, M., Thiel, H. J., Gerstberger, R., Kobayashi, S., & Kaneko, T. (2004). Identification of sympathetic premotor neurons in medullary raphe regions mediating fever and other thermoregulatory functions. *Journal of Neuroscience*, *24*(23), 5370–5380. https://doi.org/10.1523/JNEUROSCI.1219-04.2004

Nakamura, K., Matsumura, K., Kaneko, T., Kobayashi, S., Katoh, H., & Negishi, M. (2002). The Rostral Raphe Pallidus Nucleus Mediates Pyrogenic Transmission from the Preoptic Area. In *Soc Neuroscience*. https://www.jneurosci.org/content/22/11/4600.short

Nakamura, K., & Morrison, S. F. (2008a). A thermosensory pathway that controls body temperature. *Nature Neuroscience*, *11*(1), 62–71. https://doi.org/10.1038/nn2027

Nakamura, K., & Morrison, S. F. (2008b). Preoptic mechanism for cold-defensive responses to skin cooling. *Journal of Physiology*, *586*(10), 2611–2620. https://doi.org/10.1113/jphysiol.2008.152686

Nakamura, K., & Morrison, S. F. (2010). A thermosensory pathway mediating heat-defense responses. *Proceedings of the National Academy of Sciences of the United States of America*, *107*(19), 8848–8853. https://doi.org/10.1073/pnas.0913358107

Nakamura, K., & Morrison, S. F. (2011). Central efferent pathways for cold-defensive and febrile shivering. *Journal of Physiology*, *589*(14), 3641–3658. https://doi.org/10.1113/jphysiol.2011.210047

Nicoll, R. A., & Malenka, R. C. (1999). Expression mechanisms underlying NMDA receptor-dependent long-term potentiation. *Annals of the New York Academy of Sciences*, *868*, 515–525. https://doi.org/10.1111/j.1749-6632.1999.tb11320.x

Nilson, A. N., English, K. C., Gerson, J. E., Barton Whittle, T., Nicolas Crain, C., Xue, J., Sengupta, U., Castillo-Carranza, D. L., Zhang, W., Gupta, P., & Kayed, R. (2017). Tau oligomers associate with inflammation in the brain and retina of tauopathy mice and in neurodegenerative diseases. *Journal of Alzheimer's Disease*, *55*(3), 1083–1099. https://doi.org/10.3233/JAD-160912

Norimoto, H., Makino, K., Gao, M., Shikano, Y., Okamoto, K., Ishikawa, T., Sasaki, T.,

Hioki, H., Fujisawa, S., & Ikegaya, Y. (2018). Hippocampal ripples down-regulate synapses. *Science*, *359*(6383), 1524–1527. https://doi.org/10.1126/science.aao0702

O'Hara, B. F., Watson, F. L., Srere, H. K., Kumar, H., Wiler, S. W., Welch, S. K., Bitting, L., Heller, H. C., & Kilduff, T. S. (1999). Gene expression in the brain across the hibernation cycle. *Journal of Neuroscience*, *19*(10), 3781–3790. https://doi.org/10.1523/jneurosci.19-10-03781.1999

Oei, A. L., Vriend, L. E. M., Crezee, J., Franken, N. A. P., & Krawczyk, P. M. (2015). Effects of hyperthermia on DNA repair pathways: One treatment to inhibit them all. *Radiation Oncology*, *10*(1). https://doi.org/10.1186/s13014-015-0462-0

Ognjanovski, N., Maruyama, D., Lashner, N., Zochowski, M., & Aton, S. J. (2014). CA1 hippocampal network activity changes during sleep-dependent memory consolidation. *Frontiers in Systems Neuroscience*, *8*(1 APR). https://doi.org/10.3389/fnsys.2014.00061

Olcese, J. (2003). Circadian Signaling in the Chick Pineal Organ. *Chronobiology International*, *20*(4), 617–636. https://doi.org/10.1081/CBI-120022409

Olson, J. M., Jinka, T. R., Larson, L. K., Danielson, J. J., Moore, J. T., Carpluck, J., & Drew, K. L. (2013). Circannual rhythm in body temperature, torpor, and sensitivity to A1 adenosine receptor agonist in arctic ground squirrels. *Journal of Biological Rhythms*, *28*(3), 201–207. https://doi.org/10.1177/0748730413490667

Ootsuka, Y., & Blessing, W. W. (2005). Activation of slowly conducting medullary raphé-spinal neurons, including serotonergic neurons, increases cutaneous sympathetic vasomotor discharge in rabbit. *American Journal of Physiology - Regulatory Integrative and Comparative Physiology*, *288*(4 57-4). https://doi.org/10.1152/ajpregu.00564.2004

Ootsuka, Y., & Terui, N. (1997). Functionally different neurons are organized topographically in the rostral ventrolateral medulla of rabbits. *Journal of the Autonomic Nervous System*, *67*(1–2), 67–78. https://doi.org/10.1016/S0165-1838(97)00094-5

Palchykova, S., Deboer, T., & Tobler, I. (2002). Selective sleep deprivation after daily torpor in the Djungarian hamster. *Journal of Sleep Research*, *11*(4), 313–319. https://doi.org/10.1046/j.1365-2869.2002.00310.x

Palop, J. J., & Mucke, L. (2010). Amyloid-B-induced neuronal dysfunction in Alzheimer's disease: From synapses toward neural networks. In *Nature Neuroscience* (Vol. 13, Issue 7, pp. 812–818). Nature Publishing Group. https://doi.org/10.1038/nn.2583

Parmeggiani, P. L. (2005). Physiologic regulation in sleep. In *Principles and Practice of Sleep Medicine, 5th Edition*. https://doi.org/10.1016/C2009-0-59875-3

Partridge, L. D. (1982). The good enough calculi of evolving control systems: Evolution is not engineering. *American Journal of Physiology - Regulatory Integrative and Comparative Physiology*, *11*(2). https://doi.org/10.1152/ajpregu.1982.242.3.r173

Partridge, L., & Partridge, L. (1993). *The nervous system: Its function and its interaction with the world*.

Paul, M. J., Freeman, D. A., Jin, H. P., & Dark, J. (2005). Neuropeptide Y induces torpor-like hypothermia in Siberian hamsters. *Brain Research*, *1055*(1–2), 83–92. https://doi.org/10.1016/j.brainres.2005.06.090

Paxinos, G., & Watson, C. (2007). *The rat brain in stereotaxic coordinates*. http://www.apnet.com

Peineau, S., Taghibiglou, C., Bradley, C., Wong, T. P., Liu, L., Lu, J., Lo, E., Wu, D., Saule, E., Bouschet, T., Matthews, P., Isaac, J. T. R., Bortolotto, Z. A. A., Wang, Y. T., & Collingridge, G. L. (2007). LTP Inhibits LTD in the Hippocampus via Regulation of GSK3β. *Neuron*, *53*(5), 703–717. https://doi.org/10.1016/j.neuron.2007.01.029

Pengelley, E. T., Asmundson, S. J., Barnes, B., & Aloia, R. C. (1976). Relationship of light intensity and photoperiod to circannual rhythmicity in the hibernating ground squirrel, Citellus lateralis. *Comparative Biochemistry and Physiology -- Part A: Physiology*, *53*(3), 273–277. https://doi.org/10.1016/S0300-9629(76)80035-7

Pengelley, Eric T., & Fisher, K. C. (1963). The effect of temperature and photoperiod on the yearly hibernating behavior of captive golden-mantled ground squirrels (citellus lateralis tescorum). *Canadian Journal of Zoology*, *41*(6), 1103–1120. https://doi.org/10.1139/z63-087

Pierau, F. K., Sann, H., Yakimova, K., & Haug, P. (1998). Plasticity of hypothalamic

temperature-sensitive neurons. In *Progress in Brain Research* (Vol. 115, pp. 63–84). Elsevier B.V. https://doi.org/10.1016/s0079-6123(08)62030-0

Pietenpol, J. A., & Stewart, Z. A. (2002). Cell cycle checkpoint signaling: Cell cycle arrest versus apoptosis. *Toxicology*, *181–182*, 475–481. https://doi.org/10.1016/S0300-483X(02)00460-2

Pines, J. (1995). Cyclins and cyclin-dependent kinases: a biochemical view. In *Biochem. J* (Vol. 308). https://portlandpress.com/biochemj/article-pdf/308/3/697/620689/bj3080697.pdf

Planel, E., Miyasaka, T., Launey, T., Chui, D. H., Tanemura, K., Sato, S., Murayama, O., Ishiguro, K., Tatebayashi, Y., & Takashima, A. (2004). Alterations in Glucose Metabolism Induce Hypothermia Leading to Tau Hyperphosphorylation through Differential Inhibition of Kinase and Phosphatase Activities: Implications for Alzheimer's Disease. *Journal of Neuroscience*, *24*(10), 2401–2411. https://doi.org/10.1523/JNEUROSCI.5561-03.2004

Planel, E., Richter, K. E. G., Nolan, C. E., Finley, J. E., Liu, L., Wen, Y., Krishnamurthy, P., Herman, M., Wang, L., Schachter, J. B., Nelson, R. B., Lau, L.-F., & Duff, K. E. (2007). Neurobiology of Disease Anesthesia Leads to Tau Hyperphosphorylation through Inhibition of Phosphatase Activity by Hypothermia. *Soc Neuroscience*. https://doi.org/10.1523/JNEUROSCI.4854-06.2007

Planel, E., Yasutake, K., Fujita, S. C., & Ishiguro, K. (2001). Inhibition of Protein Phosphatase 2A Overrides Tau Protein Kinase I/Glycogen Synthase Kinase 3 and Cyclin-dependent Kinase 5 Inhibition and Results in Tau Hyperphosphorylation in the Hippocampus of Starved Mouse*. *ASBMB*. https://doi.org/10.1074/jbc.M102780200

Polderman, K. H. (2004). Keeping a cool head: How to induce and maintain hypothermia. In *Critical Care Medicine* (Vol. 32, Issue 12, pp. 2558–2560). https://doi.org/10.1097/01.CCM.0000148087.41418.0A

Pooler, A. M., Phillips, E. C., Lau, D. H. W., Noble, W., & Hanger, D. P. (2013). Physiological release of endogenous tau is stimulated by neuronal activity. *EMBO Reports*, *14*(4), 389–394. https://doi.org/10.1038/embor.2013.15

Popov, V. I., & Bocharova, L. S. (1992). Hibernation-induced structural changes in synaptic contacts between mossy fibres and hippocampal pyramidal neurons. *Neuroscience*, *48*(1), 53–62. https://doi.org/10.1016/0306-4522(92)90337-2

Popov, V. I., Bocharova, L. S., & Bragin, A. G. (1992). Repeated changes of dendritic morphology in the hippocampus of ground squirrels in the course of hibernation. *Neuroscience*, *48*(1), 45–51. https://doi.org/10.1016/0306-4522(92)90336-z

Pörtner, H. O. (2010). Oxygen- And capacity-limitation of thermal tolerance: A matrix for integrating climate-related stressor effects in marine ecosystems. *Journal of Experimental Biology*, *213*(6), 881–893. https://doi.org/10.1242/jeb.037523

Portt, L., Norman, G., Clapp, C., Greenwood, M., & Greenwood, M. T. (2011). Anti-apoptosis and cell survival: A review. In *Biochimica et Biophysica Acta - Molecular Cell Research* (Vol. 1813, Issue 1, pp. 238–259). Elsevier. https://doi.org/10.1016/j.bbamcr.2010.10.010

Puentes-Mestril, C., & Aton, S. J. (2017). Linking network activity to synaptic plasticity during sleep: Hypotheses and recent data. *Frontiers in Neural Circuits*, *11*, 61. https://doi.org/10.3389/fncir.2017.00061

Raaphorst, G. P., Ng, C. E., & Yang, D. P. (1999). Thermal radiosensitization and repair inhibition in human melanoma cells: A comparison of survival and DNA double strand breaks. *International Journal of Hyperthermia*, *15*(1), 17–27. https://doi.org/10.1080/026567399285828

Ran, C., Hoon, M. A., & Chen, & X. (2016). The coding of cutaneous temperature in the spinal cord. *Nature.Com*, *19*(9). https://doi.org/10.1038/nn.4350

Ransohoff, R. M. (2016). How neuroinflammation contributes to neurodegeneration. In *Science* (Vol. 353, Issue 6301, pp. 777–783). American Association for the Advancement of Science. https://doi.org/10.1126/science.aag2590

Regan, P., Piers, T., Yi, J. H., Kim, D. H., Huh, S., Park, S. J., Ryu, J. H., Whitcomb, D. J., & Cho, K. (2015). Tau phosphorylation at serine 396 residue is required for hippocampal LTD. *Journal of Neuroscience*, *35*(12), 4804–4812.

https://doi.org/10.1523/JNEUROSCI.2842-14.2015

Reynolds, C. H., Garwood, C. J., Wray, S., Price, C., Kellie, S., Perera, T., Zvelebil, M., Yang, A., Sheppard, P. W., Varndell, I. M., Hanger, D. P., & Anderton, B. H. (2008). Phosphorylation regulates tau interactions with Src homology 3 domains of phosphatidylinositol 3-kinase, phospholipase Cγ1, Grb2, and Src family kinases. *Journal of Biological Chemistry*, *283*(26), 18177–18186. https://doi.org/10.1074/jbc.M709715200

Ribeiro, M. O., Carvalho, S. D., Schultz, J. J., Chiellini, G., Scanlan, T. S., Bianco, A. C., & Brent, G. A. (2001). Thyroid hormone–sympathetic interaction and adaptive thermogenesis are thyroid hormone receptor isoform–specific. *Journal of Clinical Investigation*, *108*(1), 97–105. https://doi.org/10.1172/jci12584

Roberson, E. D., Halabisky, B., Yoo, J. W., Yao, J., Chin, J., Yan, F., Wu, T., Hamto, P., Devidze, N., Yu, G. Q., Palop, J. J., Noebels, J. L., & Mucke, L. (2011). Amyloid-β/fyn-induced synaptic, network, and cognitive impairments depend on tau levels in multiple mouse models of alzheimer's disease. *Journal of Neuroscience*, *31*(2), 700–711. https://doi.org/10.1523/JNEUROSCI.4152-10.2011

Roberts, W. W. (1988). Differential Thermosensor Control of Thermoregulatory Grooming, Locomotion, and Relaxed Postural Extension. *Annals of the New York Academy of Sciences*, *525*(1), 363–374. https://doi.org/10.1111/j.1749-6632.1988.tb38620.x

Romanovsky, A. A. (2004). Do fever and anapyrexia exist? Analysis of set point-based definitions. *American Journal of Physiology-Regulatory, Integrative and Comparative Physiology*, *287*(4), R992–R995. https://doi.org/10.1152/ajpregu.00068.2004

Romanovsky, A. A. (2007). Thermoregulation: Some concepts have changed. Functional architecture of the thermoregulatory system. In *American Journal of Physiology - Regulatory Integrative and Comparative Physiology* (Vol. 292, Issue 1). American Physiological Society. https://doi.org/10.1152/ajpregu.00668.2006

Romanovsky, A. A. (2018). The thermoregulation system and how it works. In *Handbook of Clinical Neurology* (Vol. 156, pp. 3–43). Elsevier B.V. https://doi.org/10.1016/B978-0-444-63912-7.00001-1

Roy, K., Kodama, S., Suzuki, K., Fukase, K., & Watanabe, M. (2000). Hypoxia Relieves X-Ray-Induced Delayed Effects in Normal Human Embryo Cells. *Radiation Research*, *154*(6), 659–666. https://doi.org/10.1667/0033-7587(2000)154[0659:HRXRID]2.0.CO;2

Royo, J., Aujard, F., & Pifferi, F. (2019). Daily Torpor and Sleep in a Non-human Primate, the Gray Mouse Lemur (Microcebus murinus). *Frontiers in Neuroanatomy*, *13*, 87. https://doi.org/10.3389/fnana.2019.00087

Ruby, N. F., Dark, J., Craig Heller, H., & Zucker, I. (1998). Suprachiasmatic nucleus: role in circannual body mass and hibernation rhythms of ground squirrels. In *Brain Research* (Vol. 782).

Ruf, T., & Geiser, F. (2015). Daily torpor and hibernation in birds and mammals. *Biological Reviews*, *90*(3), 891–926. https://doi.org/10.1111/brv.12137

Sakurai, T., Itoh, K., Liu, Y., Higashitsuji, H., Sumitomo, Y., Sakamaki, K., & Fujita, J. (2005). Low temperature protects mammalian cells from apoptosis initiated by various stimuli in vitro. *Experimental Cell Research*, *309*(2), 264–272. https://doi.org/10.1016/j.yexcr.2005.06.002

Saper, C. B., & Loewy, A. D. (1980). Efferent connections of the parabrachial nucleus in the rat. *Brain Research*, *197*(2), 291–317. https://doi.org/10.1016/0006-8993(80)91117-8

Satinoff, E. (1978). Neural organization and evolution of thermal regulation in mammals. *Science*, *201*(4350), 16–22. https://doi.org/10.1126/science.351802

Satinoff, E. (1964). Behavioral thermoregulation in response to local cooling of the rat brain. *The American Journal of Physiology*, *206*, 1389–1394. https://doi.org/10.1152/ajplegacy.1964.206.6.1389

Scanlan, T. S., Suchland, K. L., Hart, M. E., Chiellini, G., Huang, Y., Kruzich, P. J., Frascarelli, S., Crossley, D. A., Bunzow, J. R., Ronca-Testoni, S., Lin, E. T., Hatton, D., Zucchi, R., & Grandy, D. K. (2004). 3-Iodothyronamine is an endogenous and rapid-acting derivative of thyroid hormone. *Nature Medicine*, *10*(6), 638–642. https://doi.org/10.1038/nm1051

Schäfer, S. S., & Schäfer, S. (1973). The role of the primary afference in the generation of a

cold shivering tremor. *Experimental Brain Research*, *17*(4), 381–393. https://doi.org/10.1007/BF00234101

Scotto, P. (2006). *Fisiologia - Pietro Scotto - Paolo Mondola - Libro - Poletto - | IBS*. Retrieved June 8, 2020, from https://www.ibs.it/fisiologia-libro-vari/e/9788895033501

Seoane-Collazo, P., Martínez-Sánchez, N., Milbank, E., & Contreras, C. (2020). Incendiary leptin. In *Nutrients* (Vol. 12, Issue 2). MDPI AG. https://doi.org/10.3390/nu12020472

Shah, N., Groom, N., Jackson, S., Sibtain, A., & Hoskin, P. (2000). A pilot study to assess the feasibility of prior scalp cooling with palliative whole brain radiotherapy. *British Journal of Radiology*, *73*(869), 514–516. https://doi.org/10.1259/bjr.73.869.10884748

Sheriff, M. J., Fridinger, R. W., Tøien, Ø., Barnes, B. M., & Buck, C. L. (2013). Metabolic Rate and Prehibernation Fattening in Free-Living Arctic Ground Squirrels. *Physiological and Biochemical Zoology*, *86*(5), 515–527. https://doi.org/10.1086/673092

Shibao, C., Gamboa, A., Diedrich, A., Ertl, A. C., Chen, K. Y., Byrne, D. W., Farley, G., Paranjape, S. Y., Davis, S. N., & Biaggioni, I. (2007). Autonomic contribution to blood pressure and metabolism in obesity. *Hypertension*, *49*(1), 27–33. https://doi.org/10.1161/01.HYP.0000251679.87348.05

Shibasaki, M., Wilson, T. E., & Crandall, C. G. (2006). Neural control and mechanisms of eccrine sweating during heat stress and exercise. In *Journal of Applied Physiology* (Vol. 100, Issue 5, pp. 1692–1701). https://doi.org/10.1152/japplphysiol.01124.2005

Shiomi, H., & Tamura, Y. (2000). Pharmacological aspects of mammalian hibernation: Central thermoregulation factors in hibernation cycle. In *Folia Pharmacologica Japonica* (Vol. 116, Issue 5, pp. 304–312). https://doi.org/10.1254/fpj.116.304

Siegel, J. M. (2010). Sleep in Animals: A State of Adaptive Inactivity. In *Principles and Practice of Sleep Medicine: Fifth Edition* (pp. 126–138). https://doi.org/10.1016/B978-1-4160-6645-3.00010-4

Sies, H. (1997). Oxidative stress: Oxidants and antioxidants. In *Experimental Physiology* (Vol. 82, Issue 2, pp. 291–295). Blackwell Publishing Ltd. https://doi.org/10.1113/expphysiol.1997.sp004024

Silva, J. E., & Rabelo, R. (1997). Regulation of the uncoupling protein gene expression. In *European Journal of Endocrinology* (Vol. 136, Issue 3, pp. 251–264). BioScientifica Ltd. https://doi.org/10.1530/eje.0.1360251

Silvani, A., Cerri, M., Zoccoli, G., & Swoap, S. J. (2018). Is adenosine action common ground for nrem sleep, torpor, and other hypometabolic states? In *Physiology* (Vol. 33, Issue 3, pp. 182–196). American Physiological Society. https://doi.org/10.1152/physiol.00007.2018

Silverthorn, D., Ober, W., Agnati, L., & Silverthorn, A. (2007). *Fisiologia: un approccio integrato*.

Sjöberg, M. K., Shestakova, E., Mansuroglu, Z., Maccioni, R. B., & Bonnefoy, E. (2006). Tau protein binds to pericentromeric DNA: A putative role for nuclear tau in nucleolar organization. *Journal of Cell Science*, *119*(10), 2025–2034. https://doi.org/10.1242/jcs.02907

Smith, F., & Grenan, M. M. (1951). Effect of hibernation upon survival time following whole-body irradiation in the marmot (Marmota monax). *Science*, *113*(2946), 686–688. https://doi.org/10.1126/science.113.2946.686

Spangenberger, H., Nikmanesh, F. G., & Igelmund, P. (1995). Long-term potentiation at low temperature is stronger in hippocampal slices from hibernating Turkish hamsters compared to warm-acclimated hamsters and rats. *Neuroscience Letters*, *194*(1–2), 127–129. https://doi.org/10.1016/0304-3940(95)11723-A

Spirou, S. V., Basini, M., Lascialfari, A., Sangregorio, C., & Innocenti, C. (2018). Magnetic hyperthermia and radiation therapy: Radiobiological principles and current practice. In *Nanomaterials* (Vol. 8, Issue 6). MDPI AG. https://doi.org/10.3390/nano8060401

Standish, A., Enquist, L. W., Escardo, J. A., & Schwaberl, J. S. (1995). Central Neuronal Circuit Innervating the Rat Heart Defined by Transneuronal Transport of Pseudorabies Virus. In *The Journal of Neuroscience*. https://www.jneurosci.org/content/15/3/1998.short

Stanton, T. L., Craft, C. M., & Reiter, R. J. (1986). Pineal melatonin: Circadian rhythm and

variations during the hibernation cycle in the ground squirrel,Spermophilus lateralis. *Journal of Experimental Zoology*, *239*(2), 247–254. https://doi.org/10.1002/jez.1402390212

Staples, J. F. (2016). Metabolic Flexibility: Hibernation, Torpor, and Estivation. Metabolic Flexibility: Hibernation, Torpor, and Estivation. *Compr Physiol*, *6*, 737–771. https://doi.org/10.1002/cphy.c140064

Steriade, M., Timofeev, I., & Grenier, F. (2001). Natural waking and sleep states: A view from inside neocortical neurons. *Journal of Neurophysiology*, *85*(5), 1969–1985. https://doi.org/10.1152/jn.2001.85.5.1969

Stieler, J. T., Bullmann, T., Kohl, F., Tøien, O., Brückner, M. K., Härtig, W., Barnes, B. M., & Arendt, T. (2011). The physiological link between metabolic rate depression and tau phosphorylation in mammalian hibernation. *PLoS ONE*, *6*(1), e14530. https://doi.org/10.1371/journal.pone.0014530

Storey, K. B., & Storey, J. M. (1990). Metabolic rate depression and biochemical adaptation in anaerobiosis, hibernation and estivation. *Quarterly Review of Biology*, *65*(2), 145–174. https://doi.org/10.1086/416717

Stornetta, R. L., Rosin, D. L., Simmons, J. R., McQuiston, T. J., Vujovic, N., Weston, M. C., & Guyenet, P. G. (2005). Coexpression of vesicular glutamate transporter-3 and γ-aminobutyric acidergic markers in rat rostral medullary raphe and intermediolateral cell column. *Journal of Comparative Neurology*, *492*(4), 477–494. https://doi.org/10.1002/cne.20742

Stricker, E. M., & Hainsworth, F. R. (1970). Evaporative cooling in the rat: Effects of hypothalamic lesions and chorda tympani damage. *Canadian Journal of Physiology and Pharmacology*, *48*(1), 11–17. https://doi.org/10.1139/y70-002

Strijkstra, A. M., & Daan, S. (1997). Sleep during arousal episodes as a function of prior torpor duration in hibernating European ground squirrels. *Journal of Sleep Research*, *6*(1), 36–43. https://doi.org/10.1046/j.1365-2869.1997.00024.x

Strijkstra, A. M., & Daan, S. (1998). Dissimilarity of slow-wave activity enhancement by

torpor and sleep deprivation in a hibernator. *American Journal of Physiology - Regulatory Integrative and Comparative Physiology*, *275*(4 44-4). https://doi.org/10.1152/ajpregu.1998.275.4.r1110

Strijkstra, A. M., Hut, R. A., De Wilde, M. C., Stieler, J., & Van Der Zee, E. A. (2003). Hippocampal synaptophysin immunoreactivity is reduced during natural hypothermia in ground squirrels. *Neuroscience Letters*, *344*(1), 29–32. https://doi.org/10.1016/S0304-3940(03)00399-9

Su, B., Wang, X., Drew, K. L., Perry, G., Smith, M. A., & Zhu, X. (2008). Physiological regulation of tau phosphorylation during hibernation. *Journal of Neurochemistry*, *105*(6), 2098–2108. https://doi.org/10.1111/j.1471-4159.2008.05294.x

Sultan, S., Mandairon, N., Kermen, F., Garcia, S., Sacquet, J., & Didier, A. (2010). Learning-dependent neurogenesis in the olfactory bulb determines long-term olfactory memory. *The FASEB Journal*, *24*(7), 2355–2363. https://doi.org/10.1096/fj.09-151456

Sunagawa, G. A., & Takahashi, M. (2016). Hypometabolism during Daily Torpor in Mice is Dominated by Reduction in the Sensitivity of the Thermoregulatory System. *Scientific Reports*, *6*(1), 1–14. https://doi.org/10.1038/srep37011

Swoap, S. J., Rathvon, M., & Gutilla, M. (2007). AMP does not induce torpor. *American Journal of Physiology - Regulatory Integrative and Comparative Physiology*, *293*(1). https://doi.org/10.1152/ajpregu.00888.2006

Székely, M., Pétervári, E., Pákai, E., Hummel, Z., & Szelényi, Z. (2005). Acute, subacute and chronic effects of central neuropeptide Y on energy balance in rats. *Neuropeptides*, *39*(2), 103–115. https://doi.org/10.1016/j.npep.2005.01.005

Szolcsányi, J. (2015). Effect of capsaicin on thermoregulation: an update with new aspects. In *Temperature* (Vol. 2, Issue 2, pp. 277–296). Routledge. https://doi.org/10.1080/23328940.2015.1048928

T Hammel, B. H. (1968). *Regulation of internal body temperature1,2 further annual reviews*. www.annualreviews.org

Tai, H. C., Serrano-Pozo, A., Hashimoto, T., Frosch, M. P., Spires-Jones, T. L., & Hyman, B.

T. (2012). The synaptic accumulation of hyperphosphorylated tau oligomers in alzheimer disease is associated with dysfunction of the ubiquitin-proteasome system. *American Journal of Pathology*, *181*(4), 1426–1435. https://doi.org/10.1016/j.ajpath.2012.06.033

Tajino, K., Matsumura, K., Kosada, K., Shibakusa, T., Inoue, K., Fushiki, T., Hosokawa, H., & Kobayashi, S. (2007). Application of menthol to the skin of whole trunk in mice induces autonomic and behavioral heat-gain responses. *American Journal of Physiology-Regulatory, Integrative and Comparative Physiology*, *293*(5), R2128–R2135. https://doi.org/10.1152/ajpregu.00377.2007

Takahashi, T. M., Sunagawa, G. A., Soya, S., Abe, M., Sakurai, K., Ishikawa, K., Yanagisawa, M., Hama, H., Hasegawa, E., Miyawaki, A., Sakimura, K., Takahashi, M., & Sakurai, T. (2020). A discrete neuronal circuit induces a hibernation-like state in rodents. *Nature*. https://doi.org/10.1038/s41586-020-2163-6

Takashima, Y., Daniels, R. L., Knowlton, W., Teng, J., Liman, E. R., & McKemy, D. D. (2007). Diversity in the neural circuitry of cold sensing revealed by genetic axonal labeling of transient receptor potential melastatin 8 neurons. *Journal of Neuroscience*, *27*(51), 14147–14157. https://doi.org/10.1523/JNEUROSCI.4578-07.2007

Talaei, F., Bouma, H. R., Van der Graaf, A. C., Strijkstra, A. M., Schmidt, M., & Henning, R. H. (2011). Serotonin and Dopamine Protect from Hypothermia/Rewarming Damage through the CBS/ H2S Pathway. *PLoS ONE*, *6*(7), e22568. https://doi.org/10.1371/journal.pone.0022568

Talaei, F., Hylkema, M. N., Bouma, H. R., Boerema, A. S., Strijkstra, A. M., Henning, R. H., & Schmidt, M. (2011). Reversible remodeling of lung tissue during hibernation in the Syrian hamster. *Journal of Experimental Biology*, *214*(8), 1276–1282. https://doi.org/10.1242/jeb.052704

Tamura, Y., Shintani, M., Inoue, H., Monden, M., & Shiomi, H. (2012). Regulatory mechanism of body temperature in the central nervous system during the maintenance phase of hibernation in Syrian hamsters: Involvement of β-endorphin. *Brain Research*, *1448*, 63–70. https://doi.org/10.1016/j.brainres.2012.02.004

Tamura, Y., Shintani, M., Nakamura, A., Monden, M., & Shiomi, H. (2005). Phase-specific

central regulatory systems of hibernation in Syrian hamsters. *Brain Research*, *1045*(1–2), 88–96. https://doi.org/10.1016/j.brainres.2005.03.029

Tan, C. L., Cooke, E. K., Leib, D. E., Lin, Y. C., Daly, G. E., Zimmerman, C. A., & Knight, Z. A. (2016). Warm-Sensitive Neurons that Control Body Temperature. *Cell*, *167*(1), 47-59.e15. https://doi.org/10.1016/j.cell.2016.08.028

Tanaka, M., Mckinley, M. J., & Mcallen, R. M. (2011). Preoptic-Raphé Connections for Thermoregulatory Vasomotor Control. *Soc Neuroscience*. https://doi.org/10.1523/JNEUROSCI.6433-10.2011

Tanaka, M., McKinley, M. J., & McAllen, R. M. (2009). Roles of two preoptic cell groups in tonic and febrile control of rat tail sympathetic fibers. *American Journal of Physiology-Regulatory, Integrative and Comparative Physiology*, *296*(4), R1248–R1257. https://doi.org/10.1152/ajpregu.91010.2008

Tanaka, M., Owens, N. C., Nagashima, K., Kanosue, K., & McAllen, R. M. (2006). Reflex activation of rat fusimotor neurons by body surface cooling, and its dependence on the medullary raphé. *Journal of Physiology*, *572*(2), 569–583. https://doi.org/10.1113/jphysiol.2005.102400

Tansey, E. A., & Johnson, C. D. (2015). Recent advances in thermoregulation. *Advances in Physiology Education*, *39*(3), 139–148. https://doi.org/10.1152/advan.00126.2014

Tao, Z., Zhao, Z., & Lee, C. C. (2011). 5'-adenosine monophosphate induced hypothermia reduces early stage myocardial ischemia/reperfusion injury in a mouse model. *American Journal of Translational Research*, *3*(4), 351–361. https://www.ncbi.nlm.nih.gov/pmc/articles/PMC3158737/

Tashiro, K., Hasegawa, M., Ihara, Y., & Iwatsubo, T. (1997). Somatodendritic localization of phosphorylated tau in neonatal and adult rat cerebral cortex. *NeuroReport*, *8*(12), 2797–2801. https://doi.org/10.1097/00001756-199708180-00029

Tinganelli, W., Hitrec, T., Romani, F., Simoniello, P., Squarcio, F., Stanzani, A., Piscitiello, E., Marchesano, V., Luppi, M., Sioli, M., Helm, A., Compagnone, G., Morganti, A. G., Amici, R., Negrini, M., Zoccoli, A., Durante, M., & Cerri, M. (2019). Hibernation and

radioprotection: Gene expression in the liver and testicle of rats irradiated under synthetic torpor. *International Journal of Molecular Sciences*, *20*(2). https://doi.org/10.3390/ijms20020352

Tinganelli, W., Ma, N.-Y., Von Neubeck, C., Maier, A., Schicker, C., Kraft-Weyrather, W., & Durante, M. (2013). *Influence of acute hypoxia and radiation quality on cell survival*. https://doi.org/10.1093/jrr/rrt065

Tobler, I., & Borbély, A. A. (1986). Sleep EEG in the rat as a function of prior waking. *Electroencephalography and Clinical Neurophysiology*, *64*(1), 74–76. https://doi.org/10.1016/0013-4694(86)90044-1

Tøien, Drew, K. L., Chao, M. L., & Rice, M. E. (2001). Ascorbate dynamics and oxygen consumption during arousal from hibernation in arctic ground squirrels. *American Journal of Physiology - Regulatory Integrative and Comparative Physiology*, *281*(2 50-2). https://doi.org/10.1152/ajpregu.2001.281.2.r572

Tononi, G., & Cirelli, C. (2003). Sleep and synaptic homeostasis: a hypothesis. *Brain Research Bulletin*, *62*, 143–150. https://doi.org/10.1016/j.brainresbull.2003.09.004

Tononi, G., & Cirelli, C. (2014). Sleep and the Price of Plasticity: From Synaptic and Cellular Homeostasis to Memory Consolidation and Integration. In *Neuron* (Vol. 81, Issue 1, pp. 12–34). Cell Press. https://doi.org/10.1016/j.neuron.2013.12.025

Tononi, G., & Cirelli, C. (2019). Sleep and synaptic down-selection. *European Journal of Neuroscience*, *51*(1), 413–421. https://doi.org/10.1111/ejn.14335

Trachsel, L., Edgar, D. M., & Heller, H. C. (1991). Are ground squirrels sleep deprived during hibernation? *American Journal of Physiology - Regulatory Integrative and Comparative Physiology*, *260*(6 29-6). https://doi.org/10.1152/ajpregu.1991.260.6.r1123

Troynikov, O., Watson, C. G., & Nawaz, N. (2018). *Sleep environments and sleep physiology: A review*. https://doi.org/10.1016/j.jtherbio.2018.09.012

Tupone, D., Madden, C. J., & Morrison, S. F. (2013). Central Activation of the A1 Adenosine Receptor (A1AR) Induces a Hypothermic, Torpor-Like State in the Rat. *Soc Neuroscience*. https://doi.org/10.1523/JNEUROSCI.1980-13.2013

Twente, J. W., & Twente, J. (1978). Autonomic regulation of hibernation by citellus and eptesicus. In *Strategies in Cold* (pp. 327–373). https://doi.org/10.1016/b978-0-12-734550-5.50015-6

Vander, A., Sherman, J., & Luciano, D. (2001). Human Physiology: The Mechanism of Body Function. 2001. *McGraw Hill*.

Vaněček, J., Janský, L., Illnerová, H., & Hoffmann, K. (1984). Pineal melatonin in hibernating and aroused golden hamsters (Mesocricetus auratus). *Comparative Biochemistry and Physiology Part A: Physiology*, *77*(4), 759–762. https://doi.org/10.1016/0300-9629(84)90197-X

Vendrik, A. J. (1959). The regulation of body temperature in man. Introduction. *Nederlands Tijdschrift Voor Geneeskunde*, *103*(5), 240–244. https://pubmed.ncbi.nlm.nih.gov/13644357/

Vicent, M. A., Borre, E. D., & Swoap, S. J. (2017). Central activation of the A1 adenosine receptor in fed mice recapitulates only some of the attributes of daily torpor. *Journal of Comparative Physiology B: Biochemical, Systemic, and Environmental Physiology*, *187*(5–6), 835–845. https://doi.org/10.1007/s00360-017-1084-7

Violet, M., Delattre, L., Tardivel, M., Sultan, A., Chauderlier, A., Caillierez, R., Talahari, S., Nesslany, F., Lefebvre, B., Bonnefoy, E., Buée, L., & Galas, M.-C. (2014). A major role for Tau in neuronal DNA and RNA protection in vivo under physiological and hyperthermic conditions. *Frontiers in Cellular Neuroscience*, *8*(MAR), 84. https://doi.org/10.3389/fncel.2014.00084

Von Bernhardi, R., Eugenín-Von Bernhardi, L., & Eugenín, J. (2017). What is neural plasticity? *Advances in Experimental Medicine and Biology*, *1015*, 1–15. https://doi.org/10.1007/978-3-319-62817-2_1

Von Der Ohe, C. G., Darian-Smith, C., Garner, C. C., & Craig Heller, H. (2006). *Development/Plasticity/Repair Ubiquitous and Temperature-Dependent Neural Plasticity in Hibernators*. https://doi.org/10.1523/JNEUROSCI.2874-06.2006

Von Der Ohe, C. G., Garner, C. C., Darian-Smith, C., & Craig Heller, H. (2007).

Development/Plasticity/Repair Synaptic Protein Dynamics in Hibernation. https://doi.org/10.1523/JNEUROSCI.4385-06.2007

Vyazovskiy, Vladyslav V., Cirelli, C., Pfister-Genskow, M., Faraguna, U., & Tononi, G. (2008). Molecular and electrophysiological evidence for net synaptic potentiation in wake and depression in sleep. *Nature Neuroscience*, *11*(2), 200–208. https://doi.org/10.1038/nn2035

Vyazovskiy, Vladyslav V., Cirelli, C., & Tononi, G. (2011). Electrophysiological correlates of sleep homeostasis in freely behaving rats. In *Progress in Brain Research* (Vol. 193, pp. 17–38). Elsevier B.V. https://doi.org/10.1016/B978-0-444-53839-0.00002-8

Vyazovskiy, V V, Palchykova, S., Achermann, P., Tobler, I., & Deboer, T. (2017). Different Effects of Sleep Deprivation and Torpor on EEG Slow-Wave Characteristics in Djungarian Hamsters. *Cerebral Cortex*, *27*, 950–961. https://doi.org/10.1093/cercor/bhx020

Walker, H. C., & Romsos, D. R. (1993). Similar effects of NPY on energy metabolism and on plasma insulin in adrenalectomized ob/ob and lean mice. *American Journal of Physiology - Endocrinology and Metabolism*, *264*(2 27-2). https://doi.org/10.1152/ajpendo.1993.264.2.e226

Wang, H., & Siemens, J. (2015). TRP ion channels in thermosensation, thermoregulation and metabolism. *Temperature*, *2*(2), 178–187. https://doi.org/10.1080/23328940.2015.1040604

Wang, L. C. H. (1978). Energetic and field aspects of mammalian torpor: the richardson's ground squirrel. In *Strategies in Cold* (pp. 109–145). https://doi.org/10.1016/b978-0-12-734550-5.50009-0

Wang, Y., & Mandelkow, E. (2016). Tau in physiology and pathology. In *Nature Reviews Neuroscience* (Vol. 17, Issue 1, pp. 5–21). Nature Publishing Group. https://doi.org/10.1038/nrn.2015.1

Wang, Y. Y., Zheng, W., Ng, C. H., Ungvari, G. S., Wei, W., & Xiang, Y. T. (2017). Meta-analysis of randomized, double-blind, placebo-controlled trials of melatonin in

Alzheimer's disease. In *International Journal of Geriatric Psychiatry* (Vol. 32, Issue 1, pp. 50–57). John Wiley and Sons Ltd. https://doi.org/10.1002/gps.4571

Ward, J. M., & Armitage, K. B. (1981). Circannual rhythms of food consumption, body mass, and metabolism in yellow-bellied marmots. *Comparative Biochemistry and Physiology -- Part A: Physiology*, *69*(4), 621–626. https://doi.org/10.1016/0300-9629(81)90146-8

Werner, J. (1980). The concept of regulation for human body temperature. *Journal of Thermal Biology*, *5*(2), 75–82. https://doi.org/10.1016/0306-4565(80)90003-0

Wilson, W. R., & Hay, M. P. (2011). Targeting hypoxia in cancer therapy. In *Nature Reviews Cancer* (Vol. 11, Issue 6, pp. 393–410). https://doi.org/10.1038/nrc3064

Wilz, M., & Heldmaier, G. (2000). Comparison of hibernation, estivation and daily torpor in the edible dormouse, Glis glis. *Journal of Comparative Physiology - B Biochemical, Systemic, and Environmental Physiology*, *170*(7), 511–521. https://doi.org/10.1007/s003600000129

Wu, C.-W., & Storey, K. B. (2012). Cell Cycle Pattern of cellular quiescence over the hibernation cycle in liver of thirteen-lined ground squirrels. *Cell Cycle*, *11*(9), 1714–1726. https://doi.org/10.4161/cc.19799

Xiao, C., Liu, N., Jacobson, K. A., Gavrilova, O., & Reitman, M. L. (2019). Physiology and effects of nucleosides in mice lacking all four adenosine receptors. *PLoS Biology*, *17*(3). https://doi.org/10.1371/journal.pbio.3000161

Zagar, T. M., Oleson, J. R., Vujaskovic, Z., Dewhirst, M. W., Craciunescu, O. I., Blackwell, K. L., Prosnitz, L. R., & Jones, E. L. (2010). Hyperthermia combined with radiation therapy for superficial breast cancer and chest wall recurrence: A review of the randomised data. In *International Journal of Hyperthermia* (Vol. 26, Issue 7, pp. 612–617). https://doi.org/10.3109/02656736.2010.487194

Zetner, D., Andersen, L. P. H., & Rosenberg, J. (2016). Melatonin as Protection Against Radiation Injury: A Systematic Review. In *Drug Research* (Vol. 66, Issue 6, pp. 281–286). Georg Thieme Verlag. https://doi.org/10.1055/s-0035-1569358

Zhang, F., Wang, S., Luo, Y., Ji, X., Nemoto, E. M., & Chen, J. (2009). When hypothermia

meets hypotension and hyperglycemia: the diverse effects of adenosine 5′-monophosphate on cerebral ischemia in rats. *Journal of Cerebral Blood Flow & Metabolism*, *29*(5), 1022–1034. https://doi.org/10.1038/jcbfm.2009.28

Zhao, H. W., Christian, S. L., Castillo, M. R., Bult-Ito, A., & Drew, K. L. (2006). Distribution of NMDA receptor subunit NR1 in Arctic ground squirrel central nervous system. *Journal of Chemical Neuroanatomy*, *32*(2–4), 196–207. https://doi.org/10.1016/j.jchemneu.2006.09.002

Zhao, Z. D., Yang, W. Z., Gao, C., Fu, X., Zhang, W., Zhou, Q., Chen, W., Ni, X., Lin, J. K., Yang, J., Xu, X. H., & Shen, W. L. (2017). A hypothalamic circuit that controls body temperature. *Proceedings of the National Academy of Sciences of the United States of America*, *114*(8), 2042–2047. https://doi.org/10.1073/pnas.1616255114

Zoccoli, G., & Amici, R. (2020). Sleep and autonomic nervous system. In *Current Opinion in Physiology* (Vol. 15, pp. 128–133). Elsevier Ltd. https://doi.org/10.1016/j.cophys.2020.01.002

Zucchelli, M., Bastianini, S., Ventrella, D., Barone, F., Elmi, A., Romagnoli, N., Hitrec, T., Berteotti, C., Di Cristoforo, A., Luppi, M., Amici, R., Bacci, M. L., & Cerri, M. (2020). Autonomic effects induced by pharmacological activation and inhibition of Raphe Pallidus neurons in anaesthetized adult pigs. *Clinical and Experimental Pharmacology and Physiology*, *47*(2), 281–285. https://doi.org/10.1111/1440-1681.13194

ACKNOWLEDGMENTS

I would like to thank all the members of my lab group for their support, help and teachings during these three years of my doctorate. In particular, I would like to express my gratitude to my supervisor Prof. Roberto Amici for allowing me to take my first step towards my desire to work in the research field and for always being an essential guidance throughout my doctorate. I would also like to thank Dr. Marco Luppi, who was the first to welcome me in the laboratory, thanks also for all the kind and exhaustive explanations. Dr. Matteo Cerri for all the stimulating conversations and to find the critical points in my ideas, pushing me to always look for better ideas and solutions. Dr. Davide Martelli and Dr. Domenico Tupone for all the useful advice and teachings.

Special thanks go to Dr. Timna Hitrec who probably taught me more things than most teachers I have had so far.

Finally, I would like to thank my colleagues Dr. Alessandra Occhinegro and Dr. Emiliana Piscitiello for creating a collaborative, supportive and even fun working environment.